The Research Council of Norway (NFR)

NORSAR

NORSAR Scientific Report No. 2-93/94

Semiannual Technical Summary

1 October 1993 – 31 March 1994

Kjeller, May 1994

UNCLASSIFIED
SECURITY CLASSIFICATION OF THIS PAGE

REPORT DOCUMENTATION PAGE

1a. REPORT SECURITY CLASSIFICATION **UNCLASSIFIED**	1b. RESTRICTIVE MARKINGS **NOT APPLICABLE**
2a. SECURITY CLASSIFICATION AUTHORITY **NOT APPLICABLE**	3. DISTRIBUTION / AVAILABILITY OF REPORT **APPROVED FOR PUBLIC RELEASE** **DISTRIBUTION UNLIMITED**
2b. DECLASSIFICATION / DOWNGRADING SCHEDULE **NOT APPLICABLE**	
4. PERFORMING ORGANIZATION REPORT NUMBER(S) Scientific Report 2--93/94	5. MONITORING ORGANIZATION REPORT NUMBER(S) Scientific Report 2-93/94
6a. NAME OF PERFORMING ORGANIZATION NFR/NORSAR 6b. OFFICE SYMBOL *(If applicable)*	7a. NAME OF MONITORING ORGANIZATION HQ/AFTAC/TTS
6c. ADDRESS *(City, State, and ZIP Code)* Post Box 51 N-2007 Kjeller, Norway	7b. ADDRESS *(City, State, and ZIP Code)* Patrick AFB, FL 32925-6001
8a. NAME OF FUNDING / SPONSORING ORGANIZATION Advanced Research Projects Agency 8b. OFFICE SYMBOL *(If applicable)* NMRO	9. PROCUREMENT INSTRUMENT IDENTIFICATION NUMBER
8c. ADDRESS *(City, State, and ZIP Code)* 3701 N. Fairfax Dr. #717 Arlington, VA 22203-1714	10. SOURCE OF FUNDING NUMBERS PROGRAM ELEMENT NO. R&D PROJECT NO. NORSAR Phase 3 TASK NO. SOW Task 5.0 WORK UNIT ACCESSION NO. Seq.no. 003A2

11. TITLE *(Include Security Classification)*
SEMIANNUAL TECHNICAL SUMMARY, 1 OCTOBER 1993 - 31 MARCH 1994 (UNCLASSIFIED)

12. PERSONAL AUTHOR(S)

13a. TYPE OF REPORT	13b. TIME COVERED	14. DATE OF REPORT *(Year, Month, Day)*	15. PAGE COUNT
Scientific Summary	FROM 1 Oct 93 TO 31 Mar 94	May 1994	147

16. SUPPLEMENTARY NOTATION
NOT APPLICABLE

17. COSATI CODES			18. SUBJECT TERMS *(Continue on reverse if necessary and identify by block number)*
FIELD	GROUP	SUB-GROUP	**NORSAR, Norwegian Seismic Array**
8	11		

19. ABSTRACT *(Continue on reverse if necessary and identify by block number)*

This Semiannual Technical Summary describes the operation, maintenance and research activities at the Norwegian Seismic Array (NORSAR), the Norwegian Regional Seismic Array (NORESS), the Arctic Regional Seismic Array (ARCESS) and the experimental Spitsbergen regional array for the period 1 October 1993 - 31 March 1994. Statistics are also presented for additional seismic stations, which through cooperative agreements with institutions in the host countries provide continuous data to the NORSAR Data Processing Center (NPDC). These stations comprise the Finnish Experimental Seismic Array (FINESS), the German Experimental Seismic Array (GERESS), and an experimental regional seismic array in Apatity, Russia.

(cont.)

20. DISTRIBUTION / AVAILABILITY OF ABSTRACT ☐ UNCLASSIFIED/UNLIMITED ☐ SAME AS RPT. ☐ DTIC USERS	21. ABSTRACT SECURITY CLASSIFICATION
22a. NAME OF RESPONSIBLE INDIVIDUAL Mr. Michael C. Baker	22b. TELEPHONE *(Include Area Code)* (407) 494-7665 22c. OFFICE SYMBOL AFTAC/TTS

DD FORM 1473, 84 MAR 83 APR edition may be used until exhausted. All other editions are obsolete.

SECURITY CLASSIFICATION OF THIS PAGE
UNCLASSIFIED

Abstract (cont.)

This Semiannual Report also presents statistics from operation of the Intelligent Monitoring System (IMS). The IMS has been operated in an experimental mode, and the performance has been very satisfactory. Since October 1991, a new version of the IMS that accepts data from an arbitrary number of arrays and single 3-component stations has been operated.

The NORSAR Detection Processing system has been operated throughout the period with an average uptime of 98.3% as compared to 97.3% for the previous reporting period. A total of 1226 seismic events have been reported in the NORSAR monthly seismic bulletin. The performance of the continuous alarm system and the automatic bulletin transfer by telex to AFTAC has been satisfactory. The system for direct retrieval of NORSAR waveform data through an X.25 connection has been used successfully for acquiring such data by AFTAC. Processing of requests for full NORSAR and regional array data on magnetic tapes has progressed according to established schedules.

Since 1 October 1991, an effort has been undertaken to carry out a complete technical refurbishment of the NORSAR array. This project is funded jointly by AFTAC, ARPA and NFR. During the reporting period, we have finalized our evaluation of technical options for field instrumentation, in particular broad-band seismometers, state-of-the-art A/D converters, data acquisition and synchronization devices. In addition, we are converting the NORSAR Detection/Event Processing software to be compatible with our UNIX-based workstations. Our detailed status report regarding this work is reported on separately. We have, after approval by AFTAC and ARPA, placed orders for broad-band seismometers with Teledyne Brown Engineering, and for 24-bit digitizers and array controllers with Science Horizons. Delivery is expected during summer/fall 1994.

As an intermediate step in the NORSAR Refurbishment, a modified version of the NORSAR data acquisition system was implemented on 1 January 1994. The main reason for this change, which utilizes a previously established backup solution, was to circumvent some data timing problems due to deteriorating hardware. At the same time, this change has provided valuable experience in preparing the full refurbishment.

On-line detection processing and data recording at the NORSAR Data Processing Center (NDPC) of NORESS, ARCESS, FINESS and GERESS data have been conducted throughout the period. Data from two experimental small-aperture arrays at sites in Spitsbergen and Apatity, Kola Peninsula, have been recorded and processed in an experimental mode. Monthly processing statistics for the arrays as well as results of the IMS analysis for the reporting period are given.

Maintenance activities in the period comprise preventive/corrective maintenance in connection with all the NORSAR subarrays, NORESS and ARCESS. Other activities have involved testing of the NORSAR communications systems and work in connection with the experimental small-aperture arrays in Spitsbergen and Russia.

Summaries of five scientific contributions are presented in Chapter 7 of this report.

Section 7.1 outlines the principles for global continuous Threshold Monitoring (TM), and summarizes the status of our efforts to develop and implement a prototype, workstation-based Threshold Monitoring System for the GSETT-3 International Data Center (IDC). We have until now concentrated on the development of the interactive tools necessary for conducting extensive off-line testing of the TM method, and some work still remains. The system will initially offer certain basic services, but will be able to evolve and adapt to future requirements that may be specified, and as tests and experiments are conducted.

Within the context of IDC operation for GSETT-3 we envisage that the TM-system will be able to provide the following services.

1) A near real-time global assessment of upper magnitude limits based on generic (average) attenuation relations for a fixed number of grid points. The visual/numerical results from this process can be presented in several ways:

   - A computerized world map with continuously updated TM levels displayed on a screen at the IDC.
   - A hard-copy of the map with TM levels/contours (detection thresholds) for an instant in time or the maximum within some predefined time interval. This is a service that can be provided upon request from the National Data Centers (NDCs).
   - TM traces for the grid points used in the global assessment or other predefined targets, along with statistics on the distribution of the TM levels, and explanation on the TM peaks. This can also be provided upon request from the NDCs and sent in terms of postscript files or other formats.

2) A more precise assessment of upper mantle magnitude limits for a limited number of predefined regions or target sites using region-specific or site-specific attenuation relations. This can only be done for regions or sites for which previously recorded events (with good magnitude estimates) are available. The number of targets subjected to site-specific TM can be increased over time as additional calibration information is accumulated.

Section 7.2 describes a technical investigation with the purpose of compiling statistics for the time-lag in the ESAL (Expert System for Association and Location, the knowledge-based system which locates events in IMS) processing, as well as identifying the cause for each of these lags. It was expected that such an exercise would provide considerable insight into the complexity of the task of keeping a system like IMS running at close to real-time. In this paper, the results from the first six months of monitoring time lags (October 1993 - March 1994) are reported. The study offers several suggestions and also raises some essential questions that should be addressed in an actual monitoring environment.

Section 7.3 addresses signal detection and waveform extraction in the coda of a strong, interfering event, using the adaptive optimal group filtering (AOGF) method. Several scenarios are discussed; with main focus on the case when the locations of the strong interfering event and the possible hidden signal are both known. This scenario is of interest, e.g.,

when trying to extract a small surface wave for a known event following a large earthquake, or if one wants to focus upon a particular potential test site during the earthquake coda. It is demonstrated, both theoretically and by examples, that the spatial rejection characteristics of the AOGF method result in an undistorted waveform of the "hidden" signal, whereas the often-used method of beam subtraction produces a distorted spectrum (energy loss at low frequencies).

Section 7.4 describes some recent improvements to the regional array detectors in operation at the NORSAR data center. These improvements take into account recent research results in Bochum, Germany, regarding the GERESS array. In particular, improved use is made of horizontal components for secondary phase detection. It is shown that the application to ARCESS, GERESS and NORESS of coherent beams of rotated horizontal components clearly increases the S-phase detection capabilities of these arrays, especially in the case of relatively strong SH-wave radiation from the source to the array. Therefore, the new beams have also led to a larger number of events defined and located by automatic processes (e.g., RONAPP and GBF).

Some changes in the procedures for automatically selecting time window (i.e., length and position relative to the estimated onset time) for the fk-analysis and prefiltering the single traces were tested, and were found to stabilize the fk-results. For ARCESS, FINESS, GERESS and NORESS the "rel. fk-power" increases in the mean and especially the erroneous estimates of phase velocity and azimuth based on fk-results with very low "rel. fk-power" are reduced. This also improves the results of the automatic data analysis for all kinds of seismic phases.

Section 7.5 describes a study of satellite imagery in connection with the 31 December 1992 seismic event on Novaya Zemlya. This small (m_b 2.5) event has attracted considerable attention in the nuclear monitoring research community. In particular, it has been used as an example to test the effectiveness of seismic identification tools. Using specially processed high-quality satellite images from SPOT and Landsat, a detailed investigation has been made of five different location estimates proposed for the seismic event. It is concluded that the satellite images fail to show any certain signs of human activity that can be related to the 31 December 1992 event. This conclusion is based on experience gained during the satellite study of the Novaya Zemlya nuclear underground test site in the nearby Shumilikha valley on the southwestern side of the Matochkin Shar. The infrastructure and main feature related to the testing activities here are visible and have been mapped using satellite images. SPOT's 10 m resolution is, however, not fully satisfactory since a lot of the medium and almost all the fine details are lost. This has to be taken into account when the results of the 31 December 1992 event are evaluated.

AFTAC Project Authorization	:	T/9141/B/PKP
ARPA Order No.	:	4138 AMD # 16
Program Code No.	:	0F10
Name of Contractor	:	Royal Norwegian Council for Scientific and Industrial Research (NTNF)
Effective Date of Contract	:	1 Oct 1988
Contract Expiration Date	:	30 Sep 1994
Project Manager	:	Frode Ringdal (06) 81 71 21
Title of Work	:	The Norwegian Seismic Array (NORSAR) Phase 3
Amount of Contract	:	$ 13,052,032
Contract Period Covered by Report	:	1 October 93 - 31 March 94

The views and conclusions contained in this document are those of the authors and should not be interpreted as necessarily representing the official policies, either expressed or implied, of the Advanced Research Projects Agency, the Air Force Technical Applications Center or the U.S. Government.

This research was supported by the Advanced Research Projects Agency of the Department of Defense and was monitored by AFTAC, Patrick AFB, FL32925, under contract no. F08606-89-C-0005 and F08650-93-C-0002.

NORSAR Contribution No. 514

Table of Contents

1 Summary

This Semiannual Technical Summary describes the operation, maintenance and research activities at the Norwegian Seismic Array (NORSAR), the Norwegian Regional Seismic Array (NORESS), the Arctic Regional Seismic Array (ARCESS) and the experimental Spitsbergen regional array for the period 1 October 1993 - 31 March 1994. Statistics are also presented for additional seismic stations, which through cooperative agreements with institutions in the host countries provide continuous data to the NORSAR Data Processing Center (NPDC). These stations comprise the Finnish Experimental Seismic Array (FINESS), the German Experimental Seismic Array (GERESS), and an experimental regional seismic array in Apatity, Russia.

This Semiannual Report also presents statistics from operation of the Intelligent Monitoring System (IMS). The IMS has been operated in an experimental mode, and the performance has been very satisfactory. Since October 1991, a new version of the IMS that accepts data from an arbitrary number of arrays and single 3-component stations has been operated.

The NORSAR Detection Processing system has been operated throughout the period with an average uptime of 98.3% as compared to 97.3% for the previous reporting period. A total of 1226 seismic events have been reported in the NORSAR monthly seismic bulletin. The performance of the continuous alarm system and the automatic bulletin transfer by telex to AFTAC has been satisfactory. The system for direct retrieval of NORSAR waveform data through an X.25 connection has been used successfully for acquiring such data by AFTAC. Processing of requests for full NORSAR and regional array data on magnetic tapes has progressed according to established schedules.

Since 1 October 1991, an effort has been undertaken to carry out a complete technical refurbishment of the NORSAR array. This project is funded jointly by AFTAC, ARPA and NFR. During the reporting period, we have finalized our evaluation of technical options for field instrumentation, in particular broad-band seismometers, state-of-the-art A/D converters, data acquisition and synchronization devices. In addition, we are converting the NORSAR Detection/Event Processing software to be compatible with our UNIX-based workstations. Our detailed status report regarding this work is reported on separately. We have, after approval by AFTAC and ARPA, placed orders for broad-band seismometers with Teledyne Brown Engineering, and for 24-bit digitizers and array controllers with Science Horizons. Delivery is expected during summer/fall 1994.

As an intermediate step in the NORSAR Refurbishment, a modified version of the NORSAR data acquisition system was implemented on 1 January 1994. The main reason for this change, which utilizes a previously established backup solution, was to circumvent some data timing problems due to deteriorating hardware. At the same time, this change has provided valuable experience in preparing the full refurbishment.

On-line detection processing and data recording at the NORSAR Data Processing Center (NDPC) of NORESS, ARCESS, FINESS and GERESS data have been conducted throughout the period. Data from two experimental small-aperture arrays at sites in Spits-

bergen and Apatity, Kola Peninsula, have been recorded and processed in an experimental mode. Monthly processing statistics for the arrays as well as results of the IMS analysis for the reporting period are given.

Maintenance activities in the period comprise preventive/corrective maintenance in connection with all the NORSAR subarrays, NORESS and ARCESS. Other activities have involved testing of the NORSAR communications systems and work in connection with the experimental small-aperture arrays in Spitsbergen and Russia.

Summaries of five scientific contributions are presented in Chapter 7 of this report.

Section 7.1 outlines the principles for global continuous Threshold Monitoring (TM), and summarizes the status of our efforts to develop and implement a prototype, workstation-based Threshold Monitoring System for the GSETT-3 International Data Center (IDC). We have until now concentrated on the development of the interactive tools necessary for conducting extensive off-line testing of the TM method, and some work still remains. The system will initially offer certain basic services, but will be able to evolve and adapt to future requirements that may be specified, and as tests and experiments are conducted.

Within the context of IDC operation for GSETT-3 we envisage that the TM-system will be able to provide the following services.

1) A near real-time global assessment of upper magnitude limits based on generic (average) attenuation relations for a fixed number of grid points. The visual/numerical results from this process can be presented in several ways:

   - A computerized world map with continuously updated TM levels displayed on a screen at the IDC.

   - A hard-copy of the map with TM levels/contours (detection thresholds) for an instant in time or the maximum within some predefined time interval. This is a service that can be provided upon request from the National Data Centers (NDCs).

   - TM traces for the grid points used in the global assessment or other predefined targets, along with statistics on the distribution of the TM levels, and explanation on the TM peaks. This can also be provided upon request from the NDCs and sent in terms of postscript files or other formats.

2) A more precise assessment of upper mantle magnitude limits for a limited number of predefined regions or target sites using region-specific or site-specific attenuation relations. This can only be done for regions or sites for which previously recorded events (with good magnitude estimates) are available. The number of targets subjected to site-specific TM can be increased over time as additional calibration information is accumulated.

Section 7.2 describes a technical investigation with the purpose of compiling statistics for the time-lag in the ESAL (Expert System for Association and Location, the knowledge-based system which locates events in IMS) processing, as well as identifying the cause for each of these lags. It was expected that such an exercise would provide considerable

insight into the complexity of the task of keeping a system like IMS running at close to real-time. In this paper, the results from the first six months of monitoring time lags (October 1993 - March 1994) are reported. The study offers several suggestions and also raises some essential questions that should be addressed in an actual monitoring environment.

Section 7.3 addresses signal detection and waveform extraction in the coda of a strong, interfering event, using the adaptive optimal group filtering (AOGF) method. Several scenarios are discussed; with main focus on the case when the locations of the strong interfering event and the possible hidden signal are both known. This scenario is of interest, e.g., when trying to extract a small surface wave for a known event following a large earthquake, or if one wants to focus upon a particular potential test site during the earthquake coda. It is demonstrated, both theoretically and by examples, that the spatial rejection characteristics of the AOGF method result in an undistorted waveform of the "hidden" signal, whereas the often-used method of beam subtraction produces a distorted spectrum (energy loss at low frequencies).

Section 7.4 describes some recent improvements to the regional array detectors in operation at the NORSAR data center. These improvements take into account recent research results in Bochum, Germany, regarding the GERESS array. In particular, improved use is made of horizontal components for secondary phase detection. It is shown that the application to ARCESS, GERESS and NORESS of coherent beams of rotated horizontal components clearly increases the S-phase detection capabilities of these arrays, especially in the case of relatively strong SH-wave radiation from the source to the array. Therefore, the new beams have also led to a larger number of events defined and located by automatic processes (e.g., RONAPP and GBF).

Some changes in the procedures for automatically selecting time window (i.e., length and position relative to the estimated onset time) for the fk-analysis and prefiltering the single traces were tested, and were found to stabilize the fk-results. For ARCESS, FINESS, GERESS and NORESS the "rel. fk-power" increases in the mean and especially the erroneous estimates of phase velocity and azimuth based on fk-results with very low "rel. fk-power" are reduced. This also improves the results of the automatic data analysis for all kinds of seismic phases.

Section 7.5 describes a study of satellite imagery in connection with the 31 December 1992 seismic event on Novaya Zemlya. This small (m_b 2.5) event has attracted considerable attention in the nuclear monitoring research community. In particular, it has been used as an example to test the effectiveness of seismic identification tools. Using specially processed high-quality satellite images from SPOT and Landsat, a detailed investigation has been made of five different location estimates proposed for the seismic event. It is concluded that the satellite images fail to show any certain signs of human activity that can be related to the 31 December 1992 event. This conclusion is based on experience gained during the satellite study of the Novaya Zemlya nuclear underground test site in the nearby Shumilikha valley on the southwestern side of the Matochkin Shar. The infrastructure and main feature related to the testing activities here are visible and have been mapped using satellite images. SPOT's 10 m resolution is, however, not fully satisfactory since a lot of the medium and almost all the fine details are lost. This has to be taken into account when the results of the 31 December 1992 event are evaluated.

2 NORSAR Operation

2.1 Detection Processor (DP) operation

There have been 98 breaks in the otherwise continuous operation of the NORSAR online system within the current 6-month reporting interval. The uptime percentage for the period is 98.3 as compared to 97.3 for the previous period.

Fig. 2.1.1 and the accompanying Table 2.1.1 both show the daily DP downtime for the days between 1 October 1993 and 31 March 1994. The monthly recording times and percentages are given in Table 2.1.2.

The breaks can be grouped as follows:

a)	Hardware failure	4
b)	Stops related to program work or error	0
c)	Hardware maintenance stops	0
d)	Power jumps and breaks	1
e)	TOD error correction	0
f)	Communication lines	93

The total downtime for the period was 47 hours and 4 minutes. The mean-time-between-failures (MTBF) was 1.4 days, as compared to 2.8 for the previous period.

J. Torstveit

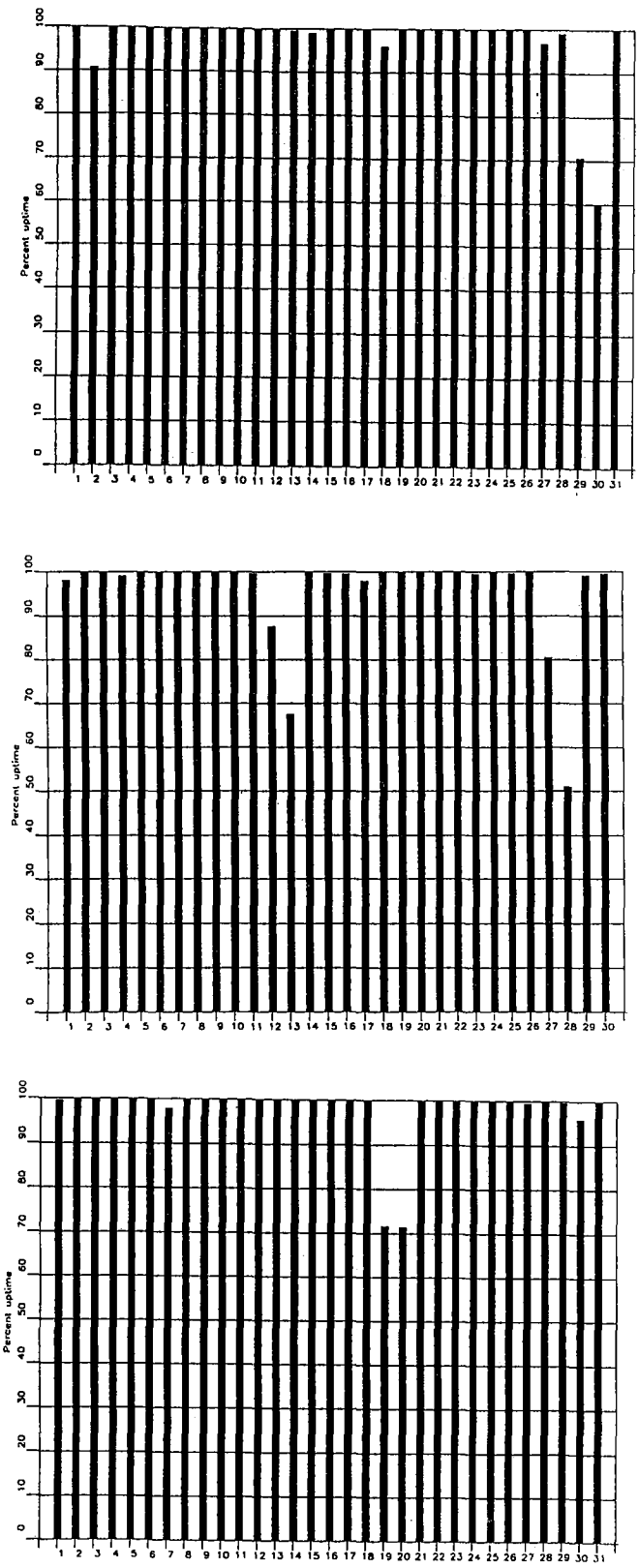

Fig. 2.1.1. Detection Processor uptime for October (top), November (middle) and December (bottom) 1993.

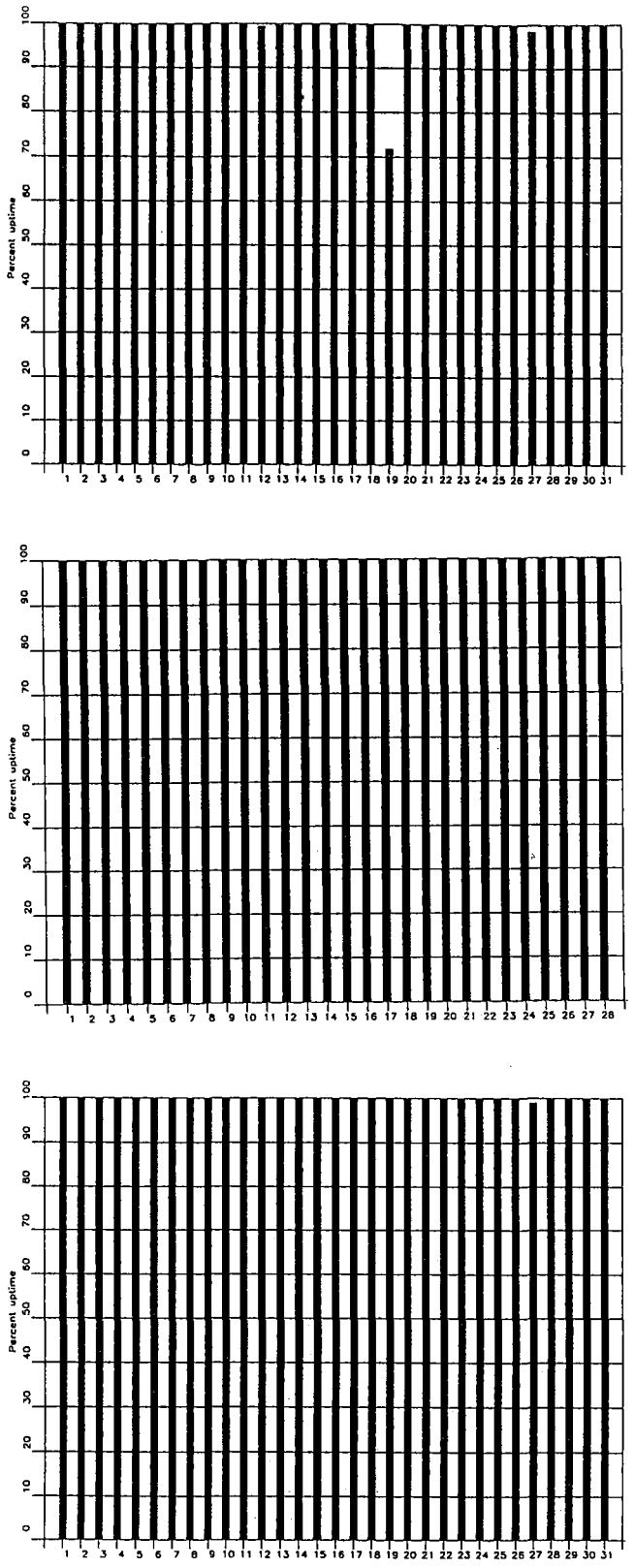

Fig. 2.1.1. Detection Processor uptime for January (top), February (middle) and March (bottom) 1994.

Date	Time	Cause
02 Oct	0915 - 1130	Line failure
18 Oct	1309 - 1356	Line failure
27 Oct	1227 - 1306	Line failure
29 Oct	1700 -	Line failure
30 Oct	- 0936	
01 Nov	1303 - 1328	Hardware failure
12 Nov	2105 -	Line failure
13 Nov	- 0745	
17 Nov	0735 - 0751	Line failure
27 Nov	1256 - 1348	Hardware failure
27 Nov	2012 -	Line failure
28 Nov	- 1144	
07 Dec	0759 - 0830	Line failure
19 Dec	1712 -	Power failure HUB
20 Dec	- 0652	
29 Dec	2358 -	Hardware failure
30 Dec	- 0051	
19 Jan	0741 - 1428	Hardware failure
27 Jan	1315 - 1337	Hardware failure
27 Mar	1244 - 1259	Line failure

Table 2.1.1. The major downtimes in the period 1 October 1993 - 31 March 1994.

Month	DP Uptime Hours	DP Uptime %	No. of DP Breaks	No. of Days with Breaks	DP MTBF* (days)
Oct 93	735.24	97.03	35	22	0.7
Nov 93	705.09	95.86	43	25	0.5
Dec 93	728.10	97.86	17	13	1.3
Jan 94	736.43	99.02	2	2	7.9
Feb 94	671.56	99.99	0	0	24.0
Mar 94	743.42	99.96	1	1	12.0
		98.29	98	63	1.4

*Mean-time-between-failures = total uptime/no. of up intervals.

Table 2.1.2. Online system performance, 1 October 1993 - 31 March 1994.

2.2 Array Communications

As detailed in the monthly NORSAR Management reports, there were significant communications problems with several subarrays during the first part of the reporting period. Some of this was related to a Modcomp problem regarding timing/synchronization, but mostly the problems were caused by progressive failure of deteriorating system components at NDPC.

As an intermediate solution, it was decided on 1 January 1994 to implement a backup version of the NORSAR recording system, thus eliminating the Modcomp/SLEM-based recording. This change succeeded in improving both the timing reliability and the individual subarray uptimes. Thus, during March 1994 all subarray communication lines were operational for essentially 100% of the time.

This intermediate solution will remain in effect until the NORSAR Refurbishment project is completed. This is scheduled to happen during the fall of 1994.

A simplified daily summary of the communications performance for the seven individual subarray lines is summarized, on a month-by-month basis, in Table 2.2.1.

F. Ringdal

Table 2.2.1 (page 1 of 6)
NORSAR Communication Status Report
Month: October 1993

Day	Subarray						
	01A	01B	02B	02C	03C	04C	06C
01	X	I	X	I	X	X	X
02	X	I	X	I	X	X	X
03	X	I	X	I	X	X	X
04	X	I	X	I	X	X	X
05	X	I	X	I	X	X	X
06	X	I	X	I	X	X	X
07	X	I	X	I	X	X	X
08	I	I	X	I	X	X	X
09	I	I	X	I	X	X	X
10	I	I	X	I	X	X	X
11	X	I	X	I	X	X	X
12	X	I	X	I	X	X	X
13	X	I	X	I	X	X	X
14	X	I	X	I	X	X	X
15	X	I	X	I	X	X	X
16	X	I	X	I	X	X	X
17	X	I	X	I	X	X	X
18	X	I	X	I	X	X	X
19	X	I	X	I	X	X	X
20	X	I	X	I	X	X	X
21	X	I	X	I	X	X	X
22	X	I	X	I	X	X	X
23	X	I	X	I	X	X	X
24	X	I	X	I	X	X	X
25	X	I	X	I	X	X	X
26	X	I	X	I	X	X	X
27	X	I	X	I	X	X	X
28	X	I	X	I	X	X	X
29	X	I	X	I	X	X	X
30	X	I	X	I	X	X	X
31	X	I	X	I	X	X	X
Total hours normal operation	650	0	744	0	744	744	744
% normal operation	87.3	0	100	0	100	100	100

Legend :

X : Normal operations
A : All channels masked for more than 12 hours that day
B : All SP channels masked for more than 12 hours that day
C : All LP channels masked for more than 12 hours that day
I : Communication outage for more than 12 hours

Table 2.2.1 (page 2 of 6)
NORSAR Communication Status Report
Month: November 1993

Day	Subarray						
	01A	01B	02B	02C	03C	04C	06C
01	X	I	X	I	X	X	X
02	X	I	X	I	X	X	X
03	X	I	X	I	X	X	X
04	X	I	X	I	X	X	X
05	X	I	X	I	X	X	X
06	X	I	X	I	X	X	X
07	X	I	X	I	X	X	X
08	X	I	X	I	X	X	X
09	X	I	X	I	X	X	X
10	X	I	X	I	X	X	X
11	X	I	X	I	X	X	X
12	X	I	I	I	X	X	X
13	X	I	I	I	X	X	X
14	X	I	I	I	X	X	X
15	X	I	I	I	X	X	X
16	X	I	X	I	X	X	X
17	X	I	X	I	X	X	X
18	I	I	X	I	X	X	X
19	I	I	X	I	X	X	X
20	X	I	X	I	X	X	X
21	X	I	X	I	X	X	X
22	X	I	X	I	X	X	X
23	X	I	X	I	X	X	X
24	X	I	I	I	X	X	X
25	X	I	I	I	X	X	X
26	X	I	X	I	X	X	X
27	X	I	X	I	X	X	X
28	X	I	X	I	X	X	X
29	I	I	X	I	X	X	X
30	I	I	X	I	X	X	X
31							
Total hours normal operation	624	0	576	0	720	720	720
% normal operation	87	0	80	0	100	100	100

Legend :

X : Normal operations
A : All channels masked for more than 12 hours that day
B : All SP channels masked for more than 12 hours that day
C : All LP channels masked for more than 12 hours that day
I : Communication outage for more than 12 hours

Table 2.2.1 (page 3 of 6)
NORSAR Communication Status Report
Month: December 1993

Day	Subarray						
	01A	01B	02B	02C	03C	04C	06C
01	X	I	X	I	X	X	X
02	X	I	I	I	X	X	X
03	X	I	I	I	X	X	X
04	X	I	I	I	X	X	X
05	I	I	I	I	X	X	X
06	I	I	I	I	X	X	X
07	X	I	X	I	X	X	X
08	X	I	X	I	X	X	X
09	X	I	X	I	X	X	X
10	X	I	X	I	X	X	X
11	X	I	X	I	X	X	X
12	X	I	X	I	X	X	X
13	X	I	X	I	X	X	X
14	X	I	X	I	X	X	X
15	X	I	X	I	X	X	X
16	X	I	X	I	X	X	X
17	X	I	X	I	X	X	X
18	X	I	X	I	X	X	X
19	X	I	I	I	X	X	X
20	X	I	I	I	X	X	X
21	X	I	I	I	X	X	X
22	X	I	I	I	X	X	X
23	X	I	X	I	X	X	X
24	X	I	X	I	X	X	X
25	X	I	X	I	X	X	X
26	X	I	X	I	X	X	X
27	X	I	X	I	X	X	X
28	X	I	X	I	X	X	X
29	X	I	X	I	X	X	X
30	X	I	X	I	X	X	X
31	X	I	X	I	X	X	X
Total hours normal operation	696	0	528	0	744	744	744
% normal operation	94	0	71	0	100	100	100

Legend :

X : Normal operations
A : All channels masked for more than 12 hours that day
B : All SP channels masked for more than 12 hours that day
C : All LP channels masked for more than 12 hours that day
I : Communication outage for more than 12 hours

Table 2.2.1 (page 4 of 6)
NORSAR Communication Status Report
Month: January 1994

Day	Subarray						
	01A	01B	02B	02C	03C	04C	06C
01	I	X	I	X	I	I	X
02	I	X	I	X	I	I	X
03	I	X	I	X	I	I	X
04	I	X	I	X	I	I	X
05	I	X	I	X	I	I	X
06	X	X	I	X	I	I	X
07	X	X	X	X	I	I	X
08	X	X	X	X	I	I	X
09	X	X	X	X	I	I	X
10	X	X	X	X	I	I	X
11	X	X	X	X	I	I	X
12	X	X	X	X	I	I	X
13	X	X	X	X	I	I	X
14	X	X	X	X	I	I	X
15	X	X	X	X	I	I	X
16	X	X	X	X	I	I	X
17	X	X	X	X	I	I	X
18	X	X	X	X	I	I	X
19	X	X	I	X	I	I	X
20	X	X	I	X	I	I	X
21	X	X	I	X	I	I	X
22	X	X	I	X	I	I	X
23	X	X	X	X	I	I	X
24	X	X	X	X	I	I	X
25	X	X	X	X	I	I	X
26	X	X	X	X	I	I	X
27	X	X	X	X	I	I	X
28	X	X	X	X	I	I	X
29	X	X	X	X	I	I	X
30	X	X	X	X	I	I	X
31	X	X	X	X	I	X	X
Total hours normal operation	624	744	600	744	24	24	744
% normal operation	84	100	81	100	3	3	100

Legend :

X : Normal operations
A : All channels masked for more than 12 hours that day
B : All SP channels masked for more than 12 hours that day
C : All LP channels masked for more than 12 hours that day
I : Communication outage for more than 12 hours

Table 2.2.1 (page 5 of 6)
NORSAR Communication Status Report
Month: February 1994

Day	Subarray						
	01A	01B	02B	02C	03C	04C	06C
01	X	X	X	X	X	X	X
02	X	X	X	X	X	X	X
03	X	X	X	X	X	X	X
04	X	X	X	X	X	X	X
05	X	X	X	X	X	X	X
06	X	X	X	X	X	X	X
07	X	X	X	X	X	X	X
08	X	X	X	X	X	X	X
09	X	I	X	X	X	X	X
10	X	I	X	X	X	X	X
11	X	I	X	X	X	X	X
12	X	I	X	X	X	X	X
13	X	I	X	X	X	X	X
14	X	I	X	X	X	X	X
15	X	I	X	X	X	X	X
16	X	I	X	X	X	X	X
17	X	X	X	X	X	X	X
18	X	X	X	X	X	X	X
19	X	X	X	X	X	X	X
20	X	X	X	X	X	X	X
21	X	X	X	X	X	X	X
22	X	X	X	X	X	X	X
23	X	X	X	X	X	X	X
24	X	X	X	X	X	X	X
25	X	X	X	X	X	X	X
26	X	X	X	X	X	X	X
27	X	X	X	X	X	X	X
28	X	X	X	X	X	X	X
29							
30							
31							
Total hours normal operation	672	480	672	672	672	672	672
% normal operation	100	71	100	100	100	100	100

Table 2.2.1 (page 6 of 6)
NORSAR Communication Status Report
Month: March 1994

Day	Subarray						
	01A	01B	02B	02C	03C	04C	06C
01	X	X	X	X	X	X	X
02	X	X	X	X	X	X	X
03	X	X	X	X	X	X	X
04	X	X	X	X	X	X	X
05	X	X	X	X	X	X	X
06	X	X	X	X	X	X	X
07	X	X	X	X	X	X	X
08	X	X	X	X	X	X	X
09	X	X	X	X	X	X	X
10	X	X	X	X	X	X	X
11	X	X	X	X	X	X	X
12	X	X	X	X	X	X	X
13	X	X	X	X	X	X	X
14	X	X	X	X	X	X	X
15	X	X	X	X	X	X	X
16	X	X	X	X	X	X	X
17	X	X	X	X	X	X	X
18	X	X	X	X	X	X	X
19	X	X	X	X	X	X	X
20	X	X	X	X	X	X	X
21	X	X	X	X	X	X	X
22	X	X	X	X	X	X	X
23	X	X	X	X	X	X	X
24	X	X	X	X	X	X	X
25	X	X	X	X	X	X	X
26	X	X	X	X	X	X	X
27	X	X	X	X	X	X	X
28	X	X	X	X	X	X	X
29	X	X	X	X	X	X	X
30	X	X	X	X	X	X	X
31	X	X	X	X	X	X	X
Total hours normal operation	744	744	744	744	744	744	744
% normal operation	100	100	100	100	100	100	100

Legend :

X : Normal operations
A : All channels masked for more than 12 hours that day
B : All SP channels masked for more than 12 hours that day
C : All LP channels masked for more than 12 hours that day
I : Communication outage for more than 12 hours

2.3 NORSAR Event Detection operation

In Table 2.3.1 some monthly statistics of the Detection and Event Processor operation are given. The table lists the total number of detections (DPX) triggered by the on-line detector, the total number of detections processed by the automatic event processor (EPX) and the total number of events accepted after analyst review (teleseismic phases, core phases and total). Note that due to the system change-over the Event Processor was operated using a higher threshold than normal during January 1994, resulting in fewer reported events (see Section 4.1).

	Total DPX	Total EPX	Accepted events		Sum	Daily
			P-phases	Core Phases		
Oct 93	10,475	1371	200	57	257	8.3
Nov 93	11,625	1454	202	45	247	8.2
Dec 93	12,693	1482	153	54	207	6.7
Jan 94	11,897	885	50	4	54	1.7
Feb 94	10,627	877	186	49	235	8.4
Mar 94	13,167	849	172	54	226	7.3
			963	263	1226	6.8

Table 2.3.1. Detection and Event Processor statistics, 1 October 1993 - 31 March 1994.

NORSAR Detections

The number of detections (phases) reported by the NORSAR detector during day 274, 1993, through day 090, 1994, was 69,853, giving an average of 384 detections per processed day (182 days processed). Table 2.3.2 shows daily and hourly distribution of detections for NORSAR.

B. Paulsen

NAO .DPX Hourly distribution of detections

Day	00	01	02	03	04	05	06	07	08	09	10	11	12	13	14	15	16	17	18	19	20	21	22	23	Sum	Date
274	13	14	15	19	21	18	6	12	6	3	13	14	11	12	13	16	10	10	15	15	15	16	25	17	329	Oct 01 Friday
275	12	18	22	22	19	23	19	12	20	5	0	2	8	14	21	6	16	16	18	21	23	24	15	18	374	Oct 02 Saturday
276	17	19	19	27	12	21	17	19	17	18	17	8	15	14	15	11	9	13	7	18	9	9	17	18	366	Oct 03 Sunday
277	20	22	12	15	8	12	9	5	0	4	3	5	5	11	10	15	11	9	9	9	15	11	14	15	249	Oct 04 Monday
278	24	10	28	15	18	26	6	5	1	1	6	2	8	6	18	9	17	6	5	10	19	19	15	16	290	Oct 05 Tuesday
279	22	18	12	21	20	13	4	3	2	17	7	5	15	8	17	9	11	13	14	11	12	15	13	13	295	Oct 06 Wednesday
280	15	12	9	10	6	20	11	1	5	11	14	4	17	8	7	7	6	8	11	12	8	10	8	9	229	Oct 07 Thursday
281	8	12	11	10	7	16	2	6	7	8	14	21	23	6	12	13	15	15	9	11	15	12	13	10	276	Oct 08 Friday
282	14	13	17	11	18	16	14	15	10	8	14	16	19	9	21	18	11	7	18	13	4	14	16	6	322	Oct 09 Saturday
283	15	11	9	11	7	10	8	9	7	11	10	3	18	6	6	7	5	5	16	2	10	7	12	11	216	Oct 10 Sunday
284	12	11	9	9	7	10	2	2	2	2	5	3	7	19	16	10	19	5	4	11	3	11	14	8	201	Oct 11 Monday
285	15	12	17	16	15	9	5	10	4	4	10	4	16	5	9	12	7	5	12	11	22	15	11	13	259	Oct 12 Tuesday
286	10	24	27	24	14	17	12	12	10	13	12	7	19	9	9	16	5	17	13	16	17	9	14	21	347	Oct 13 Wednesday
287	20	11	15	25	21	12	23	15	6	11	10	6	10	10	7	7	28	1	14	7	11	6	6	12	294	Oct 14 Thursday
288	10	16	8	13	12	5	2	8	8	2	1	14	13	8	10	10	5	15	7	14	21	14	24	15	255	Oct 15 Friday
289	20	14	24	24	10	13	12	14	13	15	15	24	28	15	17	14	27	19	26	21	20	19	22	16	442	Oct 16 Saturday
290	24	13	16	28	25	13	20	26	17	23	17	16	19	18	15	14	16	18	23	11	19	15	14	13	433	Oct 17 Sunday
291	16	18	14	19	14	15	10	6	8	9	6	11	17	36	21	21	19	18	17	23	22	8	19	16	383	Oct 18 Monday
292	16	13	14	20	19	22	13	5	10	10	17	10	9	21	16	16	18	15	14	17	13	21	22	14	365	Oct 19 Tuesday
293	13	24	18	20	12	19	9	9	19	11	5	27	8	17	13	7	20	16	9	12	16	22	12	16	354	Oct 20 Wednesday
294	19	28	14	14	23	21	9	6	11	10	11	9	21	22	14	5	16	14	10	15	5	14	14	12	337	Oct 21 Thursday
295	15	14	17	19	10	18	9	11	7	7	16	7	11	22	16	21	15	11	15	12	13	23	24	17	350	Oct 22 Friday
296	15	15	29	27	30	34	18	17	22	9	11	14	15	21	20	22	23	15	35	26	24	28	22	31	523	Oct 23 Saturday
297	22	21	25	16	21	18	34	26	23	18	18	14	15	12	16	18	18	24	19	16	26	17	23	18	478	Oct 24 Sunday
298	21	29	30	27	29	22	15	5	12	9	22	6	21	14	26	10	14	14	12	17	18	18	21	16	428	Oct 25 Monday
299	26	19	24	14	20	21	10	13	10	12	17	24	11	10	13	14	15	17	15	16	20	8	19	19	387	Oct 26 Tuesday
300	22	16	16	19	17	18	7	9	10	11	13	9	25	9	22	11	13	11	12	16	19	26	10	12	353	Oct 27 Wednesday
301	16	21	20	17	20	16	31	5	10	10	11	21	8	39	27	16	15	19	13	12	15	24	22	14	422	Oct 28 Thursday
302	35	18	21	17	21	17	14	10	15	9	5	40	9	12	5	4	10	1	0	0	0	0	0	0	263	Oct 29 Friday
303	0	0	0	0	0	0	0	0	0	17	11	14	13	15	19	17	19	20	28	15	14	9	19	24	254	Oct 30 Saturday
304	21	15	15	21	26	18	15	25	20	18	9	10	18	13	10	11	9	18	16	17	19	11	16	8	379	Oct 31 Sunday
305	17	27	17	15	8	18	16	4	3	7	11	11	23	8	30	12	4	10	11	9	9	8	11	11	300	Nov 01 Monday
306	9	16	15	12	15	6	4	6	3	10	9	11	6	10	10	1	3	9	5	17	14	14	9	12	226	Nov 02 Tuesday
307	12	18	6	18	10	6	4	6	11	9	4	20	22	10	17	7	20	8	16	12	10	16	7	14	283	Nov 03 Wednesday
308	15	18	18	14	18	17	21	4	6	4	24	8	31	29	29	29	16	10	7	13	18	10	24	18	401	Nov 04 Thursday
309	21	16	31	23	24	14	9	13	2	18	20	13	13	18	13	9	20	15	17	22	16	19	24	12	402	Nov 05 Friday
310	21	12	17	12	28	26	19	19	7	11	12	27	15	18	16	17	16	10	21	15	13	16	14	20	402	Nov 06 Saturday
311	19	21	25	18	18	20	26	15	24	19	21	13	16	23	22	8	24	11	16	15	11	20	12	28	445	Nov 07 Sunday
312	16	16	18	15	19	14	13	11	4	11	14	6	17	18	13	6	20	20	23	23	17	19	18	14	365	Nov 08 Monday
313	20	22	30	28	23	19	4	9	16	12	9	5	7	14	17	7	21	15	18	9	15	16	26	23	385	Nov 09 Tuesday
314	39	22	22	22	22	16	8	10	18	16	15	9	14	11	12	15	17	23	21	15	16	38	28	13	442	Nov 10 Wednesday
315	25	21	27	18	31	23	11	9	12	10	26	16	16	12	26	11	14	13	15	18	16	15	22	24	431	Nov 11 Thursday
316	21	31	18	24	19	16	10	11	24	11	14	27	11	26	23	22	15	15	17	18	10	0	0	0	383	Nov 12 Friday
317	0	0	0	0	0	0	0	4	20	19	21	22	13	17	11	14	5	17	9	16	12	17	15	16	248	Nov 13 Saturday
318	15	20	19	16	12	18	16	16	16	20	20	16	22	21	18	23	9	15	11	15	22	20	14	17	411	Nov 14 Sunday
319	17	25	19	16	18	15	9	1	5	7	12	10	6	8	11	19	7	9	13	14	8	0	0	0	249	Nov 15 Monday
320	28	20	27	35	31	24	17	4	9	8	9	9	13	35	17	24	21	16	11	11	11	12	16	19	427	Nov 16 Tuesday
321	16	13	20	10	22	15	8	13	12	7	9	20	12	23	18	15	18	16	17	21	18	14	22	12	371	Nov 17 Wednesday
322	10	22	24	17	27	25	12	17	15	33	9	38	51	62	126	31	18	11	12	13	17	19	16	16	641	Nov 18 Thursday
323	26	28	18	23	27	9	8	6	9	9	13	10	37	15	27	14	16	12	25	15	15	16	21	20	419	Nov 19 Friday
324	24	23	18	25	24	16	22	25	24	16	20	19	39	15	17	19	19	21	12	33	26	18	27	23	525	Nov 20 Saturday
325	18	24	23	20	14	16	13	18	22	26	17	18	16	11	25	25	17	18	18	24	18	24	23	34	482	Nov 21 Sunday
326	18	22	32	27	22	22	15	15	11	16	13	19	17	6	16	13	9	16	24	19	11	13	22	21	419	Nov 22 Monday
327	32	17	26	12	15	19	13	6	28	9	9	10	18	19	16	21	14	21	21	9	14	16	13	19	397	Nov 23 Tuesday
328	22	17	12	17	12	16	14	6	4	8	10	9	18	9	19	16	11	12	12	13	14	12	20	11	314	Nov 24 Wednesday
329	21	14	13	18	10	7	25	6	15	10	14	8	9	19	15	28	11	12	14	13	22	20	18	14	356	Nov 25 Thursday

Table 2.3.2 (Page 1 of 4)

NAO ..DPX Hourly distribution of detections

Day	00	01	02	03	04	05	06	07	08	09	10	11	12	13	14	15	16	17	18	19	20	21	22	23	Sum	Date
330	16	17	13	23	22	22	7	11	19	32	19	16	8	20	14	14	15	21	21	14	19	18	23	17	421	Nov 26 Friday
331	8	18	24	17	17	16	25	12	17	17	12	13	6	5	27	57	58	38	38	28	9	0	0	0	462	Nov 27 Saturday
332	0	0	0	0	0	0	0	0	0	0	0	15	19	17	27	20	32	11	22	19	21	24	16	19	262	Nov 28 Sunday
333	16	21	19	11	14	15	15	9	8	11	12	6	17	19	18	17	16	10	7	11	20	9	11	11	323	Nov 29 Monday
334	16	17	8	17	14	19	9	14	10	24	10	10	9	14	34	21	15	12	7	17	19	19	26	16	377	Nov 30 Tuesday
335	12	16	21	12	14	18	11	9	13	13	25	8	6	14	19	18	23	14	24	26	14	14	25	10	379	Dec 01 Wednesday
336	17	13	21	0	0	3	25	7	11	11	11	13	17	19	21	17	15	15	24	14	16	16	26	22	354	Dec 02 Thursday
337	20	18	21	12	11	24	10	10	13	12	17	24	22	14	15	15	19	29	22	16	17	14	11	17	403	Dec 03 Friday
338	25	36	16	27	31	28	63	24	16	25	6	17	18	19	21	35	25	30	16	21	17	27	27	23	593	Dec 04 Saturday
339	14	27	19	17	18	26	45	19	22	15	31	13	22	21	20	17	17	16	24	19	20	13	26	29	510	Dec 05 Sunday
340	26	23	27	26	23	22	14	9	16	6	9	17	10	36	13	28	19	20	14	18	13	16	16	20	441	Dec 06 Monday
341	13	26	17	16	30	23	12	8	17	9	19	14	18	14	10	11	53	14	15	13	16	17	13	15	413	Dec 07 Tuesday
342	25	17	16	14	24	11	10	6	9	26	11	12	37	5	30	15	7	13	10	13	10	20	5	19	365	Dec 08 Wednesday
343	7	14	15	22	32	24	13	7	15	16	20	31	9	3	7	10	15	9	13	12	7	20	11	22	354	Dec 09 Thursday
344	17	23	22	8	19	11	15	11	4	16	13	19	14	2	8	12	12	5	12	11	11	12	12	15	304	Dec 10 Friday
345	20	14	14	9	19	15	11	15	17	22	19	13	20	14	24	8	19	19	9	22	16	22	10	22	393	Dec 11 Saturday
346	13	11	20	17	19	26	27	23	32	17	20	19	16	14	20	23	14	26	27	17	20	5	17	20	463	Dec 12 Sunday
347	18	19	16	25	20	15	4	8	5	14	6	7	18	4	23	9	13	15	15	10	15	17	13	22	331	Dec 13 Monday
348	14	34	24	15	10	13	18	34	9	10	4	10	11	18	10	15	18	25	11	18	19	14	15	16	385	Dec 14 Tuesday
349	18	17	15	12	9	12	14	16	14	6	10	11	22	7	24	33	20	15	14	16	10	10	28	17	370	Dec 15 Wednesday
350	11	19	23	23	32	13	31	7	10	11	12	14	14	22	10	9	7	14	14	16	20	11	8	14	365	Dec 16 Thursday
351	24	20	10	16	12	16	4	4	8	6	11	8	16	13	22	18	18	14	16	12	20	20	24	18	350	Dec 17 Friday
352	22	24	19	19	16	18	20	12	8	26	21	17	32	16	14	20	28	23	25	29	22	18	22	22	493	Dec 18 Saturday
353	21	23	35	26	29	29	25	23	21	25	27	26	17	22	19	23	16	3	0	0	0	0	0	0	410	Dec 19 Sunday
354	0	0	0	0	0	0	16	4	4	9	8	6	8	10	22	5	8	10	16	11	17	17	9	13	193	Dec 20 Monday
355	17	11	17	13	8	15	14	11	14	12	12	18	17	23	22	15	30	18	14	11	19	18	22	23	394	Dec 21 Tuesday
356	12	27	27	25	14	24	11	14	10	4	12	14	16	23	7	19	12	13	18	16	29	19	21	18	405	Dec 22 Wednesday
357	22	16	25	18	26	17	24	14	14	14	27	14	14	17	25	17	17	15	16	10	19	16	17	10	424	Dec 23 Thursday
358	11	19	18	12	11	11	13	7	11	12	10	26	23	18	22	25	27	13	21	20	22	25	13	19	409	Dec 24 Friday
359	21	24	25	22	33	19	24	28	29	24	32	21	22	20	32	32	20	24	25	27	22	31	16	21	594	Dec 25 Saturday
360	20	29	21	16	22	21	19	13	25	16	20	20	15	28	19	20	19	10	12	16	9	10	9	18	427	Dec 26 Sunday
361	10	12	16	14	17	18	17	9	11	9	7	3	9	13	14	14	23	22	15	16	22	14	24	20	349	Dec 27 Monday
362	12	32	14	23	29	14	18	13	18	17	16	14	24	27	17	12	17	22	26	16	28	14	19	18	460	Dec 28 Tuesday
363	23	20	16	15	19	16	14	12	34	11	28	17	19	34	23	16	17	22	15	18	24	17	26	16	472	Dec 29 Wednesday
364	2	23	28	18	17	26	23	17	17	17	10	30	21	17	25	15	13	13	24	17	20	18	23	20	454	Dec 30 Thursday
365	21	16	13	26	23	27	15	15	32	9	13	25	15	16	12	7	17	12	26	20	13	15	24	24	436	Dec 31 Friday
1	27	22	20	23	26	21	17	21	29	22	17	15	20	26	20	20	17	25	13	17	14	17	21	25	495	Jan 01 Saturday
2	27	23	25	32	34	26	30	31	23	23	17	20	18	14	21	22	14	22	13	16	20	19	17	24	531	Jan 02 Sunday
3	16	25	15	26	35	23	28	8	11	22	24	11	17	44	21	24	21	43	34	31	42	40	44	27	632	Jan 03 Monday
4	26	32	22	37	26	26	9	14	35	11	14	7	6	8	13	11	10	7	9	5	9	5	11	20	373	Jan 04 Tuesday
5	18	17	10	5	15	8	5	6	3	6	10	9	11	18	7	5	6	8	7	8	4	16	7	15	224	Jan 05 Wednesday
6	13	17	15	14	13	10	6	6	7	9	17	8	20	13	8	4	9	11	10	10	16	9	15	14	274	Jan 06 Thursday
7	11	10	16	11	7	10	5	5	5	21	6	9	12	8	9	6	10	5	17	15	17	23	18	16	272	Jan 07 Friday
8	21	15	24	24	24	15	21	12	17	4	8	12	8	11	9	16	13	18	13	18	17	11	18	13	362	Jan 08 Saturday
9	13	16	21	22	22	28	12	24	19	24	25	17	24	15	23	26	17	14	19	21	15	16	18	24	475	Jan 09 Sunday
10	18	15	23	18	22	21	8	5	6	6	21	10	16	4	16	18	29	19	11	14	19	20	20	17	376	Jan 10 Monday
11	27	23	18	20	11	14	14	23	14	17	13	6	9	12	19	18	23	15	15	26	18	11	19	19	404	Jan 11 Tuesday
12	23	22	14	11	14	11	15	12	7	11	33	14	15	18	9	14	11	22	11	23	28	16	17	20	391	Jan 12 Wednesday
13	17	24	34	17	26	24	22	13	24	13	8	12	21	6	24	10	18	15	11	10	18	17	12	16	412	Jan 13 Thursday
14	27	21	12	18	21	11	11	8	3	11	11	8	18	7	13	23	14	15	18	23	24	20	13	14	364	Jan 14 Friday
15	23	15	25	21	29	13	27	34	21	20	19	26	22	15	25	19	26	26	18	27	18	17	26	30	542	Jan 15 Saturday
16	16	21	19	19	18	21	16	17	13	14	11	9	8	12	13	18	18	24	17	15	20	19	20	23	401	Jan 16 Sunday
17	11	34	23	30	19	16	15	15	11	21	11	14	20	18	19	21	17	9	16	17	20	13	19	30	439	Jan 17 Monday
18	27	20	16	27	14	18	10	9	12	4	16	17	15	15	19	28	16	21	15	21	21	21	23	26	431	Jan 18 Tuesday
19	24	19	35	18	16	23	12	18	15	11	13	7	0	0	11	25	19	20	18	16	29	20	14	14	397	Jan 19 Wednesday
20	16	22	18	12	13	11	20	5	8	13	8	18	11	11	5	7	15	11	13	14	13	10	17	20	311	Jan 20 Thursday

Table 2.3.2. (Page 2 of 4)

NAO .DPX Hourly distribution of detections

Day	00	01	02	03	04	05	06	07	08	09	10	11	12	13	14	15	16	17	18	19	20	21	22	23	Sum	Date
21	23	28	38	17	23	15	13	9	17	13	8	17	10	18	17	8	23	10	19	13	7	6	6	9	367	Jan 21 Friday
22	8	5	10	11	13	12	4	15	10	12	11	19	15	18	13	16	11	6	9	5	8	7	8	6	252	Jan 22 Saturday
23	10	21	10	14	16	17	14	8	2	5	5	4	9	15	8	10	11	16	12	9	13	14	13	11	267	Jan 23 Sunday
24	8	6	8	10	10	16	7	6	3	9	6	5	11	3	11	13	5	13	19	17	23	17	16	26	268	Jan 24 Monday
25	21	28	16	13	15	20	12	23	12	10	16	12	17	13	15	19	13	24	17	21	10	16	12	12	387	Jan 25 Tuesday
26	22	20	22	15	17	16	12	14	5	9	13	20	12	9	18	16	14	15	9	18	10	22	23	17	368	Jan 26 Wednesday
27	12	31	21	23	18	21	17	19	16	5	24	17	18	16	21	8	10	13	13	13	15	10	12	16	389	Jan 27 Thursday
28	13	24	12	10	15	14	7	15	3	5	12	15	22	18	15	19	7	27	14	10	17	18	9	13	334	Jan 28 Friday
29	15	17	25	21	20	28	16	35	21	18	17	18	18	13	19	20	11	20	23	20	20	20	24	17	476	Jan 29 Saturday
30	21	23	25	24	26	16	20	11	20	8	9	10	7	6	5	4	9	4	13	5	3	12	5	2	288	Jan 30 Sunday
31	5	4	6	9	12	10	10	7	18	12	9	17	12	9	7	8	13	11	12	6	7	13	12	14	243	Jan 31 Monday
32	12	20	10	17	13	10	11	3	18	26	24	17	8	15	9	10	22	22	10	7	21	19	25	13	362	Feb 01 Tuesday
33	17	16	20	21	16	10	14	12	8	8	10	13	16	12	8	13	27	19	12	18	13	21	15	23	362	Feb 02 Wednesday
34	13	12	21	13	10	5	3	6	4	10	16	9	7	10	14	9	9	8	30	7	10	9	6	16	257	Feb 03 Thursday
35	19	22	17	10	16	12	11	7	8	7	5	16	20	9	10	11	18	15	19	20	17	17	16	11	333	Feb 04 Friday
36	19	24	19	18	24	20	21	13	21	21	19	16	22	7	22	18	19	24	19	25	23	30	21	22	487	Feb 05 Saturday
37	31	28	27	26	23	19	25	24	24	13	16	21	17	19	14	17	23	18	21	14	19	24	18	18	499	Feb 06 Sunday
38	19	27	25	15	30	13	13	12	5	12	9	7	14	7	7	26	24	16	21	13	20	7	9	21	372	Feb 07 Monday
39	17	18	18	28	16	25	16	10	7	10	11	10	27	11	9	12	11	11	14	16	16	19	19	22	373	Feb 08 Tuesday
40	28	27	25	22	21	20	9	5	8	11	16	4	5	22	3	3	18	15	11	13	7	9	7	5	314	Feb 09 Wednesday
41	8	13	15	6	7	3	10	1	3	12	12	17	6	3	8	10	9	0	4	5	5	0	4	11	172	Feb 10 Thursday
42	16	11	10	13	8	12	5	6	6	4	4	15	12	10	16	18	12	23	14	9	10	21	13	16	284	Feb 11 Friday
43	18	17	23	27	27	16	22	28	19	25	13	10	19	17	26	19	22	23	28	27	25	17	22	16	506	Feb 12 Saturday
44	14	17	24	13	25	27	26	21	17	28	22	26	19	25	21	16	22	22	30	23	24	35	19	26	542	Feb 13 Sunday
45	27	27	24	26	19	27	20	13	12	17	20	27	21	7	14	20	13	14	14	24	18	20	24	21	469	Feb 14 Monday
46	17	18	22	14	19	15	11	11	6	8	23	12	13	13	4	17	4	26	23	14	17	23	32	18	380	Feb 15 Tuesday
47	20	21	18	10	22	12	12	29	10	9	17	29	10	13	17	15	16	13	15	18	27	20	17	17	407	Feb 16 Wednesday
48	14	11	23	23	11	18	11	3	7	5	8	12	7	12	9	10	7	2	16	17	13	15	17	20	291	Feb 17 Thursday
49	22	17	16	16	17	5	9	11	17	16	14	11	11	13	14	13	16	10	6	13	8	9	17	20	321	Feb 18 Friday
50	21	8	20	16	14	21	21	14	13	15	11	9	21	10	8	11	18	22	19	23	15	20	13	14	377	Feb 19 Saturday
51	13	22	30	17	17	15	12	18	13	10	19	17	13	10	4	9	10	8	7	12	17	19	23	19	354	Feb 20 Sunday
52	21	16	26	17	16	18	3	5	11	9	4	15	4	12	9	15	6	5	8	3	16	7	15	17	278	Feb 21 Monday
53	11	17	16	16	23	20	9	8	9	7	7	16	15	8	9	7	3	4	12	4	13	13	18	18	283	Feb 22 Tuesday
54	16	18	14	13	21	13	10	10	10	3	4	13	27	18	11	4	11	5	11	12	7	12	19	15	297	Feb 23 Wednesday
55	24	18	22	11	22	14	3	4	12	23	20	15	10	11	14	18	15	18	12	17	18	16	11	29	377	Feb 24 Thursday
56	29	21	22	16	26	12	10	15	6	5	6	18	17	20	17	5	14	24	12	15	16	32	19	14	391	Feb 25 Friday
57	24	17	20	14	27	21	20	19	13	13	26	9	25	22	18	12	13	11	18	17	38	19	20	27	463	Feb 26 Saturday
58	21	29	35	47	29	25	27	27	9	18	8	19	12	18	8	13	9	19	17	24	19	19	16	22	490	Feb 27 Sunday
59	14	19	23	19	19	15	15	6	10	17	14	12	14	14	11	5	10	17	12	11	16	20	22	21	356	Feb 28 Monday
60	15	15	23	33	21	27	14	16	11	10	8	16	12	10	16	12	17	13	18	19	18	29	11	32	416	Mar 01 Tuesday
61	29	17	19	27	24	21	12	12	11	12	15	15	11	19	21	21	15	20	19	24	17	15	20	21	437	Mar 02 Wednesday
62	19	18	13	15	24	22	13	9	15	7	9	6	6	20	26	17	34	24	20	30	13	26	31	21	438	Mar 03 Thursday
63	21	24	17	22	18	20	9	7	9	12	16	5	26	13	9	25	26	22	22	25	20	22	24	23	437	Mar 04 Friday
64	22	25	20	24	35	10	25	19	19	18	16	17	19	22	19	21	17	19	20	25	24	14	22	23	495	Mar 05 Saturday
65	34	31	25	35	27	31	25	21	25	21	23	28	18	26	21	23	14	22	22	20	17	18	21	24	572	Mar 06 Sunday
66	25	27	23	26	25	32	17	9	11	11	13	18	8	9	11	7	13	22	8	14	21	19	18	21	408	Mar 07 Monday
67	14	15	17	29	25	18	7	8	8	8	9	8	10	8	14	14	10	12	22	19	26	17	22	25	365	Mar 08 Tuesday
68	22	25	23	33	25	20	22	12	11	10	14	5	20	9	14	9	14	22	15	12	10	17	15	35	414	Mar 09 Wednesday
69	25	23	11	28	26	12	14	14	9	16	13	15	18	8	19	24	16	18	21	16	24	18	19	11	418	Mar 10 Thursday
70	17	28	30	35	41	14	15	19	7	7	13	15	13	20	12	19	18	15	23	31	13	16	11	13	445	Mar 11 Friday
71	15	18	18	12	15	15	18	17	12	13	15	9	11	14	16	18	11	19	21	16	25	15	19	32	394	Mar 12 Saturday
72	23	13	31	34	17	19	26	18	25	19	13	20	19	17	18	14	18	23	15	14	20	11	24	21	472	Mar 13 Sunday
73	20	21	15	17	25	22	5	12	11	11	7	9	8	17	12	10	18	14	17	18	16	25	22	30	382	Mar 14 Monday
74	27	22	19	39	24	19	20	6	14	7	13	21	18	6	17	5	23	9	20	24	25	21	27	26	452	Mar 15 Tuesday
75	28	21	26	30	34	21	16	17	12	33	16	14	21	4	10	19	13	10	9	17	20	21	14	22	448	Mar 16 Wednesday
76	16	30	30	23	26	15	12	8	11	8	5	17	16	13	14	13	19	9	14	16	16	15	22	17	385	Mar 17 Thursday

Table 2.3.2. (Page 3 of 4)

NAO .DPX Hourly distribution of detections

Day	00	01	02	03	04	05	06	07	08	09	10	11	12	13	14	15	16	17	18	19	20	21	22	23	Sum	Date
77	25	14	24	24	26	16	5	2	4	4	5	4	11	11	14	13	10	17	16	20	23	20	8	6	322	Mar 18 Friday
78	17	21	20	21	19	28	13	18	10	27	23	22	16	13	8	14	11	19	10	19	17	21	14	16	417	Mar 19 Saturday
79	22	26	23	21	11	16	28	16	19	28	18	16	20	10	11	7	13	14	13	16	11	21	11	19	410	Mar 20 Sunday
80	15	20	15	19	17	12	8	9	7	7	2	9	8	9	14	4	10	6	3	9	3	15	5	12	238	Mar 21 Monday
81	16	17	24	18	10	16	14	15	10	8	14	10	11	12	10	10	19	15	22	14	19	19	17	28	368	Mar 22 Tuesday
82	23	22	22	24	24	19	10	6	6	11	9	11	8	8	9	12	14	21	13	12	18	10	8	20	340	Mar 23 Wednesday
83	26	20	22	18	17	16	13	10	14	8	15	23	17	10	18	17	12	19	18	18	14	23	26	21	415	Mar 24 Thursday
84	18	20	29	13	14	13	11	3	5	6	6	7	7	11	7	10	6	33	8	8	10	20	10	15	290	Mar 25 Friday
85	21	20	19	28	21	19	20	28	19	19	21	18	28	25	22	23	27	15	21	22	25	24	23	22	530	Mar 26 Saturday
86	16	20	28	16	18	14	17	16	13	12	15	15	10	17	20	21	18	20	29	19	31	20	29	30	464	Mar 27 Sunday
87	27	24	19	21	19	11	12	11	11	7	11	3	14	21	10	12	19	19	23	24	16	19	13	11	377	Mar 28 Monday
88	16	23	25	19	15	5	15	11	15	15	20	17	13	16	13	28	18	14	27	12	18	20	16	15	406	Mar 29 Tuesday
89	18	23	27	24	21	20	9	15	13	19	19	14	22	23	13	21	33	20	28	23	18	23	16	15	477	Mar 30 Wednesday
90	15	29	36	35	25	22	28	22	13	20	22	18	21	20	17	18	15	28	27	17	18	29	40	29	564	Mar 31 Thursday
NAO	00	01	02	03	04	05	06	07	08	09	10	11	12	13	14	15	16	17	18	19	20	21	22	23		
Sum	3505	3430	3080	2225	2331	2548	2718	2768	2831	2897	3007	3203														
	3305	3553	3442	2606	2261	2463	2829	2957	2893	2907	3004	3090													69853	Total sum
182	18	19	20	19	19	17	14	12	12	13	14	14	16	15	16	15	16	16	16	16	17	17	17	18	384	Total average
129	18	20	19	18	18	16	12	10	10	11	12	13	15	14	16	14	15	15	15	15	16	16	17	17	363	Average workdays
53	18	19	21	20	20	19	20	18	17	17	16	16	18	16	17	18	17	18	18	18	18	17	18	19	435	Average weekends

Table 2.3.2. Daily and hourly distribution of NORSAR detections. For each day is shown number of detections within each hour of the day and number of detections for that day. The end statistics give total number of detections distributed for each hour and the total sum of detections during the period. The averages show number of processed days, hourly distribution and average per processed day. (Page 4 of 4)

3 Operation of regional arrays

3.1 Recording of NORESS data at NDPC, Kjeller

Table 3.1.1 lists the main outage times and reasons.

The average recording time was 96.48% as compared to 99.94% during the previous reporting period.

Date	Time	Cause
07 Dec	0759 - 0830	Transmission line failure
08 Dec	0050 - 0109	Transmission line failure
09 Dec	0726 -	Hardware/software failure
14 Dec	- 1308	
17 Dec	1305 - 1323	Software work
31 Dec	2311 - 2359	Software problem
18 Feb	0837 - 1724	Software work
19 Feb	0837 - 1724	Hardware failure NDPC
27 Mar	1756 - 1813	Transmission line failure
29 Mar	1213 - 1240	Transmission line failure
31 Mar	0040 - 0050	Software problem
31 Mar	0240 - 0250	Software problem
31 Mar	0440 - 0450	Software problem

Table 3.1.1. Interruptions in recording of NORESS data at NDPC, 1 October 1993 - 31 March 1994.

Monthly uptimes for the NORESS on-line data recording task, taking into account all factors (field installations, transmissions line, data center operation) affecting this task were as follows:

October 93	:	100.00
November	:	100.00
December	:	82.66
January 94	:	99.67
February	:	99.97
March	:	98.5

Fig. 3.1.1 shows the uptime for the data recording task, or equivalently, the availability of NORESS data in our tape archive, on a day-by-day basis, for the reporting period.

J. Torstveit

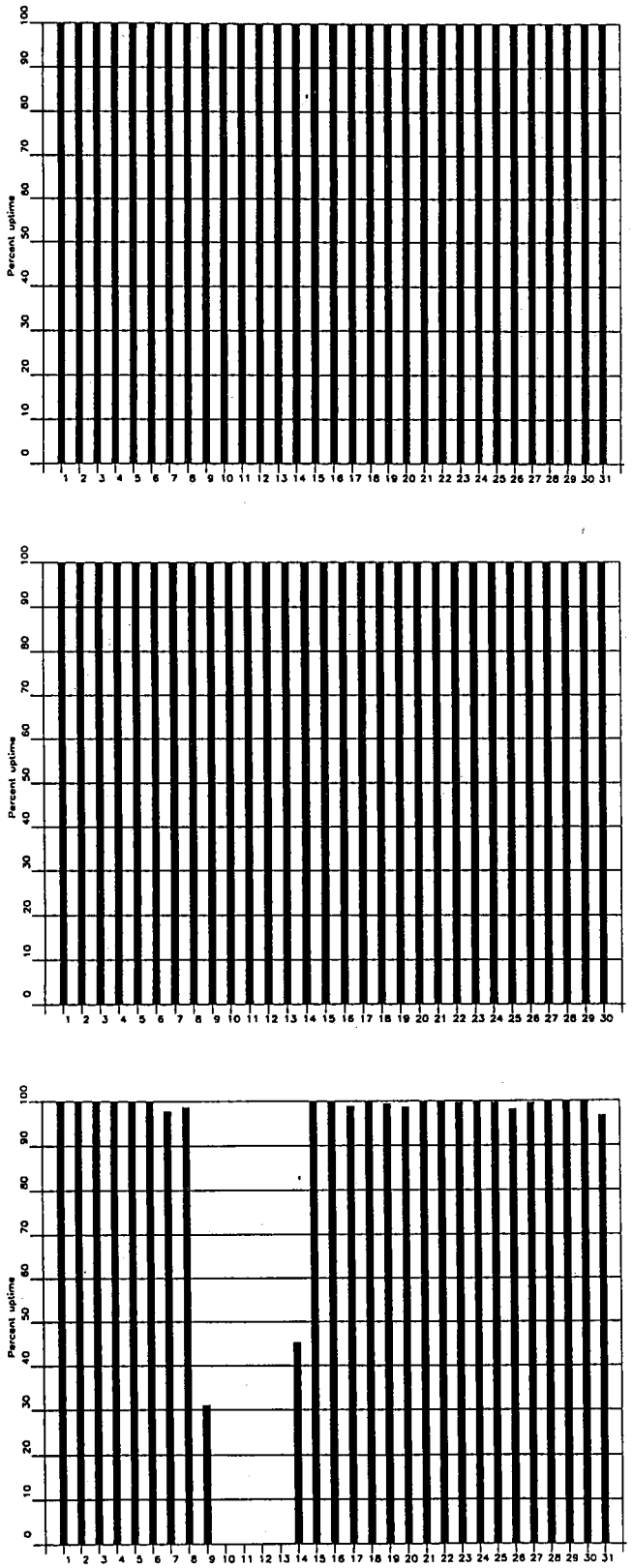

Fig. 3.1.1. NORESS data recording uptime for October (top), November (middle) and December (bottom) 1993.

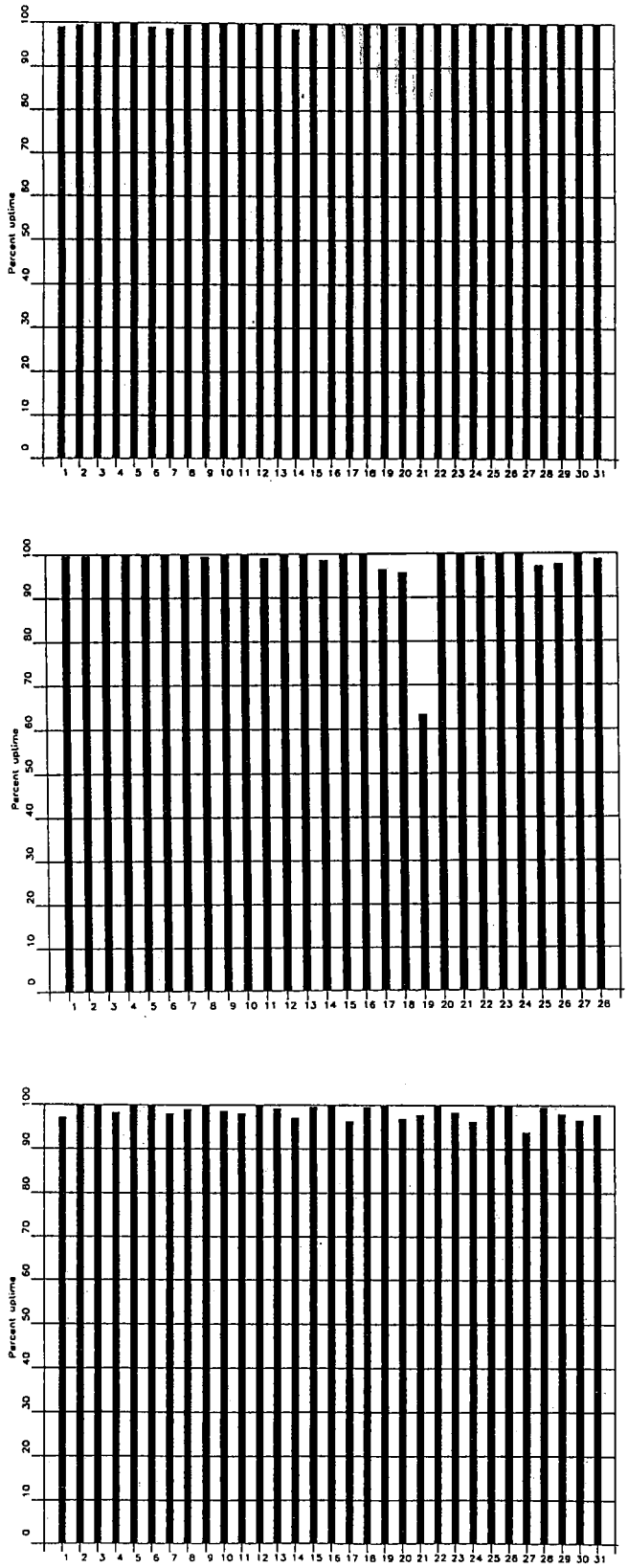

Fig. 3.1.1. (cont.) NORESS data recording uptime for January (top), February (middle) and March (bottom) 1994.

3.2 Recording of ARCESS data at NDPC, Kjeller

Table 3.2.1 lists the main outage times and reasons.

The average recording time was 99.28% as compared to 99.19% for the previous reporting period.

Date	Time	Cause
14 Oct	1159 - 1230	Transmission line failure
14 Oct	1401 - 1539	Transmission line failure
27 Oct	1700 -	Hardware failure NDPC
28 Oct	- 0655	
05 Nov	0145 - 0504	Power failure array site
16 Nov	2334 -	Hardware failure NDPC
17 Nov	- 0030	
24 Nov	1456 - 1522	Hardware failure NDPC
24 Nov	2051 - 2147	Hardware failure NDPC
25 Nov	1230 - 1242	Hardware failure NDPC
01 Dec	1150 - 1220	Satellite link failure
31 Dec	2311 - 0000	Software work

Table 3.2.1. The main interruptions in recording of ARCESS data at NDPC, 1 October 1993 - 31 March 1994.

Monthly uptimes for the ARCESS on-line data recording task, taking into account all factors (field installations, transmissions line, data center operation) affecting this task were as follows:

October 93	:	97.72%
November	:	99.19%
December	:	99.79%
January 94	:	100.00%
February	:	99.95%
March	:	100.00%

Fig. 3.2.1. shows the uptime for the data recording task, or equivalently, the availability of ARCESS data in our tape archive, on a day-by-day basis, for the reporting period.

J. Torstveit

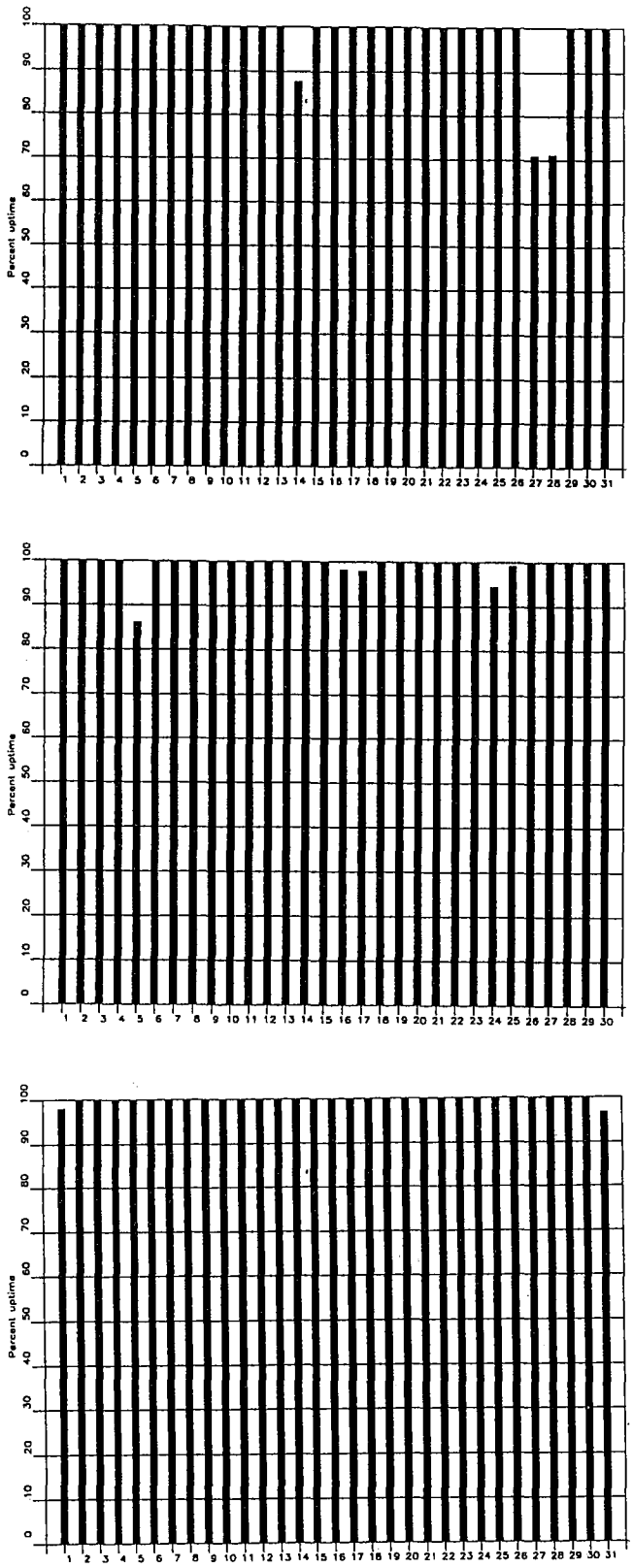

Fig. 3.2.1. ARCESS data recording uptime for October (top), November (middle) and December (bottom) 1993.

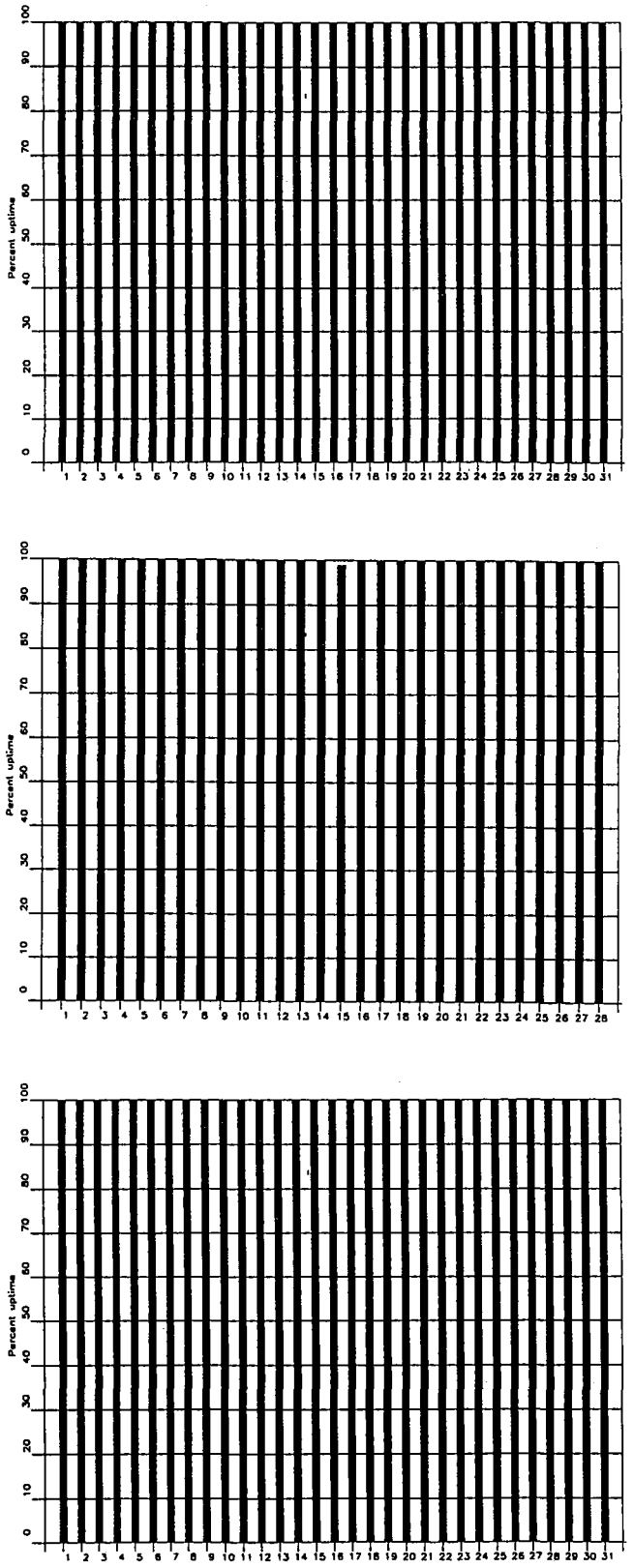

Fig. 3.2.1. ARCESS data recording uptime for January (top), February (middle) and March (bottom) 1994.

3.3 Recording of FINESS data at NDPC, Kjeller

Recording at NDPC started on 26 November when the field system came back into operation after upgrading.

Date	Time	Cause
26 Nov	- 1000	Field system upgrade
27 Nov	2247 -	Hardware failure NDPC
29 Nov	- 0401	
29 Nov	1145 - 1311	Hardware failure NDPC
10 Dec	0712 - 0828	Software work NDPC
10 Dec	0840 - 1353	Software work NDPC
03 Jan	1157 - 1251	Problems in Helsinki
07 Jan	0930 - 1157	Problems in Helsinki
08 Jan	0911 - 1137	Problems in Helsinki
09 Jan	0230 -	Problems in Helsinki
10 Jan	- 0751	
11 Jan	0634 - 0652	Problems in Helsinki
17 Jan	1614 - 1627	Transmission line failure
14 Feb	1721 -	Transmission line failure
15 Feb	- 0839	
16 Feb	0808 - 1218	Problems in Helsinki
25 Feb	0605 -	Problems in Helsinki
28 Feb	- 0704	
14 Mar	0748 - 0856	Software work in Helsinki
22 Mar	2001 - 2350	Power failure in Helsinki

Table 3.3.1. The main interruptions in recording of FINESS data at NDPC, 26 November 1993 - 31 March 1994.

Monthly uptimes for the FINESS on-line data recording task, taking into account all factors (field installations, transmission lines, data center operation) affecting this task were as follows:

October 93	:	0.00%
November	:	11.02%
December	:	99.13%
January 94	:	95.12%
February	:	86.32%
March	:	99.33%

Fig. 3.3.1 shows the uptime for the data recording task, or equivalently, the availability of FINESS data in our tape archive, on a day-by-day basis, for the reporting period.

J. Torstveit

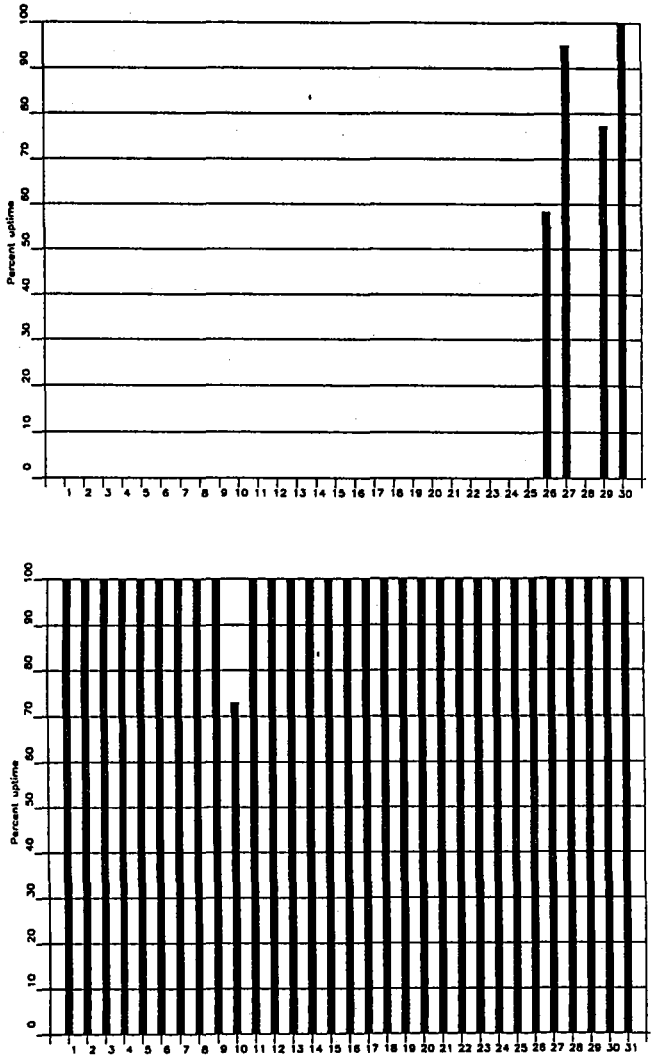

Fig. 3.3.1. FINESS data recording uptime for November (top) and December (bottom) 1993.

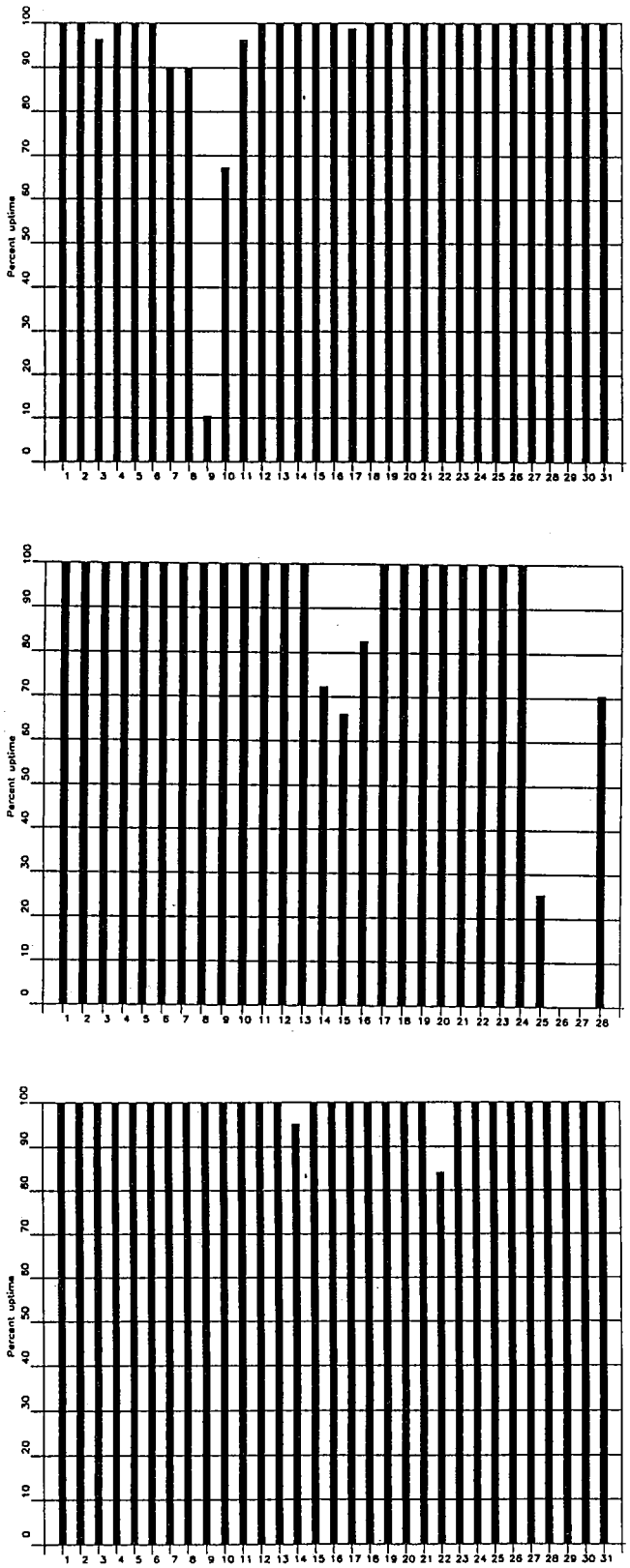

Fig. 3.3.1. FINESS data recording uptime for January (top), February (middle) and March (bottom) 1994.

3.4 Recording of Spitsbergen data at NDPC, Kjeller

The average recording time was 88.39%.

The main reasons for downtime follow:

Date	Time	Cause
14 Oct	1035 - 1133	Communication line failure
14 Oct	1147 - 1155	Communication line failure
01 Nov	1439 - 2107	Hardware failure NDPC
04 Nov	0227 - 0329	Communication line failure
16 Nov	0846 - 0910	Communication line failure
26 Nov	0119 - 0208	Hardware failure NDPC
14 Dec	1622 - 1637	Communication line failure
19 Dec	1700 - 1800	Communication line failure
20 Dec	2139 -	Communication line failure
21 Dec	- 0016	
26 Dec	1732 - 1822	Communication line failure
12 Jan	1803 - 1851	Communication line failure
15 Jan	1758 - 1824	Communication line failure
17 Jan	0853 -	Hardware failure Spitsbergen
04 Feb	- 1428	
05 Feb	1114 - 1307	Communication line failure
12 Feb	2348 -	Communication line failure
13 Feb	- 0938	
13 Feb	1558 -	Communication line failure
14 Feb	- 1959	
15 Feb	1506 - 1544	Communication line failure
16 Feb	1108 - 1205	Communication line failure
25 Feb	1213 - 1259	Communication line failure
26 Feb	1211 - 1235	Communication line failure
27 Feb	0518 - 0604	Communication line failure
27 Feb	1210 - 1225	Communication line failure
28 Feb	1211 - 1239	Communication line failure
01 Mar	1216 - 1309	Communication line failure

Monthly uptimes for the Spitsbergen online data recording task, taking into account all factors (field installations, transmission line, data center operation) affecting this task were as follows:

October 93	:	99.62%
November	:	98.67%
December	:	99.22%
January 94	:	52.63%

February	:	80.42%
March	:	99.78%

Fig. 3.4.1 shows the uptime for the data recording task, or equivalently, the availability of Spitsbergen data in our tape archive, on a day-by-day basis for the reporting period.

J. Torstveit

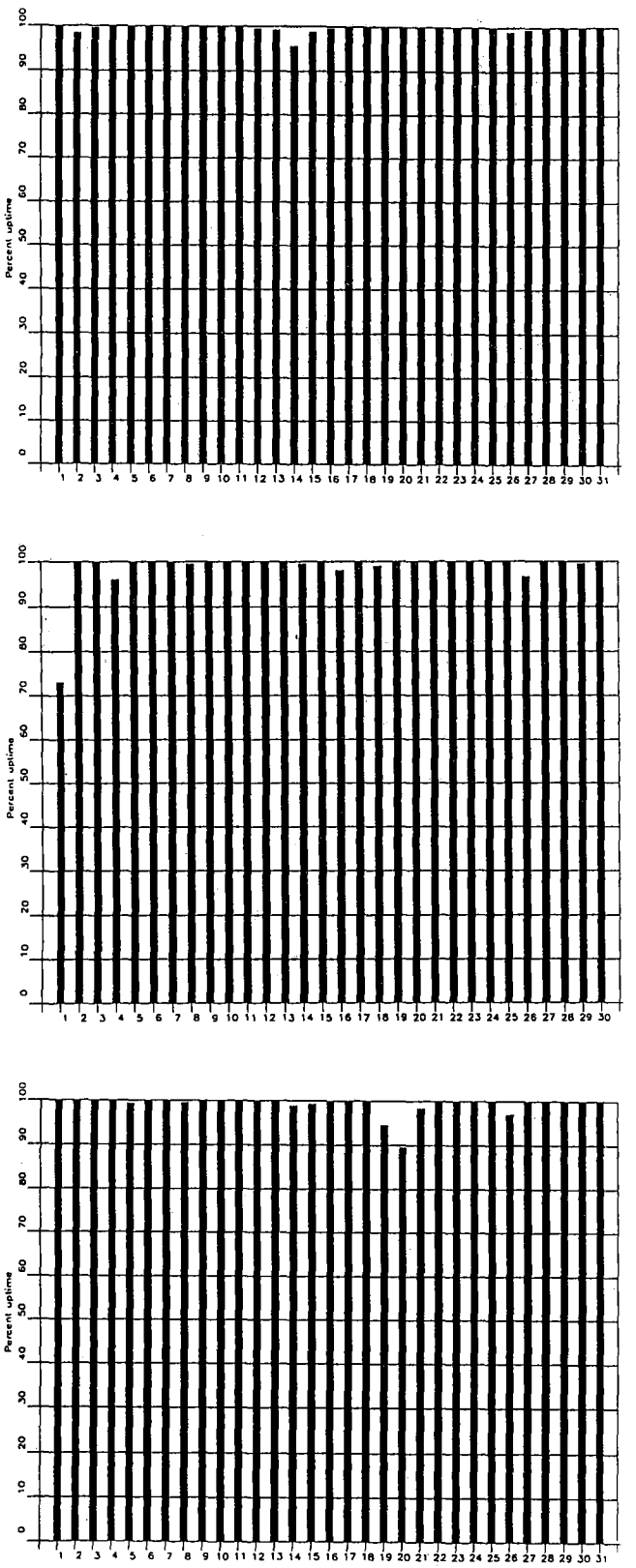

Fig. 3.4.1. Spitsbergen data recording uptime for October (top), November (middle) and December (bottom) 1993.

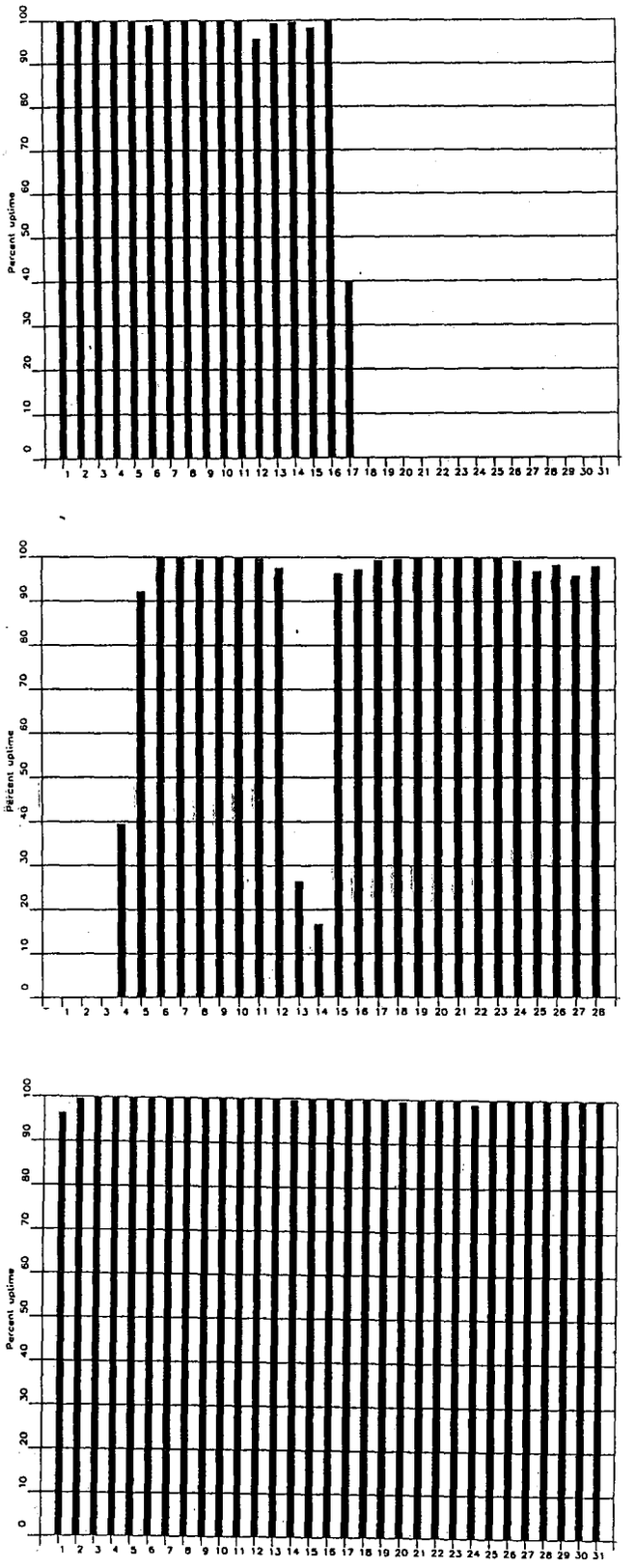

Fig. 3.4.1. Spitsbergen data recording uptime for January (top), February (middle) and March (bottom) 1994.

3.5 Event detection operation

This section reports results from one-array automatic processing using signal processing recipes and "ronapp" recipes for the ep program (NORSAR Sci. Rep. No 2-88/89).

Three systems are in parallel operation to associate detected phases and locate events:

1. The ep program with "ronapp" recipes is operated independently on each array to obtain simple one-array automatic solutions.
2. The Generalized Beamforming method (GBF) (see F. Ringdal and T. Kværna (1989), A mulitchannel processing approach to real time network detection, phase association and threshold monitoring, BSSA Vol 79, no 6, 1927-1940) processes the four arrays jointly and presents locations of regional events.
3. The IMS system is operated on the same set of arrivals as ep and GBF and reports also teleseismic events in addition to regional ones.

IMS results are reported in section 3.6.

In addition to these three event association processes, we are running test versions of the so-called Threshold Monitoring (TM) process. This is a process that monitors the seismic amplitude level at the four regional arrays continuously in time to estimate the upper magnitude limit of an event that might go undetected by the network. The current TM process is beamed to several sites of interest, including the Novaya Zemlya test site. Simple displays of so-called threshold curves reveal instants of particular interest; i.e., instants when events above a certain magnitude threshold may have occurred in the target region. Results from the three processes described above are used to help resolve what actually happened during these instances.

NORESS detections

The number of detections (phases) reported from day 274, 1993, through day 090, 1994, was 31,321, giving an average of 172 detections per processed day (182 days processed).

Table 3.5.1 shows daily and hourly distribution of detections for NORESS.

Events automatically located by NORESS

During days 274, 1993, through 090, 1994, 1919 local and regional events were located by NORESS, based on automatic association of P- and S-type arrivals. This gives an average of 10.5 events per processed day (182 days processed). 65% of these events are within 300 km, and 88% of these events are within 1000 km.

ARCESS detections

The number of detections (phases) reported during day 274, 1993, through day 090, 1994, was 71,665, giving an average of 394 detections per processed day (182 days processed).

Table 3.5.2 shows daily and hourly distribution of detections for ARCESS.

Events automatically located by ARCESS

During days 274, 1993, through 090, 1994, 3338 local and regional events were located by ARCESS, based on automatic association of P- and S-type arrivals. This gives an average 18.3 events per processed day (182 days processed). 52% of these events are within 300 km, and 85% of these events are within 1000 km.

FINESS detections

The number of detections (phases) reported during day 274, 1993, through day 090, 1994, was 39,944, giving an average of 307 detections per processed day (130 days processed).

Table 3.5.3 shows daily and hourly distribution of detections for FINESS.

Events automatically located by FINESS

During days 274, 1993, through 090, 1994, 1734 local and regional events were located by FINESS, based on automatic association of P- and S-type arrivals. This gives an average of 13.3 events per processed day (130 days processed). 77% of these events are within 300 km, and 89% of these events are within 1000 km.

GERESS detections

The number of detections (phases) reported from day 274, 1993, through day 090, 1994, was 31,409, giving an average of 173 detections per processed day (182 days processed).

Table 3.5.4 shows daily and hourly distribution of detections for GERESS.

Events automatically located by GERESS

During days 274, 1993, through 090, 1994, 2984 local and regional events were located by GERESS, based on automatic association of P- and S-type arrivals. This gives an average of 16.4 events per processed day (182 days processed). 71% of these events are within 300 km, and 90% of these events are within 1000 km.

Apatity array detections

The number of detections (phases) reported from day 274, 1993, through day 090, 1994, was 71,476, giving an average of 516 detections per processed day (139 days processed).

As described in earlier reports, the data from the Apatity array are transferred by one-way (simplex) radio links to Apatity city. The transmission suffers from radio disturbances that

result in a large number of small data gaps and spikes in the data. Although the communication protocol may correct such errors by requesting retransmission of data, this cannot be done at Apatity. For such error corrections, a two-way radio link is needed (duplex radio). However, it should be noted that noise from cultural activities and from the nearby lakes cause most of the unwanted detections. These unwanted detections are "filtered" in the signal processing, as they give seismic velocities that are outside accepted limits for regional and teleseismic phase velocities.

Table 3.5.5 shows daily and hourly distribution of detections for the Apatity array.

Events automatically located by the Apatity array

During days 274, 1993, through 090, 1994, 1808 local and regional events were located by the Apatity array, based on automatic association of P- and S-type arrivals. This gives an average of 13.0 events per processed day (139 days processed). 34 % of these events are within 300 km, and 69% of these events are within 1000 km.

Spitsbergen array detections

The number of detections (phases) reported from day 274, 1993, through day 090, 1994, was 21,392, giving an average of 130 detections per processed day (165 days processed).

Table 3.5.6 shows daily and hourly distribution of detections for the Spitsbergen array.

Events automatically located by the Spitsbergen array

During days 274, 1993, through 090, 1994, 1284 local and regional events were located by the Spitsbergen array, based on automatic association of P- and S-type arrivals. This gives an average of 7.8 events per processed day (165 days processed). 67 % of these events are within 300 km, and 82% of these events are within 1000 km.

U. Baadshaug

NRS .FKX Hourly distribution of detections

Day	00	01	02	03	04	05	06	07	08	09	10	11	12	13	14	15	16	17	18	19	20	21	22	23	Sum	Date
274	4	7	5	1	15	4	8	3	3	7	3	7	9	18	8	6	9	8	2	7	12	7	7	1	161	Oct 01 Friday
275	2	6	2	12	8	2	10	2	14	27	13	7	23	9	4	4	6	14	3	5	6	3	5	6	193	Oct 02 Saturday
276	3	2	6	9	3	6	8	8	8	6	3	4	6	5	10	1	8	8	5	6	1	2	5	7	130	Oct 03 Sunday
277	5	5	0	5	3	3	4	3	1	1	7	4	5	13	4	7	16	4	5	2	19	2	0	5	123	Oct 04 Monday
278	8	0	10	4	5	10	2	2	6	6	7	9	6	5	16	2	7	4	6	7	2	9	2	1	136	Oct 05 Tuesday
279	3	3	2	2	2	4	4	6	3	14	4	10	11	6	18	10	9	8	1	5	1	2	1	11	140	Oct 06 Wednesday
280	3	0	3	7	8	3	0	1	2	4	26	6	15	19	23	33	30	27	22	7	4	16	10	11	280	Oct 07 Thursday
281	20	11	17	23	31	30	15	9	5	6	7	9	15	10	8	10	6	8	9	3	4	0	1	8	265	Oct 08 Friday
282	1	16	1	3	4	5	1	6	4	10	8	9	14	18	13	10	11	10	11	5	3	9	5	3	180	Oct 09 Saturday
283	3	2	0	2	3	1	1	5	3	7	9	21	27	26	33	29	30	45	41	30	22	15	15	18	388	Oct 10 Sunday
284	15	18	14	14	13	15	5	2	7	7	13	9	10	15	27	7	13	5	12	15	13	8	7	11	275	Oct 11 Monday
285	12	6	14	15	11	9	2	3	8	2	14	5	13	14	10	9	4	7	10	7	11	9	8	3	206	Oct 12 Tuesday
286	0	3	9	7	3	8	4	2	2	9	8	7	10	14	9	12	7	3	10	8	6	10	11	11	173	Oct 13 Wednesday
287	7	8	11	4	6	3	3	5	1	7	7	8	6	6	8	4	26	9	5	4	13	5	8	9	173	Oct 14 Thursday
288	15	17	17	4	8	16	4	1	5	4	3	13	11	12	23	8	1	4	4	3	5	15	5	0	198	Oct 15 Friday
289	2	0	4	6	1	4	5	5	1	4	4	8	5	7	1	4	13	6	8	2	15	11	0	1	117	Oct 16 Saturday
290	9	7	4	7	1	5	7	3	6	8	3	5	7	8	5	6	2	0	40	3	6	10	3	2	157	Oct 17 Sunday
291	2	3	2	1	3	5	1	1	1	2	2	7	9	4	14	6	14	6	25	2	3	8	5	1	127	Oct 18 Monday
292	4	0	1	2	7	6	2	0	0	4	6	7	7	13	12	8	9	4	2	8	0	6	8	3	119	Oct 19 Tuesday
293	1	2	0	2	0	6	2	5	4	11	6	22	15	9	16	5	3	4	0	8	2	3	5	2	133	Oct 20 Wednesday
294	4	1	2	2	1	5	6	3	8	7	6	12	20	10	26	9	9	11	5	4	5	8	4	4	172	Oct 21 Thursday
295	1	5	0	1	1	5	5	4	4	3	9	8	10	10	4	14	7	3	4	4	3	8	2	14	129	Oct 22 Friday
296	2	2	2	11	7	6	7	13	2	3	6	4	9	3	5	6	5	5	9	4	1	4	9	9	134	Oct 23 Saturday
297	5	7	2	6	6	10	12	7	10	1	2	2	1	6	4	9	4	2	5	1	0	2	5	6	115	Oct 24 Sunday
298	5	6	4	2	3	4	7	1	3	1	11	10	12	6	11	2	2	0	5	4	5	3	4	4	115	Oct 25 Monday
299	2	4	2	3	7	2	0	6	0	3	4	16	2	2	14	2	2	1	0	6	6	7	8	0	99	Oct 26 Tuesday
300	2	1	2	6	4	3	14	1	12	3	7	7	8	6	19	15	3	2	4	11	1	16	0	0	147	Oct 27 Wednesday
301	2	3	5	2	5	2	9	2	10	9	6	2	3	17	9	19	6	0	0	5	0	13	3	5	137	Oct 28 Thursday
302	5	6	7	5	9	2	2	13	8	11	7	36	4	14	8	9	2	6	4	7	4	21	6	17	213	Oct 29 Friday
303	6	6	5	5	4	5	8	6	6	12	4	2	16	0	5	8	3	17	17	5	9	12	7	11	179	Oct 30 Saturday
304	12	12	6	22	16	17	9	5	4	0	1	3	5	11	10	9	9	18	6	7	8	5	4	3	202	Oct 31 Sunday
305	19	5	3	4	5	2	7	0	1	3	6	3	15	4	14	11	1	3	7	18	12	3	5	2	153	Nov 01 Monday
306	6	10	23	14	16	20	3	10	6	9	10	8	7	18	8	3	4	14	14	16	19	4	1	2	245	Nov 02 Tuesday
307	4	10	1	5	9	4	3	0	9	3	15	17	24	7	15	5	5	4	16	8	5	17	21	24	231	Nov 03 Wednesday
308	43	26	40	41	43	48	33	7	8	9	12	23	17	22	31	17	4	1	5	2	10	1	6	20	469	Nov 04 Thursday
309	6	2	7	8	3	2	2	7	2	10	7	5	11	9	5	10	1	4	5	4	8	2	14	0	134	Nov 05 Friday
310	3	1	3	3	6	5	10	3	1	3	3	7	10	0	19	2	1	6	6	5	2	5	2	11	117	Nov 06 Saturday
311	5	5	2	5	1	5	4	3	13	2	6	6	8	16	5	6	5	8	13	5	5	8	5	14	155	Nov 07 Sunday
312	10	6	8	5	4	4	5	3	0	4	3	5	2	9	11	4	3	4	0	5	9	9	2	2	117	Nov 08 Monday
313	1	6	10	7	6	6	1	1	5	6	6	5	9	13	24	4	0	2	3	7	9	1	6	1	139	Nov 09 Tuesday
314	14	6	5	7	5	4	1	5	1	1	3	12	18	5	14	3	2	6	1	3	4	6	7	12	145	Nov 10 Wednesday
315	12	23	9	15	14	5	4	6	5	5	11	8	11	7	14	10	6	7	1	2	2	15	5	11	208	Nov 11 Thursday
316	7	5	6	4	6	7	3	1	12	10	11	17	15	16	11	14	2	1	1	5	2	13	3	4	176	Nov 12 Friday
317	7	10	2	7	9	6	10	8	4	8	8	12	10	8	4	10	13	3	3	4	7	8	8	10	179	Nov 13 Saturday
318	3	4	10	4	5	6	7	9	9	11	3	9	7	5	5	5	1	2	5	1	4	6	5	0	126	Nov 14 Sunday
319	3	3	9	5	3	7	6	1	2	3	3	6	5	6	11	21	6	7	6	1	11	4	9	9	147	Nov 15 Monday
320	3	9	3	6	7	3	2	1	5	2	2	6	15	27	12	24	6	8	3	4	4	7	1	3	163	Nov 16 Tuesday
321	7	3	4	9	7	6	5	9	3	1	5	20	12	20	9	13	17	4	6	6	4	4	10	2	186	Nov 17 Wednesday
322	3	7	13	5	4	8	2	18	9	20	2	1	9	8	7	7	8	9	6	11	5	19	12	5	198	Nov 18 Thursday
323	20	18	14	13	19	13	8	1	5	8	5	11	3	8	10	6	3	0	1	6	4	15	6	4	201	Nov 19 Friday
324	3	6	3	9	1	4	9	6	7	17	18	14	23	14	13	7	6	8	6	12	4	7	4	3	204	Nov 20 Saturday
325	8	14	9	10	20	10	3	18	8	13	16	6	8	1	4	5	2	10	4	8	2	4	1	3	187	Nov 21 Sunday
326	2	4	2	8	11	4	1	4	5	2	6	7	4	7	11	3	1	2	7	2	4	4	16	5	122	Nov 22 Monday
327	1	1	3	3	2	7	7	5	6	5	2	7	4	12	14	7	7	3	2	3	5	7	2	2	117	Nov 23 Tuesday
328	2	2	7	0	2	6	3	1	2	3	3	6	11	11	7	6	1	2	0	3	5	3	2	6	94	Nov 24 Wednesday
329	2	4	5	1	3	5	2	5	6	3	1	3	3	19	16	4	5	10	4	7	2	9	4	2	125	Nov 25 Thursday

Table 3.5.1. (Page 1 of 4)

NRS .FKX Hourly distribution of detections

Day	00	01	02	03	04	05	06	07	08	09	10	11	12	13	14	15	16	17	18	19	20	21	22	23	Sum	Date
330	2	1	1	5	12	9	1	1	2	6	4	9	4	13	2	3	6	6	3	6	6	15	7	2	126	Nov 26 Friday
331	9	8	2	9	3	5	20	3	2	2	10	6	2	4	9	2	5	8	9	6	3	7	6	9	149	Nov 27 Saturday
332	3	7	4	9	8	9	9	8	6	5	10	9	8	13	23	20	19	22	5	8	1	5	5	3	219	Nov 28 Sunday
333	4	2	2	1	3	4	2	9	0	7	9	5	5	16	7	5	8	3	4	3	6	3	12	0	120	Nov 29 Monday
334	4	4	2	7	6	6	0	3	4	16	3	6	4	15	20	8	12	4	6	5	8	14	5	4	166	Nov 30 Tuesday
335	2	7	5	4	0	4	2	2	3	6	13	4	18	11	13	3	5	4	4	1	5	11	5	12	144	Dec 01 Wednesday
336	1	1	1	6	2	4	1	1	1	3	5	4	22	19	18	1	11	2	6	3	4	1	12	9	138	Dec 02 Thursday
337	1	3	3	4	5	8	5	1	5	3	7	15	20	8	5	2	3	2	5	4	1	5	1	13	129	Dec 03 Friday
338	2	6	3	2	1	5	13	2	11	7	5	5	10	8	3	7	3	0	1	2	5	5	4	8	118	Dec 04 Saturday
339	9	10	9	2	2	1	10	6	4	7	2	3	4	7	3	7	9	18	9	13	18	17	11	31	212	Dec 05 Sunday
340	20	25	29	13	17	19	7	6	2	3	3	5	7	22	13	8	7	3	5	1	2	6	9	3	235	Dec 06 Monday
341	3	1	5	7	7	3	2	1	7	5	10	10	10	12	12	5	23	2	6	3	3	11	2	2	152	Dec 07 Tuesday
342	3	4	9	1	2	10	4	7	4	15	7	18	34	12	14	11	8	5	2	4	7	7	7	9	204	Dec 08 Wednesday
343	10	23	27	26	26	25	8	15	12	20	11	24	15	23	38	48	61	35	31	26	9	10	16	17	556	Dec 09 Thursday
344	51	66	0	0	0	0	0	0	0	2	14	11	13	10	0	0	0	5	4	5	6	15	2	3	207	Dec 10 Friday
345	8	4	8	3	3	4	11	5	4	2	3	7	10	8	11	11	5	4	2	3	7	4	3	3	133	Dec 11 Saturday
346	7	7	7	1	7	13	7	2	7	5	8	11	8	6	10	13	5	9	12	11	14	22	21	28	241	Dec 12 Sunday
347	29	17	22	16	29	24	11	7	0	0	0	0	0	0	0	0	0	0	0	0	0	0	0	0	155	Dec 13 Monday
348	0	0	0	0	0	0	0	0	0	0	0	0	0	19	16	8	4	16	3	5	9	14	6	9	109	Dec 14 Tuesday
349	6	9	3	3	5	2	2	1	8	4	14	2	11	11	25	26	5	5	2	1	7	1	7	4	164	Dec 15 Wednesday
350	8	3	4	11	1	9	1	4	2	9	7	14	21	17	8	8	0	4	6	4	4	3	17	1	166	Dec 16 Thursday
351	9	7	6	8	2	7	2	3	2	3	5	9	11	16	21	16	16	17	17	14	14	20	22	22	269	Dec 17 Friday
352	16	18	15	18	20	14	15	3	12	9	7	9	18	9	10	11	10	12	9	4	8	4	5	11	267	Dec 18 Saturday
353	5	6	10	1	4	2	2	2	7	2	7	9	7	7	2	3	4	0	6	3	5	3	1	5	103	Dec 19 Sunday
354	4	3	1	3	2	3	6	12	5	1	4	7	6	5	16	5	7	3	7	6	7	11	20	14	158	Dec 20 Monday
355	11	6	0	8	3	2	2	1	2	10	9	3	5	18	17	18	17	28	14	17	13	30	7	14	255	Dec 21 Tuesday
356	3	17	49	27	24	9	7	9	20	19	11	20	21	33	21	32	16	31	23	38	23	24	29	30	536	Dec 22 Wednesday
357	22	22	54	50	73	69	54	44	43	34	16	12	9	6	12	5	14	12	10	3	9	10	14	7	604	Dec 23 Thursday
358	13	9	13	7	7	18	7	4	6	12	7	10	12	7	4	2	4	6	4	2	1	8	4	4	171	Dec 24 Friday
359	1	4	3	7	4	1	6	4	3	2	16	6	9	1	10	8	6	3	0	4	3	11	1	6	119	Dec 25 Saturday
360	4	5	1	1	2	0	3	3	7	8	10	7	12	17	22	15	5	10	11	16	28	25	25	35	272	Dec 26 Sunday
361	31	27	30	35	28	34	24	30	11	9	12	11	15	11	20	45	59	57	46	38	46	44	47	29	739	Dec 27 Monday
362	41	45	41	24	24	17	14	13	17	5	12	10	17	12	1	4	9	2	10	4	13	7	3	7	352	Dec 28 Tuesday
363	5	12	5	5	3	14	7	3	24	7	10	4	10	17	9	14	5	8	8	19	11	6	7	7	220	Dec 29 Wednesday
364	8	3	4	7	2	1	9	2	4	6	19	12	18	12	15	8	7	11	4	5	15	2	2	7	183	Dec 30 Thursday
365	2	0	5	7	3	8	3	7	11	10	9	16	7	10	14	5	1	4	5	5	7	1	1	1	142	Dec 31 Friday
1	1	3	6	4	1	7	2	4	6	2	6	6	3	1	1	5	7	10	7	12	2	6	7	7	116	Jan 01 Saturday
2	8	10	11	21	21	17	15	20	14	13	10	4	3	9	3	6	10	14	8	9	9	14	13	3	265	Jan 02 Sunday
3	2	8	1	13	7	2	8	2	4	8	5	11	11	13	16	12	8	6	15	14	18	15	25	5	229	Jan 03 Monday
4	3	2	5	3	11	2	6	3	11	12	10	12	11	12	22	15	15	18	29	29	21	20	22	12	306	Jan 04 Tuesday
5	12	11	13	7	4	18	5	5	6	5	6	8	10	17	13	3	1	7	3	0	3	10	1	7	175	Jan 05 Wednesday
6	3	8	4	8	6	3	3	6	8	8	9	13	16	11	2	11	9	4	1	5	6	4	12	6	166	Jan 06 Thursday
7	3	3	8	13	9	2	3	4	1	18	6	13	7	13	4	5	6	1	3	3	6	1	19	3	154	Jan 07 Friday
8	1	0	7	5	4	2	16	2	3	1	7	3	6	1	5	2	1	2	2	3	3	2	2	3	83	Jan 08 Saturday
9	1	0	0	2	3	4	2	3	1	1	8	3	8	8	13	4	8	5	2	0	2	7	7	7	99	Jan 09 Sunday
10	1	2	2	7	1	4	0	1	3	1	8	7	10	3	11	10	23	6	6	1	8	8	4	4	131	Jan 10 Monday
11	5	10	5	3	4	6	2	6	7	15	9	3	5	11	10	9	9	1	1	1	1	2	10	12	147	Jan 11 Tuesday
12	3	4	3	5	1	8	4	2	4	14	28	10	10	8	9	12	2	6	3	10	3	2	5	8	164	Jan 12 Wednesday
13	3	5	4	4	7	7	4	3	7	7	10	11	12	6	18	7	5	4	2	3	7	2	3	4	145	Jan 13 Thursday
14	7	1	0	3	3	3	5	0	4	5	6	5	17	10	5	5	0	4	2	5	2	8	2	5	107	Jan 14 Friday
15	7	2	2	3	12	2	10	6	4	3	1	4	7	5	12	6	4	9	6	2	3	4	7	6	127	Jan 15 Saturday
16	4	2	3	5	11	17	5	4	5	1	3	2	4	10	4	10	1	6	4	6	5	4	3	3	122	Jan 16 Sunday
17	8	9	5	5	3	5	2	5	2	5	2	3	12	11	14	7	6	1	6	7	15	13	4	11	161	Jan 17 Monday
18	4	2	5	3	2	9	7	3	2	1	4	5	12	7	12	15	8	9	2	1	7	0	4	6	130	Jan 18 Tuesday
19	1	6	11	7	6	9	2	4	5	3	6	9	9	14	16	8	10	7	1	0	1	13	1	0	149	Jan 19 Wednesday
20	5	5	0	0	2	0	5	2	3	5	2	8	5	13	14	5	5	3	0	1	3	0	2	12	100	Jan 20 Thursday

Table 3.5.1. (Page 2 of 4)

NRS .FKX Hourly distribution of detections

Day	00	01	02	03	04	05	06	07	08	09	10	11	12	13	14	15	16	17	18	19	20	21	22	23	Sum	Date
21	2	8	8	3	3	1	2	1	4	3	1	4	9	10	7	3	13	2	9	5	5	6	2	4	115	Jan 21 Friday
22	2	2	0	0	4	5	8	16	8	15	15	18	9	3	5	4	3	2	1	1	8	2	2	2	135	Jan 22 Saturday
23	3	3	8	3	5	3	3	3	4	1	5	0	3	5	1	3	3	6	5	1	1	7	0	3	79	Jan 23 Sunday
24	3	1	2	1	2	3	1	1	0	1	3	3	5	2	7	3	10	1	5	3	5	2	2	5	71	Jan 24 Monday
25	2	5	4	13	3	12	1	5	3	2	9	5	7	12	11	5	3	3	8	6	9	13	2	3	146	Jan 25 Tuesday
26	5	6	2	9	9	4	2	7	2	9	14	17	9	6	13	9	2	6	2	3	3	7	9	8	163	Jan 26 Wednesday
27	7	7	3	1	4	2	1	6	1	2	3	8	14	8	21	2	5	2	0	2	1	4	0	0	104	Jan 27 Thursday
28	0	10	2	1	1	1	1	4	4	3	4	6	8	3	7	11	3	12	2	4	4	9	0	0	100	Jan 28 Friday
29	3	6	2	3	7	9	5	0	4	7	4	14	5	10	3	5	2	5	8	8	3	9	9	5	136	Jan 29 Saturday
30	5	5	3	2	7	1	3	1	2	0	0	5	2	2	1	1	0	1	4	0	1	3	4	0	53	Jan 30 Sunday
31	2	2	1	3	1	2	1	1	6	3	1	6	7	15	6	4	6	4	1	3	2	0	2	3	82	Jan 31 Monday
32	0	9	2	2	3	5	5	1	10	22	15	14	5	11	9	2	6	3	2	0	9	2	5	4	146	Feb 01 Tuesday
33	1	5	5	6	3	1	2	4	3	3	0	3	6	11	8	7	13	7	3	2	2	5	12	9	121	Feb 02 Wednesday
34	3	3	3	4	2	1	0	2	1	14	9	16	18	9	17	5	4	4	16	4	14	2	6	1	158	Feb 03 Thursday
35	4	5	1	2	3	5	0	0	3	4	3	17	10	15	7	9	3	1	4	9	2	3	11	2	123	Feb 04 Friday
36	6	3	3	2	7	3	1	3	1	4	3	5	6	6	6	6	4	2	4	5	10	8	6	10	114	Feb 05 Saturday
37	12	3	8	6	3	7	9	5	1	5	4	7	3	3	1	7	3	0	7	2	3	4	2	1	106	Feb 06 Sunday
38	8	6	5	7	2	4	6	4	0	1	5	5	8	1	8	14	5	1	3	10	4	0	1	4	112	Feb 07 Monday
39	4	9	3	12	3	11	3	4	0	5	11	3	21	18	9	16	9	3	5	7	2	3	13	14	188	Feb 08 Tuesday
40	9	6	5	8	4	2	5	3	5	9	7	4	5	19	2	8	7	6	2	3	12	6	5	1	143	Feb 09 Wednesday
41	3	4	8	1	5	1	6	0	0	9	6	13	9	9	14	15	10	4	3	1	9	3	5	3	141	Feb 10 Thursday
42	11	4	3	6	3	2	0	5	5	1	3	8	12	7	6	4	3	5	7	6	6	13	4	4	128	Feb 11 Friday
43	7	4	3	6	10	0	3	11	8	2	8	8	11	7	5	4	6	8	11	4	2	7	2	2	139	Feb 12 Saturday
44	1	9	2	10	6	4	1	4	4	4	9	11	9	5	6	7	3	1	1	2	8	5	9	1	122	Feb 13 Sunday
45	4	7	3	3	4	4	6	2	1	3	5	14	12	3	8	6	9	10	4	11	3	2	7	4	135	Feb 14 Monday
46	3	8	12	3	1	3	6	5	1	4	14	8	7	16	6	13	10	7	6	5	12	14	16	13	193	Feb 15 Tuesday
47	12	10	15	3	13	2	5	9	5	10	8	16	2	5	11	3	15	4	6	8	12	9	7	6	196	Feb 16 Wednesday
48	5	11	7	6	4	3	2	2	1	5	2	17	5	11	6	13	1	7	8	9	17	11	10	9	172	Feb 17 Thursday
49	7	13	2	13	8	4	7	5	2	10	4	12	7	16	12	1	11	7	10	9	12	14	8	9	203	Feb 18 Friday
50	4	5	5	8	9	3	9	1	5	0	0	0	0	0	0	0	0	2	5	6	2	18	3	10	95	Feb 19 Saturday
51	5	11	12	21	7	5	8	6	8	3	7	7	2	5	14	2	1	1	7	2	9	4	6	6	159	Feb 20 Sunday
52	5	6	6	9	4	3	4	3	2	1	6	5	4	10	10	11	12	5	20	15	3	2	5	6	157	Feb 21 Monday
53	7	3	9	5	12	7	1	2	1	5	1	10	13	7	15	11	1	2	8	7	11	1	5	8	152	Feb 22 Tuesday
54	12	14	8	18	6	5	6	3	9	7	6	8	21	9	9	14	11	5	10	9	27	5	7	12	241	Feb 23 Wednesday
55	15	12	15	15	1	2	0	4	9	7	19	13	16	14	19	17	15	5	3	11	6	5	6	6	235	Feb 24 Thursday
56	3	11	6	7	2	5	8	6	3	4	18	12	14	12	11	4	5	3	3	14	19	3	4	12	189	Feb 25 Friday
57	1	4	21	25	2	3	4	4	3	6	10	10	23	19	9	11	22	4	6	2	11	10	9	18	237	Feb 26 Saturday
58	15	14	16	25	9	15	9	11	6	10	8	10	9	5	16	6	0	7	6	7	11	2	9	11	237	Feb 27 Sunday
59	7	1	20	4	4	5	6	3	3	11	9	10	10	13	18	4	10	11	5	6	3	7	4	9	183	Feb 28 Monday
60	11	4	2	4	10	13	8	2	3	5	9	9	10	10	13	10	9	9	7	7	4	4	1	5	169	Mar 01 Tuesday
61	4	14	15	16	16	18	12	9	2	5	12	17	11	15	3	15	11	9	1	8	4	8	8	4	237	Mar 02 Wednesday
62	2	3	5	4	4	4	2	7	9	6	5	6	6	19	21	19	21	8	1	5	6	2	10	8	183	Mar 03 Thursday
63	8	3	2	8	8	1	2	4	2	6	9	6	15	18	14	9	5	5	5	6	4	9	9	4	162	Mar 04 Friday
64	6	4	6	5	6	0	5	2	8	2	4	9	10	5	4	6	6	3	2	3	7	1	5	7	116	Mar 05 Saturday
65	4	5	5	8	1	1	3	1	5	2	6	2	2	7	8	3	3	7	0	5	1	3	2	4	88	Mar 06 Sunday
66	1	3	2	4	3	6	2	3	5	4	11	6	11	7	9	4	7	7	1	3	5	1	4	0	109	Mar 07 Monday
67	4	1	6	4	2	3	4	4	2	4	4	2	1	6	18	12	4	5	7	5	8	2	6	0	114	Mar 08 Tuesday
68	1	5	1	4	1	4	2	2	2	4	6	5	7	5	14	6	2	5	4	2	6	1	1	17	107	Mar 09 Wednesday
69	9	4	10	3	4	3	2	7	2	7	2	3	7	8	11	3	13	9	8	7	3	8	3	1	137	Mar 10 Thursday
70	2	5	4	6	7	1	5	3	9	1	5	13	8	11	5	3	4	1	2	6	10	1	1	3	116	Mar 11 Friday
71	5	4	6	3	3	1	2	8	2	6	6	7	3	4	8	5	1	13	2	1	6	1	7	7	111	Mar 12 Saturday
72	4	7	1	7	6	1	2	0	4	4	5	3	8	4	4	5	3	6	2	1	4	2	2	2	87	Mar 13 Sunday
73	3	5	7	5	15	4	11	4	2	3	6	2	9	10	8	5	17	8	1	3	5	17	21	22	193	Mar 14 Monday
74	3	5	3	4	5	3	6	2	3	0	8	11	9	2	3	4	6	5	12	29	18	13	14	5	173	Mar 15 Tuesday
75	4	7	11	12	4	4	10	8	4	21	4	10	13	14	15	6	12	1	2	3	2	7	9	12	195	Mar 16 Wednesday
76	10	7	8	4	3	9	4	1	6	12	6	8	4	6	7	11	3	4	2	4	1	3	4	4	131	Mar 17 Thursday

Table 3.5.1. (Page 3 of 4)

NRS .FKX Hourly distribution of detections

Day	00	01	02	03	04	05	06	07	08	09	10	11	12	13	14	15	16	17	18	19	20	21	22	23	Sum	Date
77	4	1	7	2	4	5	5	4	2	4	10	4	14	18	7	6	3	9	9	0	7	15	11	5	156	Mar 18 Friday
78	5	11	11	16	13	14	14	11	7	12	15	19	2	10	4	5	1	9	7	7	7	7	6	8	221	Mar 19 Saturday
79	5	4	11	12	13	14	4	8	12	10	8	5	7	5	1	3	1	15	8	2	13	10	8	4	183	Mar 20 Sunday
80	7	11	8	8	17	11	18	8	7	4	5	10	3	10	12	1	6	8	0	10	1	8	15	2	190	Mar 21 Monday
81	2	4	7	9	12	9	6	5	2	2	10	3	5	4	16	8	7	6	7	0	8	6	3	11	152	Mar 22 Tuesday
82	2	3	4	9	6	3	0	7	1	2	3	6	5	6	13	2	13	9	2	2	12	2	1	1	114	Mar 23 Wednesday
83	3	2	5	2	2	9	2	3	5	2	6	10	9	8	14	25	14	11	8	11	9	2	11	2	175	Mar 24 Thursday
84	3	0	1	7	2	5	3	1	3	13	11	9	8	10	6	6	4	1	10	14	10	15	1	5	148	Mar 25 Friday
85	3	1	3	9	5	7	5	7	5	4	7	9	2	6	9	12	3	4	8	11	4	5	5	4	138	Mar 26 Saturday
86	3	2	18	15	15	16	8	3	2	2	4	7	18	3	20	16	4	4	3	7	10	5	7	10	202	Mar 27 Sunday
87	6	17	18	14	10	8	1	4	7	4	4	3	16	12	0	7	7	6	9	8	2	7	3	7	180	Mar 28 Monday
88	3	2	6	1	3	2	3	2	10	5	5	9	6	10	2	5	1	3	11	3	10	5	1	8	116	Mar 29 Tuesday
89	1	1	0	1	0	4	2	3	0	9	2	3	12	11	7	8	3	6	2	14	7	5	3	6	110	Mar 30 Wednesday
90	2	4	10	4	2	4	6	3	2	4	20	2	16	1	8	5	5	2	9	3	5	5	8	6	136	Mar 31 Thursday
NRS	00	01	02	03	04	05	06	07	08	09	10	11	12	13	14	15	16	17	18	19	20	21	22	23		
Sum	1248	1136	1338	1284	1238	1255	867	1000	1136	916	1526	1305	1813	1759	1539	1947	1228	1351	1149	1179	1357	1273	1249	1228	31321	Total sum
182	6	7	7	7	7	7	5	5	5	6	7	8	10	10	11	8	7	7	6	6	7	7	7	7	172	Total average
129	7	7	8	7	7	7	5	4	5	6	7	9	10	11	12	9	8	6	6	7	7	8	7	7	178	Average workdays
53	5	6	6	8	6	6	7	6	6	6	7	7	8	7	8	7	6	7	7	5	6	7	6	7	157	Average weekends

Table 3.5.1. Daily and hourly distribution of NORESS detections. For each day is shown number of detections within each hour of the day, and number of detections for that day. The end statistics give total number of detections distributed for each hour and the total sum of detections during the period. The averages show number of processed days, hourly distribution and average per processed day.

ARC .FKX Hourly distribution of detections

Day	00	01	02	03	04	05	06	07	08	09	10	11	12	13	14	15	16	17	18	19	20	21	22	23	Sum	Date
274	9	11	9	6	13	4	13	28	29	20	8	20	33	67	20	16	16	14	9	5	11	7	8	19	395	Oct 01 Friday
275	4	4	3	19	17	4	17	12	13	29	22	20	23	6	16	9	9	15	8	11	5	6	14	22	308	Oct 02 Saturday
276	7	6	11	12	5	7	9	14	10	14	17	12	11	8	13	12	11	16	6	15	12	7	9	21	265	Oct 03 Sunday
277	7	6	5	3	12	4	14	17	21	21	21	17	29	25	7	27	24	13	7	28	17	8	8	17	358	Oct 04 Monday
278	11	4	11	6	9	10	8	10	9	14	6	9	7	10	14	5	5	4	3	8	11	13	5	11	203	Oct 05 Tuesday
279	3	7	11	7	6	6	4	6	1	8	14	12	22	15	19	19	5	9	25	11	11	4	7	23	255	Oct 06 Wednesday
280	12	5	11	26	27	23	13	9	21	12	15	19	29	27	21	43	61	93	75	71	74	91	96	107	981	Oct 07 Thursday
281	85	66	81	79	75	80	72	60	32	33	25	40	48	66	72	111	98	73	51	82	18	53	66	95	1561	Oct 08 Friday
282	52	16	7	13	25	7	11	15	31	27	34	31	44	13	10	7	4	7	10	19	8	10	9	26	436	Oct 09 Saturday
283	4	6	9	11	3	17	34	11	13	9	13	26	41	12	19	114	86	21	16	14	90	16	11	121	717	Oct 10 Sunday
284	102	67	86	48	23	13	19	18	13	31	5	10	12	51	102	154	111	82	42	23	37	24	30	91	1194	Oct 11 Monday
285	13	55	22	8	11	4	42	78	18	19	11	23	23	55	149	217	177	168	30	17	25	50	73	25	1313	Oct 12 Tuesday
286	28	52	30	41	37	35	20	17	14	10	12	15	33	17	18	34	17	23	15	17	13	2	3	16	519	Oct 13 Wednesday
287	15	3	7	4	3	7	6	10	3	4	2	3	7	44	0	2	7	7	8	8	8	8	6	18	190	Oct 14 Thursday
288	4	7	0	5	7	1	9	2	6	1	3	2	3	7	17	3	5	5	3	2	8	5	5	11	121	Oct 15 Friday
289	2	4	5	10	5	6	4	9	7	3	8	14	11	2	8	2	9	10	11	7	4	10	3	24	178	Oct 16 Saturday
290	5	6	6	6	8	9	20	14	10	10	10	9	19	37	21	25	18	20	8	11	6	6	4	19	307	Oct 17 Sunday
291	6	8	15	13	0	13	10	5	12	25	17	6	30	23	39	35	46	50	37	25	17	10	15	32	489	Oct 18 Monday
292	32	44	23	45	50	28	7	13	9	16	10	17	20	29	36	49	56	49	41	26	14	6	8	31	659	Oct 19 Tuesday
293	24	29	18	12	25	21	7	10	12	12	15	37	19	20	21	16	19	9	3	6	10	7	4	19	375	Oct 20 Wednesday
294	8	11	4	4	11	12	17	16	10	18	18	18	20	25	16	17	17	8	13	12	6	4	12	20	317	Oct 21 Thursday
295	20	4	11	8	7	10	8	10	5	8	15	13	28	8	6	12	14	10	4	5	10	5	7	26	254	Oct 22 Friday
296	10	5	4	5	6	4	10	15	14	12	29	8	11	9	17	43	63	20	10	4	7	6	7	24	343	Oct 23 Saturday
297	3	3	1	5	6	20	9	18	11	7	3	7	23	19	6	5	9	8	8	4	7	4	7	17	210	Oct 24 Sunday
298	6	9	5	2	6	4	7	5	1	12	20	12	16	22	15	7	20	7	8	9	10	11	8	23	245	Oct 25 Monday
299	10	6	9	5	8	9	15	24	31	31	18	25	34	38	34	43	24	21	18	8	7	10	8	23	459	Oct 26 Tuesday
300	13	1	10	8	4	13	8	20	4	10	15	24	19	9	24	19	10	3	0	0	0	0	0	0	214	Oct 27 Wednesday
301	0	0	0	0	0	0	0	5	2	3	5	4	3	4	2	2	4	0	1	0	3	3	1	9	51	Oct 28 Thursday
302	2	5	3	6	7	3	6	7	9	21	10	22	33	13	18	12	7	8	16	12	12	6	4	30	272	Oct 29 Friday
303	7	3	18	6	6	8	10	6	9	6	13	21	13	4	8	3	8	3	11	7	5	7	6	27	215	Oct 30 Saturday
304	6	3	5	6	8	8	8	5	6	1	5	7	3	4	4	4	2	14	9	5	3	2	3	15	136	Oct 31 Sunday
305	8	4	5	2	2	6	15	8	10	8	15	19	27	11	22	6	20	7	16	15	17	13	10	21	287	Nov 01 Monday
306	3	12	2	4	12	6	10	14	8	16	14	9	31	9	16	7	19	9	10	11	3	5	6	11	247	Nov 02 Tuesday
307	17	9	10	2	3	8	7	11	13	2	10	28	25	22	13	14	16	7	13	13	3	18	12	20	296	Nov 03 Wednesday
308	11	4	7	16	12	4	10	5	22	26	16	18	21	33	22	29	15	7	11	22	11	19	8	31	380	Nov 04 Thursday
309	7	2	0	0	0	10	10	29	17	34	30	26	28	27	47	24	20	18	11	15	4	14	10	23	406	Nov 05 Friday
310	15	4	8	2	13	4	12	8	6	19	22	25	17	11	21	13	8	5	6	17	21	15	22	27	321	Nov 06 Saturday
311	12	12	14	22	15	7	12	13	18	17	21	9	19	22	17	8	25	21	11	8	8	3	16	20	350	Nov 07 Sunday
312	7	17	10	9	12	7	11	7	10	15	12	16	25	18	12	9	9	18	9	8	20	7	9	4	281	Nov 08 Monday
313	5	22	11	13	9	9	18	9	12	13	6	8	7	7	15	10	10	9	18	11	6	6	12	20	266	Nov 09 Tuesday
314	13	20	7	7	9	5	12	2	11	10	11	12	29	14	22	16	17	11	8	8	14	8	14	29	309	Nov 10 Wednesday
315	17	11	3	6	9	6	17	14	14	10	24	39	26	27	37	19	30	19	21	9	10	20	5	23	416	Nov 11 Thursday
316	4	7	6	2	8	12	12	13	17	6	18	24	35	9	21	7	10	5	11	10	11	10	2	25	285	Nov 12 Friday
317	15	12	10	7	13	6	11	14	15	8	19	13	21	9	13	5	3	3	5	12	5	3	4	26	252	Nov 13 Saturday
318	7	6	22	3	3	3	5	8	9	9	8	11	7	9	9	10	9	11	9	5	5	10	7	28	213	Nov 14 Sunday
319	5	6	2	9	4	13	12	7	12	11	12	21	9	16	11	5	14	15	24	71	44	71	35	52	481	Nov 15 Monday
320	45	42	33	37	32	32	35	12	19	19	18	14	30	30	24	30	33	17	17	9	12	9	12	8	569	Nov 16 Tuesday
321	9	9	7	11	6	7	13	26	24	19	23	25	22	14	11	25	13	17	21	16	16	19	3	25	381	Nov 17 Wednesday
322	9	20	6	16	44	17	10	30	17	27	24	13	27	29	25	21	11	33	33	15	22	8	10	28	495	Nov 18 Thursday
323	10	20	11	16	14	4	5	25	23	20	21	16	17	17	17	9	6	9	3	11	23	10	16	18	341	Nov 19 Friday
324	14	21	23	26	42	46	32	26	16	14	13	15	11	13	10	13	13	17	41	15	9	9	7	27	473	Nov 20 Saturday
325	7	4	3	3	3	7	2	28	101	115	119	117	114	106	88	44	24	36	90	87	149	147	125	131	1650	Nov 21 Sunday
326	50	73	99	124	79	47	45	42	50	48	62	85	134	110	147	132	144	127	112	106	49	19	18	34	1936	Nov 22 Monday
327	6	2	8	10	15	18	25	37	46	68	72	68	88	76	78	77	122	132	134	84	73	84	86	106	1515	Nov 23 Tuesday
328	101	103	146	175	149	78	11	9	11	12	10	24	20	21	8	17	23	37	40	34	21	8	37	23	1118	Nov 24 Wednesday
329	6	20	21	9	6	3	16	8	15	16	17	38	14	19	24	34	26	16	6	39	17	13	14	18	415	Nov 25 Thursday

Table 3.5.2 (Page 1 of 4)

ARC .FKX Hourly distribution of detections

Day	00	01	02	03	04	05	06	07	08	09	10	11	12	13	14	15	16	17	18	19	20	21	22	23	Sum	Date
330	6	6	12	11	17	18	26	22	54	75	82	76	79	118	119	159	137	147	122	116	107	123	112	89	1833	Nov 26 Friday
331	115	70	74	68	62	14	43	37	45	53	62	46	52	18	11	7	10	11	8	19	2	13	15	24	879	Nov 27 Saturday
332	14	22	16	30	50	57	50	46	44	32	27	13	4	15	4	18	15	15	8	8	6	15	7	23	539	Nov 28 Sunday
333	7	13	6	4	10	24	20	42	29	21	50	53	41	45	45	35	30	10	5	13	8	6	5	25	547	Nov 29 Monday
334	10	4	7	5	3	5	5	7	5	11	7	14	17	17	9	15	16	9	7	5	14	8	8	16	224	Nov 30 Tuesday
335	11	11	9	8	9	4	12	13	16	22	17	13	19	48	34	57	83	71	99	84	26	24	16	30	736	Dec 01 Wednesday
336	19	15	8	12	8	4	4	6	8	18	14	32	20	11	10	12	13	9	15	10	8	11	11	27	305	Dec 02 Thursday
337	3	9	10	6	10	10	2	2	28	19	5	20	28	30	35	29	11	10	10	7	10	11	4	32	341	Dec 03 Friday
338	30	39	44	19	9	17	22	25	22	31	23	39	38	77	53	26	18	9	16	21	13	19	12	31	653	Dec 04 Saturday
339	8	14	5	7	4	4	14	20	20	7	27	6	15	29	12	12	19	8	17	29	18	10	25	18	348	Dec 05 Sunday
340	8	16	13	17	37	4	9	8	17	13	13	19	17	16	11	19	22	11	18	16	12	12	2	17	347	Dec 06 Monday
341	9	5	7	6	10	10	8	17	16	9	6	14	26	15	17	24	24	33	13	21	10	8	5	24	337	Dec 07 Tuesday
342	13	15	20	5	16	15	9	15	19	33	19	21	31	15	10	16	19	7	8	9	10	16	9	39	389	Dec 08 Wednesday
343	14	6	7	5	18	22	11	14	14	36	27	37	35	20	21	10	25	39	18	30	11	16	16	28	480	Dec 09 Thursday
344	1	10	16	6	20	13	12	15	7	23	25	26	43	33	11	11	11	18	31	9	10	7	8	22	388	Dec 10 Friday
345	11	5	6	8	7	13	7	12	10	13	10	9	10	7	16	11	4	7	17	11	7	8	8	37	254	Dec 11 Saturday
346	15	7	2	6	8	11	11	1	14	3	6	5	6	24	14	12	9	14	11	14	17	2	7	14	233	Dec 12 Sunday
347	7	6	4	6	18	17	8	5	9	9	14	18	25	30	32	38	48	56	56	59	66	54	48	53	686	Dec 13 Monday
348	31	23	14	17	4	10	9	20	10	13	19	12	20	9	18	15	13	8	4	12	9	9	9	18	326	Dec 14 Tuesday
349	14	3	5	10	8	7	13	12	11	9	32	23	32	33	41	31	39	37	38	42	52	35	53	42	622	Dec 15 Wednesday
350	37	25	24	17	16	20	8	10	10	10	10	15	18	11	8	11	8	16	5	23	14	7	3	22	348	Dec 16 Thursday
351	12	9	18	4	13	12	23	5	11	17	21	14	31	10	13	14	10	22	16	15	17	17	18	17	359	Dec 17 Friday
352	15	14	8	14	13	18	14	12	14	23	23	23	33	16	20	22	11	10	14	14	5	10	2	23	371	Dec 18 Saturday
353	8	5	7	2	4	7	2	12	8	6	9	17	9	9	5	9	11	6	15	14	14	15	5	25	224	Dec 19 Sunday
354	13	4	6	5	13	8	20	11	23	9	7	17	12	14	29	10	32	25	15	10	9	11	5	18	326	Dec 20 Monday
355	4	6	9	4	4	12	8	11	5	15	13	12	29	16	19	13	17	26	3	6	12	15	6	27	292	Dec 21 Tuesday
356	7	1	10	4	11	17	2	16	21	34	18	11	31	33	26	9	13	10	8	28	17	5	12	18	362	Dec 22 Wednesday
357	2	8	2	8	10	9	3	13	12	6	14	16	17	14	7	15	15	10	4	7	10	4	7	19	232	Dec 23 Thursday
358	7	11	3	12	2	10	15	6	14	10	22	6	19	14	22	4	8	12	10	6	2	14	9	24	262	Dec 24 Friday
359	12	18	15	21	21	21	34	14	24	21	34	19	17	11	18	6	15	6	6	16	12	16	9	29	415	Dec 25 Saturday
360	7	4	2	7	10	5	3	8	8	6	6	7	4	12	5	8	10	4	1	7	5	2	3	31	165	Dec 26 Sunday
361	4	0	2	7	2	17	2	15	2	9	13	13	20	13	12	15	16	9	6	15	6	16	10	26	250	Dec 27 Monday
362	12	9	1	12	11	12	8	10	12	9	11	13	17	13	10	10	12	13	7	11	7	12	9	17	258	Dec 28 Tuesday
363	3	3	4	5	7	5	7	18	32	29	12	21	29	29	32	35	36	31	31	43	22	13	4	30	481	Dec 29 Wednesday
364	6	3	5	5	4	8	13	5	10	12	38	26	31	16	18	13	18	6	11	10	16	9	4	21	308	Dec 30 Thursday
365	17	2	5	5	4	8	16	9	17	18	16	26	10	8	13	14	10	12	7	3	1	7	3	10	241	Dec 31 Friday
1	5	4	17	6	4	6	7	8	7	8	4	7	5	11	5	5	12	4	7	2	6	5	9	25	179	Jan 01 Saturday
2	8	7	11	3	9	6	9	14	15	17	21	13	23	16	23	14	18	15	13	9	14	6	11	24	319	Jan 02 Sunday
3	16	19	16	14	9	12	16	9	12	14	11	14	16	29	14	16	10	10	6	21	12	13	10	22	341	Jan 03 Monday
4	5	2	12	13	9	12	5	9	16	11	16	10	21	7	6	12	6	11	11	9	13	6	8	18	248	Jan 04 Tuesday
5	11	20	5	6	6	17	30	15	16	14	34	27	32	31	31	26	36	28	18	24	6	11	15	19	478	Jan 05 Wednesday
6	8	4	9	6	13	6	10	7	10	17	11	27	23	27	20	13	13	9	7	11	23	7	7	29	317	Jan 06 Thursday
7	10	7	10	5	8	5	10	17	5	6	13	21	9	12	15	11	5	8	11	21	9	8	6	21	253	Jan 07 Friday
8	5	0	9	10	11	7	10	9	4	7	13	11	17	8	14	12	6	16	4	25	10	11	10	10	239	Jan 08 Saturday
9	3	5	5	5	6	5	11	8	10	14	8	10	6	13	11	13	11	10	1	14	8	15	9	19	220	Jan 09 Sunday
10	5	9	2	7	6	4	8	5	9	10	15	11	12	3	8	9	37	15	11	8	9	13	5	29	250	Jan 10 Monday
11	8	12	10	8	4	13	3	11	8	8	9	12	12	15	3	21	15	9	7	18	9	3	7	29	254	Jan 11 Tuesday
12	12	4	0	2	4	4	11	8	7	9	30	20	23	22	8	7	7	9	8	10	6	8	11	31	261	Jan 12 Wednesday
13	10	10	11	4	4	9	10	7	16	16	15	15	31	20	14	10	26	17	11	13	27	12	8	28	344	Jan 13 Thursday
14	8	6	10	9	9	9	13	7	6	5	7	12	15	13	13	9	8	9	9	9	10	4	7	20	227	Jan 14 Friday
15	4	8	3	11	14	13	5	14	10	10	7	15	7	7	12	9	11	17	12	8	9	7	7	26	246	Jan 15 Saturday
16	5	6	3	5	6	6	5	11	8	6	4	8	8	12	17	13	6	12	5	14	14	4	11	18	207	Jan 16 Sunday
17	7	9	13	7	3	5	4	7	9	18	6	10	18	7	11	8	14	7	4	22	9	7	10	32	247	Jan 17 Monday
18	6	6	2	7	9	4	7	8	10	8	16	6	15	22	10	15	14	11	10	11	9	10	16	34	266	Jan 18 Tuesday
19	7	2	10	6	9	14	4	9	16	7	15	9	19	11	8	11	9	12	22	15	8	14	11	22	270	Jan 19 Wednesday
20	3	7	11	2	4	11	10	5	15	13	10	16	30	11	13	7	18	13	9	5	12	7	6	29	267	Jan 20 Thursday

Table 3.5.2. (Page 2 of 4)

ARC .FKX Hourly distribution of detections

Day	00	01	02	03	04	05	06	07	08	09	10	11	12	13	14	15	16	17	18	19	20	21	22	23	Sum	Date
21	7	9	14	14	6	3	9	1	14	11	9	8	19	10	24	9	9	8	10	10	3	11	7	27	252	Jan 21 Friday
22	7	9	5	1	7	7	8	3	1	10	4	24	5	9	9	11	7	6	8	3	12	5	6	21	168	Jan 22 Saturday
23	10	15	12	14	5	8	9	10	4	3	18	1	11	9	10	17	4	9	7	12	8	10	9	18	233	Jan 23 Sunday
24	4	3	4	1	11	10	10	7	6	14	10	10	10	12	4	16	12	15	26	6	13	4	8	15	231	Jan 24 Monday
25	8	7	6	6	12	25	11	18	21	10	12	18	18	20	14	9	9	9	12	11	14	8	10	20	308	Jan 25 Tuesday
26	2	4	8	5	11	9	5	9	9	8	19	16	32	12	19	13	6	16	12	11	9	14	13	24	286	Jan 26 Wednesday
27	16	7	9	12	9	11	6	6	17	6	15	34	25	8	7	5	7	11	11	11	7	9	7	26	282	Jan 27 Thursday
28	11	13	17	6	23	15	11	7	20	13	16	22	30	23	5	9	4	7	15	24	5	7	12	20	335	Jan 28 Friday
29	10	9	5	9	17	10	11	8	14	15	16	36	22	14	14	10	14	9	11	3	8	8	13	27	313	Jan 29 Saturday
30	9	5	8	5	19	6	8	7	10	8	6	17	6	13	4	11	10	8	6	7	14	14	26	16	243	Jan 30 Sunday
31	10	7	3	3	12	6	5	2	17	10	17	10	14	14	7	10	11	8	11	12	15	17	11	18	250	Jan 31 Monday
32	4	11	6	4	14	10	5	8	8	15	12	17	21	20	7	5	10	14	25	29	23	13	16	23	320	Feb 01 Tuesday
33	12	12	7	12	8	8	6	6	11	11	10	16	20	14	13	8	16	9	10	20	16	10	16	12	283	Feb 02 Wednesday
34	19	14	12	17	9	11	15	8	12	19	19	18	13	20	13	14	15	18	17	20	11	8	24	21	367	Feb 03 Thursday
35	14	6	7	4	6	10	7	9	13	16	21	13	38	18	21	12	7	9	10	11	5	11	10	19	297	Feb 04 Friday
36	4	3	10	5	7	20	7	9	9	5	9	26	6	6	6	10	7	5	14	14	7	1	3	35	228	Feb 05 Saturday
37	8	7	9	11	20	21	9	8	3	15	13	5	10	12	20	6	8	1	11	14	6	8	5	13	243	Feb 06 Sunday
38	8	13	7	9	9	9	10	7	14	12	13	20	17	36	71	29	8	8	9	12	23	9	6	24	383	Feb 07 Monday
39	15	11	8	13	13	19	12	6	4	16	21	17	28	16	14	12	18	6	15	12	18	11	12	27	344	Feb 08 Tuesday
40	12	10	14	12	7	6	8	8	11	14	13	20	18	23	14	7	14	13	9	15	11	10	12	18	299	Feb 09 Wednesday
41	15	9	11	3	4	8	14	12	13	16	16	21	22	15	9	9	8	11	11	6	12	7	10	24	286	Feb 10 Thursday
42	10	5	7	6	5	10	6	11	24	7	12	13	23	15	9	17	11	15	13	13	13	15	19	20	299	Feb 11 Friday
43	8	4	7	10	10	4	6	8	9	16	16	11	16	8	5	8	10	9	20	9	5	10	7	14	230	Feb 12 Saturday
44	6	13	9	8	4	12	2	9	6	2	12	7	2	4	6	7	5	8	10	9	6	11	9	21	188	Feb 13 Sunday
45	5	5	3	6	7	5	3	9	5	14	7	24	14	9	4	11	5	5	6	5	5	3	6	10	176	Feb 14 Monday
46	2	4	3	9	9	9	5	8	6	12	22	8	11	15	12	13	10	13	8	10	14	27	16	19	265	Feb 15 Tuesday
47	11	5	7	9	26	22	8	24	13	14	28	31	27	10	19	5	17	6	25	13	10	9	11	19	369	Feb 16 Wednesday
48	8	5	10	10	6	15	14	16	6	16	43	31	31	19	7	12	15	22	12	17	19	8	14	12	368	Feb 17 Thursday
49	3	6	4	6	8	9	11	16	8	12	7	7	15	4	7	4	5	2	4	2	0	1	4	10	155	Feb 18 Friday
50	6	6	5	6	4	6	3	7	4	1	12	24	15	10	10	4	10	17	14	19	6	11	10	13	223	Feb 19 Saturday
51	9	8	10	15	11	19	8	10	0	13	31	32	31	33	21	14	23	16	16	18	17	11	18	21	405	Feb 20 Sunday
52	7	7	13	13	10	8	6	4	12	12	10	16	12	20	11	11	15	18	11	5	5	8	18	48	300	Feb 21 Monday
53	19	5	4	10	6	13	8	14	13	11	15	5	14	8	18	18	22	7	10	60	24	6	22	16	348	Feb 22 Tuesday
54	4	4	5	15	8	9	34	16	26	6	13	17	15	25	38	15	3	6	19	17	52	14	28	38	427	Feb 23 Wednesday
55	9	6	11	10	10	9	7	9	11	10	16	26	32	50	49	36	27	5	16	12	10	6	6	14	397	Feb 24 Thursday
56	4	9	9	8	31	12	37	27	10	3	21	31	24	30	41	34	33	12	10	10	8	19	6	16	445	Feb 25 Friday
57	7	12	17	17	13	11	29	128	58	63	51	31	15	21	9	6	4	7	9	18	11	6	29	45	617	Feb 26 Saturday
58	30	14	7	54	32	101	22	34	54	47	32	60	61	37	86	111	60	15	10	26	40	25	30	23	1011	Feb 27 Sunday
59	16	20	9	4	12	16	15	16	31	34	11	11	27	8	9	31	35	58	13	79	82	21	7	15	580	Feb 28 Monday
60	4	8	2	16	16	9	6	9	18	10	2	9	25	13	11	24	8	4	7	13	7	9	3	15	248	Mar 01 Tuesday
61	4	3	4	7	7	6	3	10	9	15	10	11	21	17	13	11	9	7	9	10	12	36	25	33	292	Mar 02 Wednesday
62	8	4	5	3	10	12	13	10	20	20	26	27	43	18	16	47	48	26	23	25	30	45	13	30	522	Mar 03 Thursday
63	22	7	26	20	35	13	6	15	17	21	10	26	33	23	8	16	12	14	12	10	11	6	11	24	398	Mar 04 Friday
64	3	4	4	12	11	13	14	3	13	12	13	20	23	5	4	6	10	16	15	21	9	7	7	17	262	Mar 05 Saturday
65	8	13	6	16	10	7	17	8	6	4	11	15	12	5	16	13	7	11	10	13	7	9	9	25	258	Mar 06 Sunday
66	4	10	7	5	13	9	7	8	9	11	8	14	17	15	11	33	22	19	17	59	46	34	29	15	422	Mar 07 Monday
67	6	2	8	8	11	6	15	16	15	19	8	14	12	14	9	13	12	9	13	12	7	6	8	20	263	Mar 08 Tuesday
68	9	3	11	5	7	17	6	7	22	27	16	14	18	14	27	16	14	15	6	10	11	10	8	40	333	Mar 09 Wednesday
69	29	10	6	9	15	11	13	10	13	17	19	26	29	22	16	22	15	9	12	20	14	8	8	20	373	Mar 10 Thursday
70	8	9	5	13	25	8	13	22	25	10	15	30	54	12	8	22	24	20	4	9	6	7	7	18	374	Mar 11 Friday
71	14	13	9	8	6	13	4	10	5	18	3	23	8	11	17	9	5	8	10	7	13	4	5	35	258	Mar 12 Saturday
72	23	10	9	14	7	8	9	10	9	14	7	13	18	8	7	9	10	12	12	9	11	3	6	10	248	Mar 13 Sunday
73	14	12	1	0	14	14	13	6	13	4	7	11	13	19	25	8	15	24	12	11	6	17	7	22	288	Mar 14 Monday
74	5	7	6	9	5	7	13	7	4	19	19	41	24	10	15	20	11	12	14	6	14	5	8	28	309	Mar 15 Tuesday
75	15	8	9	5	7	8	13	9	12	13	10	23	23	19	26	15	22	11	10	12	13	13	13	32	341	Mar 16 Wednesday
76	3	9	13	4	8	15	11	9	19	6	13	20	39	15	8	14	16	11	11	14	5	7	11	14	295	Mar 17 Thursday

Table 3.5.2 (Page 3 of 4)

ARC .FKX Hourly distribution of detections

Day	00	01	02	03	04	05	06	07	08	09	10	11	12	13	14	15	16	17	18	19	20	21	22	23	Sum	Date
77	15	4	15	9	11	20	20	16	17	14	21	13	32	12	14	8	8	31	12	13	7	9	9	15	345	Mar 18 Friday
78	6	11	6	10	12	6	9	15	12	23	11	30	16	11	4	10	16	17	6	5	6	7	11	13	273	Mar 19 Saturday
79	4	17	6	4	3	10	3	16	8	8	13	6	18	2	16	16	14	8	8	9	8	15	14	6	232	Mar 20 Sunday
80	6	1	13	9	3	7	12	5	7	13	6	9	22	13	11	9	12	9	9	3	10	10	4	22	225	Mar 21 Monday
81	13	4	3	9	10	9	9	15	2	8	13	18	27	11	17	11	14	5	8	12	8	6	10	26	268	Mar 22 Tuesday
82	6	11	10	6	9	11	10	13	12	14	15	9	30	19	14	6	22	21	13	12	21	13	10	11	318	Mar 23 Wednesday
83	2	8	18	9	16	17	12	9	18	14	17	28	15	22	15	8	16	11	10	12	5	6	10	22	320	Mar 24 Thursday
84	4	1	9	5	5	5	7	5	17	16	15	5	18	18	8	12	14	5	10	12	9	23	6	23	252	Mar 25 Friday
85	10	10	12	5	13	8	13	8	15	10	17	12	7	9	6	12	11	12	4	25	13	20	23	69	344	Mar 26 Saturday
86	59	51	82	66	63	68	66	71	53	66	70	86	28	5	19	11	3	21	19	15	11	3	16	5	957	Mar 27 Sunday
87	8	17	8	9	9	9	15	5	17	7	11	22	14	11	7	9	8	13	9	14	15	17	12	4	270	Mar 28 Monday
88	5	5	7	25	16	7	23	16	25	24	15	21	24	10	7	24	8	10	15	12	8	15	23	10	355	Mar 29 Tuesday
89	5	3	8	13	46	15	7	36	17	20	28	15	21	8	8	9	10	12	9	11	13	4	21	11	350	Mar 30 Wednesday
90	3	6	7	6	8	6	18	20	80	74	75	92	73	71	37	13	15	23	14	16	9	7	23	15	711	Mar 31 Thursday
ARC	00	01	02	03	04	05	06	07	08	09	10	11	12	13	14	15	16	17	18	19	20	21	22	23		
Sum	2096	2212	2294	2545	3008	3687	3636	3710	3259	3198	2494	4670														
	2271	2153	2443	2281	2793	3232	4235	3635	3644	2887	2789	2493													71665	Total sum
182	12	12	12	12	13	13	13	14	15	17	18	20	23	20	20	20	20	18	16	18	15	14	14	26	394	Total average
129	12	12	12	12	13	12	12	13	14	16	17	19	25	21	22	22	22	20	17	19	16	15	14	25	403	Average workdays
53	13	11	12	13	13	14	14	16	17	19	20	22	20	16	16	16	14	12	12	14	14	12	13	27	368	Average weekends

Table 3.5.2. Daily and hourly distribution of ARCESS detections. For each day is shown number of detections within each hour of the day, and number of detections for that day. The end statistics give total number of detections distributed for each hour and the total sum of detections during the period. The averages show number of processed days, hourly distribution and average per processed day.

FIN .FKX Hourly distribution of detections

Day	00	01	02	03	04	05	06	07	08	09	10	11	12	13	14	15	16	17	18	19	20	21	22	23	Sum	Date
274	0	0	0	0	0	0	0	0	0	0	0	0	0	0	0	0	0	0	0	0	0	0	0	0	0	Oct 01 Friday
275	0	0	0	0	0	0	0	0	0	0	0	0	0	0	0	0	0	0	0	0	0	0	0	0	0	Oct 02 Saturday
276	0	0	0	0	0	0	0	0	0	0	0	0	0	0	0	0	0	0	0	0	0	0	0	0	0	Oct 03 Sunday
277	0	0	0	0	0	0	0	0	0	0	0	0	0	0	0	0	0	0	0	0	0	0	0	0	0	Oct 04 Monday
278	0	0	0	0	0	0	0	0	0	0	0	0	0	0	0	0	0	0	0	0	0	0	0	0	0	Oct 05 Tuesday
279	0	0	0	0	0	0	0	0	0	0	0	0	0	0	0	0	0	0	0	0	0	0	0	0	0	Oct 06 Wednesday
280	0	0	0	0	0	0	0	0	0	0	0	0	0	0	0	0	0	0	0	0	0	0	0	0	0	Oct 07 Thursday
281	0	0	0	0	0	0	0	0	0	0	0	0	0	0	0	0	0	0	0	0	0	0	0	0	0	Oct 08 Friday
282	0	0	0	0	0	0	0	0	0	0	0	0	0	0	0	0	0	0	0	0	0	0	0	0	0	Oct 09 Saturday
283	0	0	0	0	0	0	0	0	0	0	0	0	0	0	0	0	0	0	0	0	0	0	0	0	0	Oct 10 Sunday
284	0	0	0	0	0	0	0	0	0	0	0	0	0	0	0	0	0	0	0	0	0	0	0	0	0	Oct 11 Monday
285	0	0	0	0	0	0	0	0	0	0	0	0	0	0	0	0	0	0	0	0	0	0	0	0	0	Oct 12 Tuesday
286	0	0	0	0	0	0	0	0	0	0	0	0	0	0	0	0	0	0	0	0	0	0	0	0	0	Oct 13 Wednesday
287	0	0	0	0	0	0	0	0	0	0	0	0	0	0	0	0	0	0	0	0	0	0	0	0	0	Oct 14 Thursday
288	0	0	0	0	0	0	0	0	0	0	0	0	0	0	0	0	0	0	0	0	0	0	0	0	0	Oct 15 Friday
289	0	0	0	0	0	0	0	0	0	0	0	0	0	0	0	0	0	0	0	0	0	0	0	0	0	Oct 16 Saturday
290	0	0	0	0	0	0	0	0	0	0	0	0	0	0	0	0	0	0	0	0	0	0	0	0	0	Oct 17 Sunday
291	0	0	0	0	0	0	0	0	0	0	0	0	0	0	0	0	0	0	0	0	0	0	0	0	0	Oct 18 Monday
292	0	0	0	0	0	0	0	0	0	0	0	0	0	0	0	0	0	0	0	0	0	0	0	0	0	Oct 19 Tuesday
293	0	0	0	0	0	0	0	0	0	0	0	0	0	0	0	0	0	0	0	0	0	0	0	0	0	Oct 20 Wednesday
294	0	0	0	0	0	0	0	0	0	0	0	0	0	0	0	0	0	0	0	0	0	0	0	0	0	Oct 21 Thursday
295	0	0	0	0	0	0	0	0	0	0	0	0	0	0	0	0	0	0	0	0	0	0	0	0	0	Oct 22 Friday
296	0	0	0	0	0	0	0	0	0	0	0	0	0	0	0	0	0	0	0	0	0	0	0	0	0	Oct 23 Saturday
297	0	0	0	0	0	0	0	0	0	0	0	0	0	0	0	0	0	0	0	0	0	0	0	0	0	Oct 24 Sunday
298	0	0	0	0	0	0	0	0	0	0	0	0	0	0	0	0	0	0	0	0	0	0	0	0	0	Oct 25 Monday
299	0	0	0	0	0	0	0	0	0	0	0	0	0	0	0	0	0	0	0	0	0	0	0	0	0	Oct 26 Tuesday
300	0	0	0	0	0	0	0	0	0	0	0	0	0	0	0	0	0	0	0	0	0	0	0	0	0	Oct 27 Wednesday
301	0	0	0	0	0	0	0	0	0	0	0	0	0	0	0	0	0	0	0	0	0	0	0	0	0	Oct 28 Thursday
302	0	0	0	0	0	0	0	0	0	0	0	0	0	0	0	0	0	0	0	0	0	0	0	0	0	Oct 29 Friday
303	0	0	0	0	0	0	0	0	0	0	0	0	0	0	0	0	0	0	0	0	0	0	0	0	0	Oct 30 Saturday
304	0	0	0	0	0	0	0	0	0	0	0	0	0	0	0	0	0	0	0	0	0	0	0	0	0	Oct 31 Sunday
305	0	0	0	0	0	0	0	0	0	0	0	0	0	0	0	0	0	0	0	0	0	0	0	0	0	Nov 01 Monday
306	0	0	0	0	0	0	0	0	0	0	0	0	0	0	0	0	0	0	0	0	0	0	0	0	0	Nov 02 Tuesday
307	0	0	0	0	0	0	0	0	0	0	0	0	0	0	0	0	0	0	0	0	0	0	0	0	0	Nov 03 Wednesday
308	0	0	0	0	0	0	0	0	0	0	0	0	0	0	0	0	0	0	0	0	0	0	0	0	0	Nov 04 Thursday
309	0	0	0	0	0	0	0	0	0	0	0	0	0	0	0	0	0	0	0	0	0	0	0	0	0	Nov 05 Friday
310	0	0	0	0	0	0	0	0	0	0	0	0	0	0	0	0	0	0	0	0	0	0	0	0	0	Nov 06 Saturday
311	0	0	0	0	0	0	0	0	0	0	0	0	0	0	0	0	0	0	0	0	0	0	0	0	0	Nov 07 Sunday
312	0	0	0	0	0	0	0	0	0	0	0	0	0	0	0	0	0	0	0	0	0	0	0	0	0	Nov 08 Monday
313	0	0	0	0	0	0	0	0	0	0	0	0	0	0	0	0	0	0	0	0	0	0	0	0	0	Nov 09 Tuesday
314	0	0	0	0	0	0	0	0	0	0	0	0	0	0	0	0	0	0	0	0	0	0	0	0	0	Nov 10 Wednesday
315	0	0	0	0	0	0	0	0	0	0	0	0	0	0	0	0	0	0	0	0	0	0	0	0	0	Nov 11 Thursday
316	0	0	0	0	0	0	0	0	0	0	0	0	0	0	0	0	0	0	0	0	0	0	0	0	0	Nov 12 Friday
317	0	0	0	0	0	0	0	0	0	0	0	0	0	0	0	0	0	0	0	0	0	0	0	0	0	Nov 13 Saturday
318	0	0	0	0	0	0	0	0	0	0	0	0	0	0	0	0	0	0	0	0	0	0	0	0	0	Nov 14 Sunday
319	0	0	0	0	0	0	0	0	0	0	0	0	0	0	0	0	0	0	0	0	0	0	0	0	0	Nov 15 Monday
320	0	0	0	0	0	0	0	0	0	0	0	0	0	0	0	0	0	0	0	0	0	0	0	0	0	Nov 16 Tuesday
321	0	0	0	0	0	0	0	0	0	0	0	0	0	0	0	0	0	0	0	0	0	0	0	0	0	Nov 17 Wednesday
322	0	0	0	0	0	0	0	0	0	22	10	25	21	28	8	6	6	8	4	8	10	52	73	57	338	Nov 18 Thursday
323	55	57	25	27	70	53	47	7	9	12	17	20	16	8	17	15	9	5	8	8	10	10	8	4	517	Nov 19 Friday
324	6	11	5	6	11	4	7	19	5	14	4	7	16	56	59	20	6	7	12	36	76	105	99	82	673	Nov 20 Saturday
325	85	84	61	95	85	73	84	46	10	5	8	4	0	0	0	0	0	0	0	0	0	0	0	0	640	Nov 21 Sunday
326	0	0	0	0	0	0	0	0	0	0	0	0	0	0	0	0	0	0	0	0	0	0	0	0	0	Nov 22 Monday
327	0	0	0	0	0	0	0	0	0	10	13	13	24	21	14	15	8	13	20	23	14	16	9	6	219	Nov 23 Tuesday
328	2	6	8	23	8	4	9	6	7	19	12	12	26	10	6	9	2	10	9	15	5	11	2	10	231	Nov 24 Wednesday
329	11	11	8	10	9	3	10	4	9	8	8	19	23	16	13	12	10	13	10	14	9	6	9	5	250	Nov 25 Thursday

Table 3.5.3 (Page 1 of 4)

FIN .FKX Hourly distribution of detections

Day	00	01	02	03	04	05	06	07	08	09	10	11	12	13	14	15	16	17	18	19	20	21	22	23	Sum	Date
330	6	6	6	10	8	2	3	7	8	12	10	22	25	16	11	7	13	6	16	15	17	12	25	17	280	Nov 26 Friday
331	14	7	14	22	18	10	15	12	5	6	4	8	8	10	7	2	2	7	7	6	3	1	4	0	192	Nov 27 Saturday
332	0	0	0	0	0	0	0	0	0	0	0	0	0	0	0	0	0	0	0	0	0	0	0	0	0	Nov 28 Sunday
333	0	0	0	0	8	3	6	7	6	13	10	9	3	18	10	7	9	8	6	13	14	10	16	19	195	Nov 29 Monday
334	16	17	9	9	6	4	4	9	8	19	12	10	17	29	11	26	33	17	28	23	24	20	11	12	374	Nov 30 Tuesday
335	5	12	7	3	5	2	7	4	9	16	13	8	23	12	7	9	10	5	2	8	10	6	6	5	194	Dec 01 Wednesday
336	4	5	8	9	8	4	7	11	9	19	16	23	28	21	13	15	12	15	19	21	23	15	23	29	357	Dec 02 Thursday
337	28	32	37	56	38	25	22	16	6	10	12	25	27	18	10	6	7	7	6	8	6	6	6	4	418	Dec 03 Friday
338	5	3	5	3	1	5	6	1	4	7	7	4	4	3	5	4	1	2	3	3	6	3	2	5	92	Dec 04 Saturday
339	4	8	7	7	8	6	13	2	2	0	3	1	3	8	3	5	2	4	1	11	2	1	4	3	108	Dec 05 Sunday
340	3	6	5	2	5	1	2	2	3	6	7	14	20	17	4	4	2	2	7	9	4	7	10	16	158	Dec 06 Monday
341	17	17	15	7	4	4	0	3	10	4	5	17	15	15	11	1	18	7	9	16	9	8	10	7	229	Dec 07 Tuesday
342	12	4	8	7	6	1	2	5	6	32	26	18	29	12	7	10	7	13	7	10	6	8	14	5	255	Dec 08 Wednesday
343	3	9	3	9	5	6	5	6	6	16	10	22	24	12	8	8	10	6	6	8	9	7	8	2	208	Dec 09 Thursday
344	6	10	3	7	10	17	18	1	7	0	0	0	0	0	5	4	5	10	8	5	6	3	8	11	144	Dec 10 Friday
345	9	7	17	11	7	7	8	6	7	12	11	9	9	8	16	9	14	17	20	12	12	5	4	5	242	Dec 11 Saturday
346	8	6	6	0	9	18	15	17	17	11	19	26	32	23	19	12	8	17	13	11	21	23	19	25	375	Dec 12 Sunday
347	14	19	34	10	5	13	6	3	14	10	5	19	27	17	9	7	23	22	14	7	6	4	13	5	306	Dec 13 Monday
348	29	45	53	42	14	13	6	15	10	9	11	20	17	16	8	3	7	7	4	8	18	9	9	10	383	Dec 14 Tuesday
349	15	12	16	9	10	12	15	26	23	25	31	16	31	14	24	19	13	5	11	9	12	10	5	3	366	Dec 15 Wednesday
350	6	2	7	10	2	2	7	7	8	14	20	20	25	26	15	12	6	8	12	5	10	8	6	6	244	Dec 16 Thursday
351	9	10	6	9	5	9	4	9	22	11	22	14	30	19	5	9	11	5	7	5	11	9	7	9	257	Dec 17 Friday
352	2	5	7	7	5	17	9	2	12	10	10	9	14	6	1	4	1	6	3	1	1	3	1	6	142	Dec 18 Saturday
353	0	0	11	3	4	4	3	2	5	5	1	6	5	0	5	5	6	5	2	5	6	7	11	4	105	Dec 19 Sunday
354	11	8	11	4	7	3	3	9	10	9	10	13	20	21	9	6	11	7	10	9	10	4	7	5	217	Dec 20 Monday
355	4	8	2	7	2	4	1	9	9	14	3	18	19	13	10	8	4	4	1	6	6	5	7	7	171	Dec 21 Tuesday
356	4	4	6	7	4	7	3	2	8	14	7	15	21	27	9	2	17	10	16	11	8	10	4	6	222	Dec 22 Wednesday
357	8	10	5	5	8	5	4	8	11	8	35	19	25	10	8	4	8	5	8	4	6	5	3	2	214	Dec 23 Thursday
358	6	5	2	3	4	10	2	0	5	11	11	18	16	15	10	9	4	17	16	8	23	22	25	37	279	Dec 24 Friday
359	25	41	47	34	35	43	33	33	22	24	36	30	39	38	40	31	40	46	44	58	57	77	73	67	1013	Dec 25 Saturday
360	58	54	60	63	68	50	48	48	40	39	12	4	12	11	6	11	13	27	25	41	28	34	40	50	842	Dec 26 Sunday
361	54	33	24	18	11	10	4	7	11	10	13	20	24	15	11	19	16	29	63	49	61	44	54	56	656	Dec 27 Monday
362	45	60	58	61	47	38	37	39	39	37	45	44	42	43	57	40	31	11	10	7	19	3	9	10	832	Dec 28 Tuesday
363	24	18	10	11	9	10	8	11	21	31	12	14	20	19	12	9	6	12	11	11	14	4	7	4	308	Dec 29 Wednesday
364	4	5	5	7	3	4	8	5	8	13	17	23	20	24	14	9	14	12	9	11	5	7	5	7	239	Dec 30 Thursday
365	6	12	11	3	8	6	5	12	21	4	11	21	13	7	5	5	5	11	11	2	5	3	3	1	191	Dec 31 Friday
1	1	2	12	5	3	11	2	2	3	1	4	3	2	4	2	2	2	4	1	1	0	1	4	1	73	Jan 01 Saturday
2	1	0	6	4	10	10	0	4	3	8	1	2	4	2	10	6	7	7	8	7	9	7	4	9	129	Jan 02 Sunday
3	6	21	5	6	6	4	9	3	9	15	9	12	2	26	15	9	14	7	8	15	15	15	8	6	245	Jan 03 Monday
4	2	11	7	3	10	7	5	4	10	9	24	15	24	16	7	13	11	13	7	12	8	7	8	7	240	Jan 04 Tuesday
5	4	10	6	4	7	5	7	6	14	19	20	14	23	22	9	5	7	13	7	7	8	12	7	6	242	Jan 05 Wednesday
6	1	3	6	4	6	7	7	8	10	11	18	21	11	12	7	1	7	7	2	7	7	7	10	5	185	Jan 06 Thursday
7	4	5	6	12	10	7	3	7	6	12	0	5	19	11	9	9	7	7	6	7	10	7	5	7	181	Jan 07 Friday
8	3	3	6	7	3	5	3	4	3	3	0	0	6	3	11	3	1	0	1	3	3	5	4	0	80	Jan 08 Saturday
9	3	1	0	0	0	0	0	0	0	0	0	0	0	0	0	0	0	0	0	0	0	0	0	0	4	Jan 09 Sunday
10	0	0	0	0	0	0	0	1	11	13	11	10	23	19	11	10	17	9	6	8	8	14	2	12	185	Jan 10 Monday
11	7	8	4	6	4	2	0	11	10	12	17	21	26	16	10	7	8	9	7	8	10	4	8	4	219	Jan 11 Tuesday
12	8	8	11	6	9	4	5	7	6	17	30	15	28	23	7	5	5	11	6	10	4	8	6	3	242	Jan 12 Wednesday
13	3	10	3	1	7	1	10	4	9	8	12	27	31	21	14	6	5	12	5	8	13	12	6	4	232	Jan 13 Thursday
14	11	3	6	7	8	3	7	4	6	14	12	20	28	8	23	8	9	15	6	10	7	3	6	6	230	Jan 14 Friday
15	7	11	8	4	11	4	9	6	4	7	6	10	15	10	9	3	3	3	5	3	1	5	4	6	154	Jan 15 Saturday
16	1	1	4	5	2	3	2	4	5	5	6	4	7	7	3	4	3	7	4	7	3	9	5	7	108	Jan 16 Sunday
17	5	9	6	4	7	0	2	5	4	15	6	14	21	27	14	12	7	6	5	4	12	4	4	7	200	Jan 17 Monday
18	6	3	1	3	4	4	7	0	9	5	14	8	31	29	15	17	6	9	10	13	8	7	9	8	226	Jan 18 Tuesday
19	5	8	15	6	9	10	3	9	10	17	17	15	29	21	16	11	13	7	4	4	12	13	6	7	267	Jan 19 Wednesday
20	5	6	7	5	9	5	10	10	9	11	10	29	12	7	17	7	13	13	4	6	4	6	5	19	229	Jan 20 Thursday

Table 3.5.3 (Page 2 of 4)

FIN .FKX Hourly distribution of detections

Day	00	01	02	03	04	05	06	07	08	09	10	11	12	13	14	15	16	17	18	19	20	21	22	23	Sum	Date
21	10	9	10	7	5	4	7	4	12	8	8	19	18	10	16	8	8	6	11	7	10	7	5	8	217	Jan 21 Friday
22	9	3	6	5	5	10	7	9	7	9	7	10	10	6	11	9	5	3	3	3	13	6	7	17	180	Jan 22 Saturday
23	7	6	7	3	9	1	12	12	4	2	7	2	2	4	14	7	4	9	11	16	12	8	6	12	177	Jan 23 Sunday
24	6	6	7	7	8	7	8	3	10	7	11	16	13	13	8	6	9	17	6	11	10	13	6	6	214	Jan 24 Monday
25	9	5	5	7	8	9	8	14	15	10	15	21	16	23	25	14	13	13	14	16	8	19	13	11	311	Jan 25 Tuesday
26	13	7	14	16	23	17	8	12	11	23	24	25	22	27	18	9	10	10	7	13	9	8	8	10	344	Jan 26 Wednesday
27	8	13	15	11	7	8	4	9	6	13	25	20	30	14	8	8	8	8	2	5	6	9	11	7	255	Jan 27 Thursday
28	2	6	7	4	2	1	2	4	6	16	20	15	25	22	11	11	5	10	9	6	12	4	4	5	209	Jan 28 Friday
29	5	16	5	10	5	10	11	10	10	12	20	10	14	15	8	9	10	3	12	11	15	20	25	23	289	Jan 29 Saturday
30	35	48	56	50	51	55	55	58	57	54	57	41	40	20	14	14	10	10	20	7	9	13	8	12	794	Jan 30 Sunday
31	8	8	7	8	8	6	4	7	12	6	15	13	19	23	25	12	19	11	11	13	17	25	26	38	341	Jan 31 Monday
32	32	28	45	47	32	29	28	33	28	36	39	37	34	27	21	22	33	29	26	39	27	30	40	25	767	Feb 01 Tuesday
33	41	35	49	43	41	31	34	33	33	28	21	26	17	22	11	15	7	9	12	17	17	17	25	16	600	Feb 02 Wednesday
34	22	14	24	21	23	17	19	15	14	23	16	9	29	14	15	15	10	8	13	12	16	24	11	19	403	Feb 03 Thursday
35	15	27	37	35	50	35	43	37	43	48	31	31	37	17	7	14	13	12	9	14	14	19	23	38	649	Feb 04 Friday
36	60	59	63	66	60	58	65	67	52	23	18	27	8	8	10	7	8	5	12	7	15	29	60	48	835	Feb 05 Saturday
37	35	49	44	41	29	27	22	12	8	6	4	3	8	1	3	4	3	7	10	12	10	10	6	5	359	Feb 06 Sunday
38	15	12	9	6	8	7	8	1	7	6	8	16	22	13	15	13	11	7	12	6	17	14	10	10	253	Feb 07 Monday
39	7	4	7	7	9	9	4	6	9	9	13	15	30	28	16	15	12	11	19	10	11	12	13	8	284	Feb 08 Tuesday
40	21	14	9	10	14	8	3	5	10	17	13	15	30	20	11	11	11	12	11	12	11	18	13	12	311	Feb 09 Wednesday
41	9	14	20	9	9	4	4	7	12	11	23	22	11	14	18	10	6	9	11	9	14	15	16	32	309	Feb 10 Thursday
42	38	37	30	50	36	40	35	44	36	39	25	29	24	13	20	19	31	55	56	67	70	82	69	70	1015	Feb 11 Friday
43	76	70	61	57	80	70	69	70	64	54	52	29	20	15	9	8	9	21	43	48	58	74	69	88	1214	Feb 12 Saturday
44	69	73	67	59	54	33	37	19	14	10	6	5	3	5	5	3	3	4	12	4	9	16	7	5	522	Feb 13 Sunday
45	6	13	7	10	4	3	4	3	5	12	6	15	18	17	14	9	4	4	0	0	0	0	0	0	154	Feb 14 Monday
46	0	0	0	0	0	0	0	0	2	7	13	12	21	22	10	22	11	13	13	10	11	13	13	9	202	Feb 15 Tuesday
47	4	10	10	13	14	3	14	15	0	0	0	0	16	20	11	8	16	13	9	15	13	10	8	10	232	Feb 16 Wednesday
48	7	8	14	15	10	7	4	7	10	13	20	18	13	29	7	10	8	7	14	10	8	9	14	15	277	Feb 17 Thursday
49	11	10	12	15	17	10	9	22	19	20	16	26	34	26	10	7	11	10	10	10	9	18	21	20	373	Feb 18 Friday
50	19	10	8	12	8	9	12	11	17	10	17	14	15	10	8	10	12	8	6	6	5	1	6	0	234	Feb 19 Saturday
51	9	4	11	6	5	11	4	3	5	6	3	4	6	4	4	1	2	5	10	12	13	17	22	19	186	Feb 20 Sunday
52	20	27	32	34	29	24	21	23	17	14	20	19	24	10	12	12	11	4	7	7	13	7	9	12	408	Feb 21 Monday
53	10	10	13	17	17	31	24	21	29	17	4	25	22	18	23	10	4	3	9	10	8	9	11	14	359	Feb 22 Tuesday
54	3	6	12	16	7	4	5	3	18	25	10	18	17	27	17	10	17	12	22	11	16	12	9	6	303	Feb 23 Wednesday
55	11	9	8	2	9	2	10	6	6	8	14	7	17	19	15	20	15	13	5	8	14	10	11	8	247	Feb 24 Thursday
56	14	12	12	8	4	9	0	0	0	0	0	0	0	0	0	0	0	0	0	0	0	0	0	0	59	Feb 25 Friday
57	0	0	0	0	0	0	0	0	0	0	0	0	0	0	0	0	0	0	0	0	0	0	0	0	0	Feb 26 Saturday
58	0	0	0	0	0	0	0	0	0	0	0	0	0	0	0	0	0	0	0	0	0	0	0	0	0	Feb 27 Sunday
59	0	0	0	0	0	0	0	11	12	15	11	28	19	15	11	12	11	7	9	12	12	11	25	17	238	Feb 28 Monday
60	30	29	23	30	36	31	23	25	25	17	13	17	23	25	13	14	18	13	10	10	9	4	6	14	458	Mar 01 Tuesday
61	9	9	12	19	24	19	15	14	13	16	26	15	13	18	11	14	7	10	7	13	11	10	9	10	324	Mar 02 Wednesday
62	10	6	6	8	6	8	9	8	15	10	20	17	11	11	13	15	18	8	9	8	11	9	11	14	261	Mar 03 Thursday
63	10	13	8	13	7	9	4	7	9	23	14	13	27	14	14	12	8	9	7	8	11	11	7	11	269	Mar 04 Friday
64	13	3	11	14	7	8	2	9	9	2	6	8	10	6	3	7	5	3	1	9	4	4	3	5	152	Mar 05 Saturday
65	1	8	3	6	4	6	4	1	6	2	8	5	9	3	4	6	4	4	1	7	4	4	3	7	110	Mar 06 Sunday
66	14	10	7	15	10	13	7	10	6	11	12	24	20	21	5	12	3	8	12	3	9	7	3	6	248	Mar 07 Monday
67	6	10	6	7	9	7	9	6	5	11	19	23	18	14	9	14	11	11	4	14	10	7	5	4	239	Mar 08 Tuesday
68	5	8	1	12	6	6	11	6	8	5	13	15	16	27	8	18	8	10	7	9	4	3	9	19	234	Mar 09 Wednesday
69	20	5	10	8	8	1	3	1	10	11	9	10	27	22	13	15	13	7	5	6	6	4	6	6	226	Mar 10 Thursday
70	2	9	9	17	10	4	6	16	21	5	17	27	30	42	35	20	5	7	4	8	7	5	6	3	315	Mar 11 Friday
71	5	4	10	8	7	5	6	11	7	10	10	16	3	10	9	7	2	4	6	3	6	3	4	8	164	Mar 12 Saturday
72	3	9	3	9	5	2	1	5	4	5	3	10	7	6	8	4	4	9	11	16	12	6	6	11	159	Mar 13 Sunday
73	9	17	12	10	11	4	4	12	5	12	11	21	22	7	14	17	10	18	1	10	13	9	7	3	259	Mar 14 Monday
74	3	9	2	9	9	5	8	4	7	10	8	27	24	16	14	10	10	8	6	8	7	4	5	7	220	Mar 15 Tuesday
75	7	9	8	10	3	3	5	6	7	19	14	20	21	24	18	11	13	8	8	11	7	8	8	8	256	Mar 16 Wednesday
76	10	7	14	5	7	2	7	5	5	8	10	14	26	19	12	9	8	9	12	9	15	6	14	11	244	Mar 17 Thursday

Tsble 3.5.3 (Page 3 of 4)

FIN .FKX Hourly distribution of detections

Day	00	01	02	03	04	05	06	07	08	09	10	11	12	13	14	15	16	17	18	19	20	21	22	23	Sum	Date
77	13	9	15	5	16	27	8	6	12	14	13	24	18	15	16	10	5	10	9	16	12	8	6	7	294	Mar 18 Friday
78	13	11	14	15	11	21	14	15	5	14	13	6	8	2	7	4	9	18	22	19	21	22	19	18	321	Mar 19 Saturday
79	17	25	17	17	12	19	16	18	20	11	14	2	8	8	5	4	6	9	10	15	9	17	18	14	311	Mar 20 Sunday
80	26	21	24	28	24	13	20	21	10	14	19	10	22	16	11	9	11	8	13	23	14	31	27	25	440	Mar 21 Monday
81	47	44	43	34	23	21	18	22	23	19	16	14	17	18	9	10	13	12	8	16	0	0	0	8	435	Mar 22 Tuesday
82	25	27	27	33	30	18	12	13	6	14	7	22	21	10	15	16	7	10	6	5	6	6	7	4	347	Mar 23 Wednesday
83	5	8	6	1	5	3	1	3	7	8	10	24	20	21	12	10	10	9	8	20	6	5	8	6	216	Mar 24 Thursday
84	3	3	4	11	2	7	5	2	11	17	26	15	13	21	7	8	7	14	17	20	7	9	7	4	240	Mar 25 Friday
85	7	11	14	9	10	6	7	7	11	11	13	14	11	15	11	12	6	7	13	9	5	5	4	6	224	Mar 26 Saturday
86	7	1	8	6	2	3	5	6	9	10	8	5	6	5	4	3	9	11	13	8	6	15	17	17	184	Mar 27 Sunday
87	6	8	10	14	7	7	14	5	13	9	12	16	15	7	20	13	4	7	10	20	7	10	5	4	243	Mar 28 Monday
88	10	6	5	2	5	4	4	9	15	10	20	22	15	12	10	12	13	10	7	8	6	6	7	3	221	Mar 29 Tuesday
89	6	3	9	7	4	7	3	7	11	16	18	23	15	15	8	7	12	8	9	9	12	8	6	10	233	Mar 30 Wednesday
90	4	7	9	3	7	7	4	8	11	21	19	15	20	4	13	13	5	10	10	8	3	8	10	12	231	Mar 31 Thursday
FIN	00	01	02	03	04	05	06	07	08	09	10	11	12	13	14	15	16	17	18	19	20	21	22	23		
Sum	1835	1852	1522	1455	1772	2060	2051	1306	1302	1522	1626	1714														
	1730	1856	1745	1459	1554	1817	2398	1563	1239	1348	1551	1667													39944	Total sum
130	13	14	14	14	13	12	11	11	12	14	14	16	18	16	12	10	10	10	10	12	12	13	13	13	307	Total average
94	12	12	12	12	12	9	9	9	11	14	15	18	21	18	13	11	11	10	10	11	11	11	11	12	297	Average workdays
36	17	18	19	19	18	18	17	16	13	12	12	10	11	9	10	7	6	9	10	12	13	16	16	17	323	Average weekends

Table 3.5.3. Daily and hourly distribution of FINESS detections. For each day is shown number of detections within each hour of the day, and number of detections for that day. The end statistics give total number of detections distributed for each hour and the total sum of detections during the period. The averages show number of processed days, hourly distribution and average per processed day.

GER .FKX Hourly distribution of detections

Day	00	01	02	03	04	05	06	07	08	09	10	11	12	13	14	15	16	17	18	19	20	21	22	23	Sum	Date
274	4	1	9	3	14	6	3	2	8	8	27	25	14	7	7	7	2	2	2	1	3	5	0	0	160	Oct 01 Friday
275	10	6	9	7	5	1	3	1	3	6	6	10	4	4	7	5	11	9	1	0	3	2	4	7	124	Oct 02 Saturday
276	5	8	8	8	8	10	5	4	2	3	6	6	15	23	16	17	5	5	1	3	3	7	6	3	177	Oct 03 Sunday
277	5	2	0	14	9	3	7	9	6	11	14	22	18	5	19	11	8	4	1	4	5	7	1	3	188	Oct 04 Monday
278	3	5	7	2	11	6	1	0	7	3	26	13	18	23	22	14	5	1	9	6	3	12	5	2	204	Oct 05 Tuesday
279	3	7	2	3	17	5	9	4	5	10	13	17	26	10	6	13	2	3	3	1	0	0	4	1	164	Oct 06 Wednesday
280	2	4	7	6	1	7	5	5	13	14	29	11	15	12	10	7	8	8	2	7	3	2	7	1	186	Oct 07 Thursday
281	4	6	4	8	2	9	5	3	10	9	27	24	14	5	6	5	8	4	7	3	6	0	1	5	175	Oct 08 Friday
282	5	1	6	2	3	2	5	6	10	4	13	4	12	5	3	1	1	6	2	8	6	1	4	2	112	Oct 09 Saturday
283	0	8	5	2	1	7	2	4	6	15	5	3	16	2	3	2	3	6	8	1	3	7	7	3	119	Oct 10 Sunday
284	3	1	12	7	3	5	4	9	16	9	23	21	19	23	20	34	32	5	0	8	3	0	4	7	268	Oct 11 Monday
285	0	3	1	2	2	9	6	5	21	12	19	16	40	14	15	20	17	5	0	4	15	5	4	1	236	Oct 12 Tuesday
286	2	9	12	8	6	1	4	3	12	24	18	19	17	7	9	13	16	5	0	6	3	1	3	8	206	Oct 13 Wednesday
287	2	2	3	3	1	3	5	11	6	13	18	23	20	14	10	8	12	2	6	3	6	5	1	3	180	Oct 14 Thursday
288	7	4	8	10	7	2	2	0	10	7	10	21	14	12	8	6	2	0	4	6	10	4	8	9	171	Oct 15 Friday
289	5	1	5	8	3	1	0	3	3	3	3	12	4	1	2	8	8	2	4	1	2	10	2	2	93	Oct 16 Saturday
290	2	0	0	5	3	4	3	8	3	3	1	3	4	2	4	7	6	0	2	3	6	3	0	2	74	Oct 17 Sunday
291	3	2	1	5	3	3	1	8	8	19	20	15	11	5	18	21	7	2	2	4	3	1	5	1	168	Oct 18 Monday
292	7	4	2	0	6	0	18	19	21	12	20	20	24	17	36	24	12	6	0	7	4	4	2	3	268	Oct 19 Tuesday
293	0	3	6	4	3	1	2	7	17	34	26	20	15	27	17	24	13	5	2	2	1	11	2	3	245	Oct 20 Wednesday
294	4	3	6	2	2	1	4	5	21	18	21	26	15	17	10	5	1	3	1	3	11	6	8	8	201	Oct 21 Thursday
295	7	5	5	3	3	3	0	5	3	26	17	6	12	17	8	2	2	2	13	3	2	1	1	10	156	Oct 22 Friday
296	0	1	2	5	6	2	0	2	1	1	2	11	1	7	2	0	4	8	10	6	3	2	7	5	88	Oct 23 Saturday
297	4	1	7	7	3	1	10	1	9	1	4	1	7	1	6	6	5	4	4	0	2	2	1	1	88	Oct 24 Sunday
298	3	4	2	3	13	2	2	0	6	3	21	11	21	9	12	5	8	8	6	3	3	7	3	2	157	Oct 25 Monday
299	6	0	1	1	0	0	0	0	0	0	17	19	27	7	5	19	6	7	2	5	5	2	6	1	136	Oct 26 Tuesday
300	4	6	4	2	3	1	1	5	9	12	19	30	29	15	10	8	6	7	6	1	1	8	2	6	195	Oct 27 Wednesday
301	4	5	5	3	5	3	1	4	6	15	20	27	13	8	12	17	6	0	1	5	0	2	3	1	166	Oct 28 Thursday
302	6	4	3	4	6	6	0	7	9	12	8	20	11	11	10	7	2	3	9	1	3	0	11	5	158	Oct 29 Friday
303	8	0	0	5	5	4	3	7	2	3	3	6	3	6	7	2	2	3	9	2	1	1	2	6	90	Oct 30 Saturday
304	5	1	3	3	2	1	3	7	1	0	11	3	9	3	3	1	0	3	2	1	2	0	4	0	68	Oct 31 Sunday
305	11	6	2	7	2	3	12	7	13	8	11	6	10	18	9	5	1	11	3	9	2	6	5	2	169	Nov 01 Monday
306	3	2	1	9	3	1	3	6	9	18	21	28	30	14	16	7	1	6	2	13	2	10	4	4	213	Nov 02 Tuesday
307	0	2	1	4	6	2	2	5	16	14	21	25	27	30	27	19	3	6	12	3	5	6	7	3	246	Nov 03 Wednesday
308	6	4	4	7	2	7	11	7	12	15	31	44	22	18	13	3	8	3	18	17	7	10	4	5	278	Nov 04 Thursday
309	4	9	14	10	3	0	6	12	17	17	33	21	19	11	14	11	4	12	7	11	20	4	7	3	269	Nov 05 Friday
310	4	7	5	2	2	4	6	4	1	3	3	3	7	5	5	4	2	2	1	1	5	7	2	0	85	Nov 06 Saturday
311	2	4	0	3	5	1	4	2	5	5	3	4	0	0	0	2	4	5	0	2	3	3	3	10	70	Nov 07 Sunday
312	2	7	6	3	18	1	3	4	16	15	22	14	18	11	6	21	3	6	4	5	2	6	8	5	206	Nov 08 Monday
313	2	5	12	8	7	4	1	7	22	19	22	33	28	14	19	7	5	3	2	7	6	5	7	3	248	Nov 09 Tuesday
314	11	7	4	4	3	11	8	2	13	6	11	15	16	21	12	6	4	8	5	2	8	8	10	5	200	Nov 10 Wednesday
315	9	12	4	4	6	1	7	13	5	20	24	13	24	9	19	12	7	3	5	2	7	6	2	7	221	Nov 11 Thursday
316	5	9	6	2	6	2	8	8	8	26	16	19	18	17	9	8	8	3	6	3	2	4	5	1	199	Nov 12 Friday
317	4	13	3	1	8	2	9	9	6	13	6	8	20	18	4	1	8	2	5	1	2	4	0	3	150	Nov 13 Saturday
318	4	0	7	1	1	4	3	4	5	5	1	0	0	0	0	0	0	0	6	4	11	9	10	25	100	Nov 14 Sunday
319	22	20	7	12	10	13	7	4	23	19	11	8	2	9	13	3	10	4	2	8	1	1	2	4	215	Nov 15 Monday
320	5	6	1	8	3	0	3	13	18	8	21	24	20	12	17	15	3	4	5	4	6	4	3	2	205	Nov 16 Tuesday
321	6	0	5	8	2	7	9	4	2	4	20	11	20	6	13	2	1	0	3	1	1	4	3	3	135	Nov 17 Wednesday
322	0	0	2	2	3	5	1	5	11	16	29	27	46	20	8	16	0	8	6	11	8	2	0	1	227	Nov 18 Thursday
323	3	8	9	10	9	2	4	7	12	13	15	48	29	4	23	9	6	2	12	6	6	6	1	2	246	Nov 19 Friday
324	4	3	0	1	9	4	2	3	3	4	6	10	10	7	1	6	1	1	5	6	4	2	2	2	96	Nov 20 Saturday
325	1	1	2	0	3	1	1	4	0	2	4	0	3	3	5	1	2	4	0	4	5	8	0	4	58	Nov 21 Sunday
326	3	3	2	2	6	2	2	6	5	8	12	24	16	20	12	9	2	0	10	7	2	0	10	3	166	Nov 22 Monday
327	6	5	2	1	7	0	4	9	11	14	16	13	17	9	11	10	3	1	3	7	6	2	1	2	160	Nov 23 Tuesday
328	2	7	6	2	2	10	6	5	4	12	13	20	14	15	20	12	4	5	1	3	3	5	7	8	186	Nov 24 Wednesday
329	2	8	0	2	3	23	6	4	13	11	24	17	19	12	17	13	0	8	2	2	10	4	10	7	217	Nov 25 Thursday

Table 3.5.4 (Page 1 of 4)

GER .FKX Hourly distribution of detections

Day	00	01	02	03	04	05	06	07	08	09	10	11	12	13	14	15	16	17	18	19	20	21	22	23	Sum	Date
330	3	3	4	3	11	3	8	2	13	9	20	15	10	5	7	5	2	4	2	2	0	7	0	0	138	Nov 26 Friday
331	0	0	0	4	5	1	8	12	7	11	7	11	14	6	6	5	2	5	3	3	0	1	3	2	116	Nov 27 Saturday
332	3	6	0	3	0	0	1	3	4	4	16	5	5	4	3	0	2	8	1	8	3	4	5	3	91	Nov 28 Sunday
333	0	1	2	0	4	1	3	9	19	13	22	32	12	14	10	2	0	4	2	4	4	0	3	2	163	Nov 29 Monday
334	5	2	1	6	14	5	3	3	3	10	7	9	14	12	20	9	8	4	10	3	2	8	0	5	163	Nov 30 Tuesday
335	2	6	6	5	5	2	2	6	8	21	18	20	10	13	13	14	9	5	2	0	3	3	5	2	180	Dec 01 Wednesday
336	1	3	8	3	0	1	2	5	13	18	21	23	22	14	15	12	14	7	8	8	2	9	9	5	223	Dec 02 Thursday
337	6	3	4	5	3	4	5	6	9	20	18	8	16	17	13	2	1	2	6	1	5	0	4	3	161	Dec 03 Friday
338	3	3	0	4	6	2	2	2	7	3	4	7	3	6	3	11	7	12	12	9	4	5	4	5	124	Dec 04 Saturday
339	2	8	4	3	6	1	3	6	4	2	6	0	3	9	1	6	1	3	2	6	3	2	4	4	89	Dec 05 Sunday
340	2	3	5	2	3	3	1	13	9	10	29	20	19	13	7	8	5	2	1	2	0	2	10	5	174	Dec 06 Monday
341	4	5	4	6	1	0	2	7	15	10	22	15	18	9	35	24	12	7	5	7	8	2	10	5	233	Dec 07 Tuesday
342	7	8	6	11	5	3	1	19	15	27	40	18	29	21	17	4	4	5	5	2	13	11	18	8	297	Dec 08 Wednesday
343	7	5	3	2	12	11	12	21	31	35	47	31	28	17	16	8	0	0	0	0	0	0	0	0	286	Dec 09 Thursday
344	0	0	0	0	0	0	0	0	0	0	0	3	17	13	11	13	3	2	6	3	7	5	1	10	94	Dec 10 Friday
345	5	9	12	8	3	7	0	5	6	7	3	5	16	9	14	3	4	4	6	4	7	2	5	10	154	Dec 11 Saturday
346	3	0	2	2	5	6	7	8	5	6	14	9	5	5	4	5	1	7	11	5	6	1	2	5	124	Dec 12 Sunday
347	3	3	3	1	4	0	0	1	12	8	8	21	10	6	2	5	12	0	5	6	3	3	2	4	122	Dec 13 Monday
348	3	7	9	4	5	2	4	8	12	8	16	17	19	6	9	1	2	8	4	3	6	9	3	5	170	Dec 14 Tuesday
349	2	8	2	3	2	3	1	1	5	16	9	12	13	15	9	4	5	5	1	3	6	3	3	2	133	Dec 15 Wednesday
350	2	8	6	4	4	3	0	2	7	9	17	19	9	16	9	13	1	14	9	13	7	8	8	19	207	Dec 16 Thursday
351	15	11	13	9	8	2	5	7	7	12	14	20	9	14	2	11	8	14	3	2	0	1	6	1	194	Dec 17 Friday
352	0	1	0	0	3	6	4	3	9	6	7	14	14	8	7	3	11	7	12	22	11	11	7	7	173	Dec 18 Saturday
353	4	3	5	12	5	1	1	4	1	4	3	15	18	8	14	3	9	4	4	2	2	9	12	12	155	Dec 19 Sunday
354	14	12	6	5	7	3	0	1	10	4	12	7	6	9	8	6	13	6	14	26	7	11	4	3	194	Dec 20 Monday
355	10	2	3	3	17	11	5	6	5	8	7	17	13	6	5	5	4	7	4	6	14	12	18	14	202	Dec 21 Tuesday
356	17	21	6	7	11	7	4	4	9	6	12	16	26	12	5	6	12	12	7	5	4	12	8	9	238	Dec 22 Wednesday
357	4	2	4	11	6	13	7	10	6	0	0	0	5	4	10	3	2	3	3	2	1	2	2	0	100	Dec 23 Thursday
358	4	1	3	0	3	7	0	3	6	7	3	6	1	1	1	0	0	2	3	10	2	7	1	0	71	Dec 24 Friday
359	0	1	0	3	0	0	1	2	2	0	17	5	3	3	3	3	0	0	2	3	5	7	5	5	70	Dec 25 Saturday
360	4	1	2	1	3	1	0	3	3	1	3	0	1	4	2	2	0	1	2	2	4	3	2	0	45	Dec 26 Sunday
361	5	5	3	6	3	7	0	4	1	2	14	12	19	2	2	0	1	1	4	4	1	4	1	1	102	Dec 27 Monday
362	1	0	2	6	5	6	5	4	9	4	6	11	4	3	3	9	1	8	5	9	1	2	3	2	109	Dec 28 Tuesday
363	5	2	4	3	4	2	2	2	35	23	20	5	10	2	4	12	0	6	8	2	3	1	3	5	163	Dec 29 Wednesday
364	7	18	11	5	6	0	4	2	1	8	11	7	4	3	5	2	6	3	7	9	7	1	0	10	137	Dec 30 Thursday
365	5	2	5	15	12	19	20	19	2	10	18	5	3	4	7	6	3	2	2	2	2	0	2	7	172	Dec 31 Friday
1	8	6	4	3	3	3	4	1	3	4	2	3	6	2	0	4	0	3	1	3	5	1	2	2	73	Jan 01 Saturday
2	1	4	3	2	3	3	7	8	3	2	0	0	3	2	5	3	5	2	12	7	8	16	12	19	130	Jan 02 Sunday
3	26	14	9	5	4	7	4	5	4	15	17	4	5	15	4	1	6	4	3	8	1	6	0	2	169	Jan 03 Monday
4	0	8	9	5	11	3	0	8	8	6	9	9	10	1	4	8	3	5	1	3	10	5	1	5	132	Jan 04 Tuesday
5	3	3	4	3	6	2	4	5	19	4	15	15	6	5	6	4	5	5	3	2	3	1	0	0	123	Jan 05 Wednesday
6	1	1	2	2	3	1	0	2	6	10	11	15	14	8	2	5	2	4	1	5	3	2	3	2	105	Jan 06 Thursday
7	2	4	6	4	17	7	17	17	3	12	5	10	15	17	2	4	5	1	6	8	3	3	3	3	174	Jan 07 Friday
8	0	3	3	5	5	1	11	14	1	9	4	4	5	1	2	12	1	2	1	4	4	6	4	1	103	Jan 08 Saturday
9	4	0	1	5	1	0	0	2	5	0	5	6	6	3	2	4	2	0	2	0	0	5	6	2	61	Jan 09 Sunday
10	4	4	3	3	1	2	2	2	3	6	11	16	1	7	4	2	21	7	4	4	2	3	2	1	115	Jan 10 Monday
11	1	7	5	1	3	4	0	11	5	15	16	9	17	8	7	2	3	5	9	4	4	1	0	1	138	Jan 11 Tuesday
12	3	4	2	3	1	5	3	7	13	3	30	8	14	6	10	5	1	6	1	4	1	5	1	1	137	Jan 12 Wednesday
13	6	8	5	9	5	10	1	9	6	6	9	17	17	6	10	6	5	5	10	3	2	5	2	6	168	Jan 13 Thursday
14	6	0	0	0	2	3	5	2	9	9	20	13	9	8	7	2	5	2	4	5	1	3	2	2	119	Jan 14 Friday
15	3	3	0	6	10	7	2	3	3	2	0	10	13	7	3	1	4	6	3	3	9	2	2	4	106	Jan 15 Saturday
16	0	1	2	6	0	6	4	5	2	2	7	8	5	1	1	8	1	3	4	2	8	3	1	1	81	Jan 16 Sunday
17	3	6	4	4	5	2	4	3	3	13	12	12	16	11	8	12	7	3	5	5	6	2	5	7	158	Jan 17 Monday
18	6	4	2	2	5	4	5	3	6	7	15	9	12	5	2	14	1	11	4	3	6	2	5	4	137	Jan 18 Tuesday
19	2	3	9	7	4	5	2	5	7	8	20	11	12	17	11	2	6	5	4	1	0	7	0	0	148	Jan 19 Wednesday
20	5	3	3	1	3	1	4	14	7	9	14	7	8	7	7	4	1	8	4	2	1	2	2	12	129	Jan 20 Thursday

Table 3.5.4 (Page 2 of 4)

GER .FKX Hourly distribution of detections

Day	00	01	02	03	04	05	06	07	08	09	10	11	12	13	14	15	16	17	18	19	20	21	22	23	Sum	Date
21	4	1	8	3	6	1	2	3	4	15	13	16	3	7	7	1	6	7	5	5	9	3	5	4	138	Jan 21 Friday
22	3	0	1	1	2	3	2	2	3	4	9	2	3	2	1	2	0	0	4	1	3	0	1	0	49	Jan 22 Saturday
23	1	2	5	2	2	2	1	0	3	8	12	10	6	5	1	6	6	7	7	2	1	2	5	2	98	Jan 23 Sunday
24	4	7	3	4	4	5	4	7	15	10	27	16	22	19	2	7	4	2	9	9	10	3	5	0	198	Jan 24 Monday
25	0	3	2	2	6	12	8	16	5	6	7	7	14	14	10	4	14	10	7	9	6	17	10	15	204	Jan 25 Tuesday
26	18	5	7	9	8	25	7	10	6	4	27	20	18	14	17	15	3	7	7	6	1	4	4	11	253	Jan 26 Wednesday
27	21	22	14	16	28	21	23	28	27	25	45	27	36	25	16	13	18	25	24	10	4	7	10	21	506	Jan 27 Thursday
28	15	10	2	15	58	44	41	42	44	21	36	40	36	23	20	16	11	20	27	20	6	3	1	1	552	Jan 28 Friday
29	9	5	5	4	10	18	10	7	11	11	5	3	10	9	7	5	12	21	6	10	15	17	16	23	249	Jan 29 Saturday
30	21	28	20	19	30	18	3	5	23	17	14	33	12	13	20	3	3	1	3	7	9	5	9	11	327	Jan 30 Sunday
31	12	13	12	13	6	6	6	11	17	9	25	18	19	11	11	10	11	1	3	2	1	3	2	4	226	Jan 31 Monday
32	0	7	3	0	4	1	1	0	18	19	19	10	14	9	3	5	1	4	3	1	3	7	9	1	142	Feb 01 Tuesday
33	5	3	2	4	3	2	1	2	0	7	13	18	15	6	9	17	9	0	4	11	3	0	1	5	140	Feb 02 Wednesday
34	6	1	7	10	8	1	0	5	8	7	18	21	8	15	11	10	5	3	14	9	6	1	1	3	178	Feb 03 Thursday
35	4	1	5	11	7	2	6	9	9	26	24	28	34	16	12	6	5	2	1	4	3	7	4	1	227	Feb 04 Friday
36	6	0	5	0	4	11	4	4	2	1	7	5	6	4	3	7	7	3	2	2	7	0	3	3	96	Feb 05 Saturday
37	4	5	3	3	6	7	7	3	5	16	15	5	6	8	4	3	3	2	2	2	1	3	5	5	123	Feb 06 Sunday
38	8	1	0	4	2	3	3	1	8	4	18	10	11	5	3	9	4	1	7	3	5	2	8	0	120	Feb 07 Monday
39	3	4	3	13	1	10	5	4	20	7	7	15	10	8	10	4	7	14	6	5	6	4	4	6	176	Feb 08 Tuesday
40	8	1	6	6	3	2	3	5	3	10	10	40	24	13	8	2	7	9	8	11	6	7	9	3	204	Feb 09 Wednesday
41	0	3	7	0	1	4	4	2	9	6	13	8	23	3	4	3	0	2	0	0	3	2	1	1	99	Feb 10 Thursday
42	0	3	3	8	4	0	0	6	19	34	18	21	15	7	9	5	5	4	3	3	4	6	9	1	187	Feb 11 Friday
43	3	5	0	5	10	0	4	6	0	1	4	10	6	3	1	4	2	5	9	3	1	2	0	8	92	Feb 12 Saturday
44	1	3	3	1	3	1	1	1	1	1	18	3	10	18	4	8	0	1	5	3	1	2	9	2	100	Feb 13 Sunday
45	2	9	9	8	5	10	4	5	6	10	7	14	8	4	6	11	3	11	15	6	8	5	10	10	186	Feb 14 Monday
46	7	13	13	12	5	5	1	2	8	4	13	6	14	9	2	5	12	5	6	8	3	20	3	5	181	Feb 15 Tuesday
47	8	4	4	3	11	4	6	12	7	9	19	12	10	13	8	4	11	6	4	0	4	6	6	10	181	Feb 16 Wednesday
48	7	6	8	3	14	6	4	4	6	5	15	16	11	4	1	4	5	5	4	1	4	4	5	6	148	Feb 17 Thursday
49	2	2	7	1	9	4	6	3	6	15	11	23	11	11	10	8	12	5	4	5	2	2	4	1	164	Feb 18 Friday
50	8	3	9	4	9	4	8	1	6	19	6	7	11	16	1	3	4	7	0	9	2	1	0	2	140	Feb 19 Saturday
51	1	1	6	9	0	2	2	5	13	24	17	9	3	3	8	2	5	8	2	4	0	1	10	4	139	Feb 20 Sunday
52	3	2	3	6	4	5	3	23	9	11	13	2	19	11	3	11	9	7	3	1	4	1	1	7	161	Feb 21 Monday
53	1	3	1	3	8	6	4	1	7	12	20	11	16	10	5	1	7	2	3	6	3	7	5	3	145	Feb 22 Tuesday
54	5	9	4	6	6	3	3	2	13	8	11	9	18	2	16	9	5	6	9	2	2	2	4	11	165	Feb 23 Wednesday
55	13	15	8	4	1	6	0	7	11	3	17	16	15	15	4	19	10	7	5	1	8	7	2	2	196	Feb 24 Thursday
56	4	6	6	1	4	2	4	9	7	14	15	8	12	15	5	7	6	6	2	2	1	3	4	3	146	Feb 25 Friday
57	0	1	13	2	1	1	4	2	3	2	3	8	11	7	2	2	6	7	14	2	12	5	0	2	110	Feb 26 Saturday
58	1	1	1	6	2	1	1	6	0	6	4	3	8	7	1	0	0	3	2	2	2	2	11	3	73	Feb 27 Sunday
59	2	4	1	1	4	7	4	1	10	13	19	4	5	11	7	8	10	7	11	1	3	3	5	5	146	Feb 28 Monday
60	6	0	3	9	3	7	5	4	8	9	11	19	8	7	6	5	8	5	7	3	1	2	1	3	140	Mar 01 Tuesday
61	1	1	1	5	6	2	3	4	9	15	23	14	5	6	11	11	11	3	2	8	4	11	3	7	166	Mar 02 Wednesday
62	7	10	5	8	12	12	3	11	10	16	24	21	19	10	11	4	6	1	8	5	7	1	6	6	223	Mar 03 Thursday
63	8	1	5	16	3	6	1	1	12	18	18	21	10	9	3	6	5	5	4	2	1	3	12	5	175	Mar 04 Friday
64	6	3	7	2	8	5	8	3	4	2	2	4	15	15	3	4	3	3	1	8	7	4	3	5	125	Mar 05 Saturday
65	2	5	3	8	3	4	7	7	7	1	9	3	4	3	4	1	1	1	0	3	0	4	1	1	82	Mar 06 Sunday
66	4	2	4	1	2	3	0	14	15	30	31	23	19	15	19	12	7	5	9	7	5	5	11	2	245	Mar 07 Monday
67	2	1	6	6	4	2	5	7	5	4	23	17	11	7	11	9	5	7	5	7	3	12	0	5	164	Mar 08 Tuesday
68	5	6	2	7	7	5	2	10	13	10	16	16	18	9	3	10	4	6	9	0	2	0	1	12	173	Mar 09 Wednesday
69	32	9	10	7	7	9	1	8	9	21	14	14	16	10	11	6	10	9	8	9	10	1	3	5	239	Mar 10 Thursday
70	3	2	3	5	8	4	12	2	11	7	21	10	19	8	3	4	5	14	4	10	6	2	6	2	171	Mar 11 Friday
71	3	8	5	5	1	2	3	4	6	6	10	9	4	9	7	9	5	4	6	2	3	0	6	4	121	Mar 12 Saturday
72	6	0	1	11	7	13	14	16	23	18	17	22	20	24	22	25	29	28	29	22	25	21	16	13	422	Mar 13 Sunday
73	16	24	19	10	20	20	23	27	17	24	24	27	23	17	20	21	14	24	17	23	28	19	16	23	496	Mar 14 Monday
74	10	18	14	21	18	9	9	15	19	15	24	13	21	20	25	27	21	9	17	15	19	19	23	25	426	Mar 15 Tuesday
75	12	14	11	6	4	5	8	7	19	10	17	16	20	11	10	8	8	19	14	17	20	17	16	21	310	Mar 16 Wednesday
76	15	21	14	21	17	21	24	15	20	22	21	20	28	23	23	16	9	9	6	2	8	15	12	10	392	Mar 17 Thursday

Table 3.5.4 (Page 3 of 4)

GER .HFKX Hourly distribution of detections

Day	00	01	02	03	04	05	06	07	08	09	10	11	12	13	14	15	16	17	18	19	20	21	22	23	Sum	Date
77	6	0	7	5	5	3	12	9	14	22	13	19	16	11	9	5	5	3	10	4	3	4	8	9	202	Mar 18 Friday
78	17	15	18	10	17	15	12	21	11	30	20	24	14	16	13	18	17	22	18	23	17	15	3	0	386	Mar 19 Saturday
79	1	7	3	1	5	6	5	9	2	2	7	7	7	10	4	10	13	17	10	3	3	13	4	2	151	Mar 20 Sunday
80	2	12	6	5	1	4	4	4	7	14	21	19	14	11	12	6	7	4	10	6	8	11	2	0	190	Mar 21 Monday
81	4	11	3	1	4	2	3	7	10	17	14	21	11	10	9	14	7	4	8	3	4	1	3	7	178	Mar 22 Tuesday
82	3	11	1	6	1	2	0	8	10	10	5	12	18	11	19	7	7	3	6	0	4	5	4	1	154	Mar 23 Wednesday
83	1	9	6	2	4	0	2	6	9	9	17	7	12	14	9	6	15	6	9	11	10	2	4	3	173	Mar 24 Thursday
84	1	1	2	3	6	2	4	5	12	10	15	12	10	5	5	5	2	6	7	3	2	7	3	7	135	Mar 25 Friday
85	10	1	1	2	4	1	0	2	4	2	9	6	8	1	1	2	6	0	2	0	1	4	3	10	80	Mar 26 Saturday
86	0	0	6	0	1	1	3	7	1	3	6	4	5	1	3	1	1	1	0	2	6	1	2	1	56	Mar 27 Sunday
87	11	3	4	2	2	2	10	8	12	18	11	18	5	14	13	8	13	2	4	9	7	1	0	4	181	Mar 28 Monday
88	3	2	4	1	2	0	9	11	18	17	14	28	12	3	2	8	1	3	4	5	0	0	0	1	148	Mar 29 Tuesday
89	3	2	2	2	3	1	4	4	12	24	27	17	11	16	3	0	1	10	5	3	10	11	5	1	177	Mar 30 Wednesday
90	7	0	5	3	5	1	6	15	7	26	9	29	23	7	1	4	8	4	5	15	6	1	8	2	197	Mar 31 Thursday
GER	00	01	02	03	04	05	06	07	08	09	10	11	12	13	14	15	16	17	18	19	20	21	22	23		
Sum	939		926		884	1191		1959	2568		1816	1390		996		951		893		895						
	926		888	1070		857	1650		2677	2502		1594	1071		1011		899		856					31409	Total sum
182	5	5	5	5	6	5	5	7	9	11	15	14	14	10	9	8	6	5	6	5	5	5	5	5	173	Total average
129	5	6	5	5	6	5	5	7	11	12	18	17	16	11	10	9	6	6	6	5	5	5	5	5	191	Average workdays
53	4	4	4	4	5	4	4	5	5	6	7	7	8	7	5	5	5	5	5	5	5	5	5	5	123	Average weekends

Table 3.5.4. Daily and hourly distribution of GERESS detections. For each day is shown number of detections within each hour of the day, and number of detections for that day. The end statistics give total number of detections distributed for each hour and the total sum of detections during the period. The averages show number of processed days, hourly distribution and average per processed day.

APA .FKX Hourly distribution of detections

Day	00	01	02	03	04	05	06	07	08	09	10	11	12	13	14	15	16	17	18	19	20	21	22	23	Sum	Date
274	15	13	16	32	50	51	91	94	77	83	67	98	155	107	80	63	34	54	29	30	33	32	17	11	1332	Oct 01 Friday
275	5	14	16	14	19	25	29	33	31	48	27	40	33	25	39	19	37	28	7	20	9	15	19	9	561	Oct 02 Saturday
276	18	8	12	20	9	14	9	25	16	20	20	26	15	17	30	40	17	30	21	11	13	7	23	7	428	Oct 03 Sunday
277	8	7	14	25	57	63	85	83	91	90	79	64	64	60	58	63	56	24	16	15	1	21	5	3	1052	Oct 04 Monday
278	7	1	19	41	55	70	64	92	73	89	74	80	89	83	62	69	45	30	39	7	18	9	5	0	1121	Oct 05 Tuesday
279	14	16	10	25	68	54	93	84	88	75	70	61	75	83	71	61	26	51	50	20	21	36	32	16	1200	Oct 06 Wednesday
280	19	10	13	41	40	79	76	66	58	62	73	53	156	112	75	80	55	48	36	27	33	10	14	9	1245	Oct 07 Thursday
281	5	11	16	28	65	61	64	59	40	69	62	89	92	58	49	42	30	27	19	16	11	10	9	5	937	Oct 08 Friday
282	0	4	10	13	12	23	38	16	32	22	31	70	27	16	50	24	28	16	15	16	4	28	20	8	523	Oct 09 Saturday
283	9	10	15	22	22	15	19	25	17	20	14	25	21	21	24	16	16	27	19	4	9	3	18	6	397	Oct 10 Sunday
284	7	4	9	20	27	33	53	47	36	41	42	50	46	48	38	42	31	27	29	6	29	24	10	17	716	Oct 11 Monday
285	10	9	16	22	32	38	51	57	26	30	38	38	32	34	39	26	31	19	26	13	14	11	5	7	624	Oct 12 Tuesday
286	8	6	13	15	28	30	29	21	17	11	22	16	33	20	20	12	16	24	8	28	13	21	15	13	439	Oct 13 Wednesday
287	6	0	12	18	36	47	44	50	48	59	42	44	45	43	168	48	72	66	88	93	79	66	72	58	1304	Oct 14 Thursday
288	54	34	47	45	52	56	65	58	30	30	35	37	50	35	48	47	25	33	5	9	10	12	10	1	828	Oct 15 Friday
289	4	5	2	16	19	38	20	63	49	57	45	38	35	27	22	25	15	12	3	11	8	3	2	4	523	Oct 16 Saturday
290	1	3	4	4	2	6	12	7	11	45	26	13	7	20	8	5	4	6	6	8	5	5	15	4	227	Oct 17 Sunday
291	3	5	6	16	15	22	21	0	0	0	0	0	0	0	0	0	0	13	14	10	14	13	12	5	169	Oct 18 Monday
292	32	7	13	40	59	55	56	49	24	18	11	23	28	20	30	32	18	25	22	30	13	63	13	13	694	Oct 19 Tuesday
293	32	12	26	21	37	37	32	65	26	42	44	60	48	59	25	16	29	19	10	8	23	10	8	10	699	Oct 20 Wednesday
294	16	20	12	24	28	40	40	46	14	19	21	22	20	41	30	31	26	11	7	17	8	12	10	2	517	Oct 21 Thursday
295	8	18	11	19	23	42	37	53	24	27	18	25	43	24	24	26	31	15	9	6	14	40	2	13	552	Oct 22 Friday
296	13	7	7	30	8	13	18	12	9	12	17	9	9	11	10	4	13	8	8	5	12	3	4	6	248	Oct 23 Saturday
297	13	0	1	7	8	11	9	7	8	9	10	14	34	35	7	4	4	8	9	3	31	6	32	9	279	Oct 24 Sunday
298	9	4	3	7	36	14	29	32	15	15	23	13	20	26	26	21	37	29	45	30	37	8	15	13	507	Oct 25 Monday
299	19	44	16	18	19	24	28	13	44	64	41	45	53	41	59	26	36	22	13	13	20	10	9	10	687	Oct 26 Tuesday
300	2	1	11	10	12	19	31	23	20	21	68	35	24	20	12	14	8	7	5	4	6	4	4	8	369	Oct 27 Wednesday
301	8	5	11	14	21	19	45	92	113	118	132	141	148	155	146	129	130	132	133	116	132	136	117	130	2323	Oct 28 Thursday
302	156	118	93	113	127	112	77	54	66	51	57	36	26	46	15	16	20	15	16	7	17	2	9	14	1263	Oct 29 Friday
303	10	6	15	4	10	12	8	25	8	9	20	26	12	10	16	15	12	5	14	4	1	5	5	5	257	Oct 30 Saturday
304	8	12	12	45	47	96	86	53	11	6	18	14	12	12	4	20	6	10	10	9	10	23	6	10	540	Oct 31 Sunday
305	8	7	30	15	25	33	36	39	34	19	22	33	30	34	20	23	11	16	14	11	10	22	8	14	514	Nov 01 Monday
306	17	6	12	16	33	42	32	47	26	28	26	10	34	26	36	30	32	29	14	8	25	6	4	5	544	Nov 02 Tuesday
307	16	13	8	15	21	30	22	28	26	29	17	25	24	10	19	14	9	33	11	15	9	5	6	9	414	Nov 03 Wednesday
308	28	1	7	14	18	19	21	35	21	32	20	8	25	34	12	10	10	12	6	9	5	4	7	6	364	Nov 04 Thursday
309	6	7	13	15	12	16	22	25	27	7	20	10	21	47	14	12	12	13	8	3	3	3	4	1	321	Nov 05 Friday
310	0	2	2	4	11	11	23	54	12	8	13	26	3	6	15	5	4	5	3	0	2	1	1	8	219	Nov 06 Saturday
311	1	1	4	5	3	5	1	9	10	4	5	7	4	3	4	23	10	35	23	24	4	0	1	11	197	Nov 07 Sunday
312	18	12	7	13	10	8	13	18	8	7	7	5	11	15	14	30	29	31	23	42	30	31	14	11	407	Nov 08 Monday
313	6	7	23	31	20	28	29	40	18	29	29	24	50	25	22	27	20	34	12	34	11	17	23	8	567	Nov 09 Tuesday
314	18	10	9	17	29	13	37	28	27	11	17	10	32	7	9	14	10	18	4	5	11	7	12	4	359	Nov 10 Wednesday
315	9	6	3	20	23	22	27	58	22	20	26	19	31	11	20	18	19	21	8	16	3	2	5	7	416	Nov 11 Thursday
316	9	7	8	13	28	27	23	17	39	47	16	27	53	31	24	23	15	12	16	25	27	15	14	5	521	Nov 12 Friday
317	15	30	11	33	17	19	25	35	18	37	27	23	54	23	31	22	23	18	8	16	16	28	25	21	575	Nov 13 Saturday
318	22	24	28	26	10	14	21	25	19	9	6	8	5	18	9	17	1	9	7	5	3	12	3	7	308	Nov 14 Sunday
319	3	3	5	14	85	38	53	38	38	38	30	25	26	38	36	56	41	29	13	8	14	3	3	7	644	Nov 15 Monday
320	14	10	20	27	28	34	45	39	42	36	31	40	42	25	34	57	19	18	19	3	8	4	8	5	608	Nov 16 Tuesday
321	8	4	9	19	23	43	26	49	41	22	25	34	31	19	11	9	14	11	11	11	6	10	10	13	459	Nov 17 Wednesday
322	13	6	17	20	22	27	28	29	21	23	23	19	14	22	9	16	15	21	13	16	8	6	9	8	405	Nov 18 Thursday
323	2	19	14	16	35	21	24	24	37	27	41	22	25	47	9	22	14	11	4	3	5	8	6	6	442	Nov 19 Friday
324	4	8	7	4	15	13	18	31	30	29	26	34	21	54	9	9	13	8	21	25	5	11	34	21	450	Nov 20 Saturday
325	24	21	20	3	1	11	7	19	4	12	7	6	10	9	6	16	4	13	6	12	24	24	38	18	315	Nov 21 Sunday
326	31	22	33	35	33	37	57	30	31	13	21	20	21	28	16	16	17	33	36	29	43	41	51	42	736	Nov 22 Monday
327	35	33	42	39	50	43	56	32	57	46	36	38	54	37	49	60	54	36	48	56	51	43	28	63	1086	Nov 23 Tuesday
328	26	7	6	16	23	21	27	33	31	25	12	16	31	34	25	17	10	5	3	5	3	2	8	5	391	Nov 24 Wednesday
329	14	7	5	15	22	32	22	35	23	38	11	19	12	20	21	20	3	11	4	15	13	11	5	12	390	Nov 25 Thursday

Table 3.5.5 (Page 1 of 4)

APA .FKX Hourly distribution of detections

Day	00	01	02	03	04	05	06	07	08	09	10	11	12	13	14	15	16	17	18	19	20	21	22	23	Sum	Date
330	1	0	20	14	28	30	17	16	18	30	39	26	42	25	24	34	54	32	33	15	21	30	38	39	626	Nov 26 Friday
331	30	14	15	8	11	10	16	13	14	28	35	19	13	13	2	18	8	13	0	5	8	8	7	7	315	Nov 27 Saturday
332	1	0	11	7	4	10	3	5	5	5	0	6	6	8	2	6	0	7	3	3	3	5	12	11	123	Nov 28 Sunday
333	5	3	14	15	29	45	39	48	38	19	26	29	38	29	30	31	25	13	11	28	45	17	0	3	580	Nov 29 Monday
334	1	3	11	10	21	28	26	22	20	27	12	25	29	21	17	17	10	6	22	27	22	26	30	27	460	Nov 30 Tuesday
335	27	33	36	39	37	28	16	40	31	27	20	48	49	21	17	22	23	25	18	15	22	26	18	29	667	Dec 01 Wednesday
336	44	47	42	30	29	35	31	30	38	23	24	46	18	37	25	14	31	25	43	40	43	55	60	36	846	Dec 02 Thursday
337	34	30	54	80	50	77	61	80	56	53	28	45	61	50	24	33	31	49	41	53	46	49	51	46	1182	Dec 03 Friday
338	63	74	46	79	70	71	33	34	45	43	46	69	54	56	54	49	68	59	70	65	63	28	32	56	1327	Dec 04 Saturday
339	49	69	86	88	106	122	105	73	75	79	71	57	32	20	28	31	24	33	33	25	33	9	13	5	1266	Dec 05 Sunday
340	11	3	7	12	16	21	27	37	15	16	12	27	37	19	13	17	11	7	10	9	7	18	6	7	365	Dec 06 Monday
341	6	7	8	11	7	13	18	16	13	12	8	12	31	13	22	7	18	5	8	8	6	6	4	2	261	Dec 07 Tuesday
342	0	3	8	9	24	25	15	15	23	17	5	30	24	11	18	17	10	13	22	10	14	10	14	26	363	Dec 08 Wednesday
343	1	10	22	35	40	30	33	26	27	18	16	28	21	24	32	31	21	27	31	7	15	14	15	11	535	Dec 09 Thursday
344	3	9	24	19	29	26	32	29	24	33	30	29	62	18	22	13	8	16	16	16	7	4	9	3	481	Dec 10 Friday
345	8	9	3	5	0	9	17	6	0	0	0	0	0	0	0	0	0	0	0	0	0	0	0	0	57	Dec 11 Saturday
346	0	0	0	0	0	0	0	0	0	0	0	0	0	0	0	0	0	0	0	0	0	0	0	0	0	Dec 12 Sunday
347	0	0	0	0	0	0	0	0	0	0	0	0	0	0	0	0	0	0	0	0	0	0	0	0	0	Dec 13 Monday
348	0	0	0	0	0	0	0	0	0	0	0	0	0	0	0	0	0	0	0	0	0	0	0	0	0	Dec 14 Tuesday
349	0	0	0	0	0	0	0	0	0	0	0	0	0	0	0	0	0	0	0	0	0	0	0	0	0	Dec 15 Wednesday
350	0	0	0	0	0	0	0	0	0	0	0	0	0	0	0	0	0	0	0	0	0	0	0	0	0	Dec 16 Thursday
351	0	0	0	0	0	0	0	0	0	0	0	0	0	0	0	0	0	0	0	0	0	0	0	0	0	Dec 17 Friday
352	0	0	0	0	0	0	0	0	0	0	0	0	0	0	0	0	0	0	0	0	0	0	0	0	0	Dec 18 Saturday
353	0	0	0	0	0	0	0	0	0	0	0	0	0	0	0	0	0	0	0	0	0	0	0	0	0	Dec 19 Sunday
354	0	0	0	0	0	0	0	0	0	0	0	0	0	0	0	0	0	0	0	0	0	0	0	0	0	Dec 20 Monday
355	0	0	0	0	0	0	0	0	0	0	0	0	0	0	0	0	0	0	0	0	0	0	0	0	0	Dec 21 Tuesday
356	0	0	0	0	0	0	0	0	0	0	0	0	0	0	0	0	0	0	0	0	0	0	0	0	0	Dec 22 Wednesday
357	0	0	0	0	0	0	0	0	0	0	0	0	0	0	0	0	0	0	0	0	0	0	0	0	0	Dec 23 Thursday
358	0	0	0	0	0	0	0	0	0	0	0	0	0	0	0	0	0	0	0	0	0	0	0	0	0	Dec 24 Friday
359	0	0	0	0	0	0	0	0	0	0	0	0	0	0	0	0	0	0	0	0	0	0	0	0	0	Dec 25 Saturday
360	0	0	0	0	0	0	0	0	0	0	0	0	0	0	0	0	0	0	0	0	0	0	0	0	0	Dec 26 Sunday
361	0	0	0	0	0	0	0	0	0	0	0	0	0	0	0	0	0	0	0	0	0	0	0	0	0	Dec 27 Monday
362	0	0	0	0	0	0	0	0	0	0	0	0	0	0	0	0	0	0	0	0	0	0	0	0	0	Dec 28 Tuesday
363	0	0	0	0	0	0	0	0	0	0	0	0	0	0	0	0	0	0	0	0	0	0	0	0	0	Dec 29 Wednesday
364	0	0	0	0	0	0	0	0	0	0	0	0	0	0	0	0	0	0	0	0	0	0	0	0	0	Dec 30 Thursday
365	0	0	0	0	0	0	0	0	0	0	0	0	0	0	0	0	0	0	0	0	0	0	0	0	0	Dec 31 Friday
1	0	0	0	0	0	0	0	0	0	0	0	0	0	0	0	0	0	0	0	0	0	0	0	0	0	Jan 01 Saturday
2	0	0	0	0	0	0	0	0	0	0	0	0	0	0	0	0	0	0	0	0	0	0	0	0	0	Jan 02 Sunday
3	0	0	0	0	0	0	0	0	0	0	0	0	0	0	0	0	0	0	0	0	0	0	0	0	0	Jan 03 Monday
4	0	0	0	0	0	0	0	0	0	0	0	0	0	0	0	0	0	0	0	0	0	0	0	0	0	Jan 04 Tuesday
5	0	0	0	0	0	0	0	0	0	0	0	0	0	0	0	0	0	0	0	0	0	0	0	0	0	Jan 05 Wednesday
6	0	0	0	0	0	0	0	0	0	0	0	0	0	0	0	0	0	0	0	0	0	0	0	0	0	Jan 06 Thursday
7	0	0	0	0	0	0	0	0	0	0	0	0	0	0	0	0	0	0	0	0	0	0	0	0	0	Jan 07 Friday
8	0	0	0	0	0	0	0	0	0	0	0	0	0	0	0	0	0	0	0	0	0	0	0	0	0	Jan 08 Saturday
9	0	0	0	0	0	0	0	0	0	0	0	0	0	0	0	0	0	0	0	0	0	0	0	0	0	Jan 09 Sunday
10	0	0	0	0	0	0	0	0	0	0	0	0	0	0	0	0	0	0	0	0	0	0	0	0	0	Jan 10 Monday
11	0	0	0	0	0	0	0	0	0	0	0	0	0	0	0	0	0	0	0	0	0	0	0	0	0	Jan 11 Tuesday
12	0	0	0	0	0	0	0	0	0	0	0	0	0	0	0	0	0	0	0	0	0	0	0	0	0	Jan 12 Wednesday
13	0	0	0	0	0	0	0	0	0	0	0	0	0	0	0	0	0	0	0	0	0	0	0	0	0	Jan 13 Thursday
14	0	0	0	0	0	0	0	0	0	0	0	0	0	0	0	0	0	0	0	0	0	0	0	0	0	Jan 14 Friday
15	0	0	0	0	0	0	0	0	0	0	0	0	0	0	0	0	0	0	0	0	0	0	0	0	0	Jan 15 Saturday
16	0	0	0	0	0	0	0	0	0	0	0	0	0	0	0	0	0	0	0	0	0	0	0	0	0	Jan 16 Sunday
17	0	0	0	0	0	0	0	0	0	0	0	0	0	0	0	0	0	0	0	0	0	0	0	0	0	Jan 17 Monday
18	0	0	0	0	0	0	0	0	0	0	0	0	0	0	0	0	0	0	0	0	0	0	0	0	0	Jan 18 Tuesday
19	0	0	0	0	0	0	0	0	0	0	0	0	0	0	0	0	0	0	0	0	0	0	0	0	0	Jan 19 Wednesday
20	0	0	0	0	0	0	0	0	0	0	0	0	0	0	0	0	0	0	0	0	0	0	0	0	0	Jan 20 Thursday

Table 3.5.5 (Page 2 of 4)

APA .FKX Hourly distribution of detections

Day	00	01	02	03	04	05	06	07	08	09	10	11	12	13	14	15	16	17	18	19	20	21	22	23	Sum	Date
21	0	0	0	0	0	0	0	0	0	0	0	0	0	0	0	0	0	0	0	0	0	0	0	0	0	Jan 21 Friday
22	0	0	0	0	0	0	0	0	0	0	0	0	0	0	0	0	0	0	0	0	0	0	0	0	0	Jan 22 Saturday
23	0	0	0	0	0	0	0	0	0	0	0	0	0	0	0	0	0	0	0	0	0	0	0	0	0	Jan 23 Sunday
24	1	4	3	5	3	15	16	6	21	17	5	4	11	6	7	4	1	6	12	3	8	3	1	1	163	Jan 24 Monday
25	9	1	5	7	11	22	21	21	16	12	14	25	15	12	6	11	6	9	9	5	3	6	9	2	257	Jan 25 Tuesday
26	5	3	10	9	19	6	29	33	20	10	28	9	39	18	20	15	8	4	9	10	4	8	6	6	328	Jan 26 Wednesday
27	10	5	6	13	10	26	11	19	28	16	12	10	17	10	4	21	13	9	4	5	8	6	7	4	274	Jan 27 Thursday
28	10	5	18	9	14	15	19	22	10	9	31	16	43	10	3	21	8	12	14	6	0	1	13	7	316	Jan 28 Friday
29	15	1	4	4	3	3	4	4	15	3	11	31	17	4	2	5	7	5	2	2	5	0	2	2	151	Jan 29 Saturday
30	5	5	6	3	16	10	5	3	6	8	12	13	5	7	8	8	9	2	6	4	11	9	7	17	185	Jan 30 Sunday
31	13	10	14	4	21	15	11	20	13	17	11	11	16	18	6	8	11	9	12	13	5	4	3	10	275	Jan 31 Monday
32	2	11	9	3	10	7	18	12	14	17	8	4	8	9	5	16	8	3	6	14	0	2	10	7	203	Feb 01 Tuesday
33	3	6	3	15	15	13	25	22	7	23	14	23	12	12	10	15	16	7	9	5	16	6	11	8	296	Feb 02 Wednesday
34	9	11	17	11	22	19	19	17	17	28	15	30	16	14	6	19	7	14	43	30	32	13	6	4	419	Feb 03 Thursday
35	6	9	12	5	9	14	17	10	10	9	13	14	20	23	19	14	9	6	1	0	0	7	13	35	275	Feb 04 Friday
36	21	7	5	6	6	12	9	13	14	18	10	40	39	11	31	8	6	7	10	3	0	1	7	49	333	Feb 05 Saturday
37	4	3	1	6	13	18	4	8	56	15	50	4	37	2	4	4	5	1	0	16	29	34	46	5	365	Feb 06 Sunday
38	8	2	0	10	12	16	24	21	11	19	22	16	4	9	16	14	5	2	4	5	3	3	0	4	230	Feb 07 Monday
39	1	3	2	18	10	15	21	21	7	6	16	20	37	8	10	55	16	4	2	10	9	3	1	2	297	Feb 08 Tuesday
40	1	0	4	15	9	31	11	31	13	5	18	9	9	23	17	7	15	6	5	3	8	2	5	2	249	Feb 09 Wednesday
41	20	5	20	15	14	16	15	19	13	6	8	60	31	14	11	21	9	6	15	12	18	22	19	14	403	Feb 10 Thursday
42	29	14	10	6	15	10	27	12	27	5	21	27	30	15	20	14	10	14	11	9	14	17	23	3	383	Feb 11 Friday
43	7	12	3	14	12	10	7	12	18	12	31	25	9	9	4	0	5	9	27	10	8	10	2	2	258	Feb 12 Saturday
44	9	2	2	4	7	9	17	30	8	7	4	9	8	5	5	4	2	5	6	3	2	3	1	16	168	Feb 13 Sunday
45	5	8	4	6	10	5	17	13	13	14	23	32	10	8	6	8	3	6	5	7	11	19	10	14	257	Feb 14 Monday
46	2	18	11	14	9	11	10	11	18	8	38	23	12	27	11	51	42	32	26	50	19	69	26	17	555	Feb 15 Tuesday
47	12	9	12	15	27	11	17	13	17	11	20	51	16	18	8	18	5	15	6	7	3	3	17	13	344	Feb 16 Wednesday
48	21	12	16	18	25	28	41	58	46	23	18	25	29	19	11	11	9	12	40	31	16	17	25	16	567	Feb 17 Thursday
49	4	20	20	16	28	52	46	34	25	36	20	47	36	32	15	22	9	16	16	12	13	11	40	63	633	Feb 18 Friday
50	61	83	161	180	167	82	77	99	102	117	99	73	55	28	7	8	11	8	6	8	19	10	5	9	1475	Feb 19 Saturday
51	6	4	7	6	12	3	2	10	4	3	14	9	2	8	3	21	5	9	10	10	1	12	18	15	194	Feb 20 Sunday
52	6	2	9	8	43	29	40	36	33	26	13	14	7	11	4	5	5	8	5	4	2	3	2	2	317	Feb 21 Monday
53	4	2	2	9	15	20	22	20	26	19	28	19	15	13	8	16	10	12	6	7	7	22	8	9	319	Feb 22 Tuesday
54	1	4	6	18	10	38	22	18	26	25	26	22	10	11	12	16	7	8	13	3	4	2	8	9	319	Feb 23 Wednesday
55	19	3	0	18	21	34	54	39	30	25	21	30	44	15	17	18	11	12	17	9	6	9	1	7	460	Feb 24 Thursday
56	6	10	9	34	22	34	44	40	47	37	22	30	34	57	92	61	62	59	60	59	60	60	60	61	1060	Feb 25 Friday
57	59	60	61	60	64	65	62	87	69	29	21	30	34	6	14	25	30	28	30	20	20	38	15	28	955	Feb 26 Saturday
58	24	3	22	54	35	27	24	33	16	3	8	14	31	13	19	17	12	8	3	8	5	8	5	2	394	Feb 27 Sunday
59	7	4	9	15	26	27	24	34	16	20	16	26	20	14	21	22	23	14	18	8	12	5	6	3	390	Feb 28 Monday
60	10	6	13	42	35	51	46	55	15	21	26	12	32	7	14	13	20	7	6	14	5	5	4	8	467	Mar 01 Tuesday
61	13	11	12	21	11	16	15	10	15	20	18	11	18	10	7	8	4	5	4	7	3	8	5	4	256	Mar 02 Wednesday
62	8	5	9	17	28	64	90	58	39	31	11	26	31	15	10	18	32	20	17	8	9	11	6	15	578	Mar 03 Thursday
63	21	5	17	20	33	46	51	35	61	31	36	54	56	26	14	9	13	6	20	8	7	6	6	13	594	Mar 04 Friday
64	1	1	6	13	10	10	24	9	18	8	8	20	22	3	4	9	18	24	10	26	42	17	9	10	322	Mar 05 Saturday
65	6	13	30	25	21	24	25	22	34	46	32	49	50	61	55	52	32	42	42	49	45	73	32	22	882	Mar 06 Sunday
66	6	21	28	33	41	36	50	21	30	33	28	11	29	30	23	16	17	12	6	4	5	0	0	8	488	Mar 07 Monday
67	3	4	7	10	3	8	5	14	6	13	20	3	7	1	2	3	5	14	8	10	8	5	2	9	170	Mar 08 Tuesday
68	1	3	5	9	31	15	18	21	13	12	15	24	18	14	13	21	1	3	3	7	20	14	2	26	309	Mar 09 Wednesday
69	7	6	3	9	17	12	23	38	23	27	22	11	0	2	9	5	8	11	3	14	8	1	8	25	292	Mar 10 Thursday
70	1	5	2	21	19	44	51	38	44	24	29	22	30	20	12	11	6	1	10	9	2	14	2	2	419	Mar 11 Friday
71	3	1	12	2	11	12	15	5	4	20	4	24	8	6	6	11	3	2	1	3	0	0	1	5	159	Mar 12 Saturday
72	0	0	3	5	2	11	2	35	18	3	1	2	7	3	4	6	2	3	4	1	5	3	0	0	120	Mar 13 Sunday
73	4	1	3	3	16	11	11	28	20	20	12	19	9	16	28	20	5	6	7	10	9	34	21	30	343	Mar 14 Monday
74	25	11	9	13	31	40	44	20	33	40	21	62	43	42	56	57	20	11	20	8	31	25	26	17	705	Mar 15 Tuesday
75	16	15	13	10	23	20	57	26	27	24	26	43	29	22	19	18	19	6	10	2	7	6	6	10	454	Mar 16 Wednesday
76	9	2	10	17	23	38	32	44	21	11	6	18	39	28	10	5	9	14	6	0	7	0	3	12	364	Mar 17 Thursday

Table 3.5.5 (Page 3 of 4)

APA .FKX Hourly distribution of detections

Day	00	01	02	03	04	05	06	07	08	09	10	11	12	13	14	15	16	17	18	19	20	21	22	23	Sum	Date
77	6	5	9	6	24	31	42	29	58	31	35	28	44	16	3	11	8	10	15	3	7	0	1	2	424	Mar 18 Friday
78	2	21	2	6	8	15	17	12	5	18	8	27	1	6	2	7	9	21	9	11	7	2	0	5	221	Mar 19 Saturday
79	0	4	3	5	15	15	14	8	7	18	6	3	6	3	5	12	11	7	11	5	4	5	7	4	178	Mar 20 Sunday
80	2	1	8	19	18	47	67	47	25	20	14	24	20	17	23	19	18	21	11	6	13	14	8	3	465	Mar 21 Monday
81	6	6	3	7	35	18	39	47	30	21	26	33	115	189	91	20	23	13	15	15	8	7	9	5	781	Mar 22 Tuesday
82	4	9	7	30	27	45	69	51	34	22	10	17	59	14	22	25	30	25	14	10	21	15	17	13	590	Mar 23 Wednesday
83	8	9	15	22	27	27	18	30	17	42	16	23	16	30	18	21	20	20	42	19	10	4	6	14	474	Mar 24 Thursday
84	15	9	11	17	34	38	66	57	35	51	28	17	63	18	21	23	14	9	4	12	19	15	17	21	614	Mar 25 Friday
85	19	26	28	32	47	76	94	65	103	69	94	118	111	83	58	46	59	57	49	62	34	57	40	20	1447	Mar 26 Saturday
86	17	11	13	14	30	9	36	14	3	15	9	23	18	7	15	2	8	5	6	0	3	5	12	12	287	Mar 27 Sunday
87	16	2	10	32	27	45	44	41	32	80	24	12	19	18	17	8	5	17	7	11	0	3	4	6	480	Mar 28 Monday
88	18	2	22	29	41	35	56	4	9	8	5	2	12	12	13	12	11	7	8	3	0	3	3	3	318	Mar 29 Tuesday
89	3	5	17	19	18	17	10	42	16	15	32	27	13	11	10	6	5	11	10	8	17	9	1	1	323	Mar 30 Wednesday
90	8	2	14	12	16	45	20	10	10	5	24	7	26	21	10	9	3	8	7	5	10	7	22	12	313	Mar 31 Thursday
APA	00	01	02	03	04	05	06	07	08	09	10	11	12	13	14	15	16	17	18	19	20	21	22	23		
Sum	1589	2853	4100	4555	3756	3940	3577	3056	2463	2084	2090	1861														
	1838	2083	3634	4531	3872	3535	4376	3154	2523	2286	2094	1896													71746	Total sum
139	13	11	15	21	26	29	33	33	28	27	25	28	31	26	23	22	18	18	16	15	15	15	14	13	516	Total average
99	13	10	14	20	28	31	36	35	30	29	26	29	35	29	25	25	20	19	18	16	16	16	14	14	546	Average workdays
40	14	15	18	22	22	25	24	26	23	23	23	26	22	17	16	16	14	15	13	13	13	13	14	12	439	Average weekends

Table 3.5.5. Daily and hourly distribution of Apatity array detections. For each day is shown number of detections within each hour of the day, and number of detections for that day. The end statistics give total number of detections distributed for each hour and the total sum of detections during the period. The averages show number of processed days, hourly distribution and average per processed day.

SPI .FKX Hourly distribution of detections

Day	00	01	02	03	04	05	06	07	08	09	10	11	12	13	14	15	16	17	18	19	20	21	22	23	Sum	Date
274	9	1	0	1	0	3	1	3	12	8	1	7	4	2	3	4	0	2	6	3	0	1	5	2	78	Oct 01 Friday
275	2	3	2	3	1	3	3	2	4	4	3	1	3	2	6	6	2	10	2	7	0	4	2	3	78	Oct 02 Saturday
276	10	0	1	1	3	4	3	6	2	8	0	2	5	4	0	6	0	1	8	3	3	0	1	1	72	Oct 03 Sunday
277	6	0	0	2	3	1	6	1	1	2	0	0	5	1	1	6	3	10	13	8	0	2	4	1	76	Oct 04 Monday
278	7	2	8	7	11	5	2	2	13	4	6	1	5	2	2	4	4	5	1	5	4	17	8	5	130	Oct 05 Tuesday
279	9	6	4	7	3	7	6	6	7	3	2	4	3	3	12	2	4	3	4	3	2	5	3	6	114	Oct 06 Wednesday
280	3	1	4	12	6	1	2	0	10	3	6	3	4	1	2	2	1	5	10	3	0	0	1	0	80	Oct 07 Thursday
281	1	2	0	0	2	2	1	2	2	5	2	1	3	2	2	0	0	0	3	1	3	3	1	1	39	Oct 08 Friday
282	1	1	2	0	4	0	0	1	1	4	0	1	0	2	4	1	2	5	0	1	0	1	1	8	40	Oct 09 Saturday
283	2	5	5	3	3	2	0	1	0	0	2	7	6	1	0	0	0	3	2	1	0	2	1	2	48	Oct 10 Sunday
284	0	0	5	6	2	5	0	9	6	3	1	7	0	8	6	0	4	1	4	7	1	1	2	1	79	Oct 11 Monday
285	1	4	1	1	2	3	1	3	2	3	0	10	1	6	2	7	8	5	0	6	4	8	7	1	86	Oct 12 Tuesday
286	2	4	6	7	6	4	2	4	3	2	0	1	0	3	3	5	2	2	2	1	2	0	1	1	63	Oct 13 Wednesday
287	2	3	3	2	0	3	1	6	5	2	1	3	5	5	3	2	1	1	3	2	3	2	2	7	67	Oct 14 Thursday
288	3	1	0	4	4	5	7	0	2	3	2	2	4	3	1	0	3	5	1	3	9	0	1	1	64	Oct 15 Friday
289	2	3	0	3	5	1	3	2	12	5	1	6	7	6	2	5	10	10	8	7	7	6	5	3	119	Oct 16 Saturday
290	8	5	4	1	1	2	13	2	0	2	0	9	0	13	1	2	3	2	3	5	12	6	2	7	103	Oct 17 Sunday
291	12	2	8	1	1	1	4	3	4	14	4	0	6	6	4	7	1	7	2	1	4	6	3	7	108	Oct 18 Monday
292	4	0	1	3	6	7	2	2	0	1	3	1	2	14	0	2	0	0	5	0	0	3	1	16	73	Oct 19 Tuesday
293	34	4	7	4	0	3	1	2	1	1	3	1	9	10	1	2	13	2	4	2	0	3	3	0	110	Oct 20 Wednesday
294	6	1	3	6	3	27	9	6	5	5	9	4	3	2	3	5	2	1	2	6	4	1	7	4	124	Oct 21 Thursday
295	4	2	1	3	2	4	4	1	0	0	2	3	1	2	0	1	2	5	0	1	8	2	1	0	49	Oct 22 Friday
296	2	5	3	4	2	8	0	1	2	3	6	18	16	18	4	18	7	28	24	15	12	2	2	1	201	Oct 23 Saturday
297	4	9	5	3	6	0	7	3	11	10	6	0	1	2	2	4	0	2	4	1	3	1	8	0	92	Oct 24 Sunday
298	2	15	4	5	0	2	0	2	1	11	6	5	0	6	5	1	5	0	1	2	1	5	3	4	86	Oct 25 Monday
299	10	4	4	5	2	3	0	3	9	2	1	18	3	8	2	2	0	2	1	2	5	3	0	3	92	Oct 26 Tuesday
300	6	1	7	3	4	6	5	0	0	3	0	1	5	3	0	3	4	0	1	1	1	2	1	4	61	Oct 27 Wednesday
301	0	1	2	0	1	1	2	1	4	1	0	0	2	1	1	2	2	0	6	3	5	3	2	1	41	Oct 28 Thursday
302	4	6	0	6	5	1	0	3	4	0	0	3	3	1	0	2	0	1	3	0	2	0	0	0	44	Oct 29 Friday
303	0	0	1	2	0	1	0	0	7	0	3	2	7	5	0	2	3	3	3	4	4	1	8	0	56	Oct 30 Saturday
304	11	8	0	3	2	4	0	0	0	4	4	0	1	1	2	2	1	5	4	2	9	3	1	3	70	Oct 31 Sunday
305	5	5	2	2	5	15	5	4	1	3	2	7	3	4	4	0	0	0	0	0	0	4	3	0	74	Nov 01 Monday
306	0	2	1	1	2	2	1	2	2	0	0	2	3	1	4	2	3	1	0	5	9	1	16	6	66	Nov 02 Tuesday
307	5	1	2	1	5	2	1	2	4	5	10	10	8	9	6	3	5	1	10	6	2	0	2	4	104	Nov 03 Wednesday
308	7	2	1	0	1	7	6	14	13	1	7	2	1	6	0	7	1	0	1	0	0	2	9	3	91	Nov 04 Thursday
309	2	0	1	0	1	3	1	9	0	3	5	1	2	3	2	4	4	6	5	4	4	4	4	6	74	Nov 05 Friday
310	4	2	8	7	6	5	12	11	11	5	4	3	2	1	11	6	2	2	12	0	6	1	2	12	135	Nov 06 Saturday
311	2	0	4	6	0	3	3	3	8	2	2	3	0	12	5	5	0	4	2	0	3	1	0	4	72	Nov 07 Sunday
312	3	7	3	3	1	0	6	9	2	3	2	4	3	2	5	2	4	3	3	0	5	2	0	1	73	Nov 08 Monday
313	0	1	2	2	4	8	1	23	0	6	4	2	12	3	1	2	0	2	2	1	3	2	0	0	81	Nov 09 Tuesday
314	9	3	4	2	1	5	5	4	13	22	29	12	26	10	19	8	6	6	5	0	1	2	3	1	196	Nov 10 Wednesday
315	11	1	0	5	3	1	6	2	0	2	2	1	1	2	0	2	0	3	1	4	1	0	2	1	51	Nov 11 Thursday
316	6	0	2	2	1	2	2	13	8	10	15	31	7	7	2	3	7	5	1	2	5	7	1	3	142	Nov 12 Friday
317	3	7	4	1	2	6	11	6	2	6	1	8	2	5	10	0	2	0	2	4	0	6	2	1	91	Nov 13 Saturday
318	2	0	8	0	4	1	5	0	1	1	3	3	7	9	0	1	2	1	0	0	0	1	1	6	56	Nov 14 Sunday
319	2	4	2	3	3	13	2	0	1	0	1	2	2	12	10	14	1	9	0	3	3	4	3	1	95	Nov 15 Monday
320	3	1	2	1	3	2	14	21	6	1	6	3	1	1	0	9	34	2	19	13	6	16	3	4	171	Nov 16 Tuesday
321	9	5	3	2	1	2	5	2	5	6	7	10	4	2	0	9	2	2	10	5	1	5	5	5	107	Nov 17 Wednesday
322	2	4	2	6	1	5	5	5	3	7	0	1	6	10	0	1	3	2	8	4	8	1	9	1	94	Nov 18 Thursday
323	0	7	17	18	13	7	10	14	7	2	6	5	4	2	7	2	3	2	3	2	2	4	5	3	145	Nov 19 Friday
324	2	6	0	5	0	2	0	1	2	3	0	1	6	1	6	4	2	1	5	3	2	0	6	6	64	Nov 20 Saturday
325	4	4	2	5	1	5	6	2	2	6	6	5	2	4	6	14	8	7	8	11	4	6	9	7	134	Nov 21 Sunday
326	11	6	4	9	5	7	0	2	2	3	1	1	4	2	2	2	3	0	3	3	0	1	4	0	75	Nov 22 Monday
327	7	4	1	3	2	6	10	3	4	5	1	5	4	19	10	5	9	3	13	10	5	3	7	4	143	Nov 23 Tuesday
328	4	10	14	3	5	3	9	3	7	4	4	4	2	2	0	1	1	3	1	6	8	4	1	4	103	Nov 24 Wednesday
329	3	0	1	6	4	2	0	0	1	4	1	1	6	1	0	3	2	5	3	1	0	1	3	6	54	Nov 25 Thursday

Table 3.5.6 (Page 1 of 4)

SPI .FKX Hourly distribution of detections

Day	00	01	02	03	04	05	06	07	08	09	10	11	12	13	14	15	16	17	18	19	20	21	22	23	Sum	Date
330	3	0	0	2	4	1	2	7	4	5	2	2	1	1	1	1	0	4	6	7	4	2	4	0	63	Nov 26 Friday
331	0	4	3	0	3	4	6	6	2	0	0	1	1	3	5	5	0	3	3	2	4	1	12	18	86	Nov 27 Saturday
332	13	27	2	1	1	9	0	4	3	0	2	4	5	3	4	1	5	3	5	2	2	3	1	2	102	Nov 28 Sunday
333	6	7	12	5	29	7	6	4	1	4	3	5	10	3	1	3	2	5	4	1	7	2	0	2	129	Nov 29 Monday
334	1	3	5	0	1	3	1	4	2	6	4	6	1	4	2	22	3	1	2	0	1	4	0	1	77	Nov 30 Tuesday
335	1	1	3	2	5	1	3	3	2	5	4	2	10	7	0	4	1	1	9	4	13	6	6	0	93	Dec 01 Wednesday
336	2	2	3	2	2	3	7	1	2	7	0	4	3	1	3	3	4	0	0	2	0	0	1	6	58	Dec 02 Thursday
337	0	0	1	3	0	9	2	0	0	0	0	1	1	0	0	1	0	0	0	0	1	1	0	1	21	Dec 03 Friday
338	0	1	0	0	0	0	2	0	0	1	1	11	1	1	1	0	1	0	0	0	4	2	4	2	32	Dec 04 Saturday
339	1	0	1	4	0	0	0	0	2	1	2	1	1	6	1	0	4	2	0	2	2	0	0	2	32	Dec 05 Sunday
340	4	1	1	2	2	2	0	2	15	4	3	4	1	4	8	2	2	0	3	3	0	5	3	3	74	Dec 06 Monday
341	1	1	10	4	4	1	6	8	4	7	5	9	14	9	5	7	10	5	8	9	5	5	0	2	139	Dec 07 Tuesday
342	4	10	16	1	10	10	6	7	5	11	6	1	16	7	4	3	10	13	11	10	5	7	8	5	186	Dec 08 Wednesday
343	7	12	3	2	10	7	3	5	9	8	1	8	4	9	1	2	3	2	1	1	2	1	5	3	109	Dec 09 Thursday
344	0	1	2	6	7	0	2	0	0	4	4	1	2	2	0	1	0	0	0	1	1	0	0	1	35	Dec 10 Friday
345	0	0	2	0	0	1	2	1	1	2	2	2	1	2	1	2	2	1	2	0	1	0	1	1	27	Dec 11 Saturday
346	1	5	2	5	1	1	2	0	1	1	1	0	3	3	4	1	2	2	2	1	5	3	0	0	46	Dec 12 Sunday
347	8	0	2	0	1	1	2	0	0	2	1	2	0	1	0	0	0	1	0	0	2	1	0	1	25	Dec 13 Monday
348	3	6	5	13	1	0	3	2	2	3	0	3	2	1	0	0	1	1	0	1	1	3	2	0	53	Dec 14 Tuesday
349	3	0	3	6	1	5	6	4	5	2	2	12	2	2	0	1	8	11	6	2	8	11	18	3	121	Dec 15 Wednesday
350	3	3	7	6	2	4	0	1	9	0	1	0	2	2	5	6	2	3	0	0	6	0	2	5	69	Dec 16 Thursday
351	0	0	6	1	1	5	0	0	1	8	0	3	2	1	0	0	0	3	1	2	4	1	3	2	44	Dec 17 Friday
352	1	4	4	3	1	1	6	0	0	4	1	3	4	1	0	2	0	2	0	3	6	1	0	0	47	Dec 18 Saturday
353	1	2	8	0	6	0	2	0	0	0	4	2	1	1	0	1	0	0	1	1	0	0	5	1	36	Dec 19 Sunday
354	4	2	0	0	0	1	1	1	0	2	1	2	1	1	4	2	1	0	0	0	2	1	0	0	26	Dec 20 Monday
355	2	8	8	3	2	1	0	1	5	10	1	2	6	4	2	1	1	7	0	4	0	4	3	2	77	Dec 21 Tuesday
356	2	5	1	3	9	10	9	1	0	1	0	4	0	1	5	1	2	6	2	7	4	0	4	7	84	Dec 22 Wednesday
357	2	2	6	8	4	12	3	5	7	1	2	4	7	8	2	9	7	2	11	13	9	15	23	23	185	Dec 23 Thursday
358	34	34	21	24	19	24	13	9	4	6	13	2	5	0	13	3	4	4	1	4	14	5	17	22	295	Dec 24 Friday
359	9	14	3	3	1	1	2	0	0	0	1	4	6	0	0	3	0	5	0	0	0	23	1	1	77	Dec 25 Saturday
360	0	0	0	2	0	1	0	0	4	0	1	0	2	2	4	2	5	0	0	0	0	0	1	0	24	Dec 26 Sunday
361	0	2	1	1	1	5	0	8	4	2	3	3	0	4	5	3	6	3	3	1	9	5	7	7	83	Dec 27 Monday
362	4	0	3	7	16	11	10	4	1	3	3	7	0	1	1	0	4	1	5	1	5	0	5	2	94	Dec 28 Tuesday
363	0	3	0	1	0	1	1	0	9	0	3	3	3	3	1	0	10	3	5	2	5	1	0	6	60	Dec 29 Wednesday
364	1	0	1	0	0	0	3	2	0	12	3	0	0	3	7	3	1	0	3	0	8	7	2	5	61	Dec 30 Thursday
365	2	3	8	4	8	1	0	0	0	1	1	7	0	0	1	2	1	0	1	2	0	0	2	0	44	Dec 31 Friday
1	1	0	0	0	0	1	0	1	3	2	1	3	1	0	1	0	0	0	1	0	0	1	1	1	18	Jan 01 Saturday
2	1	0	0	1	9	0	0	5	3	2	0	0	0	2	0	0	1	0	0	0	0	1	0	6	31	Jan 02 Sunday
3	3	0	1	2	0	5	5	0	1	0	1	0	0	6	0	0	0	0	2	1	0	9	0	0	36	Jan 03 Monday
4	1	0	1	7	0	2	1	4	0	0	0	0	8	0	0	2	3	0	3	1	0	0	3	13	49	Jan 04 Tuesday
5	3	7	1	2	5	1	2	2	8	0	0	0	0	6	1	0	4	1	1	1	2	0	0	4	51	Jan 05 Wednesday
6	0	1	1	5	7	1	0	0	2	3	1	4	0	3	2	1	0	0	0	1	0	2	0	0	34	Jan 06 Thursday
7	7	2	0	3	1	0	0	2	0	2	1	4	0	0	0	0	0	2	0	1	1	6	0	0	32	Jan 07 Friday
8	0	0	0	0	0	0	9	0	0	0	0	6	0	1	2	1	1	0	2	1	4	0	1	1	29	Jan 08 Saturday
9	3	0	0	2	0	1	0	3	2	2	0	0	1	0	1	3	0	3	3	2	3	4	5	9	47	Jan 09 Sunday
10	12	7	11	12	3	1	8	2	6	2	6	5	6	9	10	14	22	32	44	28	35	24	15	8	322	Jan 10 Monday
11	9	11	6	2	4	6	4	15	5	19	3	5	2	1	3	2	4	4	3	2	2	7	13	3	135	Jan 11 Tuesday
12	1	0	5	2	0	10	3	1	1	11	11	3	11	6	6	8	3	8	0	15	11	15	12	21	164	Jan 12 Wednesday
13	20	11	12	12	23	15	14	16	14	14	12	18	14	5	17	31	13	33	25	19	38	47	30	32	485	Jan 13 Thursday
14	42	33	26	34	28	34	31	18	22	16	22	22	12	14	9	4	6	18	5	13	12	7	8	15	451	Jan 14 Friday
15	11	8	4	10	7	11	3	26	12	6	5	4	8	3	5	7	5	8	7	9	3	7	7	10	186	Jan 15 Saturday
16	2	5	3	5	0	2	1	4	6	6	3	7	6	13	1	5	2	5	12	4	0	11	3	8	114	Jan 16 Sunday
17	7	4	3	2	3	1	3	11	5	0	0	0	0	0	3	0	0	0	0	0	0	0	0	0	42	Jan 17 Monday
18	0	0	0	0	0	0	0	0	0	0	0	0	0	0	0	0	0	0	0	0	0	0	0	0	0	Jan 18 Tuesday
19	0	0	0	0	0	0	0	0	0	0	0	0	0	0	0	0	0	0	0	0	0	0	0	0	0	Jan 19 Wednesday
20	0	0	0	0	0	0	0	0	0	0	0	0	0	0	0	0	0	0	0	0	0	0	0	0	0	Jan 20 Thursday

Table 3.5.6 (Page 2 of 4)

SPI .FKX Hourly distribution of detections

Day	00	01	02	03	04	05	06	07	08	09	10	11	12	13	14	15	16	17	18	19	20	21	22	23	Sum	Date
21	0	0	0	0	0	0	0	0	0	0	0	0	0	0	0	0	0	0	0	0	0	0	0	0	0	Jan 21 Friday
22	0	0	0	0	0	0	0	0	0	0	0	0	0	0	0	0	0	0	0	0	0	0	0	0	0	Jan 22 Saturday
23	0	0	0	0	0	0	0	0	0	0	0	0	0	0	0	0	0	0	0	0	0	0	0	0	0	Jan 23 Sunday
24	0	0	0	0	0	0	0	0	0	0	0	0	0	0	0	0	0	0	0	0	0	0	0	0	0	Jan 24 Monday
25	0	0	0	0	0	0	0	0	0	0	0	0	0	0	0	0	0	0	0	0	0	0	0	0	0	Jan 25 Tuesday
26	0	0	0	0	0	0	0	0	0	0	0	0	0	0	0	0	0	0	0	0	0	0	0	0	0	Jan 26 Wednesday
27	0	0	0	0	0	0	0	0	0	0	0	0	0	0	0	0	0	0	0	0	0	0	0	0	0	Jan 27 Thursday
28	0	0	0	0	0	0	0	0	0	0	0	0	0	0	0	0	0	0	0	0	0	0	0	0	0	Jan 28 Friday
29	0	0	0	0	0	0	0	0	0	0	0	0	0	0	0	0	0	0	0	0	0	0	0	0	0	Jan 29 Saturday
30	0	0	0	0	0	0	0	0	0	0	0	0	0	0	0	0	0	0	0	0	0	0	0	0	0	Jan 30 Sunday
31	0	0	0	0	0	0	0	0	0	0	0	0	0	0	0	0	0	0	0	0	0	0	0	0	0	Jan 31 Monday
32	0	0	0	0	0	0	0	0	0	0	0	0	0	0	0	0	0	0	0	0	0	0	0	0	0	Feb 01 Tuesday
33	0	0	0	0	0	0	0	0	0	0	0	0	0	0	0	0	0	0	0	0	0	0	0	0	0	Feb 02 Wednesday
34	0	0	0	0	0	0	0	0	0	0	0	0	0	0	0	0	0	0	0	0	0	0	0	0	0	Feb 03 Thursday
35	0	0	0	0	0	0	0	0	0	0	0	0	0	0	0	5	1	5	3	6	2	4	0	1	27	Feb 04 Friday
36	2	2	3	1	2	0	0	0	1	0	2	2	0	4	0	0	1	4	0	5	0	3	0	5	37	Feb 05 Saturday
37	2	0	4	1	3	1	3	1	1	2	2	0	2	0	1	0	3	3	4	4	1	2	0	0	40	Feb 06 Sunday
38	3	0	1	7	1	2	0	0	1	2	5	7	1	1	3	2	2	3	2	1	0	0	4	0	48	Feb 07 Monday
39	6	0	5	7	5	5	5	2	2	0	0	2	0	1	0	0	0	4	11	1	7	4	1	0	68	Feb 08 Tuesday
40	3	1	3	5	4	0	2	0	3	5	9	4	4	20	18	4	12	3	2	8	6	13	11	21	161	Feb 09 Wednesday
41	12	16	19	8	10	10	6	11	2	6	0	8	13	8	10	0	1	4	13	2	1	7	3	3	173	Feb 10 Thursday
42	0	2	0	4	0	1	4	0	6	11	3	10	1	10	4	0	2	10	4	3	4	15	6	5	105	Feb 11 Friday
43	12	5	2	0	2	9	2	10	13	9	26	24	5	16	35	39	27	32	33	35	31	17	15	13	412	Feb 12 Saturday
44	0	0	0	0	0	0	0	0	0	21	25	44	43	57	48	24	0	0	0	0	0	0	0	0	262	Feb 13 Sunday
45	0	0	0	0	0	0	0	0	0	0	0	0	0	0	0	0	0	0	0	0	0	2	10	7	19	Feb 14 Monday
46	10	1	3	4	5	8	6	7	5	6	3	8	7	9	13	7	13	17	9	6	17	13	11	8	196	Feb 15 Tuesday
47	3	6	3	8	4	8	1	17	2	10	1	4	5	17	11	9	24	21	20	15	21	16	24	27	277	Feb 16 Wednesday
48	14	12	18	21	17	13	15	6	10	9	10	9	10	10	15	15	10	4	13	8	1	3	3	12	258	Feb 17 Thursday
49	5	7	4	4	5	5	5	9	2	1	3	8	1	1	1	3	9	8	11	13	14	15	25	25	184	Feb 18 Friday
50	33	32	32	41	36	26	19	18	15	15	15	10	11	7	10	7	6	3	12	3	1	12	15	15	394	Feb 19 Saturday
51	14	11	11	6	3	4	4	0	1	0	4	3	2	4	8	1	1	3	5	2	0	2	5	6	100	Feb 20 Sunday
52	2	5	8	7	4	8	3	2	2	3	1	0	1	2	2	8	6	8	3	9	7	4	3	14	112	Feb 21 Monday
53	9	6	15	17	11	16	19	17	17	18	20	17	16	18	16	27	23	27	33	44	35	27	29	15	492	Feb 22 Tuesday
54	35	38	34	35	35	22	23	10	17	13	8	6	7	9	10	6	11	16	7	6	26	14	24	36	448	Feb 23 Wednesday
55	20	15	20	20	20	16	9	26	15	7	26	11	14	20	8	17	16	20	13	10	11	7	12	14	367	Feb 24 Thursday
56	11	13	18	24	8	12	9	12	16	20	15	10	3	12	17	18	23	14	23	12	14	19	11	7	341	Feb 25 Friday
57	14	4	17	14	32	16	14	11	27	13	28	10	9	19	20	11	12	19	17	10	12	8	19	5	361	Feb 26 Saturday
58	16	7	10	10	19	5	12	17	16	3	8	7	7	9	5	8	19	9	2	5	4	4	4	1	207	Feb 27 Sunday
59	13	16	7	5	3	9	6	8	1	4	2	2	3	13	5	3	11	3	3	3	15	2	3	0	140	Feb 28 Monday
60	4	2	4	12	2	0	0	6	3	5	9	1	0	7	2	4	4	3	2	0	2	1	4	1	78	Mar 01 Tuesday
61	4	2	7	5	1	10	8	3	13	5	1	2	3	19	3	13	4	2	2	2	5	5	5	1	125	Mar 02 Wednesday
62	1	6	4	5	3	1	6	2	7	4	2	0	9	14	6	39	47	21	27	31	14	13	8	13	283	Mar 03 Thursday
63	7	0	3	2	0	3	1	4	4	0	8	1	5	8	5	4	4	0	21	2	5	1	1	3	92	Mar 04 Friday
64	2	1	1	5	7	6	10	10	6	10	4	0	7	2	1	1	6	5	7	12	6	3	22	10	144	Mar 05 Saturday
65	19	5	4	14	0	2	4	6	4	5	1	1	2	3	7	4	7	15	3	13	7	17	47	69	259	Mar 06 Sunday
66	11	15	15	17	19	17	37	20	59	76	70	89	101	171	103	115	76	54	62	26	26	45	29	20	1273	Mar 07 Monday
67	26	17	22	20	15	8	12	4	3	3	1	7	3	5	2	0	8	6	4	1	2	4	4	2	179	Mar 08 Tuesday
68	3	2	16	0	9	7	6	10	3	0	2	5	0	5	2	7	2	0	3	2	1	3	3	19	110	Mar 09 Wednesday
69	6	0	0	1	10	0	0	1	1	0	3	2	3	5	3	1	3	3	4	6	12	2	7	1	74	Mar 10 Thursday
70	1	12	13	6	1	17	3	3	5	4	3	5	1	9	3	7	3	3	7	8	0	6	1	1	122	Mar 11 Friday
71	0	2	14	5	1	4	1	3	6	1	0	0	2	6	3	4	2	1	0	2	1	1	1	2	62	Mar 12 Saturday
72	1	0	0	3	2	5	1	3	0	1	4	4	9	5	1	1	6	12	4	0	8	0	4	3	77	Mar 13 Sunday
73	8	3	9	4	8	5	6	1	4	5	6	3	4	10	1	2	5	4	2	3	8	7	1	0	109	Mar 14 Monday
74	0	8	0	5	0	0	6	4	3	3	1	4	1	4	0	2	4	2	8	4	6	6	3	1	75	Mar 15 Tuesday
75	4	7	2	3	4	5	10	4	2	4	13	12	6	8	26	31	20	3	6	18	9	1	7	13	218	Mar 16 Wednesday
76	4	0	1	2	10	1	5	5	12	8	0	3	0	2	6	8	4	2	0	0	2	2	2	2	81	Mar 17 Thursday

Table 3.5.6 (Page 3 of 4)

SPI .FKX Hourly distribution of detections

Day	00	01	02	03	04	05	06	07	08	09	10	11	12	13	14	15	16	17	18	19	20	21	22	23	Sum	Date
77	9	0	0	1	3	2	0	2	4	0	1	0	0	1	2	2	18	6	17	6	9	3	0	3	89	Mar 18 Friday
78	0	12	4	0	1	0	0	5	1	4	1	8	3	6	4	0	2	6	17	3	2	1	0	0	80	Mar 19 Saturday
79	5	6	1	0	1	3	3	5	1	4	1	4	5	2	2	2	11	2	0	2	2	6	2	4	74	Mar 20 Sunday
80	4	3	3	10	6	5	5	9	10	9	12	7	3	4	1	12	0	0	6	11	0	11	6	3	140	Mar 21 Monday
81	1	5	6	5	9	4	6	14	6	1	3	4	1	3	20	1	10	5	0	1	3	8	5	7	128	Mar 22 Tuesday
82	1	7	12	13	1	6	16	5	6	7	6	9	8	4	15	7	9	4	7	2	2	9	18	8	182	Mar 23 Wednesday
83	9	12	12	9	7	8	5	4	0	1	1	5	5	3	5	11	10	10	5	4	2	4	2	2	136	Mar 24 Thursday
84	1	5	1	2	11	9	0	6	5	11	6	3	7	5	7	7	8	12	10	7	10	8	20	8	169	Mar 25 Friday
85	5	10	1	1	1	2	2	5	8	7	15	20	10	13	5	13	18	21	37	17	16	16	18	25	286	Mar 26 Saturday
86	15	14	13	5	12	11	15	35	38	16	2	2	14	5	3	5	4	3	3	6	6	10	5	17	259	Mar 27 Sunday
87	7	12	6	12	5	2	3	19	3	3	3	2	8	3	3	2	1	5	5	3	1	5	4	7	124	Mar 28 Monday
88	8	4	3	9	8	6	6	3	13	7	10	4	2	3	4	10	6	19	12	4	9	22	10	4	186	Mar 29 Tuesday
89	10	9	7	12	7	12	3	4	0	6	6	18	10	12	1	4	9	4	6	6	8	4	2	7	167	Mar 30 Wednesday
90	9	4	4	9	5	2	3	2	3	3	2	25	8	4	10	16	20	3	4	12	20	11	4	10	193	Mar 31 Thursday
SPI	00	01	02	03	04	05	06	07	08	09	10	11	12	13	14	15	16	17	18	19	20	21	22	23		
Sum	828		893		855		856		852		938		1087		960		898		819		895		968			
	956		848		830		789		865		778		855		875		939		1000		886		922		21392	Total sum
165	6	5	5	5	5	5	5	5	5	5	5	6	5	7	5	6	6	5	6	5	5	5	6	6	130	Total average
116	6	5	5	6	5	6	5	5	5	5	5	5	5	7	5	6	6	5	6	5	6	6	6	6	132	Average workdays
49	5	5	4	4	4	4	4	5	5	4	4	6	5	6	5	5	4	5	6	5	4	4	5	6	115	Average weekends

Table 3.5.6. Daily and hourly distribution of Spitsbergen array detections. For each day is shown number of detections within each hour of the day, and number of detections for that day. The end statistics give total number of detections distributed for each hour and the total sum of detections during the period. The averages show number of processed days, hourly distribution and average per processed day.

3.6 IMS operation

The Intelligent Monitoring System (IMS) was installed at NORSAR in December 1989 and was operated at NORSAR from 1 January 1990 for automatic processing of data from ARCESS and NORESS. A second version of IMS that accepts data from an arbitrary number of arrays and single 3-component stations was installed at NORSAR in October 1991, and regular operation of the system comprising analysis of data from the 4 arrays ARCESS, NORESS, FINESS and GERESS started on 15 October 1991. As opposed to the first version of IMS, the one in current operation also locates events at teleseismic distance.

On 14 December 1992, phase detections from the Apatity array were included in the automatic phase association. Due to a malfunctioning power amplifier in the satellite ground station in Apatity, no Apatity data were available to IMS between 11 December 1993 and 26 January 1994. FINESS data were not used between 16 May 1993 and 12 January 1994 because of damage due to ligthning, and later an upgrade of the array. On 12 January 1994, phase detections from the Spitsbergen array were included in the automatic phase association.

The operational stability of IMS has been very good during the reporting period. In fact the IMS event processor (pipeline) has had no downtime of its own; i.e., all data available to IMS have been processed by IMS.

Phase and event statistics

Table 3.6.1 gives a sumary of phase detections and events declared by IMS. From top to bottom the table gives the total number of detections by the IMS, the number of detections that are associated with events automatically declared by the IMS, the number of detections that are not associated with any events, the number of events automatically declared by the IMS, the total number of events defined by the analyst, and finally the number of events accepted by the analyst without any changes (i.e., from the set of events automatically declared by the IMS)

Due to reductions in the FY94 funding for IMS activities (relative to previous years), new criteria for event analysis, effective from January 1, 1994 were introduced. Since that date, only regional events in areas of special interest (e.g, Spitsbergen, since it is necessary to acquire new knowledge in this region) or other significant events (e.g, felt earthquakes and large industrial explosions) have been thoroughly analyzed. Teleseismic events are analyzed as before. This is the reason for the drop in "No. of events accepted without modifications" in Table 3.6.1. Before January 1, 1994, all events declared by IMS were considered for manual analysis. Some were accepted unchanged, some were discarded as false alarms and the rest were modified in some way or another (phases had their phase-identification changed or their arrival time corrected etc.). After January 1, only interesting events (see above) are selected for manual analysis, and they are always corrected (one exception in January). The uninteresting events are discarded, whether they are real events or false alarms.

	Oct 93	Nov 93	Dec 93	Jan 94	Feb 94	Mar 94	Total
Phase detections	47242	44674	33345	26538	45452	48053	245304
-Associated phases	5540	6008	4988	5392	6672	7578	36178
-Unassociated phases	41702	38666	28357	21146	38780	40475	209126
Events automatically declared by IMS	1765	1873	1552	1712	2004	2305	11211
No. of events defined by the analyst	1483	1588	1309	301	361	422	5464
No. of events accepted without modifications	1005	1160	1119	1	0	0	3285

Table 3.6.1. IMS phase detections and event summary.

U. Baadshaug
B. Ferstad
B.Kr. Hokland
L.B. Loughran
B. Paulsen

4 Improvements and Modifications

4.1 NORSAR

NORSAR data acquisition

The NORSAR data acquisition system was changed on January 1, 1994.

Up to this date, the data was recorded on a 30-hours circular disk buffer on an IBM 4381 VM/CMS system, and archived onto 1/2 inch magnetic tapes. The data from the 7 subarrays were transmitted over 2400 bps leased lines between the Short and Long Period Electronic Modules (SLEMs) in the subarray vaults and a MODCOMP computer at NDPC. The timing was done centrally from one clock at NDPC by sending time commands from NDPC to SLEMs. Modernization of telecommunications led to severe problems for this system, that was using special modems for analog fixed telephone lines. New digital lines, speedconversions and unknown routings could no longer ensure the data quality and timing precision that the system was designed for.

As a consequence of the communication problems, and as a result of evaluations for the NORSAR refurbishment project, we installed a backup system during the last quarter of 1993. This backup system was put into operation on January 1, 1994.

Each subarray is now equipped with Nanometric digitizers and GPS clocks. The 6 SP instruments are sampled at 40 Hz, and the LP instrument is sampled at 1 Hz. The analog signals from the remote SP sensors are transmitted via the buried cables, and all data is digitized at the Central Terminal Vault - CTV. The digital data is transmitted over the old leased data lines, which has been upgraded to 9600 bauds with new modems. The data are now recorded on a SUN system in a 48-hour circular disk buffer, and archived on Exabyte casettes. A consequence of the system change is that the old format data tapes are no longer used, and data are formatted to CSS 3.0 for data requests.

The MODCOMP and IBM computers have been shut down.

The current NORSAR array center, subarray 02B, where sensor 00 has ISC code **NB2**, is used as reference station name for NORSAR readings.

See also the section on NORSAR refurbishment.

NORSAR detection processing

The NORSAR detection processor has been running satisfactorily on both the IBM 4381 computer and SUN computers up to December 31, 1993, and is now running on SUN computers only from January 1, 1994.

To maintain consistent detection capability, the NORSAR beam tables have not been changed. The DP program (Fyen, 1987) accepts commands for beamforming either specified by given velocity and azimuth or by given time delays. For NORSAR, all beams are

specified by time delays, such that time delay corrections can be included. Due to the size of the NORSAR array, beamforming using plane wave time delays alone, leads to significant loss of beam power. The 180 coherent and 64 inchorent beams are thus specified by time delays including the old known time delay corrections. (Berteussen, 1974).

Detection statistics for the NORSAR array are given in section 2.

NORSAR event processing

The routine processing of NORSAR events, using the IBM system, was cut off on December 31, 1993.

Routine event processing is now done on a SUN computer using the "old" IBM time delay correction data base that has been converted to SUN/OS-unix. The automatic solutions produced are equal to or better than the old system with a lower false alarm rate. Alert messages are sent to the USGS and European centers for events above magnitude 4.9.

All waveform data for all events are now automatically saved as CSS 3.0 files, and archived as event files on Exabyte tar casettes when the disk gets full. Events are plotted on Sparcprinter laser. An interactive analysis tool for NORSAR data has been developed, based on the EP program system, (Fyen, 1989), and the analysts have all events available on disk for quick reprocessing whenever necessary. The need for "rerun" has been reduced significantly as compared to the "old" system.

Some modifications in the NORSAR processing has been done, and we will introduce these in the following by describing large array processing techniques as opposed to regional array processes. The NORSAR processing differs from the regional array processing in the way of obtaining a slowness estimate. The sensor separation of the NORSAR array is up to 60 km as opposed to, e.g., 3 km for the NORESS array. The effect on the observed signal is that the large array has less coherent signals and it is a well known fact that the signals observed at the NORSAR array have great amplitude variations. So the size of the array leads to much larger time delays and less coherent signals, and the fk-analysis used for regional arrays to obtain an estimate of the slowness vector does not work well for the larger array. The technique used for the larger array is to beamform in the time domain to find the beam with the largest power. This process is called *beampacking*. The slowness that corresponds to the beam with maximum power (or STA) is then the observed slowness. This larger size of the array leads to much better resolution in apparent velocity as compared to the regional array. For a regional array the velocity component from fk-analysis can be used to classify the type of seismic phase. For the NORSAR array, the slowness can be used to classify the phase type and also used to obtain the epicentral distance from a slowness-distance table derived from some earth model. For a small array a location can be obtained by associating a P and S type regional phase with approximately the same azimuth. For a network of regional arrays, the observed slownesses for teleseimsic phases can be used to define and locate events at teleseismic distances. For the NORSAR array, the observed slowness alone is used to obtain a location estimate.

The NORSAR array is designed and used only to detect and locate events at teleseismic distances.

An example of an automatic event plot and bulletin for the NORSAR array is shown in Fig. 4.1.

When observing teleseismic phases across the NORSAR array, the estimated delays calculated for a plane wavefront do not fit exactly with observed delays. Using plane wave time delays for beamforming leads to a loss in beam power. By introduction of time delay corrections, significant improvement of beam power is obtained. (Berteussen,1974. See also Table 4.1)

In addition to building a data base with time delay corrections, a data base with slowness corrections for location calibration was established in 1974. This data base still give valuable corrections for the NORSAR array, but the data base itself is technically based on old IBM architecture disk files. The correction subroutines and disk file access routines have been converted to give identical results on SUN and the old IBM system. However, this data base is in today's technology outdated, and an effort to create a new data base is much needed.

Different methods have been developed to compensate for the amplitude variation over the NORSAR array. Weighted beamforming is one approach that has now been implemented in the new NORSAR event processor. RMS max values are computed for filtered, single sensors, and used as weights during the beampacking process and in the estimation of the best beam.

For automatic onset determination, the same process that is used for IMS arrival time estimation is applied. Amplitudes and periods are determined by a peak-to-trough search.

In addition to beampacking which starts with the detection beam slowness and searches the slowness space in a limited area, a new process called *beamscanning* form beams over the full slowness space, and the result is reported if the resulting beam power exceeds that of the beampacking process.

NORSAR array beams illustrating effects of time delay corrections and RMS weighting are shown in Table 4.1 and Fig. 4.2. It is clearly demonstrated that time delay corrections are important. Moreover, weighted beamforming gives a gain in signal amplitudes which is important both for detection and estimation of amplitude. An investigation of amplitude variations may be used to establish a fixed set of weights for the detecting beams.

Table 4.2 illustrates the location precision obtained by NORSAR alone compared to other agencies.

NORSAR refurbishment

During this reporting period we purchased 6 AIM24-1 digitizers and one AIM24-3 digitizer from Science Horizons. These 7 digitizers together with 7 GPS clocks were tested in the subarray 06C vault. We performed successfull recording of data at NDPC using an experimental VSAT communication link. The equipment has been returned for technical upgrade.

As a consequence of the testing and in agreement with AFTAC, we placed an order for 42 AIM24-1 and 7 AIM24-3 BB digitizers together with GPS clocks, and a communication and acquisition system at Science Horizons. Delivery is expected early July 1994.

Both short period and long period instruments from the old installation are functioning well although the long period instruments require a high amount of manual calibration. In accordance with AFTAC requirements, an order for 7 KS54000P broadband instruments from Teledyne Brown Engineering has been ordered. These instruments will replace the long period instruments.

The NORSAR array was built during the years 1967-1970. The array was originally over 100 km in diameter with 22 subarrays, each having 6 short period instruments and one three-component set of LP instruments. The array was reduced to 7 subarrays October 1, 1976. Each short period instrument is mounted in a 6 - 12 meter borehole in a Short Period Vault - SPV. There are 5 remote SPV's in each subarray in addition to a Long Period Vault - LPV and a Central Terminal Vault - CTV. The LPV houses the long period instruments and the 6th SP instrument. The CTV has AC power, telecommunication to NDPC and provides DC power to the remote SPV sites and the LPV. The LPV and SPV's are connected to the CTV with buried cables. The buried cable system is complicated. Typically a 12 pair cable goes to one SPV, and from that, two 6 pair cables go to two other SPVs. This leaves 2 pairs for communication and 2 pairs for power to three sites. The DC voltage is regulated to maximum 60 Volts DC, and the current delivered to the remote sites will be limited to 300 mA. The NORSAR refurbishment plan includes only partial replacement of these buried cables. The small number of pairs in each cable limits the possibilities for power and communication techniques. Some of the pairs are broken, which is OK for the existing system, but the new system requires all pairs. In such cases, the whole cable must be replaced.

The AIM24-1 digitizers will be placed in the SPV's. The HS-10 seismometers will not be replaced, but otherwise only the zinc tank of the SPV will be kept. See Fig. 4.3 for a description of the SPV.

The current Geotech 8700 LP seismometers will be removed from the LPV's together with all old electronics. AIM24-3BB will be installed, and boreholes will be prepared for the KS54000P instruments as well as for the 6th SP instrument. See Fig. 4.4 for a description of the LPV.

The CTV's will also be completely refurbished. The old electronic mounting racks will be kept to install new Communication Interface Modules - CIM, modem lightning protection, batteries etc.

Fig. 4.5 shows an overview of the new digitizer system components that will be installed.

At the NDPC, the refurbishment will be mostly upgrading of workstations and installation of the new data acquisition system.

4.2 Regional Arrays

DP - *Detection processing*

The routine detection processing of the arrays is running satisfactorily on each of the array's SUN-3/280 or Sparcstation 1 acquisition systems. The same program is used for NORSAR, NORESS, ARCESS, FINESS, GERESS, Apatity and Spitsbergen, but with different "recipes". The beam tables for NORESS and ARCESS are found in NORSAR Sci. Rep. No. 1-89/90. The beam tables for FINESS and GERESS are found in NORSAR Sci. Rep. No. 1-90/91. The beam table for Apatity is found in NORSAR Sci. Rep. No. 1-92/93, and that for Spitsbergen is found in NORSAR Sci. Rep. No. 2-92/93.

SUN 3's have been replaced with Sparcstations. This led to problems for the NORESS and ARCESS acquisition systems which are using SUN-3 dependent interfaces and code. The conversion to SUN-4 architecture is going on. One SUN-3 is still operational for ARCESS for data acquisition. During this reporting period, NORESS recording has not had the same uptime quality due to the SUN-4 problems.

Detection statistics are summarized in section 3.

EP_SigPro - *Signal processing. Phase estimation*

This process performs fk and polarization analysis for each detection to determine phase velocity, azimuth and type of phase, and the results are put into the ORACLE detection and arrival tables for use by the IMS.

Some modifications have been done as a result of IDC testing.

EP_Ronapp - *Event Processing. Plot and epicenter determination*

A description of single-array event processing is found in NORSAR Sci. Rep. No. 2-88/89, and NORSAR Sci. Rep. No. 2-89/90.

For the GERESS array, new recipes have been used for all three processes. Together with the staff at the Ruhr University, Bochum, we have implemented rotation of three-component sites to perform coherent beamforming for different azimuths using radial and transverse components of the 4 three-component sites in the GERESS array. This has led to significantly better detectability of S-type phases. Together with modified recipes for fk analysis, the one-array event processing done at Bochum is now improved.

J. Fyen

References

Berteussen, K.A. (1974): NORSAR Location calibrations and time delay corrections, NORSAR Scientific Report No. 2-73/74, Kjeller, Norway.

Fyen, J. (1987): Improvements and modifications, *NORSAR Semiannual Tecnical Summary, 1 Oct 1986 - 31 Mar 1987*, NORSAR Sci. rep. No. 2-86/87, Kjeller, Norway.

Fyen, J. (1989): Event processor program package, *NORSAR Semiannual Tecnical Summary, 1 Oct 1988 - 31 Mar 1989*, NORSAR Sci. rep. No. 2-86/87, Kjeller, Norway.

Beam	Amplitude No weight	Amplitude RMS weight
01A	66418	67127
01B	94858	94939
02B	107064	112697
02C	39642	36842
03C	109106	119881
04C	153386	156242
06C	107999	120939
Array - No TC, No RMS	30163	
Array - TC, No RMS	76308	
Array - TC, RMS	87961	93530

Table 4.1. NORSAR array beam amplitudes for the event in Fig. 4.1. The table lists the 7 subarray beams and the array beam for different combinations of applying time delay corrections and RMS weights. The left column lists peak amplitude on the subarray beam when the beams are made with no weights. (And no time delay correction, since this is available for subarray center only). The right column gives amplitudes for subarray beams when RMS weights are applied. For the array beam, TC indcates that a time delay correction has been made, and RMS indicates that RMS weights have been used. RMS weights for each instrument are obtained by calculating RMS in a small time window around the arriving phase, and then normalizing these values before using them as weights.

Ref	Origin time	Lat	Lon	Dep	mb	Comment
NB2	057:02.30.52.585	38.218	56.614	33.0	5.9	Observed
NB2	057:02.30.52.585	28.760	62.603	33.0	5.9	Calibrated
SED	057:02.31.51.500	33.200	55.600	10.0	6.0	
USGS	057:02.31.17.890	31.009	61.356	33.0	5.7	
CSEM	057:02.31.16.260	32.000	60.340	33.0	5.9	
USGS	057:02.31.12.620	31.066	60.594	11.4	5.8	Reviewed
IDC	057:02.32.11.000	36.600	55.900	33.0	5.2	
YKA	057:02.31.32.000	34.000	69.000	33.0	5.9	
MAD	057:02.30.52.600	27.300	62.200	0.0	5.9	

Table 4.2. Example of automatic NORSAR (NB2) event processing and location results. All solutions are automatic, except for the reviewed USGS solution. The list is distributed automatically by the Swiss Seismological Service (SED). The NORSAR location is obtained by slowness lookup in Herrin travel time tables. Two locations are given: by observed slowness and by calibrated slowness using the current calibration data base.

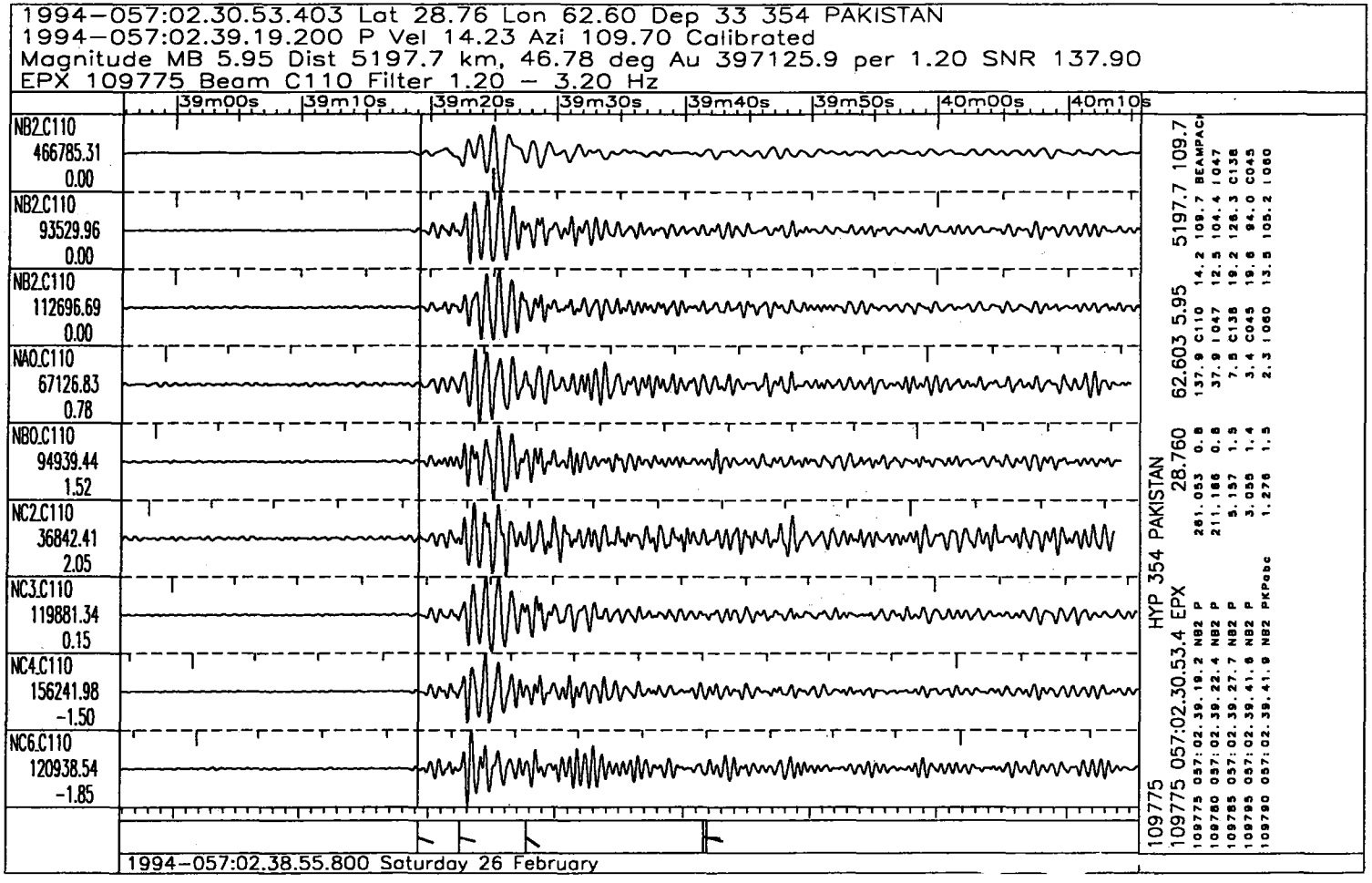

Fig. 4.1. Automatic event plot for the event in Table 4.1.

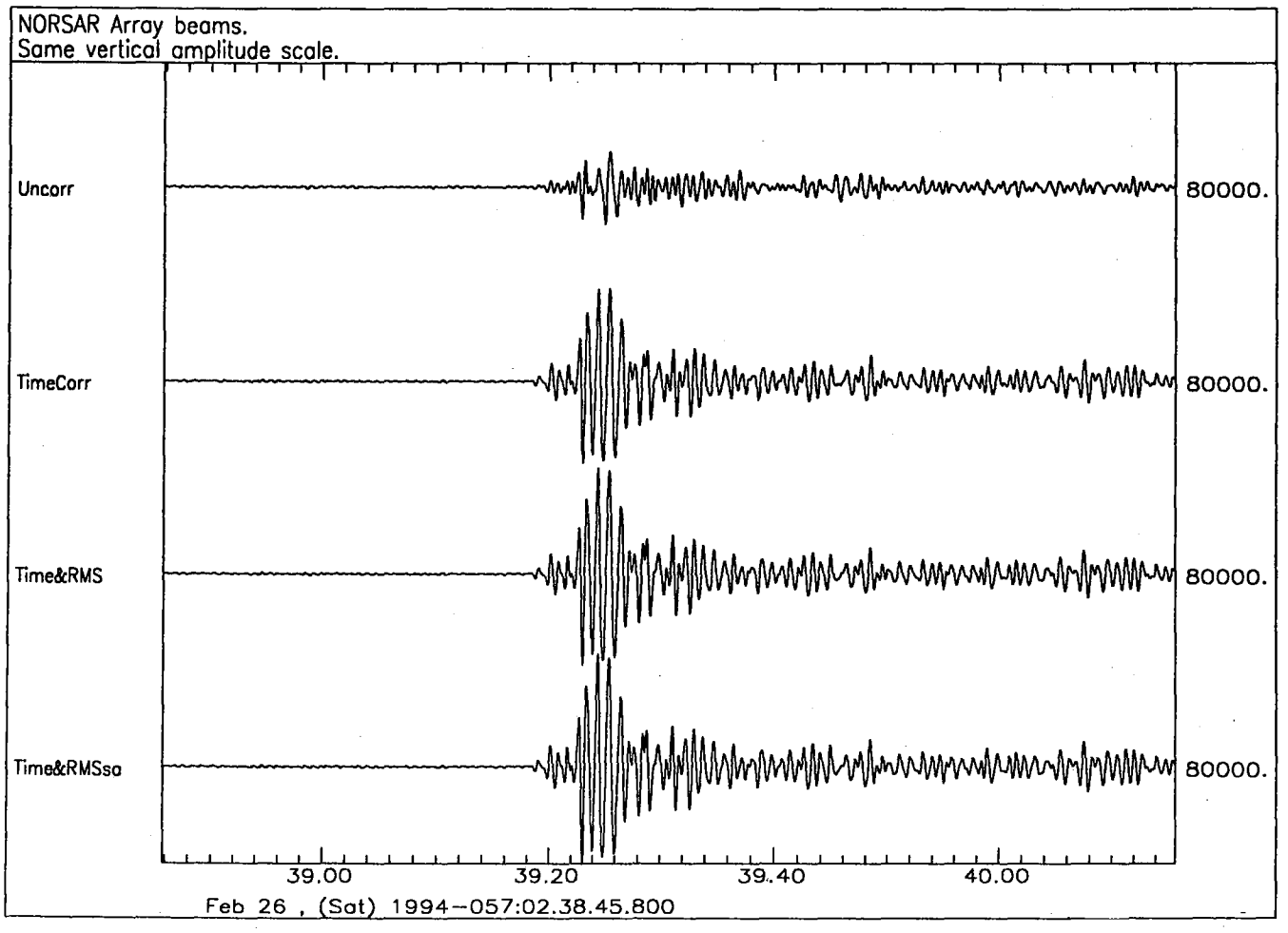

Fig. 4.2. NORSAR array beamforming. The upper trace "Uncorr" is a "standard" array beam. The next trace, "TimeCorr", is an array beam where time delay corrections are used in addition to plane wave time delays. The two lower traces are array beams with time delay corrections and RMS weighting, where RMS weights are applied on subarray beams for "Time&RMS" and for all instruments on "Time&RMSsa".

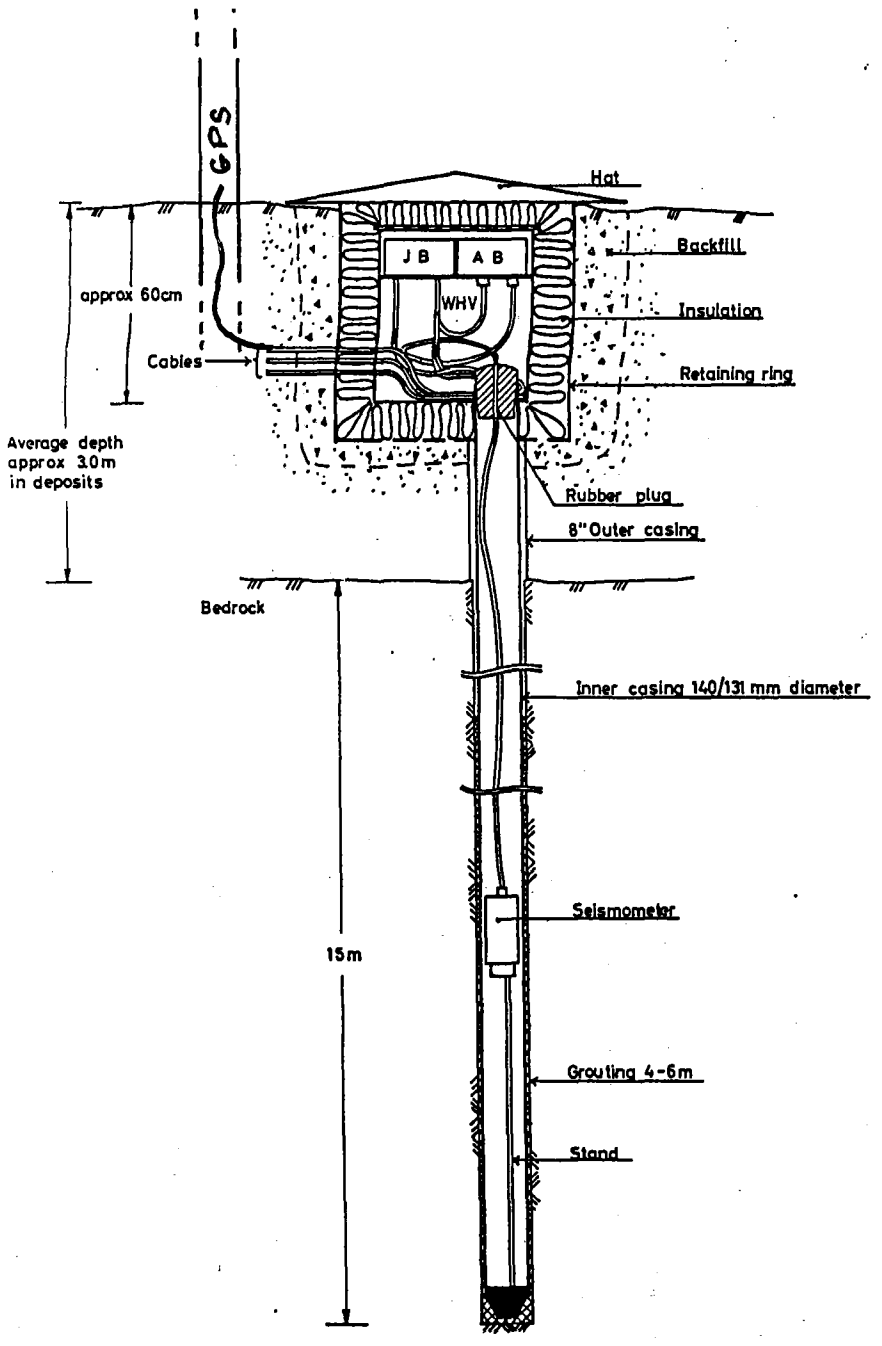

Fig. 4.3. Configuration of a typical seismometer site - SPV, at an outstation. There are 35 such sites at NORSAR (5 per subarray), each with an HS-10-1 SPZ seismometer installed in a shallow borehole (22 sites have 3.5 m borehole, 13 sites has 6 - 12 m borehole). The inside diameter of the borehole is 132mm. Two existing boxes with old electronics will be replaced with one AIM24-1 and two new boxes with batteries, battery charger and monitor electronics, modems and lightening protections will be installed. The battieries will be used for digitizer startup and otherwise charged by the DC power from the CTV. A new outside cable will be inserted to carry signals from new GPS clock, which will be mounted on a protective stand.

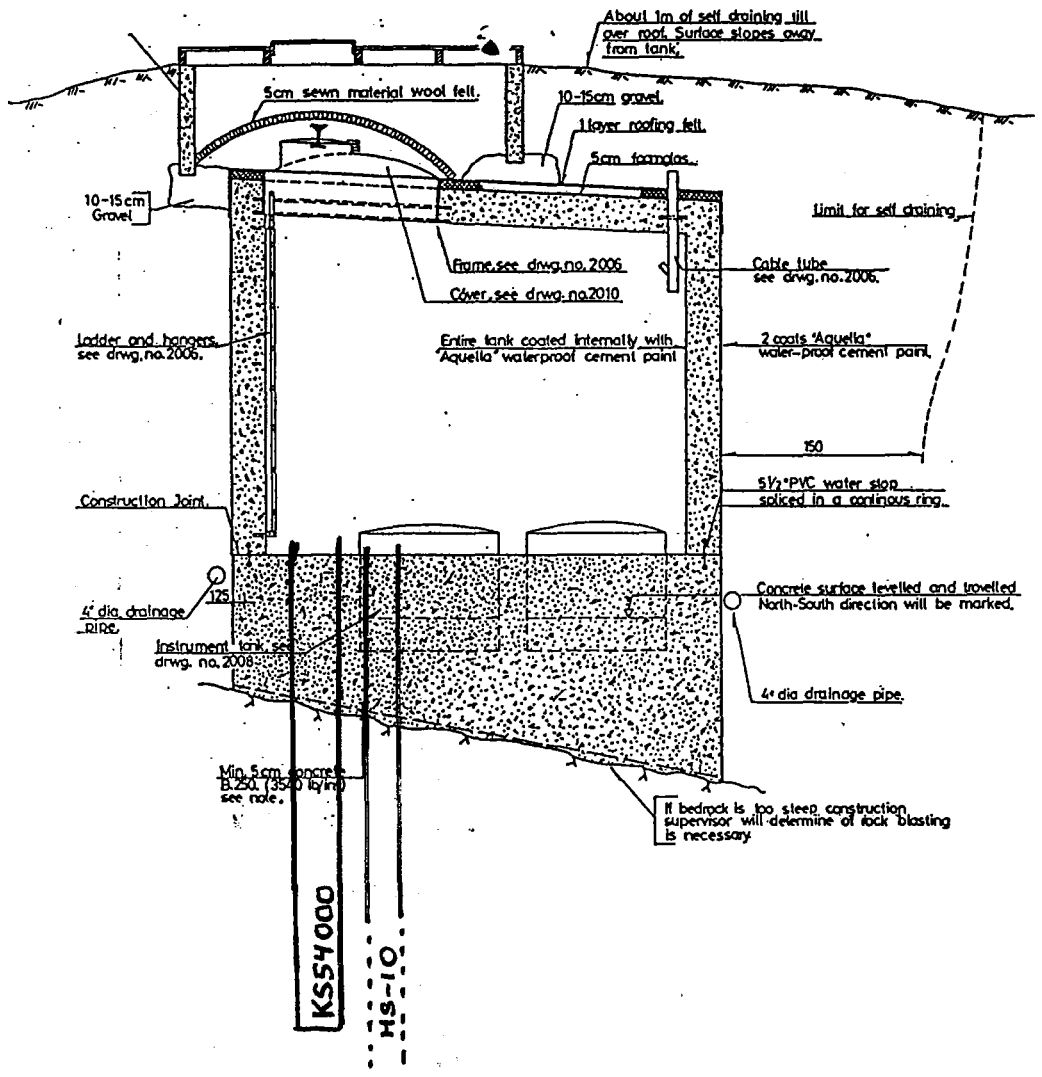

Fig. 4.4. Long Period Vault (LPV) configuration. There are 7 LPVs within NORSAR, co-located with each CTV. The LPVs will be used for KS54000P broadband seismometers and a central SPZ (HS-10) seismometer (in 3.5 m borehole). New boreholes will be made for installation of KS54000P and HS-10. The current HS-10 is mounted on the floor.

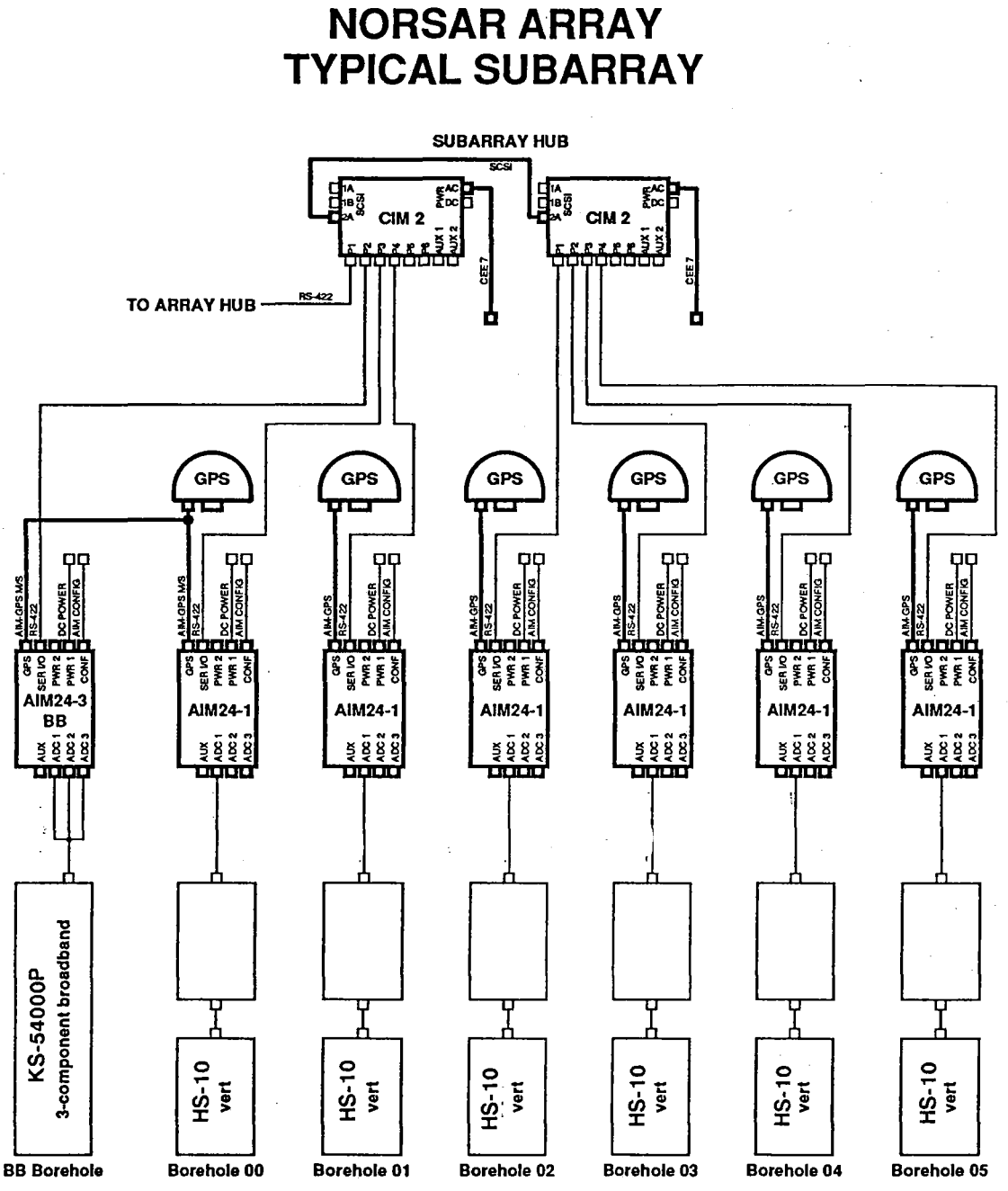

Fig. 4.5. Schematic of the field part of the new data acquistion to be installed. The CTV will have Communication Interface Modules - CIMs which will communicate with the AIM24s. One AIM24-3BB and one AIM24-1 will be close to the CTV, whereas the 5 remote AIM24-1's will use buried cables and modems for communication. The communication line to NDPC has been upgraded to 9600 baud with new modems.

5 Maintenance Activities

Activities in the field and at the Maintenance Center

This section summarizes the activities at the Maintenance Center (NMC) Hamar, and NDPC activities related to monitoring and control of NORSAR, including monitoring of NORESS, ARCESS, FINESS, GERESS and the Apatity and Spitsbergen arrays.

Activities involve preventive and corrective maintenance, planning and activities related to NORSAR refurbishment (NMC/06C).

NORSAR

Visits to subarrays in connection with:

- Adjustment of gain and offset, SP/LP channels
- Adjustment of LP seismometers, Z, EW and NS
- Cable splicing
- Installation of temporary new data acquisition equipment

NMC

- Continuing the NORSAR refurbishment preparations

NORESS

- Adjustment of offset site D8
- Fiber optical link repair

NORESS

- Replaced outdoor unit and antenna cable (VSAT)

Spitsbergen

- Defective batteries and windmill

Subarray/ area	Task	Date
NORSAR		October
01B	Adjusted gain SP ch 1, 3 and the 3 LP ch Adjusted DC offset SP ch 2, 3 and 4 Adjusted MP, all seismometers Adjusted FP, NS and EW	15 Oct
01B	Cable splicing SP-02 Modem/line test with new modems	26 Oct 28-29 Oct
02B	Adjusted MP and FP, all LP seismometers LP-vertical instrument repaired	13 Oct 14 Oct
02C	Adjusted gain, SP ch 2, 3 and 4 Adjusted MP, all LP instruments SLEM removed and brought to 01B for test	25 Oct 26 Oct 29 Oct
03C	Adjusted DC offset, all SP ch Adjusted gain, SP ch 5 and 6 Adjusted MP, NS-seismometer	14 Oct
04C	Adjusted gain, SP ch 2 Adjusted DC offset, SP ch 3 Adjusted MP/FP, all instruments Adjusted MP/FP, vertical LP and MP, LP EW ch	8 Oct
06C	Changed cable route SP-03 Replaced FP relay EW seismometer Replaced RA-5 SP-03	20 Oct 21 Oct
NMC	VSAT equipment has been installed at the 06C subarray to enable transfer of test data to the NDPC. Also at the same subarray, testing of a NORAC acquisition system and AIM 24 bit digitizers has been carried out.	October
NPDC	Daily checks of the following arrays have been carried out, i.e., NORSAR, NORESS, ARCESS, FINESS, GERESS, Apatity and Spitsbergen. SP/LP instruments have been calibrated (NORSAR). Free Period (FP) and Mass Pos. (MP) were measured. Those outside specifications adjusted (when feasible from NDPC).	October

Subarray/ area	Task	Date
NORSAR		November
01A	Adjusted gain, SP ch 1 and 5 Adjusted MP/FP, all LP seismomters Replaced RA-5, SP02 SLEM power supply repaired Power connector, SLEM power supply repaired	10 Nov 18 Nov 19 Nov 30 Nov
02B	Main power failure Adjusted all MP, LP instruments SLEM reset	10 Nov 16 Nov 25 Nov
03C	Found SP04 cable broken Cable splicing SP04	2 Nov 4 Nov
NMC	Worked with VSAT equipment Replaced outdoor unit and antenna cable NORSAR refurbishment preparations	November
NDPC	Daily checks of the following arrays have been carried out, i.e., NORSAR, NORESS, ARCESS, FINESS, Apatity and Spitsbergen (partly). SP/LP instruments have been calibrated (NORSAR), excl. week 20. FP/ MP were measured. Those outside specifications adjusted (when feasible from NDPC).	November
NORSAR		December
01B	Installation of new data acquisition equipment: RD6 digitizer and modem	13,15 Dec
02C	Installation of new data acquisition equipment: RD6 digitizer and modem	21,23 Dec
NMC	NORSAR refurbishment preparations	December
NDPC	Daily checks of the following arrays have been carried out, i.e., NORSAR, NORESS, ARCESS, FINESS, Apatity and Spitsbergen. SP/LP instruments were calibrated (NORSAR), excl. week 26. FP/ MP were measured. Those outside specifications adjusted (when feasible from NDPC).	December

Subarray/ area	Task	Date
	1994	
NORSAR		January
01A	Installation of new data acquisition equipment: RD6 digitizer, Omega OM-DC synchronized clock and modem	6 Jan
02B	Installation of new data acquisition equipment: RD6 digitizer, Kinemetrics LF-DC synchronized digital clock and modem	7 jan
03C	Installation of new data acquisition equipment: RD6 digitizer, Omega OM-DC synchronized clock and modem	12 Jan
04C	Installation of new data acquisition equipment: RD6 digitizer, modem, GPS time receiver and battery backup	31 Jan
06C	Installation of new data acquisition equipment: RD6 digitizer, modem, GPS time receiver and battery backup	28 Jan
Spitsbergen	The windmills were defect, battery voltage was low and 6 out of 11 batteries were defect. The 5 others were brought to Longyearbyen for recharging. The windmills were brought to NMC Hamar for repair and sent back to Longyearbyen on 27 Jan. The equipment was reinstalled by local representatives from Store Norske Transportservice at the beginning of February	January
NMC	Preparation of new data acquisition equipment	January
NORSAR		February
01A	Replaced Omega OM-DC synchronized clock with GPS time receiver. Installed battery backup	9 Feb
01B	Installed battery backup	9 Feb
02B	Replaced Kinemetrics LF-DC synchronized clock with GPS time receiver. Installed battery backup	10 Feb
02C	Replaced Kinemetrics LF-DC synchronized clock with GPS time receiver. Installed battery backup	8 Feb
03C	Replaced Omega OM-DC synchronized clock with GPS time receiver. Installed battery backup	10 Feb
NMC	NORSAR refurbishment preparations	February
NORSAR		March

Subarray/ area	Task	Date
06C	Two visits to 06C, with two different well-drilling companies, to prepare for drilling of boreholes for KS54000 and HS-10 seismometers in the LPV.	March
NMC	Continued the NORSAR refurbishment preparations	March

Table 5.1. Activities in the field and the NORSAR Maintenance Center, including NDPC activities related to NORSAR, NORESS, ARCESS, FINESS, GERESS and the Apatity and Spitsbergen arrays 1 October 1993 - 31 March 1994.

P.W. Larsen
K.A. Løken

6 Documentation Developed

Baadshaug, U. and B. Ferstad (1994): Monitoring ESAL time-lags, in *Semiann. Tech. Summ. 1 Oct 93 - 31 Mar 94*, NORSAR Sci. Rep. 2-93/94, Kjeller, Norway.

Kushnir, A. and T. Kværna (1994): Signal detection and waveform extraction in the coda of a strong, interfering event, in *Semiann. Tech. Summ. 1 Oct 93 - 31 Mar 94*, NORSAR Sci. Rep. 2-93/94, Kjeller, Norway.

Kværna, T. (1993): Accurate determination of phase arrival times using autoregressive likelihood estimation, Proc. Erice Workshop, Italy, Nov 93.

Kværna, T., F. Ringdal, H. Iversen and N.H.K. Larsen (1994): A system for continuous global seismic threshold monitoring, in *Semiann. Tech. Summ. 1 Oct 93 - 31 Mar 94*, NORSAR Sci. Rep. 2-93/94, Kjeller, Norway.

Kværna, T. and F. Ringdal (1993): Intelligent post-processing of seismic events, Proc. Erice Workshop, Italy, Nov 93.

Schweitzer, J. (1994): Some improvements of the detector / SigPro-system at NORSAR, in *Semiann. Tech. Summ. 1 Oct 93 - 31 Mar 94*, NORSAR Sci. Rep. 2-93/94, Kjeller, Norway.

Semiannual Tech. Summary, 1 Apr - 30 Sep 93, NORSAR Sci. Rep. 1-93/94, NORSAR, Kjeller, Norway.

Skorve, J. (1994): The 31 December 1992 seismic event on Novaya Zemlya, in *Semiann. Tech. Summ. 1 Oct 93 - 31 Mar 94*, NORSAR Sci. Rep. 2-93/94, Kjeller, Norway.

7 Summary of Technical Reports / Papers Published

7.1 A system for continuous global seismic threshold monitoring

Summary

Continuous threshold monitoring is a technique for using a seismic network to monitor a geographical area continuously in time. The method provides, at a given confidence level, a continuous assessment of the upper magnitude limit of possible seismic events that might have occurred in the target area. Three approaches are discussed in this paper.

Site-specific threshold monitoring: By 'focusing' a seismic network on a specific target site, continuous threshold monitoring of that site is achieved. We optimize the monitoring capability by tuning the frequency filters and array beams to known characteristics from previously recorded events at the site. We define the *threshold trace* for the network as the continuous time trace of computed upper magnitude limits of seismic events in the target area, at a 90 per cent confidence level.

Regional threshold monitoring: This involves conducting site-specific monitoring of a dense grid of geographical aiming points and requires the development of generic phase attenuation relationships for covering a specific geographical region. The regional threshold monitoring approach lends itself to illustration in the form of maps with color contour displays.

Global threshold monitoring: This is a natural extension of the regional monitoring approach, but requires a somewhat different strategy for effective implementation. Using a global network, and taking into account that phase propagation time is up to several tens of minutes, it is necessary to establish elaborate travel-time and attenuation tables, and to use a much coarser geographical grid than in the regional approach.

The regional and global threshold maps have advantages over standard network capability maps in being more accurate during time intervals when interfering seismic events occur. They can also more easily reflect special conditions such a particularly favorable source-station propagation paths, and have the advantage of not being tied to specific event detection criteria.

As discussed by Ringdal and Kværna (1992), continuous threshold monitoring offers a valuable supplement to traditional seismic techniques used in nuclear test ban monitoring. The method may also be useful for monitoring earthquake activity at low magnitudes for sites of special interest, as well as for monitoring earthquake aftershock sequences.

In this paper, an overview is given of the underlying principles for continuous threshold monitoring, together with a status report for the development of a prototype system for continuous seismic threshold monitoring on a global scale.

Introduction

Traditionally, seismic monitoring of earthquakes and underground explosions has relied upon applying signal detectors to individual stations within a monitoring network, associating detected phases and locating possible events in the region of interest. It is implicitly understood that such a network will have a detection threshold that varies with time. However, with methods being used in practical operation today, no attempt is made to specify this threshold as a function of time. During time periods when the background noise level is abnormally high, the event detection capabilities of such a network may be severely degraded. It is important to retain such information along with the information on the detected events.

In practice, the event detection procedure is often supplemented by assessments of network capabilities for the target region using statistical models for the noise and signal distributions. These models include station corrections for signal attenuation and a combinational procedure to determine the detection threshold as a function of the number of phase detections required for reliable location (Sykes & Evernden 1982; Harjes, 1984; Hannon 1985; Ringdal 1986; Sereno & Bratt, 1989).

The noise models used in these capability assessments are not able to accommodate the effect of interfering signals, such as the coda of large earthquakes, which may cause the estimated thresholds to be quite unrealistic at times. Furthermore, only a statistical capability assessment is achieved, and no indication is given as to particular time intervals when the possibility of undetected seismic events is particularly high.

Another shortcoming of traditional signal detection-based monitoring is their inability to provide upper bounds on magnitudes of non-detected seismic events. This could be important, e.g., if a teleseismic network fails to detect an event that is known to have occurred (for example, through local network recordings). Even more important, it would be useful for discrimination purposes to obtain a network-based upper limit on M_S for a given seismic event for which no surface waves are detected. Again, traditional methods do not provide such "negative evidence".

The continuous threshold monitoring technique has been developed to address these problems. The basic principles were described by Ringdal & Kværna (1989), who showed that this method could be useful as a supplement to event detection analysis. In this paper we expand further on the utility of this method, with particular emphasis on seismic threshold monitoring on a global scale, using a global network. Some examples are given on how such monitoring could be achieved in a practical prototype system, which might be suitable at an International Data Center for monitoring a Comprehensive Test Ban Treaty (CTBT).

General approach

The basic idea behind the threshold monitoring method is, for any given point in time, to assess the largest magnitude of events in a given target region that might go undetected by

a monitoring network. These magnitude estimates are computed by combining observations of the amplitude of the seismic data at different arrays and/or single stations.

For computation of site-specific continuous magnitude thresholds the following procedure is required (for details, see Ringdal & Kværna, 1992):

- For each location-station-phase combination, estimate continuously the seismic amplitude levels. If the station is an array, we use short-term averages (STAs) of filtered beams to represent the amplitude levels. The steering parameters of the beams will then correspond to the apparent velocity and azimuth of the actual phase. The filter bands are chosen such that good signal-to-noise ratio (SNR) is ensured. If the observation unit is a three- or single-component station, the STA values are computed from a filtered single channel.
- When considering a potential event at a given time and location, measure the seismic amplitude levels at the expected arrival times for the relevant seismic phases. The travel times for each phase can be taken from standard travel time tables, or by processing events with known location and origin time.
- In order to relate the STA observations to actual magnitude estimates, apply the formula

$$m = \log(STA) + b(\Delta, h) \quad (1)$$

  where m is the estimated magnitude, STA is the representation of the seismic amplitude level and b is a distance-depth correction factor for each location-station-phase combination. The correction factors can be obtained by processing events with known magnitudes, or by using standard attenuation values.
- For assessing the significance of these magnitude estimates, assume that they are sampled from a normal distribution with a given standard deviation. Experience with signal amplitude variation across the NORSAR array indicates that a standard deviation of 0.2 is a good value for a small epicentral area.
- The magnitude limits computed by this algorithm are tied to a given confidence level, initially set to 0.9. This means that the estimated limits represent the largest magnitude of a possible hidden event, in the sense that there is at least a 90 per cent probability that one or more of the observed amplitude values would be exceeded by the signals from an event with magnitude above these limits.

Global threshold monitoring -- basic principles

In principle, global threshold monitoring can be achieved by conducting site-specific monitoring of a grid of target points covering the globe. The density of the grid and the interpolation technique applied will determine the quality of the results.

We have adopted the method described by Vinje et al (1992) to develop global grid point systems. This method applies triangulation of an icosaeder to construct regularly sampled

wavefronts, and provides uniform geographical coverage of the globe at a specified grid density (Kværna, 1992).

Figs. 7.1.1 to 7.1.3 show three examples of such coverage, using 162, 642 and 2562 grid points, respectively. With the coarsest sampling (162 points) the circle corresponding to each grid point has a radius of 11.0 degrees. This radius is reduced to 5.5 and 2.75 degrees for the two denser grids, respectively.

The grid density to be used in practice is mainly a cost-performance trade-off. As described later in this paper, we have chosen the 642-point grid for the initial prototype of a global threshold monitoring system.

It is important to be aware that the density of the global TM grid is quite different from the beam deployment density for the arrays in the station network. For each array, a certain number of steering points will be selected (typically less than 100 for a small or medium aperture array, and several hundred for a large array). When calculating the threshold traces for a given TM grid point, the closest beam steering point is selected. Thus, there will be a potential beam steering loss that must be taken into account when calculating the "representative" threshold for the circle covered by the TM grid point.

The beam steering loss is mainly a function of array aperture and signal frequency. An illustration for the NORESS array is given in Figs. 7.1.4-7.1.5, showing 1 dB and 3 dB beam loss contours for P-type velocities (8 km/s and up). These loss contours are circles when shown in inverse velocity space, and the steering points therefore do not translate into equidistant geographical points. Thus, if mainly teleseismic distances are considered, the number of steering points for a given worst-case loss will be modest.

Calibration and time/azimuth tolerances

Ideally, global threshold monitoring requires access to magnitude calibration statistics for each target point and each station/phase combination considered. In a practical situation it will usually be impossible to obtain the necessary number of calibration events for each target point in the grid, and a different approach is therefore required.

Our approach is to develop a set of "generic" attenuation models. This can be done as a two-step process. The first step is to divide the earth into regions that are relatively homogeneous with respect to wave propagation characteristics. Within each region, an attenuation model is then established on the basis of available calibration data.

Using this approach, the distance-depth correction factors $b\,(\Delta, h)$ in (1) can be determined individually for each seismic phase, by applying a standard global attenuation model, in combination with region-specific station corrections.

In threshold monitoring there is a trade-off between the size of the target area and the tolerances of the parameter values used in the threshold computations. With a given grid, it is necessary to make the tolerances of each aiming point compatible with the grid spacing.

An illustration of the time and azimuth tolerances is given in Figs. 7.1.6 and 7.1.7. For example, if we increase the time windows over which we measure the signal levels, this has the effect of broadening the target area for the aiming point. At the same time, some of the resolution in the regional threshold variation will be lost. As shown in Fig. 7.1.6, the necessary time window corresponding to a typical teleseismic distance (see the highlighted area of Fig. 7.1.1) is of the order of ± 1 minute. A similar consideration applies to azimuth and slowness tolerances (see Fig. 7.1.7), and we refer to Kværna (1992) for details.

Implementation considerations

A convenient way to view the threshold monitoring system is to consider it as a set of objects and attributes.

The basic objects in threshold monitoring are the *Station* and the *GridPoint*. The *Network* is the collection of *Station* objects. The *Grid* is the collection of *GridPoint* objects.

A Station can be an array, a three-component station or a single-component station. The type of seismometer, digitizer, sampling rate and response function can vary, although for the TM purpose we will restrict ourselves to the short period processing band (typically 0.5 Hz and higher).

A GridPoint is an aiming point in geographical space. In site-specific monitoring, only one GridPoint is necessary, and the Grid consequently consists of only this one GridPoint.

In regional and global threshold monitoring, the Grid will consist of many GridPoints. The number of GridPoints and their density and distribution may vary according to the available Network, the monitoring requirements and the computing facilities available.

The Station object

The Station object has the following attributes:

a) Fixed attributes
   - Latitude, longitude, height
   - Types and deployments of sensors
   - System response
   - Sampling rate

b) Parameterized attributes
   - Number of beams
   - For each beam: Ux, Uy, beam configuration, filter band

The GridPoint object

The GridPoint object has the following attributes:

- Latitude, longitude, depth

For each station:

- A 0/1 indicator for P-phase
- A 0/1 indicator for S-phase
- Similar indicators for other phases used

For each nonzero Station-Phase combination:

- A filter band
- A pointer to the nearest beam
- A magnitude bias term

Threshold processing

For a given GridPoint, Origin Time, Station and Phase, an STA value is calculated as the maximum of N consecutive 2-second STA(1) values for the appropriate beam.

This STA value is converted to magnitude using an empirical conversion from STA to A/T, and then applying Veith-Clawson or other extended distance-depth corrections and adding/subtracting the appropriate GridPoint bias.

The set of magnitudes thus obtained is converted to a 90 percent threshold using the method of Ringdal & Kværna (1992).

Parameter selection

The beam deployment is made taking into account the need for regional characterization (for non-arrays as well as arrays) and the allowable worst-case beam loss for the appropriate regional coverage.

The beam configurations are set so as to obtain the optimum SNR for the actual beam in the frequency band used. The SNR is defined as the signal strength relative to the normal noise conditions (note that this is different from the optimum SNR for "coda phases").

The Grid is determined based upon the actual monitoring requirements and the resources available.

The filter bands are set for each GridPoint-Station-Phase combination and should be designed for optimum SNR for all events of interest in the area covered by the GridPoint.

Filter parameters

Initially, the prototype system will use a set of generic, wide-band filters.

We classify the distances into 4 ranges:

A: 0-10 degrees

B: 10-20 degrees

C: 20-90 degrees

D: 90-180 degrees

We classify the Stations as follows:

S1: Good HF propagation, low HF noise

S2: Stations with low LF noise, and which are not in the S1 category

S3: All other stations

We define the generic filter bands as follows:

F1: 0.5-2 Hz

F2: 1.5-6 Hz

F3: 2.5-10 Hz

F4: 4.0-16 Hz

The initial selection is as follows, for distance ranges A, B, C, D:

S1:	F4	F3	F2	F2
S2:	F3	F2	F1	F1
S3:	F3	F2	F2	F1

These filter bands should be refined on an individual station basis as experience accumulates.

STA calibration

Since STA values are used instead of A/T as a basis for magnitude estimates, it is necessary to introduce a conversion formula. From experiments with different short-period instrument types, we have found that such a relation can be well parameterized in the following way:

$$\log (A/T) = \log (STA \times cal) + c\,(resp, filter) \qquad (2)$$

where *cal* is the instrument calibration factor at 1 Hz, and *c* is a constant that is dependent on the instrument response and the filter band used to calculate the STA value. The constant *c* is derived empirically for each instrument and the filter band, as shown in Fig. 7.1.8.

Initial IDC implementation

The initial IDC implementation will comprise the following main features:

- Continuous global TM map
- 642 grid points
- 10 seconds update rate
- 7-day diskloop of STA values
- Site-specific traces extracted on request

It should be noted that the site-specific traces will be represented by the trace of the closest global grid point. "Optimum" site-specific traces may be available in the future.

It is currently envisaged that the following Threshold Monitoring services will be provided by the IDC:

- World threshold map (e.g., postcript file) at given point in time
- Site-specific trace (taken from world map) for specified target and time period
- Either data points or trace plot provided
- Specification of IDC events associated with peaks on the TM plot
- Use of CenterView, DRM or other mechanisms for easy remote access.

Examples of typical products of the global TM system are shown in Figs. 7.1.9-7.1.12. Fig. 7.1.9 shows an example of the structure of a global threshold "snapshot". For illustration purposes, only one station is used rather than a global network (the Apatity array in NW Russia). The color scale gives an indication of the instantaneous thresholds (for a specified origin time) using this station only. It is noted that the threshold is around m_b 4.0 over large parts of the northern hemisphere, increasing toward m_b 5.5 in the shadow zone (epicentral distance 90-110 degrees) and then decreasing to m_b 4.5-5.0 in the PKP zone. Note in particular the threshold increase in a region about 10 degrees from the station. This is due to a local event occurring within a few minutes of the time of the "snapshot", which causes the threshold to increase in the region that would have corresponding P travel times. Also note that the thresholds show a slight variation with azimuth due to the formation of beams and differences in "noise suppression", especially during interfering events.

Figs. 7.1.10 and 7.1.11 are "regional threshold displays", showing sections of the global map (eastern Asia and Africa/Middle East, respectively). On these figures the grid points are especially marked. These two figures illustrate that the variability in threshold at teleseismic distances is sufficiently resolved by the 642-point global grid. There may, however, be a need for a denser grid in cases where stations at local and regional distances are available.

Fig. 7.1.12 is an example of a trace plot corresponding to a selected point on the global grid. This is an example of a site-specific application, although optimized threshold processing is not performed in this case (which is based on the "generic" global map). To

optimize the processing for areas of particular interest, it will be necessary to include detailed calibration information.

Conclusions

The continuous threshold monitoring technique represents a new approach toward achieving reliable seismic monitoring. The method is well suited to supplement the traditional methods in monitoring potential test sites for the purpose of verifying nuclear test ban treaties. The method may equally well be used to monitor earthquake activity at low magnitudes for sites of special interest, and could also be useful for monitoring earthquake aftershock sequences. The prototype system described in this paper is intended to demonstrate how the concept can be used to enable threshold monitoring on a global basis, with applications to real-time displays.

It is important to be aware that the main purpose of the threshold monitoring method is to call attention to any time instance when a given threshold is exceeded. This will enable the analyst to focus his efforts on those events that are truly of interest in a monitoring situation. He will then apply other, traditional analysis tools in detecting, locating and characterizing the source of the disturbance. Thus, the threshold monitoring method is a supplement to, and not a replacement of, traditional methods.

T. Kværna
F. Ringdal
H. Iversen
N.H.K. Larsen

References

Bache, T.C., S.R. Bratt, J. Wang, R.M. Fung, C. Kobryn & J.W. Given (1990): The Intelligent Monitoring System, *Bull. Seism. Soc. Am.*, 80, Special Issue, 1833-1851.

Hannon, W. (1985): Seismic verification of a comprehensive test ban, *Science*, 227, 251-257.

Harjes. H.-P. (1984): Global seismic network assessment for teleseismic detection of underground nuclear explosions, *Tech. Rep. C84-02*, Center for Seismic Studies, Washington, D.C.

Kværna, T. (1991): Initial development of generic relations for regional threshold monitoring, Semiannual Tech. Summ., 1 Apr - 30 Sep 1990, *NORSAR Sci. Rep. 1-90/91*, NORSAR, Kjeller, Norway.

Kværna, T. (1992): Initial results from global Generalized Beamforming, Semiannual Tech. Summ., 1 Apr - 30 Sep 1992, *NORSAR Sci. Rep. 1-92/93*, NORSAR, Kjeller, Norway.

Lilwall, R.C. & P.D. Marshall (1986): Body wave magnitudes and locations of Soviet underground explosions at the Novaya Zemlya test site, *AWRE Rep. NO 017/86*, Blacknest, U.K.

Ringdal, F. (1986): Study of magnitudes, seismicity and earthquake detectability using a global network, *Bull. Seism. Soc. Am.*, 76, 1641-1659.

Ringdal, F. & T. Kværna (1989): A multichannel processing approach to real time network detection, phase association and threshold monitoring, *Bull. Seism. Soc. Am.*, 79, 1927-1940.

Ringdal, F. & T. Kværna (1991): Continuous threshold monitoring using "regional threshold displays", Semiannual Tech. Summ., 1 Oct 90 - 31 Mar 91, *NORSAR Sci. Rep. 2-90/91*, NORSAR, Kjeller, Norway.

Ringdal, F. & T. Kværna (1992): Continuous seismic threshold monitoring, *Geophys. J. Int.*, 111, 505-514.

Sereno, T.J. & S.R. Bratt (1989): Seismic detection capability at NORESS and implications for the detection threshold of a hypothetical network in the Soviet Union, *J. Geophys. Res.*, 94, 10397-10414.

Sykes, L. & J. Evernden (1982): The verification of a comprehensive nuclear test ban, *Sci. Am.*, 247, 47-55.

Vinje, V., E. Iversen, H. Gjøystdal & K. Åstebøl (1992): Traveltime and amplitude estimation using wavefront construction. Abstract of paper presented at the 54th Meeting and Technical Exhibition of the European Association of Exploration Geophysicists, Paris, France, 1-5 June 1992.

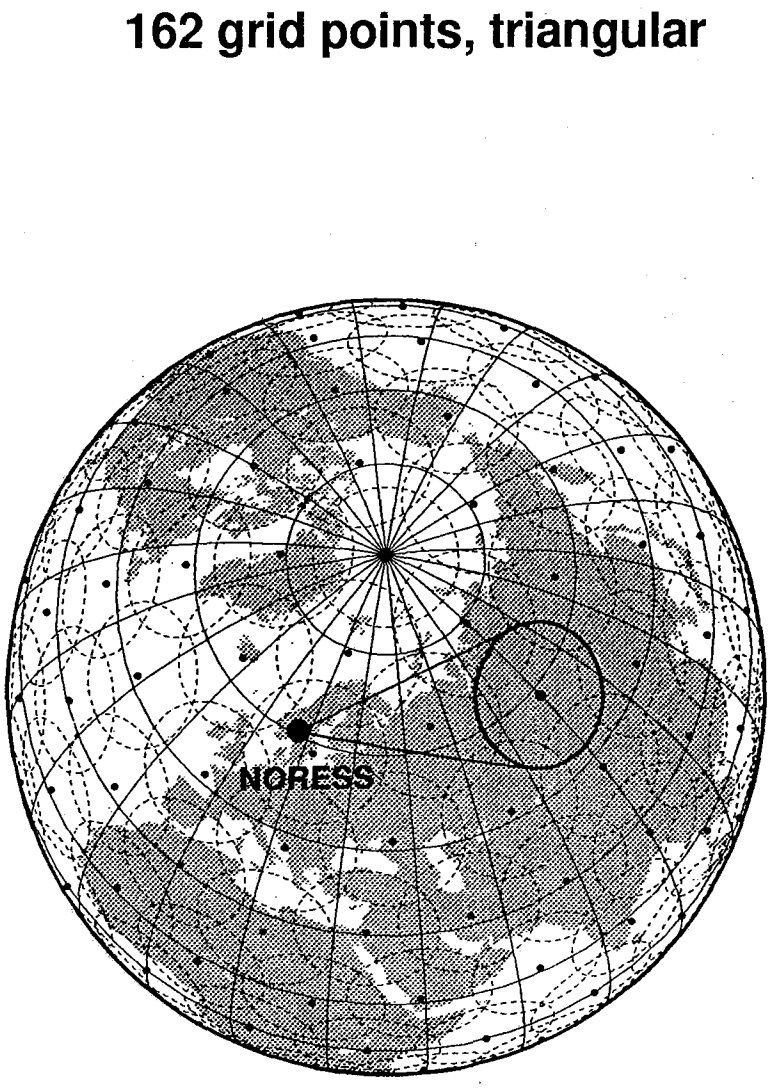

Fig. 7.1.1. A 162-point global grid system projected onto an azimuthal orthographic projection of the earth. The circular target regions are shown by dashed circles, and the highlighted target region is used as an example of time and azimuth tolerances in this study. Its center point is located 37.5 degrees from the NORESS array. Minimum and maximum azimuthal lines from NORESS to the target region are also shown.

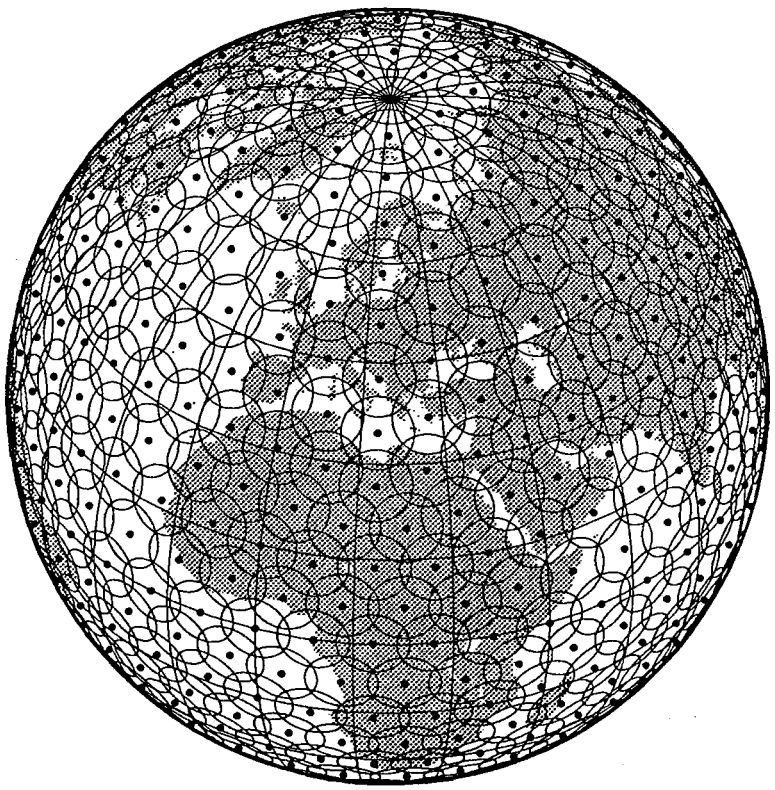

Fig. 7.1.2. Circular regions of radius 5.5 deg encompassing each grid point constructed by the triangular method. Note that the coverage is complete.

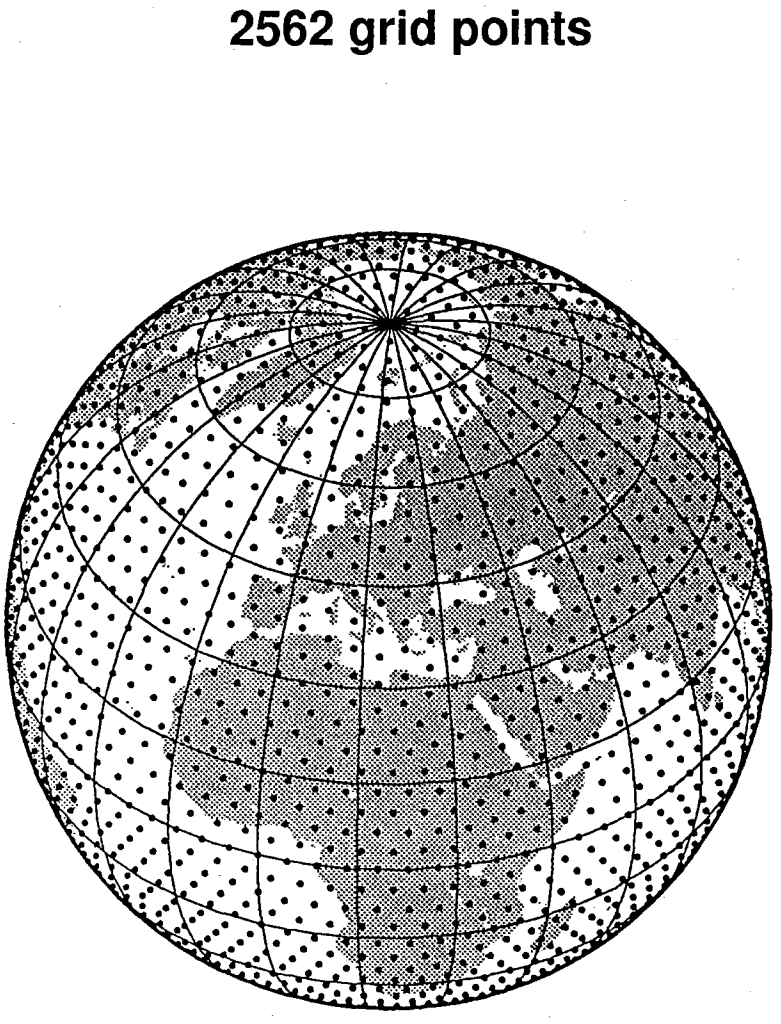

Fig. 7.1.3. A 2562-point global grid system projected onto an azimuthal orthographic projection of the earth. This grid system was obtained by a four-fold triangulation of the icosaeder, and each grid point represents a target region of 2.7 degrees radius.

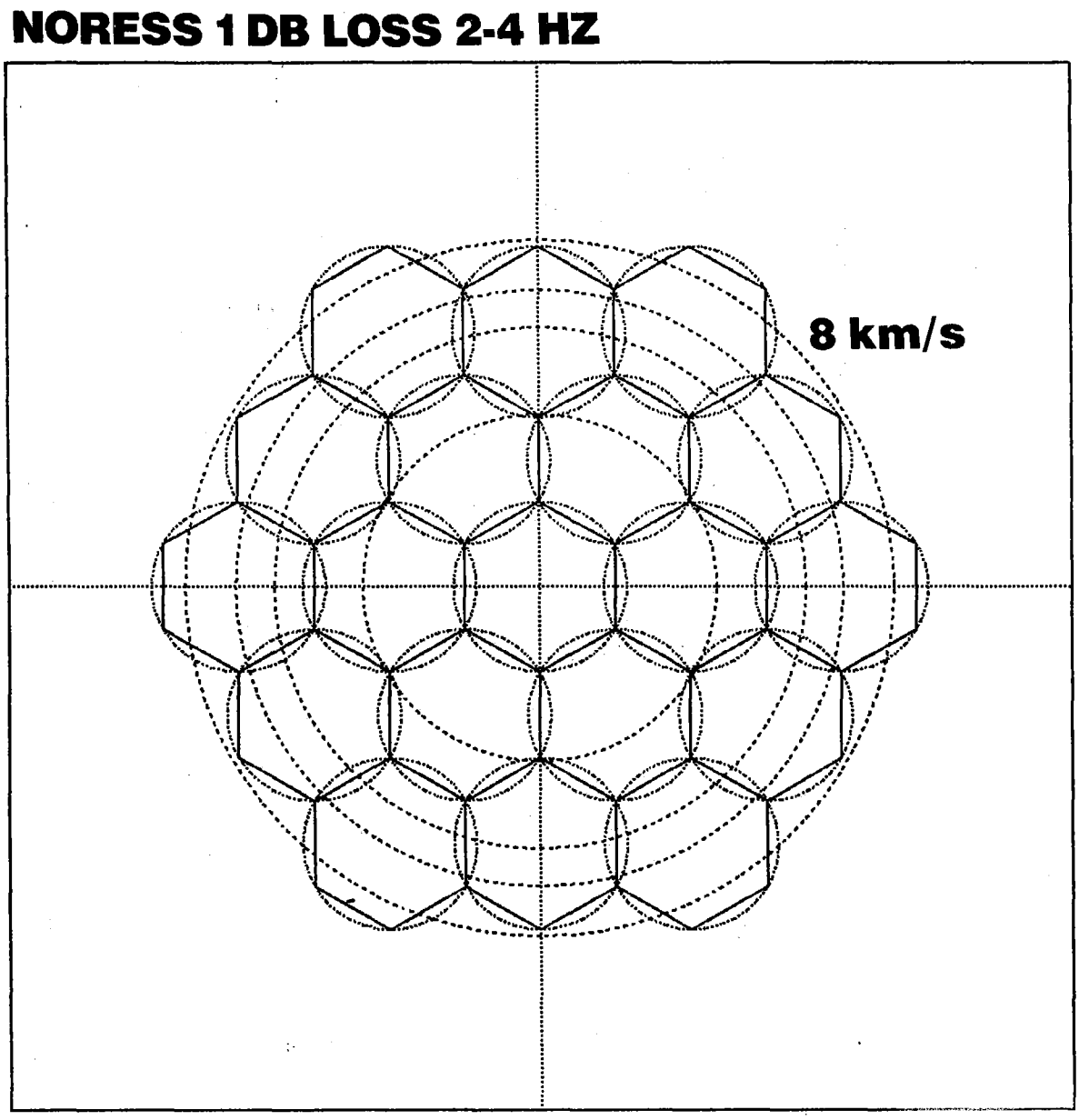

Fig. 7.1.4. Example of NORESS beam pattern, displayed in inverse velocity space, corresponding to a deployment with a worst-case beam-steering loss of 1 dB (filter band 2-4 Hz). The figure covers typical P-wave velocities for regional and teleseismic distances (8 km/s and up).

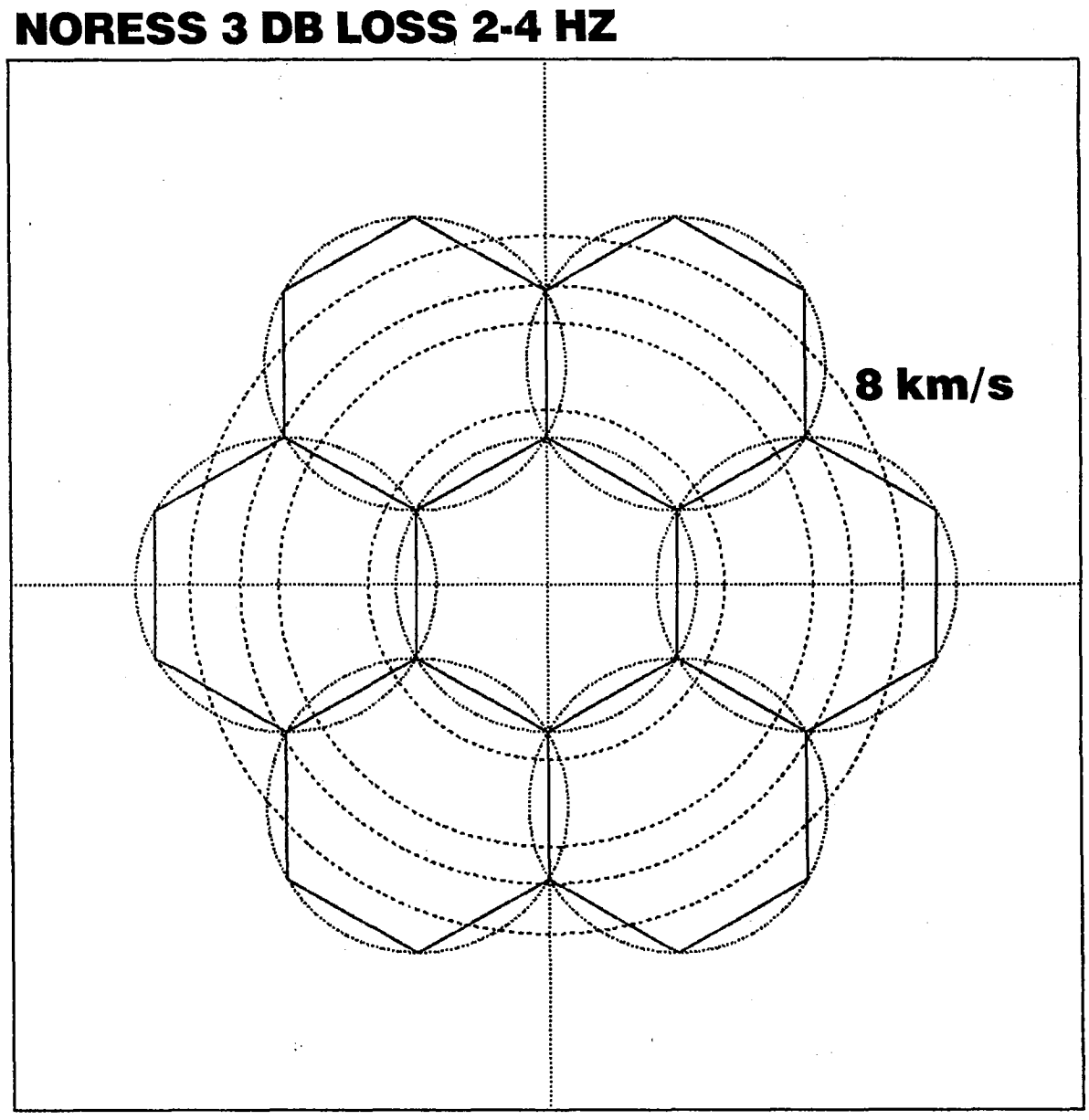

Fig. 7.1.5. Same as Fig. 7.1.4, but allowing a worst-case beam-steering loss of 3 dB. Note that the number of beams required is significantly lower than for the 1 dB loss case (7 vs 19).

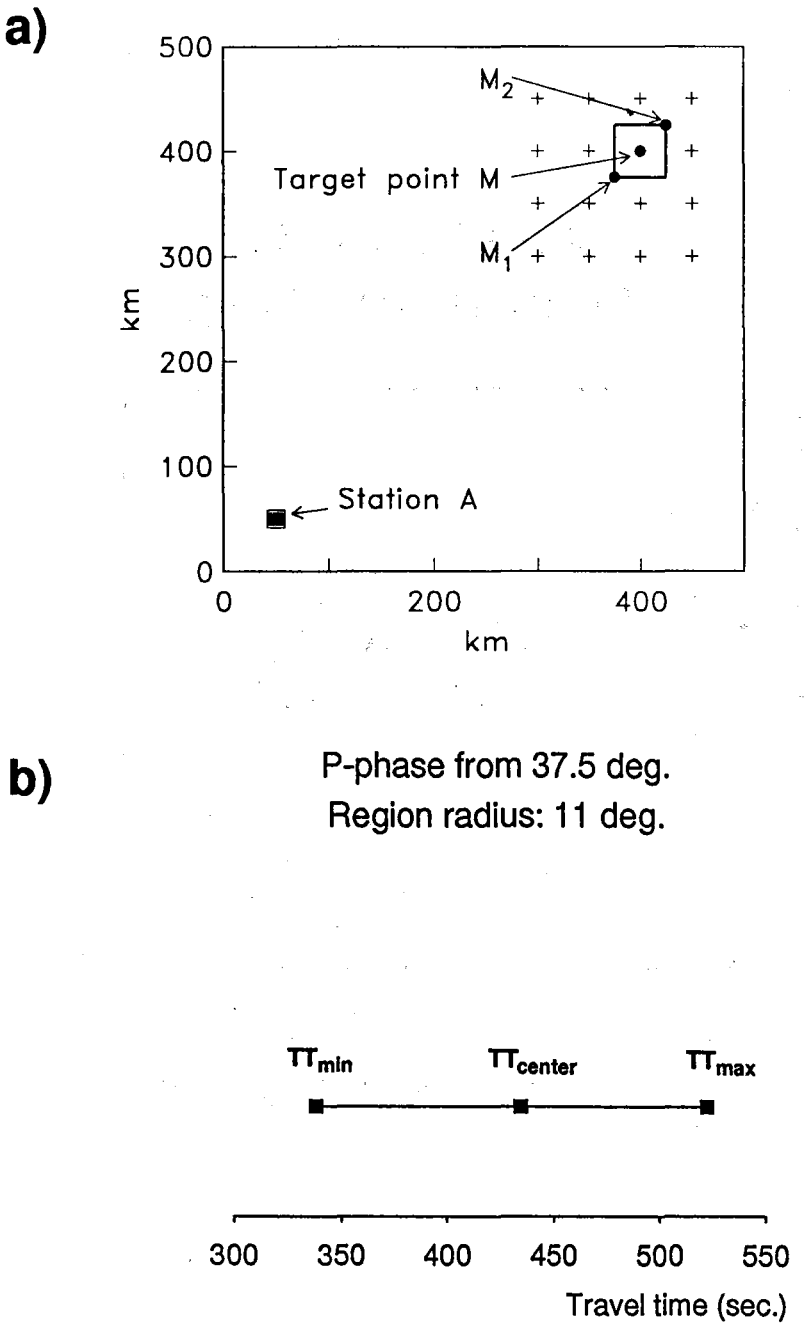

Fig. 7.1.6. The *top part* of this figure illustrates the necessity of using time tolerances when using one target point to represent an area. The plus signs indicate target points, and a rectangle surrounding one of the target points (M) is also given. The point within the rectangle with the minimum traveltime is denoted M_1, whereas the point with the maximum traveltime is denoted M_2. The *bottom part* of the figure shows the range of predicted P-wave travel times from the highlighted target region of Fig. 7.1.1 to the NORESS array.

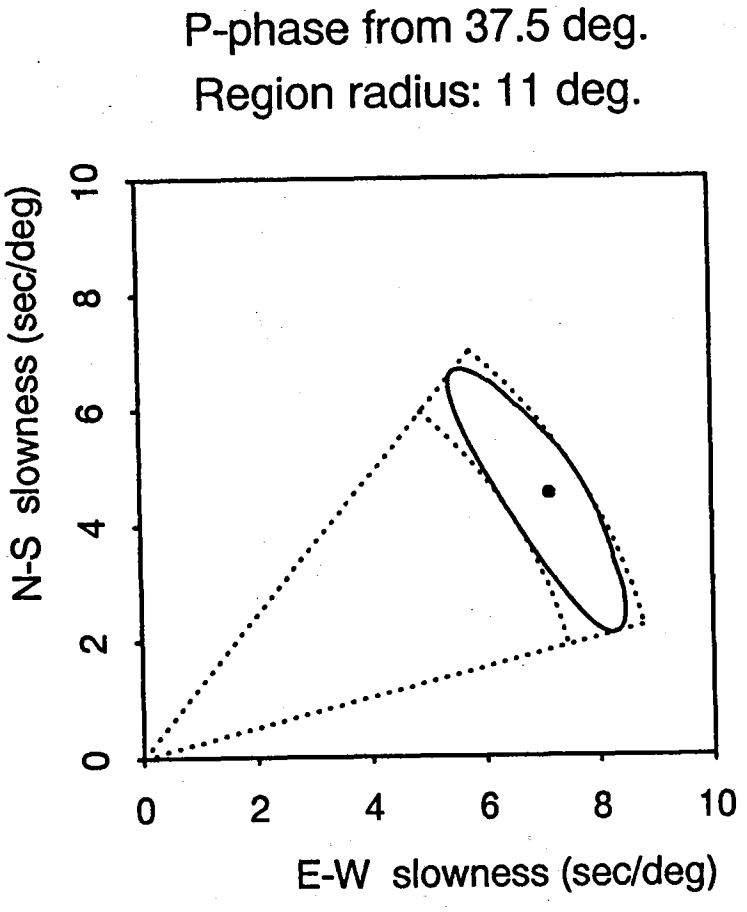

Fig. 7.1.7. In order to monitor a finite area surrounding each of the target points, a mis-steering in azimuth is introduced when the beams are steered towards the target points. This figure illustrates the range of predicted P-wave slowness vectors at NORESS for events in the highlighted target region of Fig. 7.1.1. The slowness vectors of the circular boundary of the target region are projected onto the solid line of this figure. An approximation to the area inside this solid line is given by the dotted sector segment defined by the minimum and maximum azimuths and the minimum and maximum slownesses.

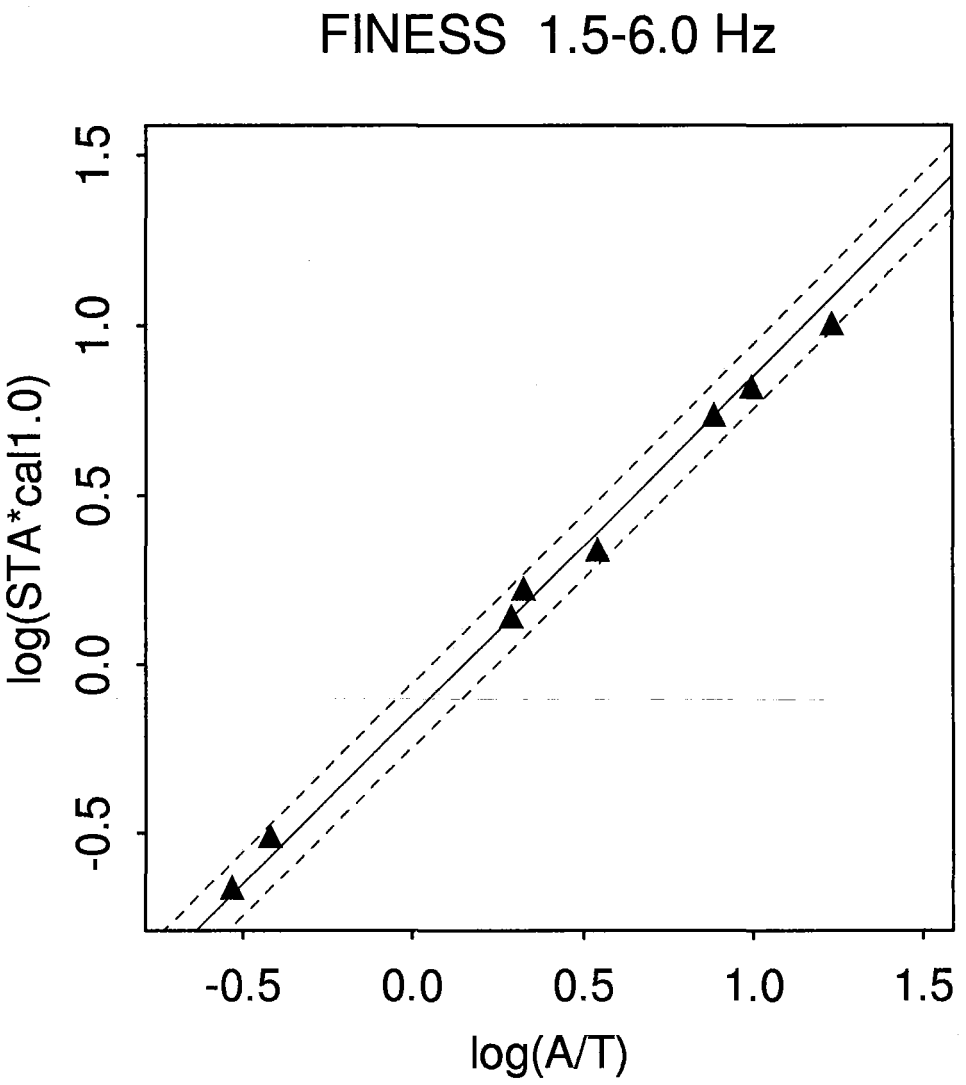

Fig. 7.1.8. Figure illustrating the linear dependency between log (A/T) and log (STA x cal). For the station FINESS and the frequency band 1.5-6.0 Hz, shown on the figure, the best-fitting straight line (with a restricted slope of 1.0) is:

$$\log (STA \times cal) = \log (A/T) - 0.15$$

Thus, in this case the constant c in formula (2) is 0.15.

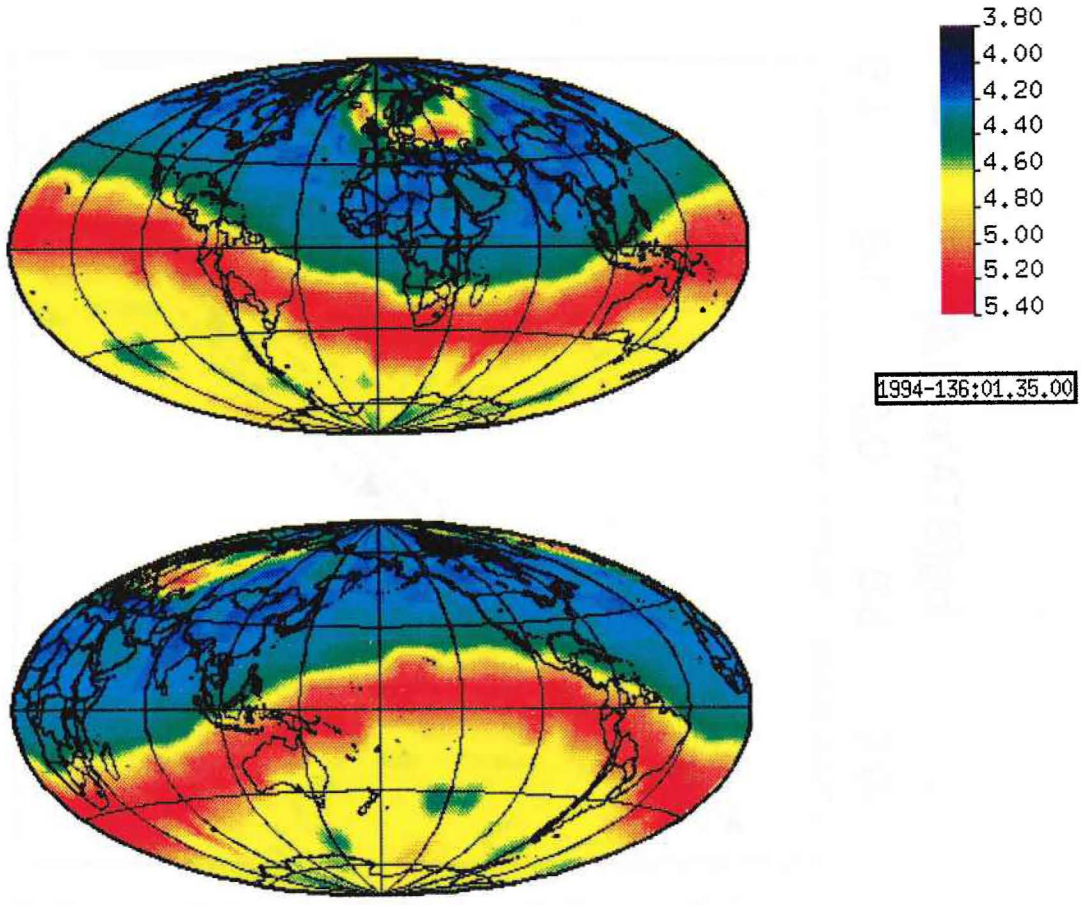

Fig. 7.1.9. Illustration of global threshold monitoring for the simplified case of a monitoring "network" consisting of one array (the Apatity station in NW Russia). The figure shows instantaneous thresholds globally (with two different world map perspectives) for a specified origin time. As illustrated by the color coding, the threshold ranges from near 4.0 in much of the northern hemisphere to about 5.5 in the shadow zone. Note the effect of a preceding local event on the threshold near Scandinavia (see text for details).

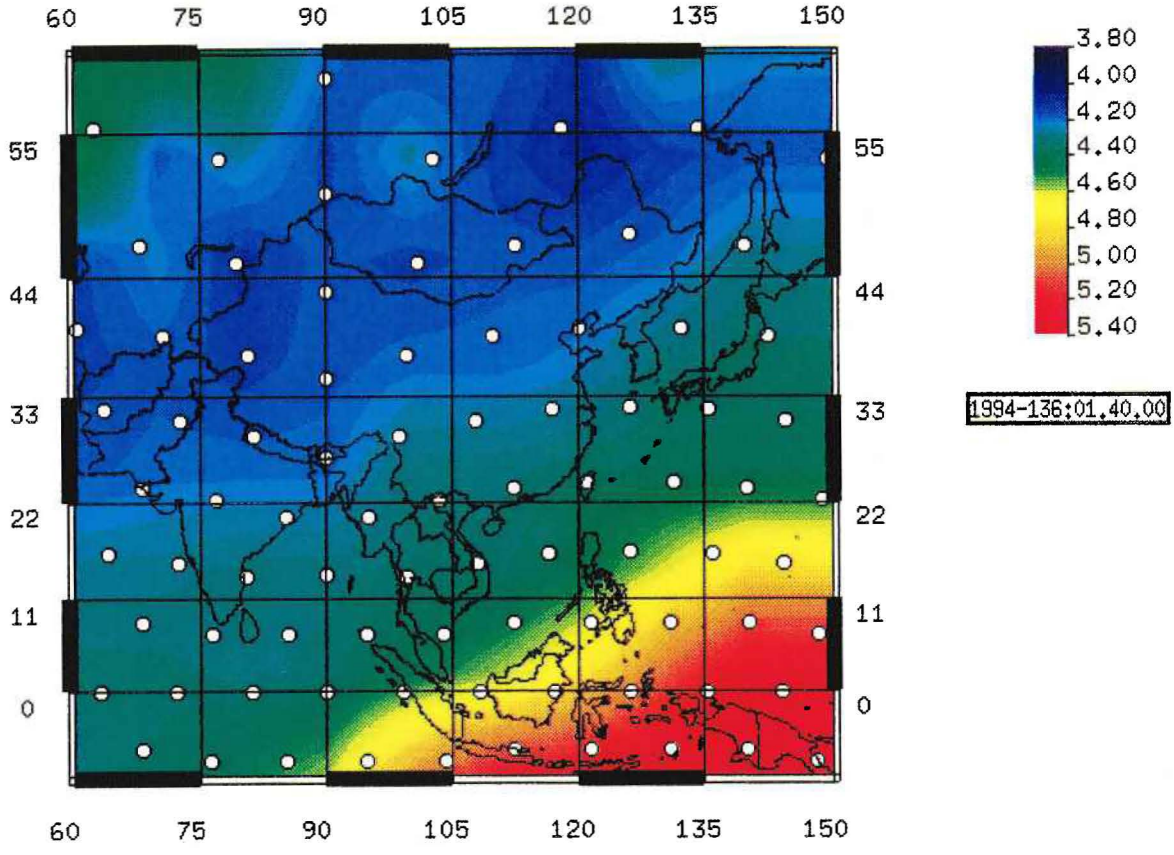

Fig. 7.1.10. A regional threshold map excerpted from the global map of Fig. 7.1.9. The figure shows the eastern Asia region, and grid points corresponding to the global 642 points triangularization (Fig. 7.1.2) are especially marked.

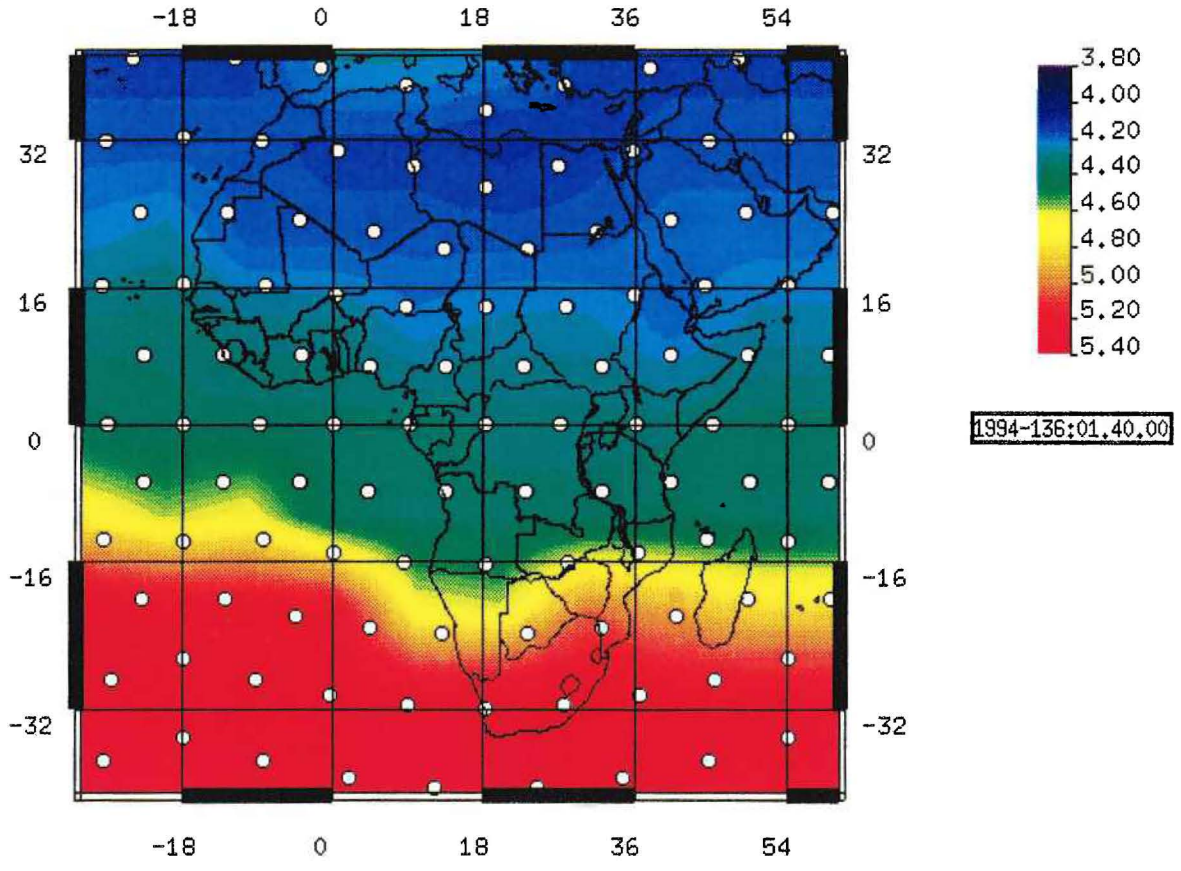

Fig. 7.1.11. Similar to Fig. 7.1.10, but covering the region of Africa/Middle East.

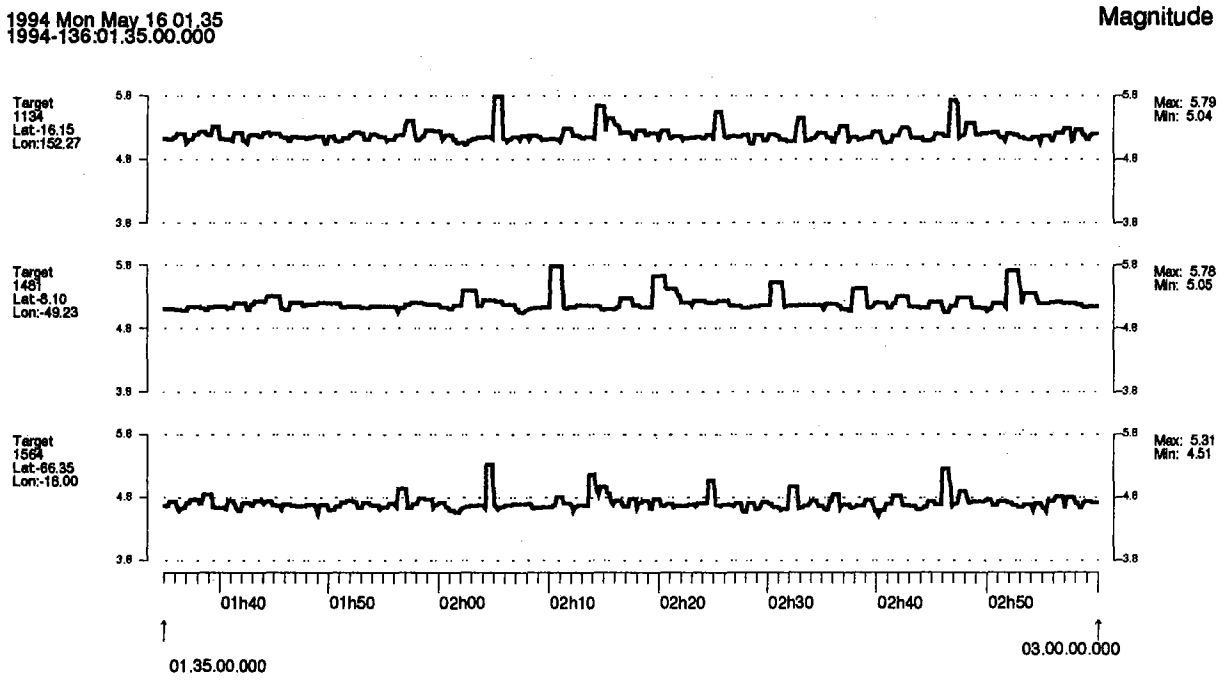

Fig. 7.1.12. Figure illustrating the display of individual threshold traces as a function of time. Traces corresponding to three grid points on the global map (all at teleseismic distances) are shown. Each trace covers about 1 1/2 hours. Such traces can be displayed interactively by clicking on the points of a global or regional map (Figs. 7.1.9-7.1.11) and specifying the desired time interval. This example is based on only one station in the "network" (the Apatity array).

7.2 Monitoring ESAL time-lag

Background

The Intelligent Monitoring System (IMS) is a software system of "a new generation of systems for automated and interactive analysis of data from a network of seismic stations to detect and locate seismic events" (Bache et al, 1991). A version of IMS that accepts data from an arbitrary number of arrays and single 3-component stations was installed at NORSAR in October 1991. The system currently processes data from the 6 arrays ARCESS, NORESS, FINESS, GERESS, Spitsbergen and Apatity.

One of the objectives of the IMS development was to improve the quality of the automatic event solutions and thus reduce the need for interactive, manual analysis. In addition to being accurate, the automatic solutions from IMS have to be quickly available to be useful in monitoring underground nuclear explosions. Ideally, the system should be operated in close to real-time to provide up-to-date explosion (and earthquake) alarms.

When IMS failed to define the Chinese test explosion on 5 October 1993 until 8 hours after the event occurred, an initiative was taken to start recording the time-lag in the ESAL (Expert System for Association and Location, the knowledge-based system which locates events in IMS) processing, as well as identifying the cause for each of these lags. It was expected that such an exercise would provide considerable insight into the complexity of the task of keeping a system like IMS running at close to real-time. In the following, the results from the first six months of monitoring time-lags (October 1993 - March 1994) are reported. The first three weeks have also been described in detail earlier (Baadshaug, 1993).

IMS architecture and design

Fig. 7.2.1 gives a broad outline of the IMS components relevant to this discussion.

The waveform data from the seismic stations are transferred to circular diskloops on acquisition computers. Signal processing programs extract detection parameters and store them in the SigPro database. Up to this point, there are separate programs for each station and all stations are processed in parallel. From here, data from all stations are processed together. Once an hour, detections from the SigPro database are copied to a second database used by ESAL. If one of the stations for some reason falls behind, the detection copying waits for that station, i.e., only detections with arrival time less than or equal to the last detection from the delayed station are copied. (See example in Tables 7.2.1 and 7.2.2) The progress of ESAL is vulnerable to all preceding processing steps. A delay at one station will propagate down the processing pipeline and delay event location.

This processing scheme is used because the IMS results are mainly used for research and bulletin production. The emphasis has been on completeness (wait for all detections from all stations) rather than speed (skip a station if it is too far behind). These are often con-

flicting criteria and in a continuous monitoring situation, the focus may have to be shifted to speed to provide early event notices.

As can be seen from Fig. 7.2.1, there are several hardware and software components in the system and therefore lots of error sources. In the current implementation, there is no redundancy or duplication of equipment. This may also have to change in a continuous monitoring situation with tight requirements on system reliability.

Collecting the time-lag data and checking ESAL progress

Every ten minutes, the UNIX system time (based on a GPS satellite clock) is written to a file together with the detection time last processed by ESAL (found in a database table - timestamp). The difference between these two times is the ESAL time-lag, i.e., the number of seconds ESAL is behind real-time.

In Fig. 7.2.2, the time-lag is shown in six plots, with one month of data in each.

The maximum time-lag was 204241 seconds, close to 57 hours, on 14 December 1993, when the communication to Apatity was down because of a satellite dish positioning problem.

The minimum time-lag was 868 seconds or 14 minutes 28 seconds. This should not be interpreted as a delay one can expect to see during normal operation with the current set-up, but rather as a result of a combination of favorable circumstances.

The median time-lag was 4770 seconds or approximately 1 hour and 20 minutes.

Table 7.2.3 shows examples of common reasons for delay.

In addition to the time-lag data, full reports of system progress are collected at less frequent intervals. These reports include the status of all processes which ESAL depends on: The last data time recorded for each station, the last detection processed, etc. Normally, it is possible to determine from these reports what caused ESAL to fall behind. This is usually done through a backward-trace where each processing step is checked in reverse succession:

1) Discover that ESAL processing is not up-to-date

2) Check if the latest detections have been copied from the SigPro- to the ESAL database.

3) Check if some signal processing job is delayed.

4) Check if the last recorded raw data are current.

It is not always possible to determine why ESAL falls behind. There may be no errors reported in log-files and the delay may have happened between two instances of the full system report.

An example showing both the backward-tracing of processing steps and some unexplained delays is seen in Figure 7.2.3. This example from April 1994 (after the reporting period) illustrates the mentioned points. The weekly ESAL time-lag plot had several peaks, meaning that location processing had fallen behind real-time. To find the reasons for the delays, the delays of the signal processing for each station were plotted. It was found that all delays were caused by the Spitsbergen SigPro. This shows how a single station can hold up all processing. The reason for the delays on April 5/6 and on April 10 were found to be large numbers of detections, overloading the computers where the signal processing software runs. The peaks on April 4 and April 8, however, remain unexplained. The one on April 8 is most likely caused by some network problem, as the SigPro programs for two other stations stopped as well. On April 4, there was no clue to the reason for the delay. The detection processor slowed down for no obvious reason and then caught up again by itself.

Problem classes and possible remedies

The reasons for delays in the ESAL-processing can largely be divided into four groups, each with their own possible remedies:

1) **Hardware**. Caused by errors and maintenance on computers, disks and communication equipment.

As mentioned above, there is no redundancy in the current IMS implementation. One way to minimize hardware downtime, would be to duplicate equipment. Fault-tolerant computer systems are commercially available with different degrees of redundancy. Parallel execution of the same program on several CPUs, disk mirroring and alternative network routes are measures that could improve the IMS uptime and reduce the time-lag.

2) **Software**. Stops due to program bugs or upgrades.

At the moment, programs in the IMS system are started manually. When a program aborts on an error, it will stay down until manually restarted. The downtime could be significantly reduced by implementing Manager programs that will detect stops and do an automatic restart. This may not, however, be desirable. Some error situations should cause a program to halt until an operator has cleared the underlying cause. A Manager program may also introduce another error source into the system as happened at the aforementioned Chinese test explosion on 5 October 1993. At that time, the detection processors for each station were checked automatically (by a program in the UNIX crontab file) on an hourly basis. This check failed, i.e., a running detector was seen as stopped, and a second detector was started. This overloaded the computer, causing the detection processing to fall hours behind in addition to creating duplicate phase detections.

3) **Data**. Missing or delayed waveforms. Most of these delays can usually be traced back to malfunctioning hardware, and belong under 1) but some are results of field work, power outages or weather conditions (e.g snow on satellite dish) and can be treated as a separate category.

Smarter or more flexible processing algorithms would handle the situations not caused by faulty hardware. At the moment, no event location or association is performed until data are available from all stations. A processing scheme where a station is left out of the processing if it is more than a predetermined interval behind, would allow events to be formed at a closer to real-time rate. Such a scheme could be adopted, and would be in accordance with the GSETT-3 IDC Alpha/Beta station processing where stations that do not have data available in real-time could contribute in the next refinement of the event solution.

4) **Seismicity**. Large number of detections, often because of temperature changes resulting in ice-cracking or thawing.

Since each phase detection initiates several processing steps (quality assurance, beaming, onset estimation, broadband FK-analysis, polarization analysis and numerous database accesses), bursts of detections will slow down the signal processing. The number of detections vary both with the time of day (working hours, cultural noise) and with the season (ice-cracking, see example below). From the start, the signal processing programs for several stations used the same SUN SparcStation 1 computer. During periods of normal seismicity, this worked well, but peak periods made the machines struggle. This problem was greatly reduced when a SUN SparcStation IPC was allocated to each SigPro process, but can probably be eliminated altogether if a better distribution of processing load is introduced. This would call for some kind of Manager program, similar to the one outlined under 1), that would detect processing bottlenecks and move the struggling programs to higher capacity computers.

At ARCESS seasonal variations related to ice-cracking/-thawing have been observed (Fyen and Hansvold, 1992) which can make the number of detections rise to 1200 - 1500 a day compared to a few hundred on a normal day, see Fig. 7.2.4a). When the ARCESS signal processing ran on a SUN SparcStation IPC, the processing load of these bursts would make the processing fall as much as 19 hours behind (See Fig. 7.2.4b). After a SparcStation 10 was introduced in the system and used for ARCESS processing, this problem has disappeared. This machine will not help when other arrays have detection bursts, unless their signal processing are moved there manually.

There seem to be two possible ways to handle increased number of detections: Upgrades to faster processing hardware or introduction of automatic distribution of the processing load.

Relevance to continuous monitoring.

We have only studied time-lags in the ESAL processing. This gives us a measure of the delay in the automatic definition of events. In a continuous monitoring situation, other delays further down the processing pipeline may be equally important. Retrieval of raw waveforms from the diskloop machines, beamforming and event plotting are tasks which have to be up-to-date to allow early event review by a human analyst.

In a monitoring situation, there will probably also be stricter limits on the delays allowed. The current deadline for including an event in the GSETT-3 IDC Alpha Event List (AEL), is about 50 minutes after recording (IDC staff, 1994). With the inherent delays in the IMS processing implementation at NORSAR (Baadshaug, 1993), lots of events will not be defined until two hours after recording, even in normal, error-free processing, and would miss this deadline.

Stead (1994) explains how the time limit policy has been enforced at the GSETT-3 IDC:

"Originally, the system functioned with a drop-dead time. This was enforced by requiring esal to run on pre-determined time intervals at pre-determined times (using cron). For example, the AEL was run every 20 minutes for a time window 20 minutes long ending at the GMT when it was run. With a 30-minute lookback, this means that the oldest data esal could look at would be detections associated with an event that had detections within 50 minutes of real time. No new events could be formed unless all the detection were within 50 minutes of realtime (at the start of the esal run). Esal normally runs in less than 10 minutes, so the events were all but guaranteed to be in the database before the hour."

In January 1994, the IDC adopted a new model where time segments of possibly non-uniform length are generated for ESAL automatically. There may also be more changes. The drop-dead times (no data will ever be included in a bulletin if it arrives late) still in use may give way to targets (IDC only tries to get the bulletin in final form by the deadline, but may be delayed, and may include late-arriving data).

When deciding which model to use, issues discussed above should be relevant. If the waveform data arrives on time but the signal processing computer is overloaded and falls behind because of detection bursts, should the detections be included? They probably should, but a decision has to be made regarding what to do with this and other types of late-arriving data.

U. Baadshaug
B. Ferstad

References

Baadshaug, U. (1993): ESAL time-lag statistics, in *NORSAR Semiannual Tech. Summ. 1 Apr 1993 - 30 Sep 1993*, Scientific Rep. No.1-93/94, Kjeller, Norway.

Bache, T.C., S.R. Bratt, J.W. Given, T.D. Schroeder, H.J. Swanger, J. Wang (1991): The Intelligent Monitoring System Version 2, *NMRD Quarterly Technical Report #7,* SAIC-91/1137, San Diego, CA.

Fyen, J. and K. Hansvold (1992): Correlation between temperature and number of detections, in *NORSAR Semiannual Tech. Summ. 1 Oct 1991 - 31 Mar 1992*, Scientific Rep. No. 2-91/92, Kjeller, Norway.

IDC Staff (1994):, *IDC Performance Report, March 5 - 18, 1994*, March 23, 1994

Stead, R (1994): *Personal communication*

Station	Detection time
NORESS	1994-050:11.58.17
GERESS	1994-050:11.58.00
ARCESS	1994-050:11.55.49
Spitsbergen	1994-050:11.52.00
Apatity	1994-050:08.29.25
FINESS	**1994-049:22.58.30**

Table 7.2.1. Times of the last processed detection for each station. (Taken from the **sigpro_time** table in the sigpro database). FINESS has fallen behind real time.

Process Class	Process Name	Time
ARS	ANALYST	1994-043:00.00.00
DetMag	ANALYST	1994-043:00.00.00
EvPlot	ANALYST	1994-043:00.00.00
bull	ANALYST	1994-043:00.00.00
bull	NRSN	1994-049:00.00.00
Beamer	APA0	1994-049:21.58.30
GetData	APA0	1994-049:21.58.30
Beamer	ARA0	1994-049:21.58.30
GetData	ARA0	1994-049:21.58.30
Beamer	FIA0	1994-049:21.58.30
GetData	FIA0	1994-049:21.58.30
Beamer	GEC2	1994-049:21.58.30
GetData	GEC2	1994-049:21.58.30
Beamer	NRA0	1994-049:21.58.30
GetData	NRA0	1994-049:21.58.30
DetMag	NRSN	1994-049:21.58.30
EvPlot	NRSN	1994-049:21.58.30
Beamer	SPA0	1994-049:21.58.30
GetData	SPA0	1994-049:21.58.30
GET_DET	NRSN	**1994-049:22.58.30**
ESAL	NRSN	1994-049:22.58.30

Table 7.2.2. Times last processed by IMS programs, taken from the **timestamp** table in the IMS database. 'ARS ANALYST' shows how far manual analysis has advanced. The 'EvPlot' entries give the time of the last analyzed ('ANALYST') and automatic ('NRSN') event plotted. 'GetData <station>' gives the time of the newest data retrieved to the IMS from the diskloop. 'GET_DET NRSN' is the GetArrivals-process (see Fig. 7.2.1) that fetches detections from the EP-SigPro database to the IMS database. It never proceeds beyond the oldest time in Table 7.2.1.

Station/Program	Error	Reason
ESAL	Machine down	Changed disk on tjalfe
ESAL	Slow processing	Unknown reason, network problem?
ESAL	Stopped	Bad Apatity detection
GetArrivals	Failed (twice)	
IMS	Database down	Parity error on vile
Sigpro	Database down	Changed disk on ve
apatity	Delayed data	
apatity	No data	Satellite dish positioning problem
apa_ep		Number of detections, gaps in the data
arcess	No data	Snow on antenna?
arcess_ep		Number of detections
arcess_ep	Stopped	Changed disk on rein
finess	No data	
finess_ep		Diskloop read error
finess_ep	Stopped	Bad data
geress		Communication down
geress_ep	Beamforming failed	Sonic boom
noress_ep		Diskloop read error
spitsbergen	Delayed data	
spitsbergen	No data	Broken power supply
spi_dp	Delayed	Unknown reason
spi_dp & apa_ep	Delayed	
spi_ep	Stopped	Bad data?

Table 7.2.3 Examples of reasons for stops or delays in ESAL processing

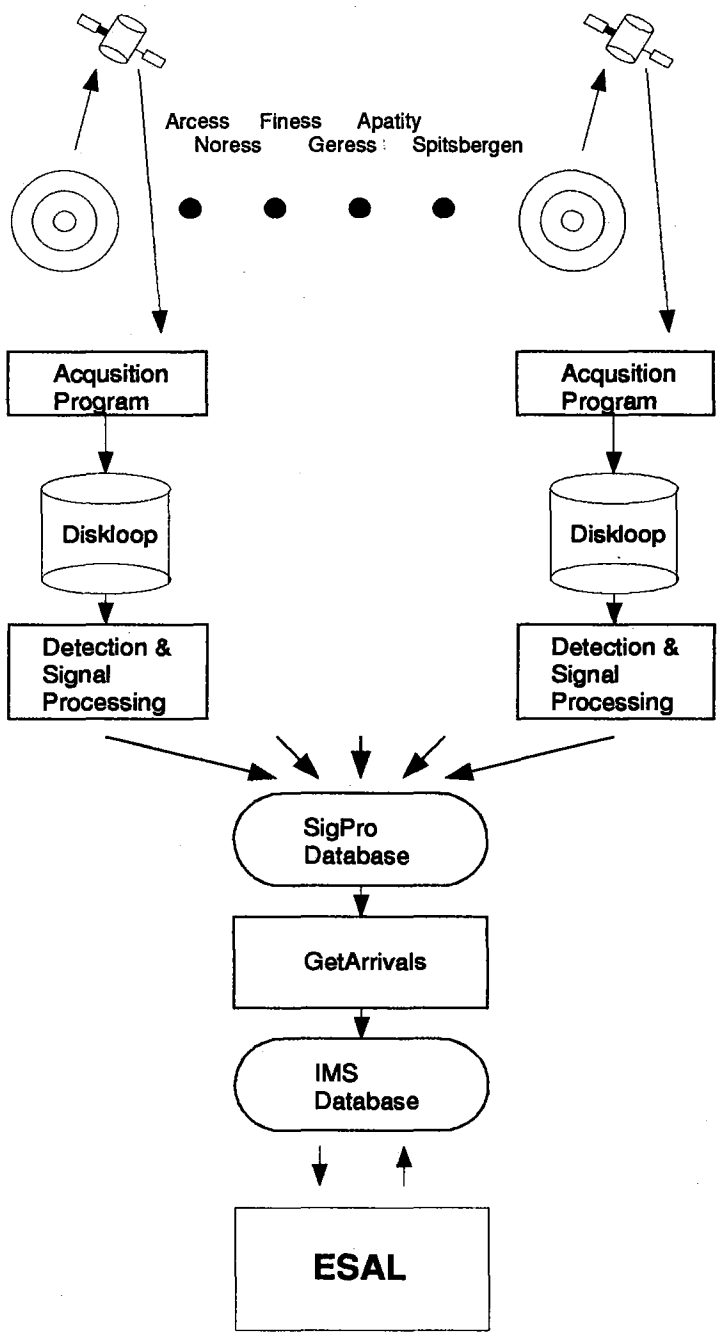

Fig. 7.2.1. Major IMS hard- and software components from seismic station to event association and location. All stations are processed separately, but in parallel, until the detections are entered into the SigPro database. From there, the detections from all stations are processed together.

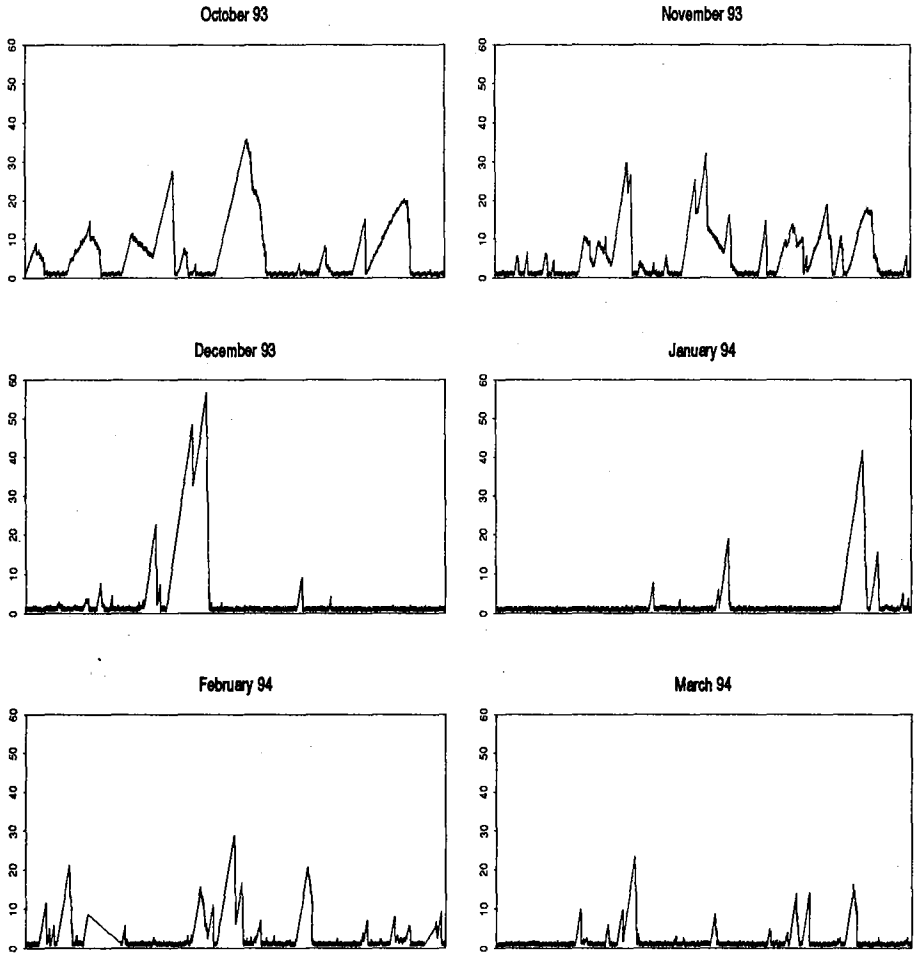

Fig. 7.2.2. ESAL time lag, October 1993 - March 1994. Each plot contains one month of time-lag data and shows the difference in hours between ESAL processing time and real time.

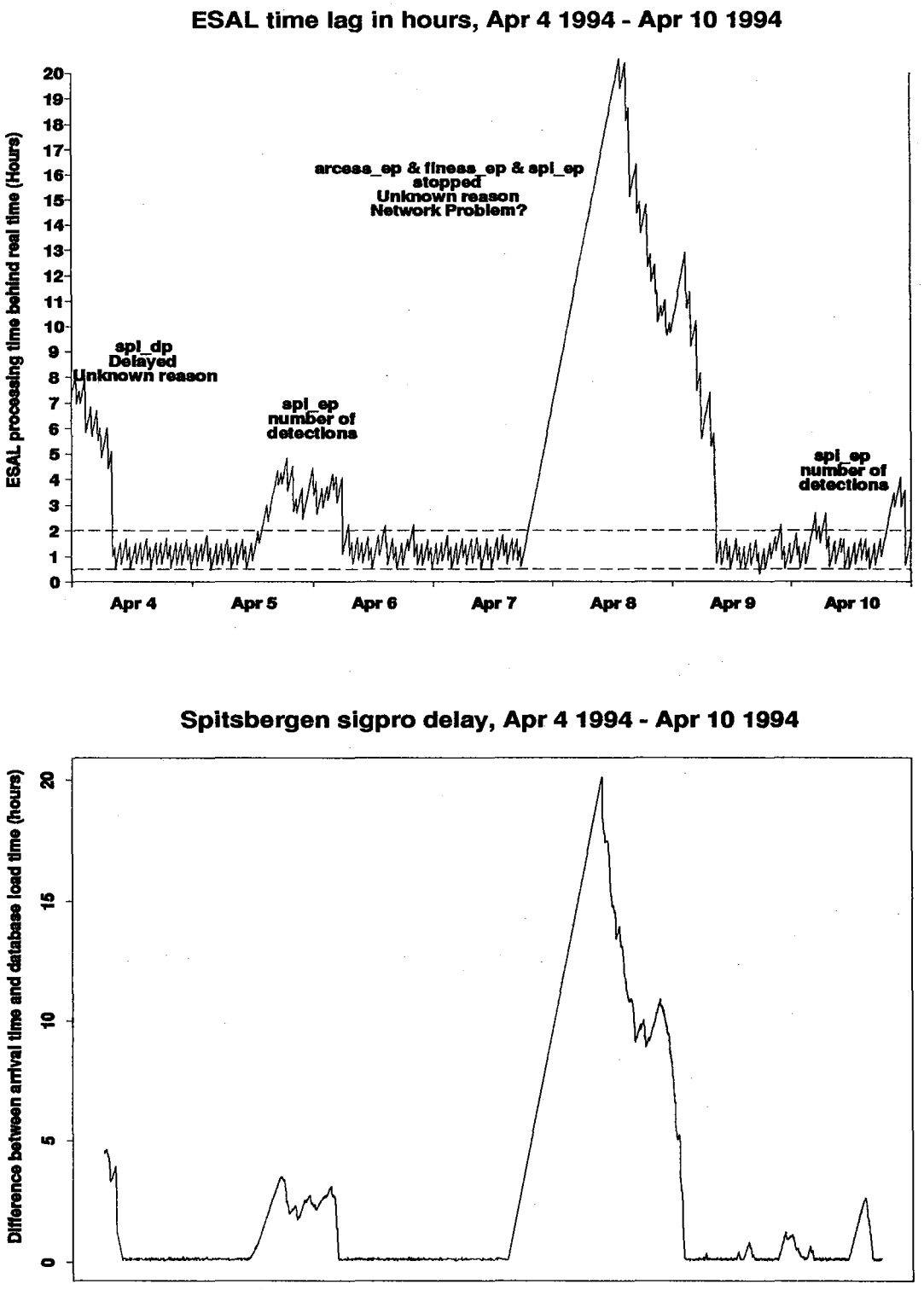

Fig. 7.2.3. ESAL time lag, April 4 - April 10, 1994 (top) and Spitsbergen signal processing delay for the same period (bottom).

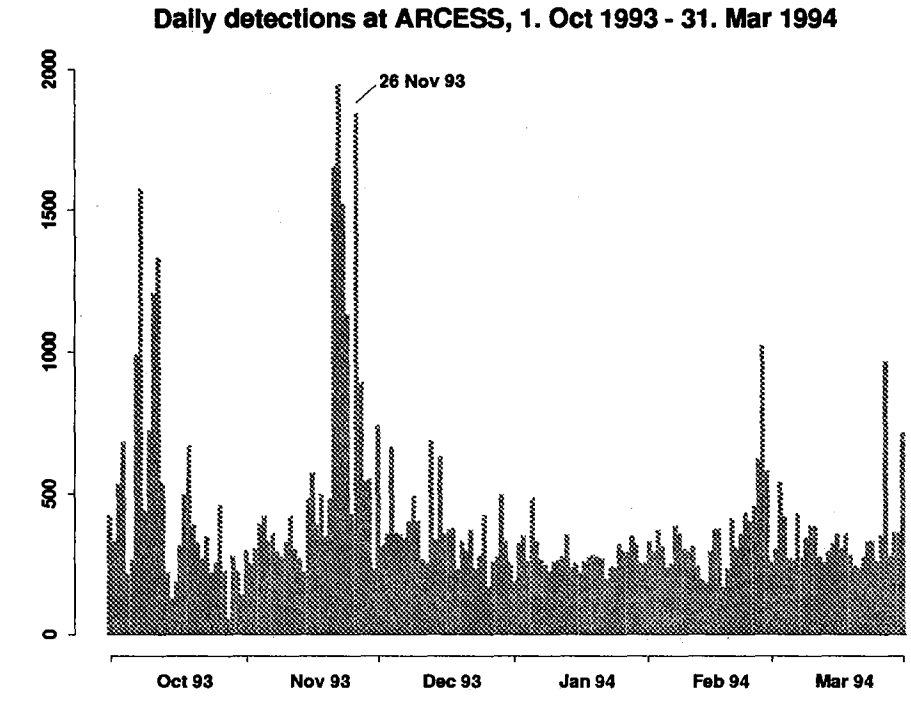

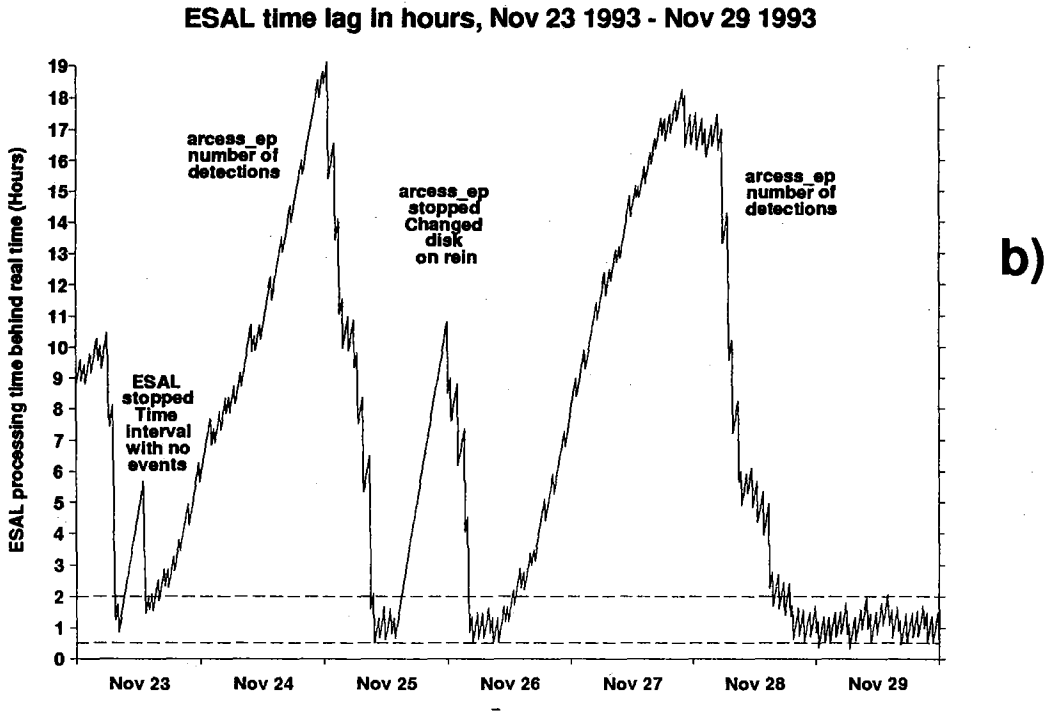

Fig. 7.2.4. a) The number of detections per day at ARCESS for the reporting period and **b)** ESAL time lag for the period with many detections in late November 1993.

7.3 Signal detection and waveform extraction in the coda of a strong, interfering event

Introduction

A possible scenario for evading a nuclear testing treaty is to hide the seismic signals from a nuclear explosion in the wavetrain of a strong interfering earthquake. At small aperture arrays, some improvement in detection and parameter estimation capability of such "hidden" signals can be obtained by conventional beamforming and filtering techniques. There are, however, other approaches that are likely to be more powerful for this purpose, and we have in this study investigated a number of such methods.

For simplicity and to avoid confusion, the "hidden" signal is in this paper called "the explosion", whereas the interfering wavetrain is called "the earthquake" or the "noise". In general, signal detection and waveform extraction in the coda of a strong interfering wavetrain can be performed under different conditions that arise in different applications:

1. The azimuths and slownesses of both the explosion and the earthquake signals are assumed to be known.
2. The azimuth and slowness of the explosion signal is known, but unknown for the earthquake, e.g., due to uncertainty of the azimuth and slowness characteristics of the earthquake coda or in the case of real time processing.
3. The azimuth and slowness of the earthquake is known, but unknown for the explosion.
4. The azimuth and slownesses are unknown for both the explosion and the earthquake.

In practical applications, scenarios 1 and 3 above would probably be the most useful. In these two cases, it is assumed that the earthquake has been well located, so that azimuth and slowness can be assumed known. The search for a potential hidden signals (the explosion) might be done without any assumptions on its location (case 3), or one might want to focus upon a site of special interest (case 1).

The scenarios 2 and 4 are most interesting for detecting potential hidden events relatively far into the coda of the earthquake. Even if the earthquake location is known, the scatter in azimuth and slowness of coda phases might make it appropriate to apply the model of an unknown earthquake source as done in these two cases.

In this paper we discuss array data processing algorithms that seem to be helpful to solve the problem under conditions 1) and 2). In these cases, the apparently best way to detect and estimate the parameters of the signal is to apply beamforming (or group filtering) procedures by which the array spatial receiver function attains its maximum gain in the direction and slowness of the explosion while minimizing the gain in the direction and azimuth of the interfering earthquake.

Spatial Rejection Filtering

When the azimuths and slownesses of both the explosion and the earthquake signals are known, we propose to use a "spatial rejection group filter" (SRGF) to improve the detection and parameter estimation capability of the "hidden" explosion. A group filter $\bar{r}(j) = (r_1(f), \ldots, r_m(f))$ is a multichannel filter that transforms the m input array data traces $\bar{x}(f) = (x_1(f), \ldots, x_m(f))^T$ (where T denotes transposition) into a scalar trace $y(f)$ via the equation

$$y(f) = \bar{r}^*(f)\,\bar{x}(f) \tag{1}$$

Equation (1) is written in the frequency domain, where f is the frequency $0 < f < f_{smp}/2$, f_{smp} is the sampling frequency and * denotes complex conjugation.

The vector frequency response of the spatial rejection group filter can be written as:

$$\bar{r}^*(f) = \frac{\bar{h}_s^*(f)\,\mathbf{B}(f)}{\bar{h}_s^*(f)\,\mathbf{B}(f)\,\bar{h}_s(f)} \tag{2}$$

where

$$\bar{h}_s(f) = e^{-i2\pi\tau_{s,k}f/f_{smp}}, \qquad k = 1, \ldots, m \tag{3}$$

is the columns vector of "signal frequency delays" corresponding to the signal time delays $\tau_{s,k}$ between the *1st* sensor and the *k-th* sensor of the array.

$$\mathbf{B}(f) = \frac{\mathbf{I} - \bar{h}_n(f)\,\bar{h}_n^*(f)}{\bar{h}_n^*(f)\,\bar{h}_n(f)} \tag{4}$$

(where **I** is the identity matrix) is the matrix spatial rejection filter designed to reject the purely coherent wave arriving from the direction and slowness of the interfering earthquake source (the "noise"). The matrix $\mathbf{B}(f)$ is determined by the "noise frequency delays"

$$\bar{h}_n(f) = e^{-i2\pi\tau_{n,k}f/f_{smp}}, \qquad k = 1, \ldots, m \tag{5}$$

corresponding to the time delays $\tau_{n,k}$ of the interfering earthquake signals.

For the problem under discussion, the residual beamforming (RB) method is often used (Gupta et al, 1990). By this method, the beam steered to the "noise" direction is subtracted from every channel to create residual traces. Then a new beam steered to the signal direction is composed from the residuals. This method can be formulated as the implementation of a group filtering procedure with the vector frequency response

$$\bar{r}_{RB}(f) = h_s^*(f)\,\mathbf{B}(f) \tag{6}$$

Both group filters (2) and (6) suppress (theoretically - completely eliminate) the interfering purely coherent "noise" wave arriving from the assigned direction. The array record of the interfering wave can be written in the frequency domain in the form $\bar{n}(f) = \bar{h}_n(f)\, n_{WF}(f)$, where $n_{WF}(f)$ is the (scalar) spectrum of the interfering wave.

Substituting $\bar{n}(f)$ into eq. (1) gives

$$z(f) = \bar{r}_{RJ}^{*}(f)\,\bar{n}(f) = 0 \quad \text{and} \quad z(f) = \bar{r}_{RB}^{*}(f)\,\bar{n}(f) = 0 \tag{7}$$

because

$$\mathbf{B}(f)\,\bar{n}(f) = \left[\frac{\bar{h}_n(f) - \bar{h}_n(f)\,\bar{h}_n^{*}(f)\,\bar{h}_n(f)}{\bar{h}_n^{*}(f)\,\bar{h}_n(f)}\right] n_{WF}(f) = 0 \tag{8}$$

Note that the RB method has a disadvantage because it distorts the frequency content of the "hidden" explosion signal, and can therefore not be regarded as "pure spatial" filtering. In contrast, the SRGF is a signal undistorting procedure. This is shown in the following:

The vector spectrum of an array record for a purely coherent "hidden" signal has the form $\bar{s}(f) = \bar{h}_s(f)\, s_{WF}(f)$, where $s_{WF}(f)$ is the scalar spectrum of the signal waveform. Substituting $\bar{s}(f)$ into eq. (1) gives for the SRGF method

$$y(f) = \frac{\bar{h}_s^{*}(f)\,\mathbf{B}(f)\,\bar{h}_s(f)\,s_{WF}(f)}{\bar{h}_s^{*}(f)\,\mathbf{B}(f)\,\bar{h}_s(f)} = s_{WF}(f) \tag{9}$$

For the RB method

$$y(f) = \bar{h}_s^{*}(f)\,\mathbf{B}(f)\,\bar{h}_s(f)\,s_{WF}(f) = \bar{h}_s^{*}(f)\left[\frac{\bar{h}_s(f) - \bar{h}_n(f)\,\bar{h}_n^{*}(f)\,\bar{h}_s(f)}{\bar{h}_n^{*}(f)\,\bar{h}_n(f)}\right] s_{WF}(f) \tag{10}$$

$$= \bar{h}_s^{*}(f)\,\bar{\rho}_s(f)\,s_{WF}(f)$$

To illustrate the difference in performance between the spatial rejection group filter (SRGF) and the residual beamforming (RB) methods, we have simulated a mixture of a two fully coherent plane waves with different azimuths and slownesses, using the sensors of the NORESS array. The signal plane wave was assumed to arrive from the Novaya Zemlya Test Site (azimuth: 32.9 deg., apparent velocity: 14.8 km/s), and the signal waveform was generated as a linear frequency modulated signal with constant amplitude ("sweep signal"). The interfering (noise) plane wave was assumed to arrive from the Hindu Kush area (azimuth: 101.0 deg., apparent velocity: 14.8 km/s), and its waveform was set equal to a real Hindu Kush P-phase observation. The ratio between the maximum amplitudes of the signal and the interfering plane wave was 0.13.

Fig. 7.3.1a shows the residuals after processing with the matrix spatial rejection filter **B**(f). We see that the interfering wave is completely suppressed, but the shape of the"hidden"

signal is distorted at low frequencies. We also note that distortions are different for the different channels.

The upper trace of Fig. 7.3.1b is the result of conventional beamforming steered to the Novaya Zemlya Test Site. In this case the low SNR hidden signal cannot be identified. The second trace of Fig. 7.3.1b is the result of the residual beamforming method realized as group filtering in the frequency domain in accordance with equations (1) and (6). The simulated interfering earthquake waveform is completely suppressed, but the "hidden" signal amplitude is strongly reduced at low frequencies. It follows from eq. (10) that these signal frequency distortions are dependent on both the array geometry and the arrival directions of the incoming signals. The third trace of Fig. 7.3.1b is the output of spatial rejection group filtering in accordance with equations (1) and (2). This group filter extracts the sweep signal from the interfering earthquake and retains the waveform of the hidden signal undistorted. The fluctuations of the signal amplitudes at the end of the trace are explained by signal frequencies approaching the Nyquist frequency of the data.

In practice, signals arriving at an array do not consist of a single plane wave component and are not fully coherent among the array sensors. To illustrate the performance of SRGF and RB under such "real" conditions, we have created an event mixture by superimposing down-scaled NORESS records of the Novaya Zemlya (NZ) explosion of 24 October 1990 in the coda of a real Hindu Kush (HK) earthquake (Origin time: Oct. 25, 1990, 04.53.59.9). The ratio between the maximum amplitudes of the explosion and the earthquake was 0.2, and the P-phase from the explosion was set to arrive 12 s after the HK P-arrival. The lower trace of Fig. 7.3.2 show the event mixture at the central element of the NORESS array. The top trace is the conventional beam steered in agreement with the delays of the NZ P-phase. Also in this case we can see that the output from the RB method (trace no. 3) contain less low frequency components for the hidden signal as compared to the output from the SRGF (trace no. 2). It should also be emphasized that high-pass filtering of the SRGF output will for the NZ P-phase provide SNR comparable to the SNR of the output from the RB method.

Adaptive Optimal Group Filtering

The late part of an earthquake coda consists of wave components arriving from very different azimuths and slownesses. To reject this type of interfering energy, it is not very meaningful to use the spatial rejection group filter. The same applies to real-time processing, when the frequency delays are unknown. In this situation (case 2 of the Introduction) the adaptive optimal group filter (AOGF) can be helpful (Kushnir et al., 1990a; Kushnir et al., 1990b). The vector frequency response of the AOGF filter is

$$\bar{r}_{AO}{}^{*}(f) = \frac{\bar{h}_s{}^{*}(f)\,\hat{\mathrm{F}}_n^{-1}(f)}{\bar{h}_s{}^{*}(f)\,\hat{\mathrm{F}}_n^{-1}(f)\,\bar{h}_s(f)} \tag{11}$$

where $\hat{\mathrm{F}}_n^{-1}(f)$ is an estimate of the inverse matrix spectral density of the array "noise" (in our case the "noise" is the interfering event). Kværna and Kushnir (1991) showed that the-

oretically an adaptation window could include the plane wave signal we wanted to retrieve without significantly degrading the performance of AOGF filtering. We will refer this type of adaptation as self-adaptation.

Fig. 7.3.3 presents the results from processing the mixture of simulated plane waves (described in the connection with Fig. 7.3.1b) using the self-adaptive AOGF. The upper trace is the result of conventional beamforming steered to the Novaya Zemlya Test Site. The second trace is the output from processing with the self-adapted AOGF and the third trace is the output from the SRGF (assuming signal from Novaya Zemlya and interfering energy from Hindu Kush). The bottom trace shows the mixture as observed on the central NORESS sensor. When comparing the second and the third trace we find that the self-adaptive AOGF in the case of two interfering plane waves performs almost as well as the spatial rejection group filter, and we emphasize that the self-adaptive AOGF does not require any information on the arrival direction of the interfering event.

However, our experiments with mixtures of real events revealed a significant reduction in the performance of the AOGF filtering when the self-adaptation was performed, as compared to adaptation to the interfering event without using the signal window. We believe that this is due to the fact that both the signal and the interfering energy deviate strongly from single plane wave components. We will in the following illustrate this problem:

In Fig. 7.3.4a, the adaptation of the AOGF was made using the pure Hindu Kush recording. The NZ signal was then mixed with the Hindu Kush event (SNR 0.1) and AOGF filtering was performed. The result is shown in traces 2 and 3, using two slightly different implementations of the algorithm. For comparison, the output from conventional beamforming and SRGF is shown in traces 1 and 4. For this artificial situation, the performance of AOGF is excellent. However, results from AOGF after self-adaptation do not give nearly as good results, see traces 2 and 3 of Fig. 7.3.4b. In Fig. 7.3.4c the SNR of the NZ signal was raised to 0.3, and we see that the both the output from AOGF after self-adaptation (traces 2 and 3) and SRGF shown in the lower trace, clearly extract the signals from the earthquake coda.

Adaptive Optimal Phase Detection

The difference in frequency content between the Novaya Zemlya explosion and the Hindu Kush earthquake may enable us to detect the explosion on the self-adapted AOGF trace even if the SNR is very small. Fig. 7.3.5 shows the result after processing the self-adapted AOGF output with an adaptive optimal phase detector (AOPD). The SNR of the NZ signal was set to 0.05, and the NZ P-phase arrived 21 sec after the Hindu Kush P-arrival. The entire self-adapted AOGF output (trace no. 3) was used for detector adaptation, resulting in an average AR-model. Then the AR-coefficients were used for calculation of the Chi-squared detector statistics (Pisarenko et al., 1987; Kushnir et al., 1991) using data within 4-sec windows moving along the self-adapted AOGF trace. The detector statistics are shown in the upper trace of Fig. 7.3.5. We see that although the explosion signal is not clearly identified on the output from the self-adapted AOGF (trace no. 3) or SRGF (trace no. 4), the AOPD (trace no. 1) gives us convincing evidence of the presence of the signal.

The high sensitivity of the AOPD can therefore be helpful as a tool to be used for signal detection and waveform extraction of signals with low SNR. A practical procedure would be first to run the AOPD on a conventional beam output to determine the approximate onset time of the signal. The second step would comprise AOGF adaptation using the interval before (and may be after) the signal arrival, and the final step would be to process the entire data segment with AOGF.

Fig. 7.3.6 illustrates the performance of such a combined procedure. A mixture of real Novaya Zemlya and Hindu Kush recordings with SNR 0.2 was created. The onset time of the Novaya Zemlya signal was set to 41 sec after the onset of the Hindu Kush P-arrival. The conventional beam steered to Novaya Zemlya is shown in the second trace, but the signal is difficult to identify. However, after running the AOPD, the presence of a signal is clear. After running AOGF adaptation on the time segment preceding the signal (0-39 sec.), the data segment (0-60 sec.) was filtered by AOGF (trace no. 3). We see that a clear signal waveform is extracted, and the quality is somewhat better than the output from SRGF shown in trace no. 4. In practice, the SRGF cannot be implemented when information on the interfering signal is unknown.

A. Kushnir, MITPAN, Moscow
T. Kværna

References

Gupta, I.N., C.S. Lynnes and R.A. Wagner (1990): Broadband F-k analysis of array data to identify sources of local scattering, *Geophys. Res. Letters*, 17, 2, 183-186.

Kushnir, A.F., V.M. Lapshin, V.I. Pinsky and J. Fyen (1990): Statistically optimal detection using small array data, *Bull. Seism. Soc. Am.*, 80, 6, 1934-1950.

Kushnir, A.F., V.I. Pinsky, S.L. Tsvang, J. Fyen, S. Mykkeltveit and F. Ringdal (1990): Optimal group filtering and noise attenuation for the NORESS and ARCESS arrays, *Semiann. Tech. Summ., 1 April - 30 September 1990*, NORSAR Sci. Rep. no. 1-90/91, Kjeller, Norway, 115-134

Kushnir, A.F., J. Fyen and T. Kværna (1991): Studying of multichannel statistical data processing algorithms in the framework of the NORSAR event processing package, *Semiann. Tech. Summ., 1 October 1990 - 31 March 1991*, NORSAR Sci. Rep. no. 2-90/91, 82-103.

Kværna, T. and A.F. Kushnir (1991): Initial testing of mixed event separation using statistically optimal adapative algorithm, *Semiann. Tech. Summ., 1 April - 30 September 1991*, NORSAR Sci. Rep. no. 1-91/92, 112-126.

Pisarenko, V.F., A.F. Kushnir and I.V. Savin (1987): Adaptive algorithms for estimation of onset moments of seismic phases, *Phys. Earth Planet. Inter.*, 47, 4-10.

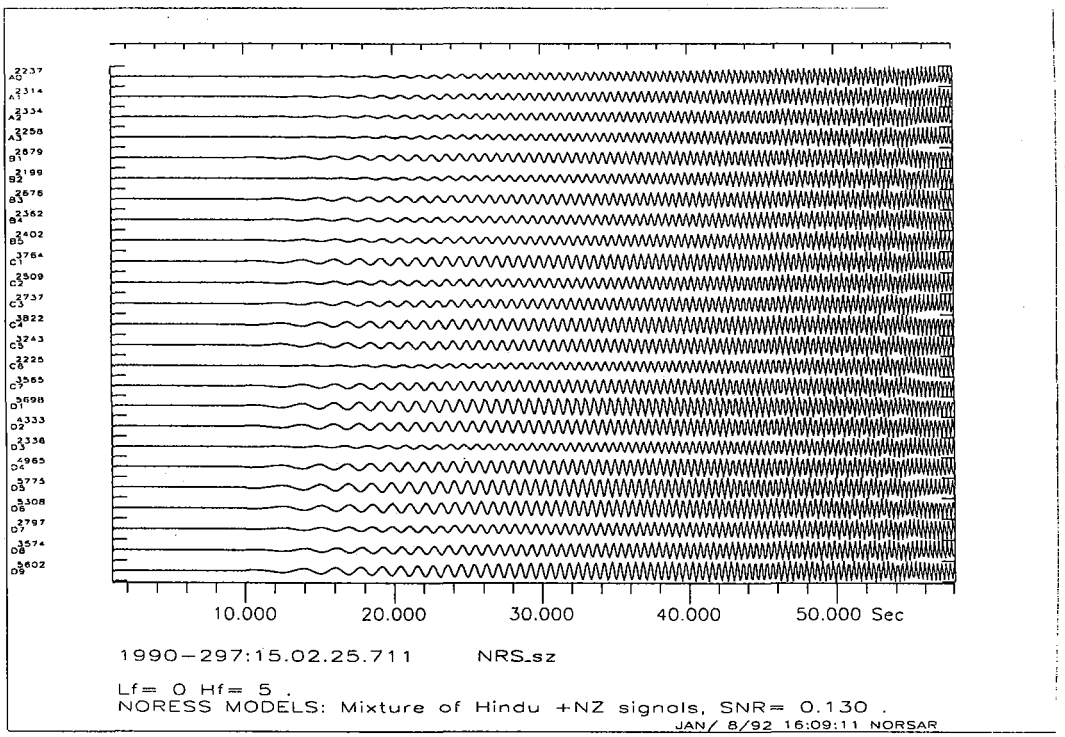

Fig. 7.3.1a. Residuals after processing a simulated mixture of two plane waves with a matrix spatial rejection filter. See text for a detailed explanation.

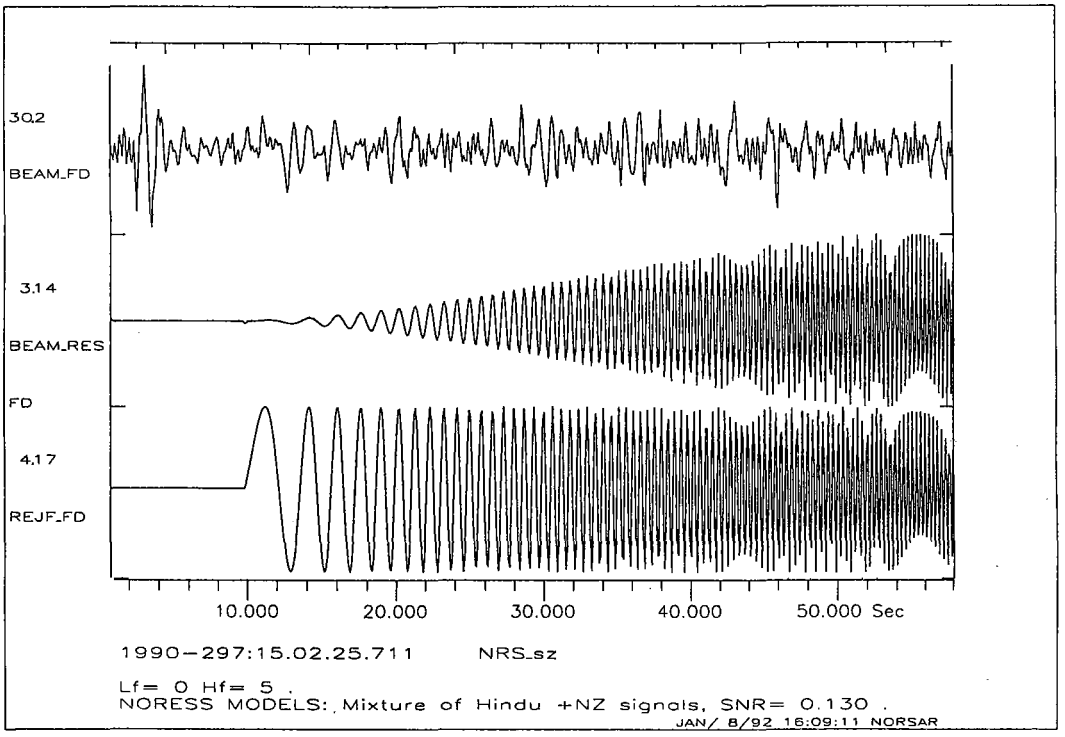

Fig. 7.3.1b. Results after processing a simulated mixture of two plane waves with three different rejection filters. The upper trace - conventional beamforming, the second trace - residual beamforming, the third trace - spatial rejection group filter. See text for detailed explanation.

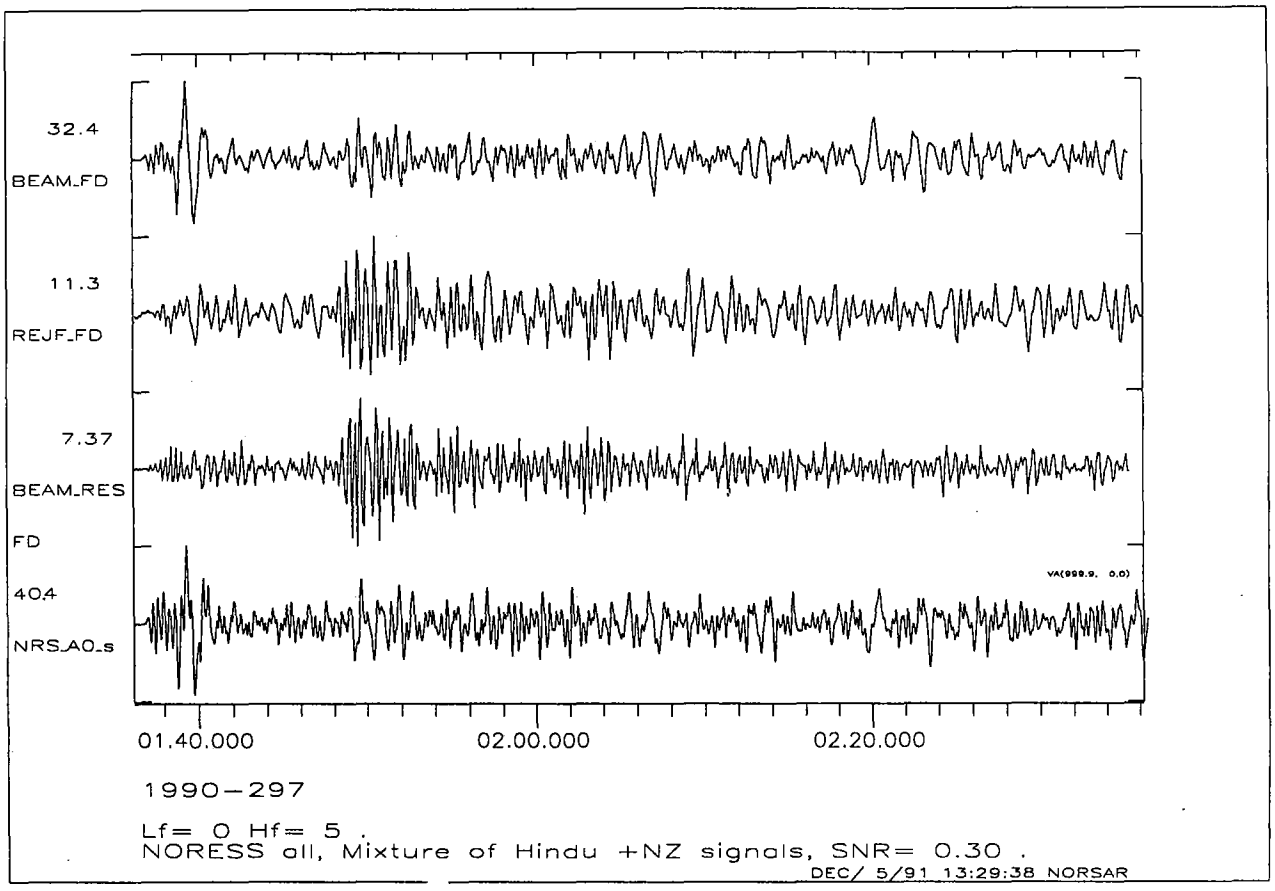

Fig. 7.3.2. Output after processing an artificial mixture of two NORESS recorded events with the spatial rejection filters.The upper trace - conventional beamforming, the second trace - spatial rejection group filter, the third trace - residual beamforming. The lower trace shows the event mixture at the central element of the NORESS array. See text for detailed explanation.

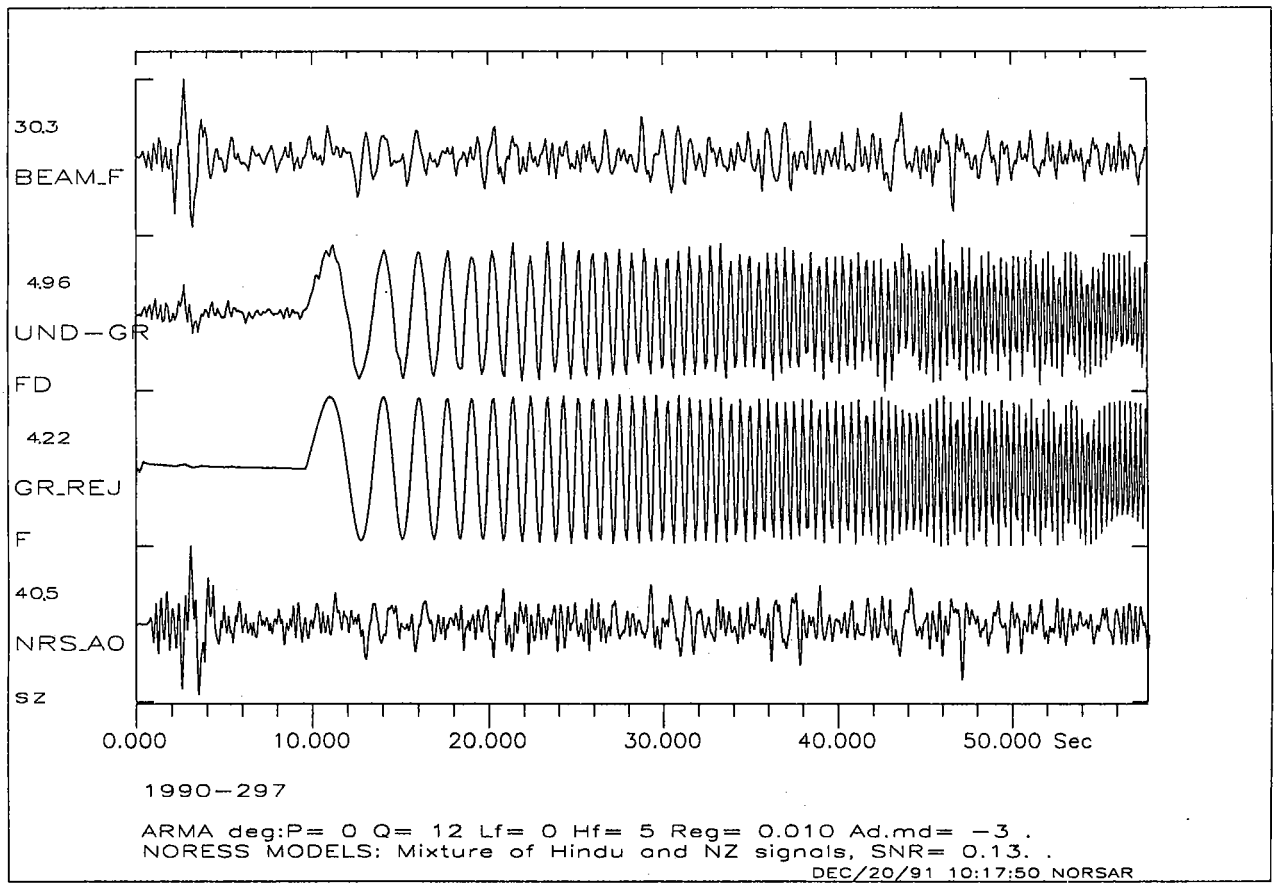

Fig. 7.3.3. Trace no. 2 shows the output after processing a simulated mixture of two plane waves with the self-adaptive optimal group filter. Trace no. 1 is the output after conventional beamforming, and trace no. 3 shows the output of the spatial rejection group filter. The lower trace shows the mixture at the central element of the NORESS array. See text for detailed explanation.

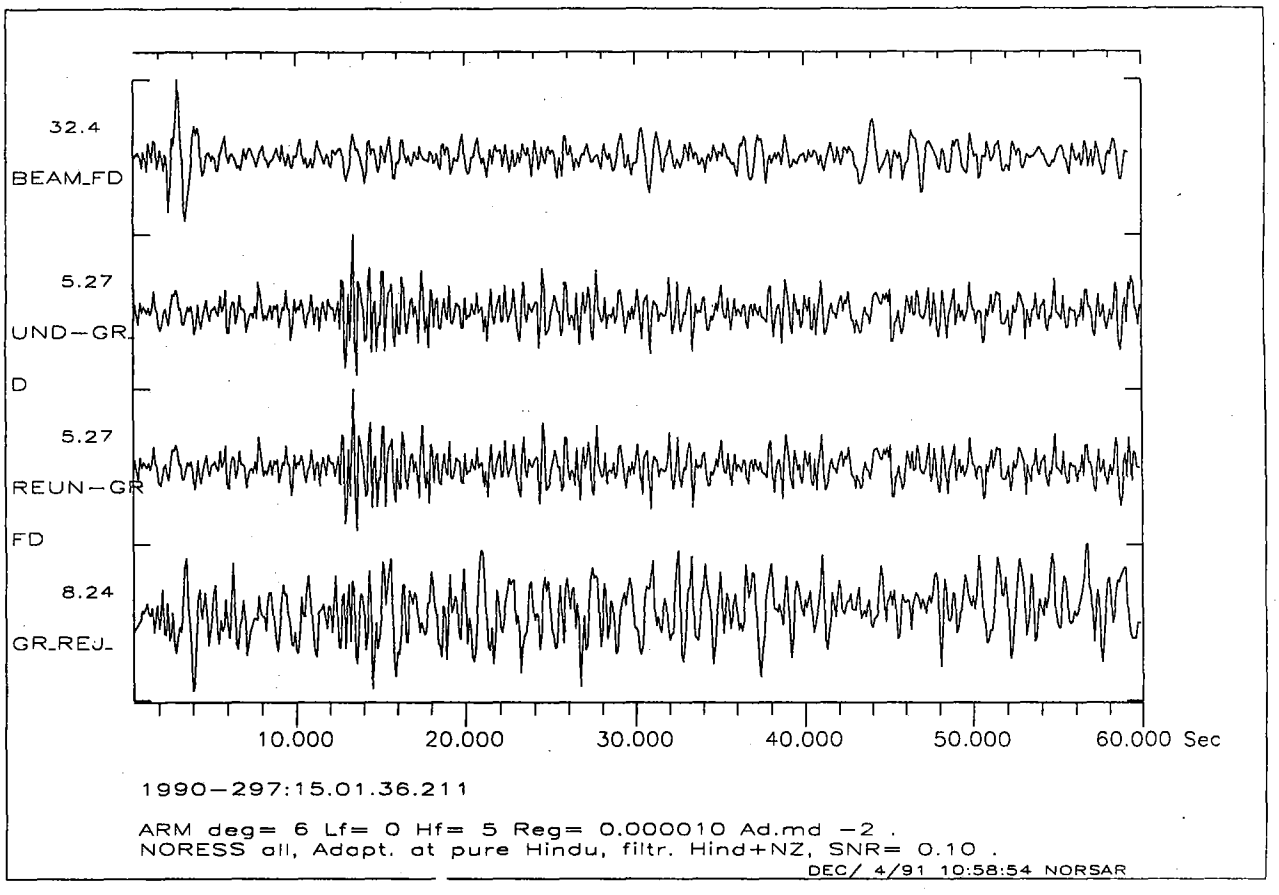

Fig. 7.3.4a. Figure illustrating the performance of the adaptive optimal group filter for separating an artificial event mixture. In this "unreal" implementation, the wanted signal (arriving at about 13 seconds) was not included in the adaptation. Traces no. 2 and no. 3 show outputs from the adaptive optimal group filter, using two slightly different implementations of the method. Trace no. 1 is the output after conventional beamforming, and trace no. 4 shows the output of the spatial rejection group filter. It is clear that in this "theoretically ideal" situation the adaptive optimal group filter has an excellent performance. See text for more details.

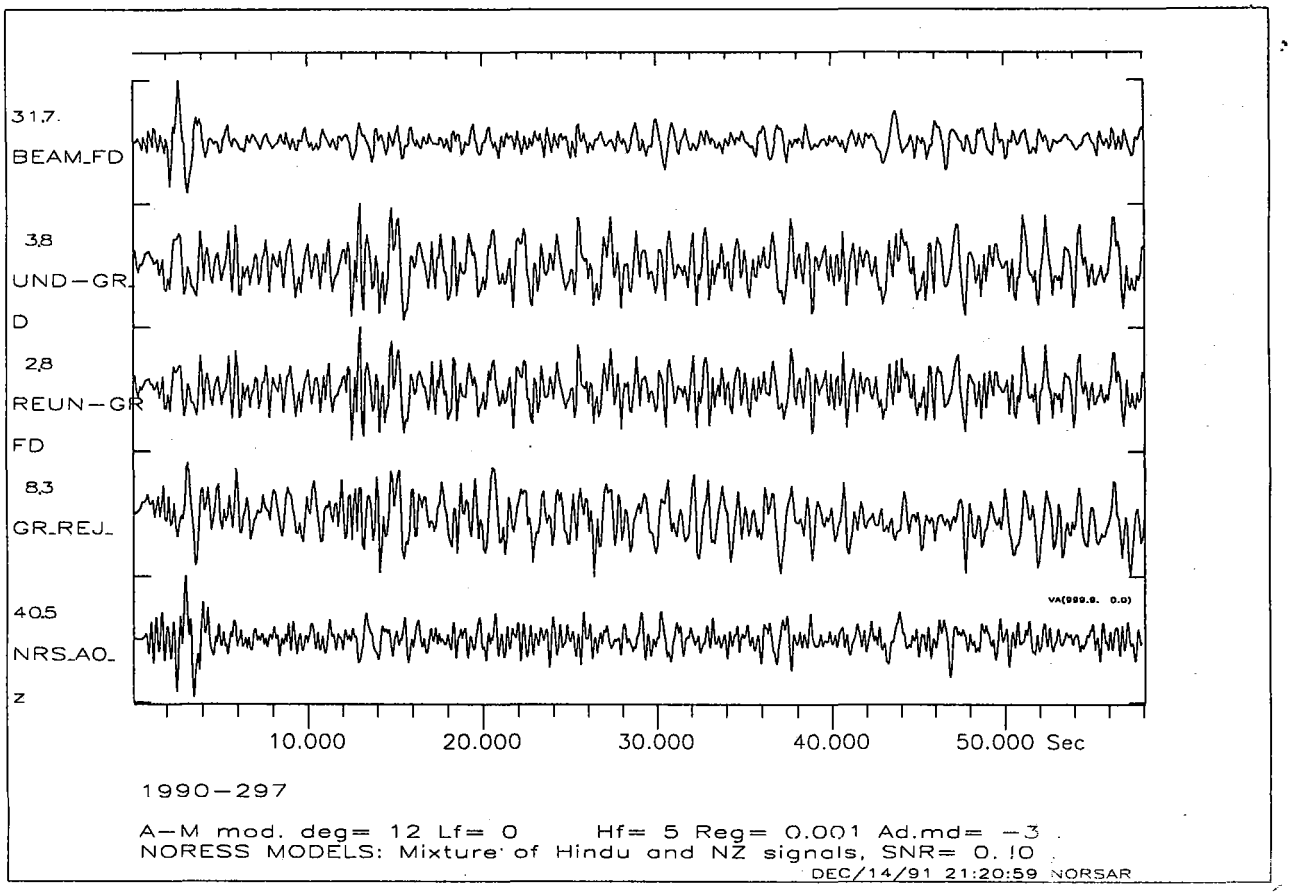

Fig. 7.3.4b. Figure illustrating the performance of the self-adaptive optimal group filter for separating an artificial event mixture. Traces 1-4 correspond to traces 1-4 of Fig. 7.3.4a. We believe that the degradation in performance relative to results shown in Fig. 7.3.4a is due to fact that both the signal and the intefering energy deviate strongly from single plane wave components.

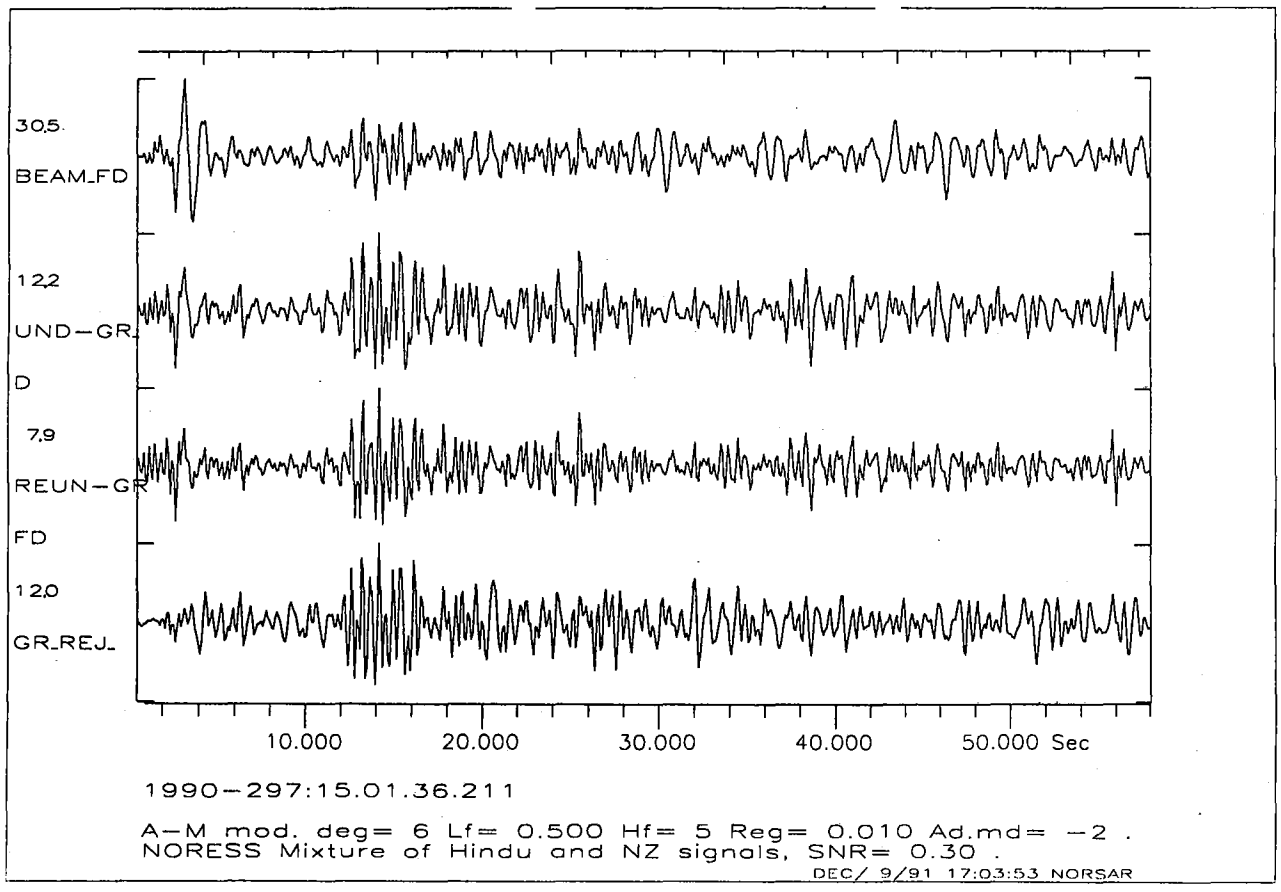

Fig. 7.3.4c. Traces 1-4 correspond to traces 1-4 of Fig. 7.3.4b, but the SNR of the signal is now raised from 0.1 to 0.3. We see that the self-adaptive optimal group filter provide results comparable to the spatial rejection group filter. However, the self-adaptive optimal group filter does not require any information on the slowness or azimuth of the interfering wavetrain.

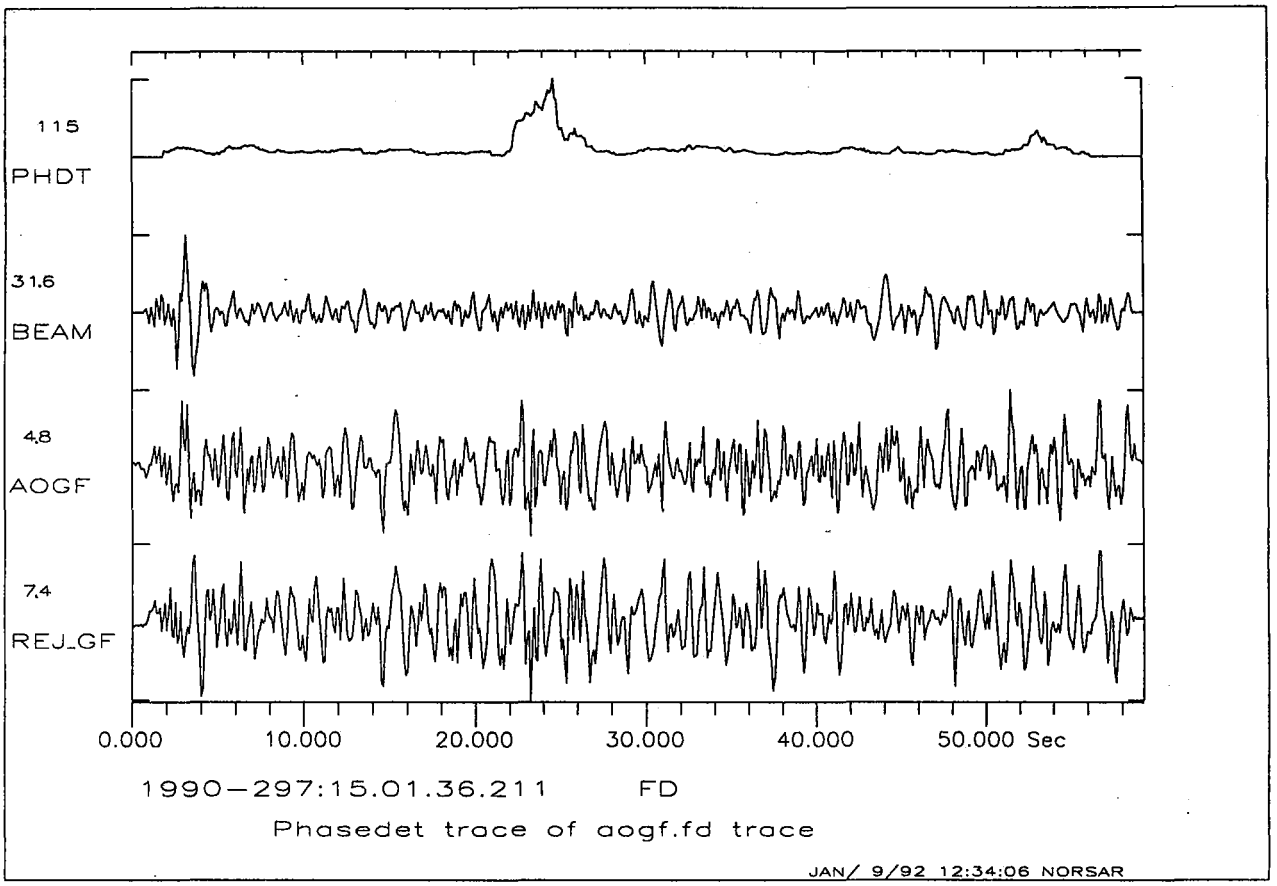

Fig. 7.3.5. Detector statistics from the adaptive optimal phase detector applied to the output from the self-adapted optimal group filter (trace no. 3). Trace no. 2 shows the conventional beam and trace no. 4 shows the spatial rejection group filter output. We see that although the signal (arriving at 21 seconds) is not clearly identified on any of the traces, the adaptive optimal group filter gives us convincing evidence of the presence of a signal.

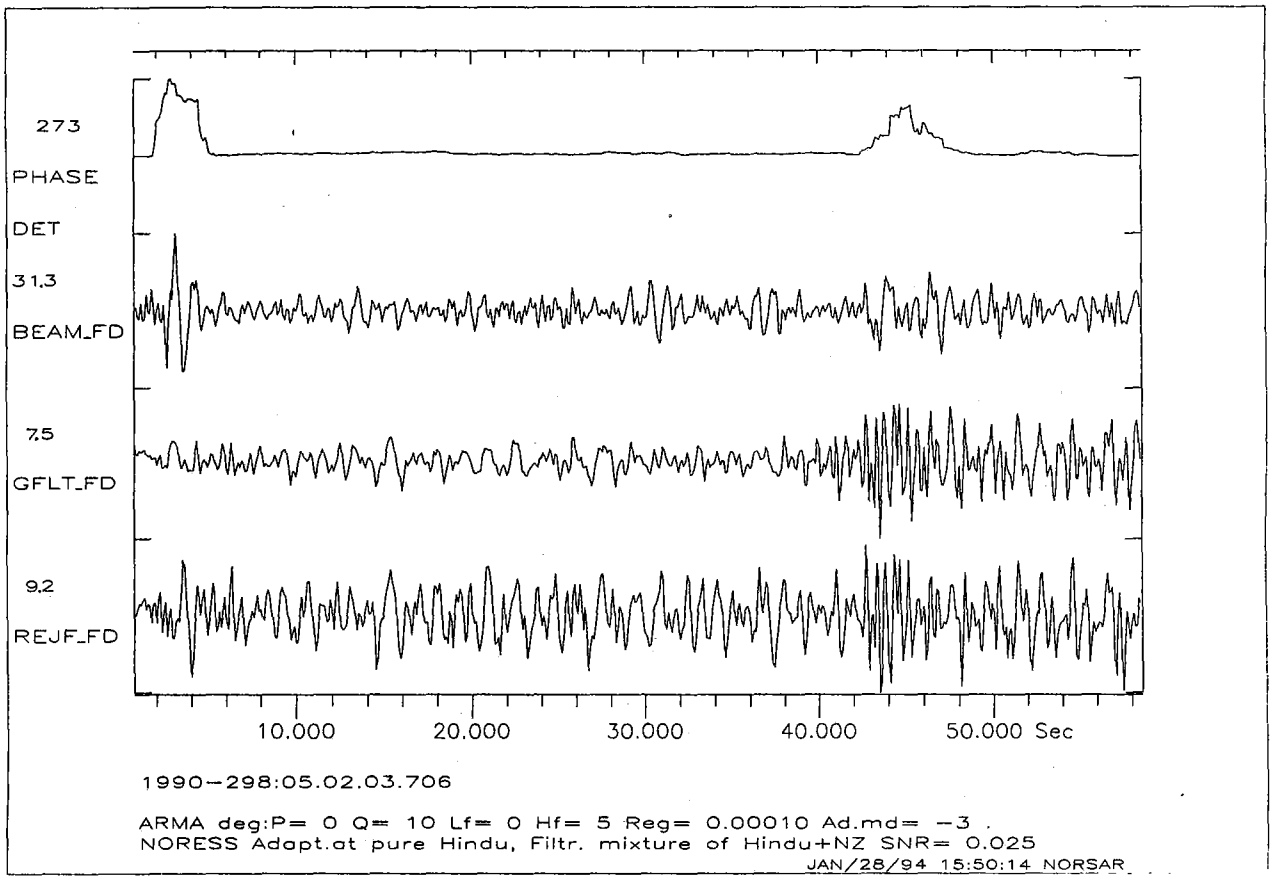

Fig. 7.3.6. Figure illustrating a combined procedure for detecting and extracting a signal with known slowness and azimuth. The signal was set to arrive 41 seconds after the onset of the interfering event, and had a SNR of 0.2. A conventional beam was steered with delays corresponding to the slowness and azimuth of the signal (trace no. 2), and the adaptive optimal phase detector was applied to this conventional beam (trace no. 1). The signal arrival was identified at 41 seconds. The group filter was adapted to the interval 0-39 seconds, and the output from the adaptive optimal group filter is shown in trace no. 3. The signal is now clearly extracted. For comparison the output from the spatial rejection group filter is shown in trace no. 4, but it should be noted that this filter cannot be implemented when information on the interfering event is unknown.

7.4 Some improvements of the detector / SigPro - system at NORSAR

Introduction

In operating the GERESS array, the Institute of Geophysics at the Ruhr-University of Bochum, Germany uses NORSAR software for analyzing the GERESS data. Due to special site conditions and a slightly different configuration of GERESS relative to the small aperture arrays in Scandinavia the application of the NORSAR software for GERESS data needed several adaptations. A systematic comparison of events defined by the automatic RONAPP system and events reported by international data centers led to the conclusion that many events were not located because the installed detector missed a lot of clearly visible S-type onsets (i.e. Sn, Sg, Lg, or Rg). This occurred when on all vertical beams (i.e., beams formed using vertical component sensor data only) these S-type onsets showed a relative small signal to noise ratio (SNR) relative to the P-phases and when the S-energy on the calculated incoherent beams using the horizontal components was smeared out instead of being concentrated. This observation led to a general modification of the detector for S-type onsets at the GERESS data center in Bochum using the horizontal components. After changing the detector in Bochum about 20% more events could be located by the automatic processing.

These modifications have now been implemented for the processing of GERESS data at NORSAR, and the same detector extensions have been tested for ARCESS and NORESS. Also for these two arrays, an improvement of the detection capabilities for S-type onsets can be observed using the new beam configurations.

In a separate study, the effect of the length of the analysis time window for the automatic fk-estimation and the effect of prefiltering the signal traces before estimating the fk-spectra were investigated. This study takes into account the different apertures of the arrays, and for all the arrays (ARCESS, FINESS, GERESS, and NORESS) an improvement of the automatic fk-results can be observed.

Coherent beams of rotated horizontal components

To detect S-phases on the horizontal components, one has to be aware that amplitudes and polarities of S-phases normally show large differences on the two horizontal components. The signal form of S-phases depends on the backazimuth of the incoming wave field, which defines the amplitude split into the two horizontals and it depends on the S-phase radiation pattern of the source, which defines the polarization of the S-onset. If the SV-radiation from the source in the direction of the observing station is relatively large, an S-phase is mostly visible on the radial and vertical components. These onsets are normally well detected by the installed beams that use the vertical components. In the case of a relatively large SH-radiation and a weak SV-radiation in the direction to the station the S-phase is mostly visible on the transverse component, and a signal may go undetected on both the coherent and the incoherent beam of vertical components.

To obtain the best SNR - especially for SH-onsets - the horizontal components must be rotated to their radial and transverse components, respectively. These rotated traces can then be used separately for further investigations. For ARCESS and NORESS, four 3-component stations are available for calculation of coherent beams with the rotated components. For GERESS, five 3-component stations are available. To form the beams, a mean S-velocity of 4 km/sec and several narrow band filters are used. The rotation angle is always the same as the assumed backazimuth for calculating the beam. Additionally, to detect weak S-type onsets with no preferred polarization (i.e. SH and SV show similarly small amplitudes) incoherent beams of the horizontal components for a phase velocity of 4 km/sec and different backazimuths are calculated. The new defined horizontal beams, which extend the old beam tables at NORSAR for ARCESS, GERESS, and NORESS are given in Table 7.4.1.

Fig. 7.4.1 shows two histograms of observed regional phases (velocity $\leq$ 12 km/sec) with and without the new beam tables. This result consists of 5 days (DOY 144-149, 1994) of data processing for ARCESS, GERESS, and NORSAR. The total increase of detections in this velocity range is obvious (55.6%), especially (and as expected) for velocities lower than 5 km/sec. To assess the contributions from the added detections, the whole event processing cycle (SigPro) was carried out and compared with the results of the current automatic processing at NORSAR (i.e., based on the beam tables without the new beams):

For DOY 98-100 and 104-107 in 1994, the GBF routine for multiple station phase association and event location (Ringdal and Kværna, 1989) was rerun with the new detections. Comparing the results with the original GBF locations, 13.3% more events (478 instead of 422) could be defined and the mean number of associated phases to an event increased (e.g. for DOY 104-107 by 40.7% from 3.76 to 5.30).

But also the number of events defined using the single array RONAPP routine (NORSAR Sci. Rep. No 2-88/89) increased for all 3 arrays by 18.6%. Table 7.4.2 gives the results for each array individually for the investigated 17 days (DOY 98-100, 104-107, 133-136, 144-149, 1994) and in Fig. 7.4.2 event locations are given for both the old and the new beam tables. Especially for the known source regions around the arrays the increase of new events is obvious and it is also clearly seen that the observable scatter of poorly located events at larger distances from the arrays has decreased.

To demonstrate the advantage of the new beam tables Fig. 7.4.3a shows as an example an event in southern Norway observed at NORESS, with an epicentral distance of about 250 km (March 14, 1994, 16:02). This event was not locatable because the Lg-phase was not detected with the old beam deployment. Fig. 7.4.3b shows results of the detector process using the new beam tables. At the top the two beams are seen with which the event could be defined, using the detection beam N077 of the P-phase (as in the old beam table) and the newly defined coherent beam NT13 using the transverse components (for definition see Table 7.1.1). Additionally, the SNR-traces of 3 detector beams related to S-phases are shown. It is clearly seen that the Lg-onset has the strongest and sharpest onset on the SNR-trace of beam NT13. The two other SNR-traces correspond to the formerly defined incoherent beams NH02 and NV04 which have the highest SNR for this Lg-onset. NH02

uses all 8 horizontal components and NV04 uses 8 vertical traces (A0, C-ring) as data. Note that the theoretical SNR increase by 8 traces should be higher than by 4 traces, but the SNR on the new beam NT13 is 1.7 to 2.0 times larger than on the incoherent beams.

We also observe that the onset times of S-phases can often be measured more precisely on the new beams than on the vertical beams because of the higher SNR on the horizontal beams, and also because the horizontal components are less disturbed by S-P conversions and scattered energy from the P-coda.

Fk-analysis for detections on the horizontal beams

Especially in the coda of stronger P-phases when the LTA on the verticals is still high (i.e. a high detection threshold) and P to SV conversions or scattered energy arrive at the station, P-type onsets on the horizontal components may also trigger some detections. Therefore the new beams increase the number of P-phases slightly. But the number of noise detections also increases, because the influence of one single (noisy) trace is much higher in the case of only 4(5) stations used for the beam forming. To avoid erroneous fk-results for these detections, the following new rules were developed for the SigPro routine and successfully tested:

For all detections on the horizontal components a first fk-estimate is derived using all available vertical traces. In most cases this gives reliable fk-results, but not if the detection on the horizontal beams is based mostly on SH-energy or on noise at some rotated traces. In these cases, the fk-results are arbitrary, the 'rel. fk-power' - a measure of the quality of the fk-estimation - is very low, and the results cannot be accepted. In these cases, a new fk-estimation is done with the following rules:

If the 'rel. fk-power' is lower than 0.20 it is assumed that the detected energy is an S-onset which is mostly visible on the horizontal traces. Therefore, the fk-analysis is repeated for the rotated components (for radial and transverse components separately) and for the summed square root traces of all horizontal components (this helps to estimate azimuth and velocity for very weak S-onsets which are a mixture of SH and SV energy). Then beams are calculated using these three fk-results and an SNR of the detected onset is remeasured on these beams. The estimated velocity and azimuth of the beam with the highest SNR are chosen as representing this detection, but they are only accepted if the estimated velocity is an S-velocity, if the SNR is higher than the detection threshold of the beam, and if the amplitude of this onset is higher than on a beam calculated with the same parameters, but using the vertical components of the 3-component sites. If these conditions are not satisfied, this detection is classified as noise.

Improvements of the fk-analysis

From off-line fk-analysis it is known that the positioning of the time window relative to the detected onset is of high importance for quality, stability, and reliability of the fk-results. In the following, different changes of the automatic fk-analysis were tested for

ARCESS, FINESS, GERESS, and NORESS. For all tests of new parameter settings more than 100 fk-analyses including different phase-velocities and frequency ranges were compared. The mean of the 'rel. fk-power' - a measure of the quality of the fk-analysis - was used to decide on the success of different parameter settings.

At the moment, the automatic fk-analysis at NORSAR uses a constant time window of 3 sec starting 0.5 sec before the estimated onset time. We can assume that the first cycles of an onset are the most coherent part of this signal. The chosen time window of 3 sec is quite appropriate for signals with a dominant period of about 1 Hz. But for more high frequent signals a 3 sec long time window includes incoherent coda energy which can easily influence the fk-results. Therefore, a frequency dependent time window for the automatic fk-analysis was defined and tested.

With the travel time of the slowest signals (~2 km/sec) crossing an array of aperture a and with the dominant period T_s measured during the onset time estimation, the length t_w of the fk-analysis time window was defined as

$$t_w = 2 * T_s + a / 2$$

This time window guarantees that at least two cycles of the signals are within the fk-analysis window for each channel. Using this time window as a guide-line, several minimum and maximum values of the fk-time window were tested. Another parameter which was varied was the time length the fk-time window starts before the estimated onset. It was found that this value must be increased slightly in the case of GERESS due to the larger aperture of this array. The time window limits with the best fk-results are given for each array in Table 7.4.3.

Additionally, it was found that the fk-results became more reliable when using prefiltered data. The reason for this is that large amplitudes outside the interesting frequency range (especially low frequent noise) can affect the fk-analysis, which uses small time windows for Fourier- transformation. Therefore the traces were prefiltered with a slightly wider pass band (+/- 20%) than the pass band used for the detecting beam.

To avoid erroneous fk-results from the numerous detections of the Glomma river Rg-noise (Kværna, 1990) in the vicinity of NORESS, two beams to detect this noise were tested successfully. These 'negative' detections can now be thrown out to reduce unwanted associations in the event processing routines, in similarity to the two beams especially formed for two know sources of acoustical noise at GERESS.

The advantage of these new rules is demonstrated as follows. For 5 days (DOY 144 - 149, 1994) a total number of 6154 new fk-results from all investigated arrays could be compared with the original NORSAR SigPro results. Fig. 7.4.4 shows 6154 differences of the 'rel. fk-power' for the new and the old SigPro recipes plotted against the dominant frequency of the onsets (Fig. 7.4.4a), and plotted against the estimated ray parameter of the onset (Fig. 7.4.4b). The size of the symbols corresponds to the number of hits for this value, respectively. The figures clearly show that the 'rel. fk-power' increase by 9.5% over the whole frequency range of analyzed signals and also for all ray parameters. Finally, Fig. 7.4.5 shows for all 6154 compared fk-results the new 'rel. fk-power' values against the cor-

responding original 'rel. fk-power' values. It is clearly visible that especially for onsets with small 'rel. fk-power' using the old recipes the quality increases significantly, i.e., the fk-results for weak onsets became more stable and reliable.

Conclusions

The investigated extensions of the beam tables for ARCESS, GERESS and NORESS using coherent beams of rotated horizontal components clearly increase the S-phase detection capabilities of these arrays, especially in the case of relatively strong SH-wave radiation from the source to the array. Therefore, the new beams also led to a larger number of events defined and located by automatic processes (e.g. RONAPP and GBF).

The tested changes of the automatically chosen time window (i.e. length and position relative to the estimated onset time) for the fk-analysis and prefiltering the single traces stabilized the fk-results. For ARCESS, FINESS, GERESS, and NORESS the 'rel. fk-power' increases in the mean and especially the erroneous estimates of phase velocity and azimuth based on fk-results with very low 'rel. fk-power' could be reduced. This also improves the results of the automatic data analysis for all kinds of seismic phases.

J. Schweitzer

References

Kværna, T. (1990): Sources of short-term fluctuations in the seismic noise level at NORESS. *Phys. Earth Planet. Int.* 63, 269-276.

Ringdal, F. and T. Kværna (1989): A multichannel processing approach to real time network detection, phase association and threshold monitoring. *Bull. Seism. Soc. Amer.* 79, 1927-1940.

BEAM	AZ deg	VEL km/sec	FILTER Hz - Hz	ORD	THR	STATION LIST	COMMENTS
New horizontal beams added to the old beam table of ARCESS (NORSAR Sci. Rep. No. 1-89/90):							
FR01 - FR12	*	4.0	0.7- 2.0	4	3.8	A0_sr C1_sr C4_sr C7_sr	radial components
FR13 - FR24	*	4.0	3.5- 5.5	3	3.5	A0_sr C1_sr C4_sr C7_sr	radial components
FR25 - FR36	*	4.0	2.0- 4.0	3	3.5	A0_sr C1_sr C4_sr C7_sr	radial components
FS01 - FS12	*	4.0	3.5- 5.5	3	3.0	A0_sn A0_se C1_sn C1_se C4_sn C4_se C7_sn C7_se	incoherent horizontals
FS13 - FS24	*	4.0	1.0- 4.0	3	3.0	A0_sn A0_se C1_sn C1_se C4_sn C4_se C7_sn C7_se	incoherent horizontals
FS25 - FS36	*	4.0	5.0-10.0	3	3.0	A0_sn A0_se C1_sn C1_se C4_sn C4_se C7_sn C7_se	incoherent horizontals
FT01 - FT12	*	4.0	0.7- 2.0	4	3.8	A0_st C1_st C4_st C7_st	transverse components
FT13 - FT24	*	4.0	3.5- 5.0	3	3.5	A0_st C1_st C4_st C7_st	transverse components
FT25 - FT36	*	4.0	2.0- 4.0	3	3.5	A0_st C1_st C4_st C7_st	transverse components
New horizontal beams added to the old beam table (as running at NORSAR since DOY 123, 1991) of GERESS:							
GR01 - GR12	*	4.0	0.7- 2.0	4	3.5	A2_sr C2_sr D1_sr D4_sr D7_sr	radial components
GR13 - GR24	*	4.0	1.0- 3.0	4	3.5	A2_sr C2_sr D1_sr D4_sr D7_sr	radial components
GR25 - GR36	*	4.0	2.0- 4.0	3	3.5	A2_sr C2_sr D1_sr D4_sr D7_sr	radial components
GS01 - GS12	*	4.0	0.7- 2.0	4	3.0	A2_sn A2_se C2_sn D2_se D1_sn D1_se D4_sn D4_se D7_sn D7_se	incoherent horizontals
GS13 - GS24	*	4.0	1.0- 4.0	3	3.0	A2_sn A2_se C2_sn D2_se D1_sn D1_se D4_sn D4_se D7_sn D7_se	incoherent horizontals
GS25 - GS36	*	4.0	6.0-10.0	3	3.0	A2_sn A2_se C2_sn D2_se D1_sn D1_se D4_sn D4_se D7_sn D7_se	incoherent horizontals
GT01 - GT12	*	4.0	0.7- 2.0	4	3.5	A2_st C2_st D1_st D4_st D7_st	transverse components
GT13 - GT24	*	4.0	1.0- 3.0	4	3.5	A2_st C2_st D1_st D4_st D7_st	transverse components
GT25 - GT36	*	4.0	2.0- 4.0	3	3.5	A2_st C2_st D1_st D4_st D7_st	transverse components
New horizontal beams added to the old beam table of NORESS (NORSAR Sci. Rep. No. 1-89/90):							
N998	100	2.8	2.0- 3.0	2	3.5	all sz	Glomma noise (Kvaerna, 1990) beam
N999	100	2.8	3.0- 4.0	2	3.5	all sz	Glomma noise (Kvaerna, 1990) beam
NR01 - NR12	*	4.0	0.7- 2.0	4	3.8	A0_sr C1_sr C4_sr C7_sr	radial components
NR13 - NR24	*	4.0	3.5- 5.5	3	3.5	A0_sr C1_sr C4_sr C7_sr	radial components
NR25 - NR36	*	4.0	2.0- 4.0	3	3.5	A0_sr C1_sr C4_sr C7_sr	radial components
NS01 - NS12	*	4.0	3.5- 5.5	3	3.0	A0_sn A0_se C1_sn C1_se C4_sn C4_se C7_sn C7_se	incoherent horizontals
NS13 - NS24	*	4.0	1.0- 4.0	3	3.0	A0_sn A0_se C1_sn C1_se C4_sn C4_se C7_sn C7_se	incoherent horizontals
NS25 - NS36	*	4.0	5.0-10.0	3	3.0	A0_sn A0_se C1_sn C1_se C4_sn C4_se C7_sn C7_se	incoherent horizontals
NT01 - NT12	*	4.0	0.7- 2.0	4	3.8	A0_st C1_st C4_st C7_st	transverse components
NT13 - NT24	*	4.0	3.5- 5.0	3	3.5	A0_st C1_st C4_st C7_st	transverse components
NT25 - NT36	*	4.0	2.0- 4.0	3	3.5	A0_st C1_st C4_st C7_st	transverse components

*

BEAM-	AZ	BEAM-	AZ	BEAM-	AZ
01 =	0 deg	13 =	0 deg	25 =	0 deg
02 =	30 deg	14 =	30 deg	26 =	30 deg
03 =	60 deg	15 =	60 deg	27 =	60 deg
04 =	90 deg	16 =	90 deg	28 =	90 deg
05 =	120 deg	17 =	120 deg	29 =	120 deg
06 =	150 deg	18 =	150 deg	30 =	150 deg
07 =	180 deg	19 =	180 deg	31 =	180 deg
08 =	210 deg	20 =	210 deg	32 =	210 deg
09 =	240 deg	21 =	240 deg	33 =	240 deg
10 =	270 deg	22 =	270 deg	34 =	270 deg
11 =	300 deg	23 =	300 deg	35 =	300 deg
12 =	330 deg	24 =	330 deg	36 =	330 deg

Table 7.4.1. List of newly tested horizontal beams to extend the former beam tables of ARCESS, GERESS, and NORESS.

Array	No. of Events		
	Old Beam Table	New Beam Table	Increase %
ARCESS	368	418	13.6
GERESS	288	372	29.2
NORESS	155	172	11.0
	811	**962**	**18.6**

Table 7.4.2. Number of located events by the single array RONAPP process (NORSAR Sci. Rep. No 2-88/89), for the old and for the new beam tables, respectively, for a total of 17 days (DOY 98-100, 104-107, 133-136, 144-149).

Array	Aperture (km)	Min. Time Window (sec)	Max. Time Window (sec)	Start Time before Onset (Sec)
ARCESS	3.0	1.75	2.50	0.50
FINESS	2.0	2.00	2.50	0.50
GERESS	4.0	2.0	3.50	0.75
NORESS	3.0	1.75	2.50	0.50

Table 7.4.3. Parameters for setting the frequency dependent fk-time window for the investigated arrays in order to obtain the highest 'rel. fk-power'.

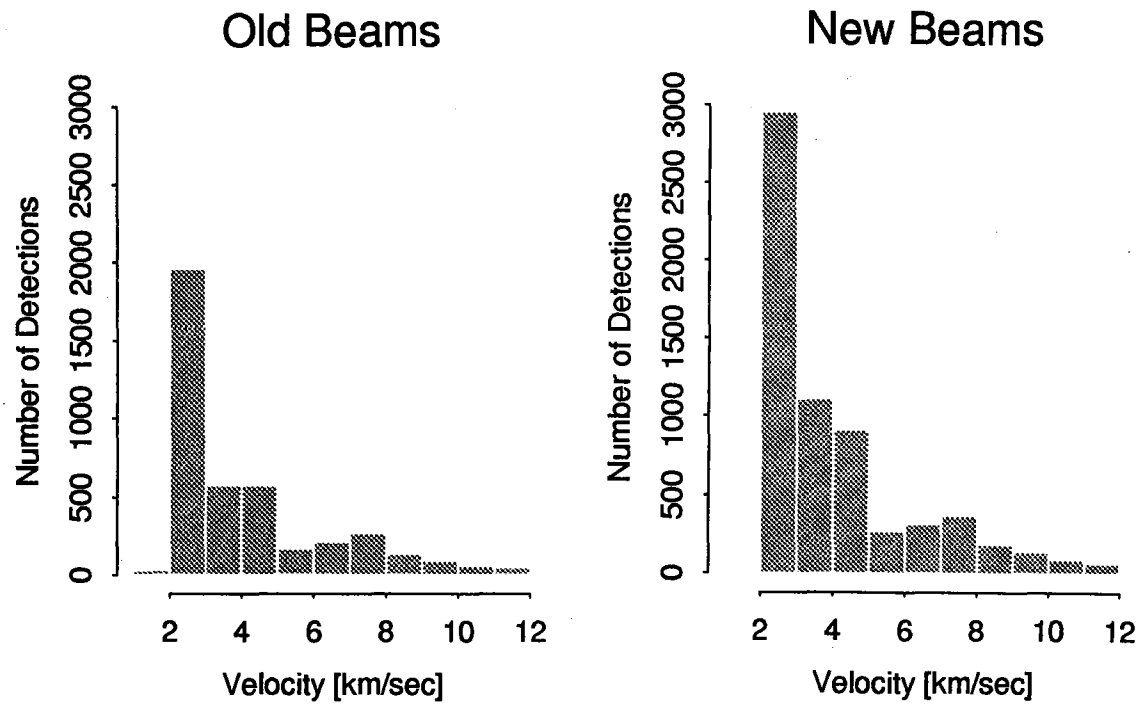

Fig. 7.4.1. Number of observed phases vs. the estimated velocities for the old and the new beam tables. The histograms show the results for ARCESS, GERESS, and NORESS together.

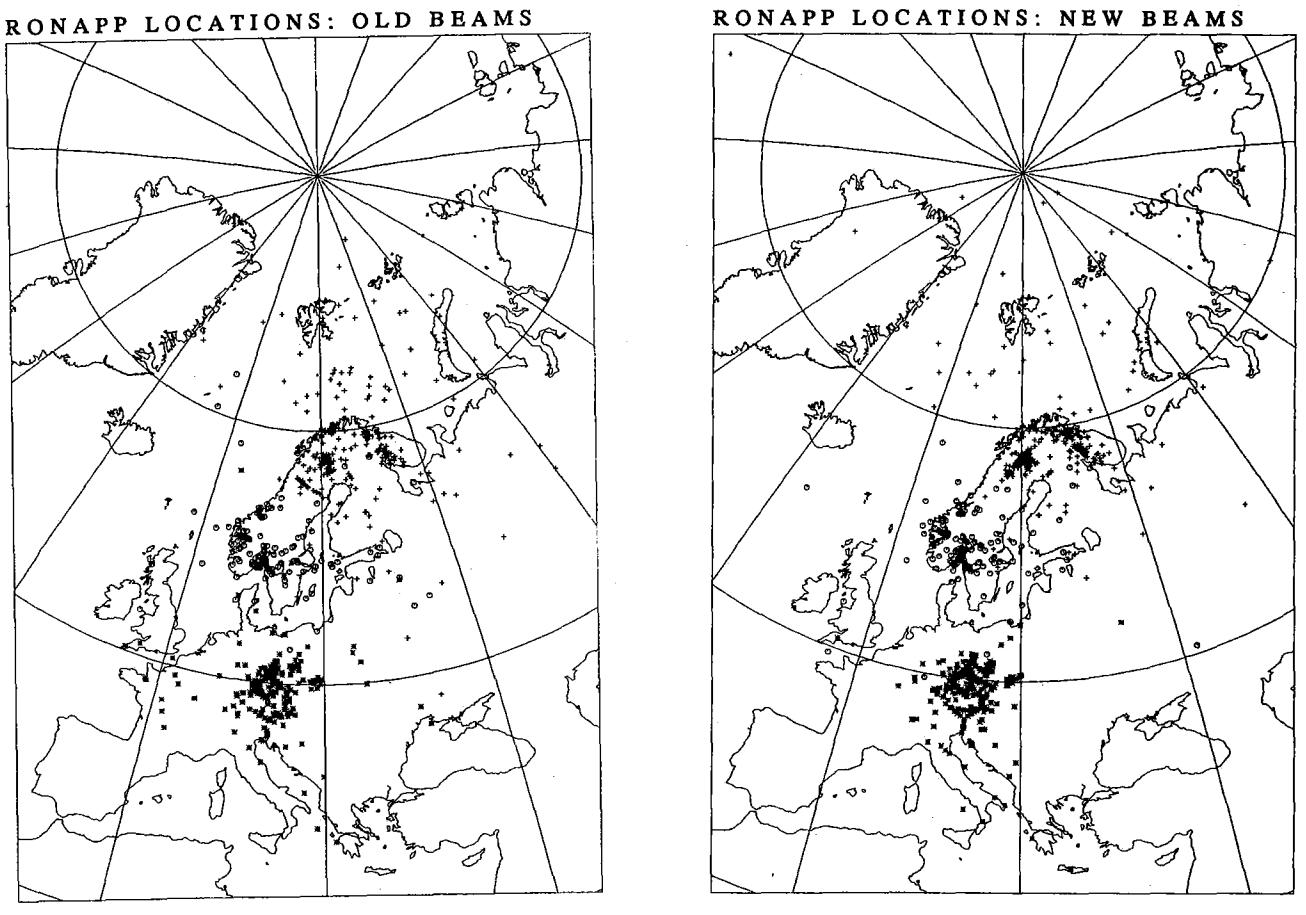

Fig. 7.4.2. Events located with the old and the new beam tables for the 17 days analyzed.

a)

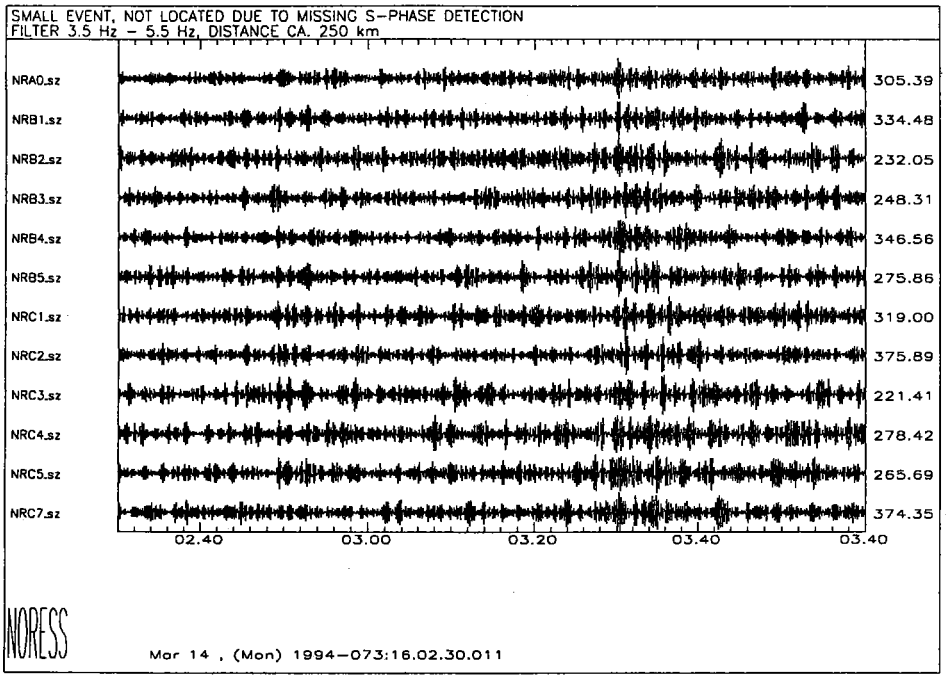

b)

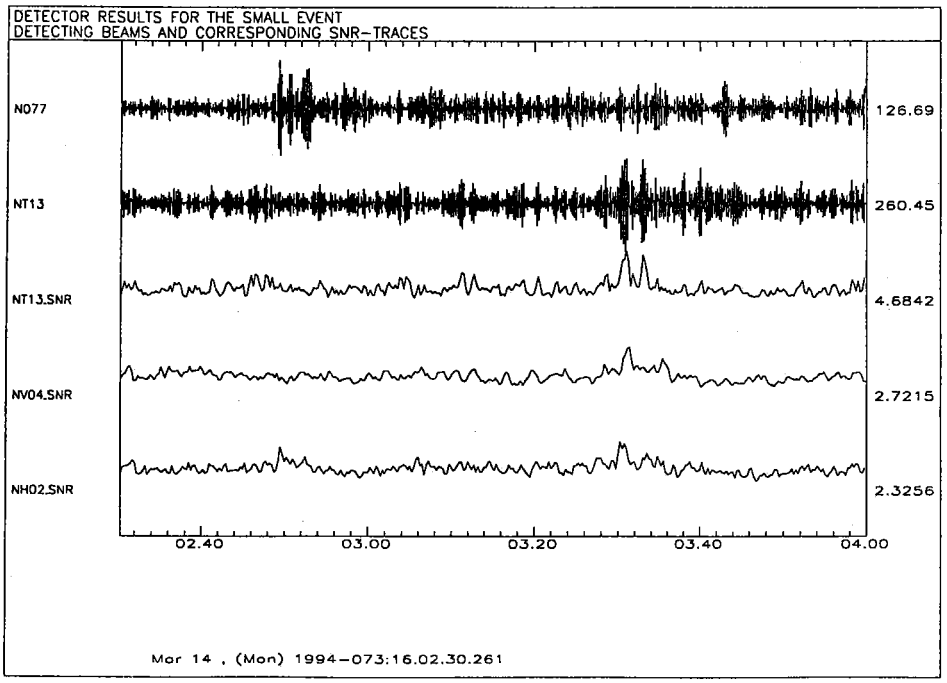

Fig. 7.4.3. An example of an event that was not locatable with the old beam set due to missing S-phase detection. A selection of band pass filtered (3.5 Hz - 5.5 Hz) single traces showing the clearly visible S-phase onset for this NORESS event (Fig. 7.4.3a). Detector beams of P-onset and S-onset and SNR-traces for several beams to detect S-phases of the discussed example (Fig. 7.4.3b).

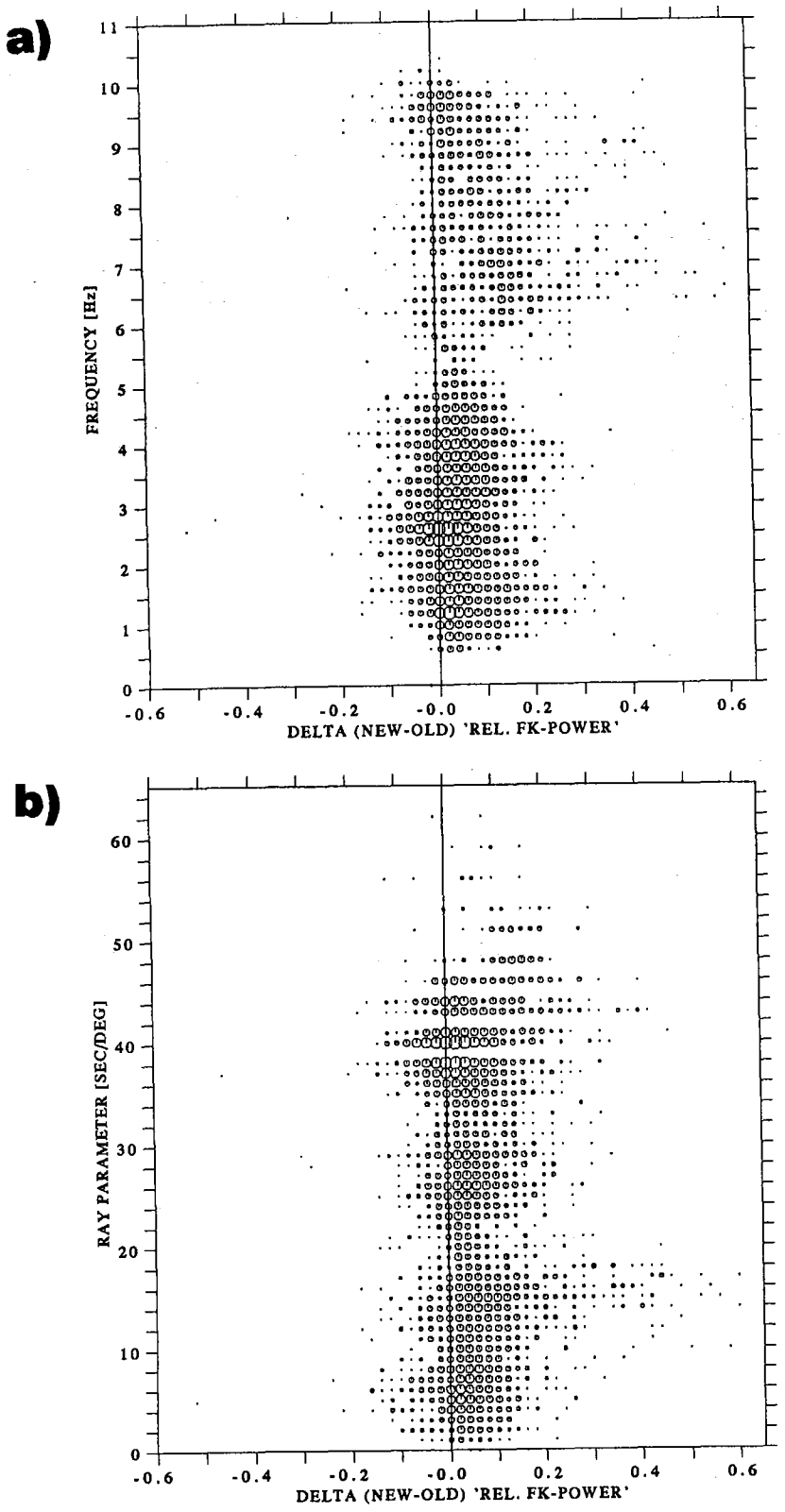

Fig. 7.4.4. Differences between the new and the old 'rel. fk-power' for 6154 estimations plotted against the signal frequency (Fig. 7.4.4a) and against the signal ray parameter (Fig. 7.4.4b).

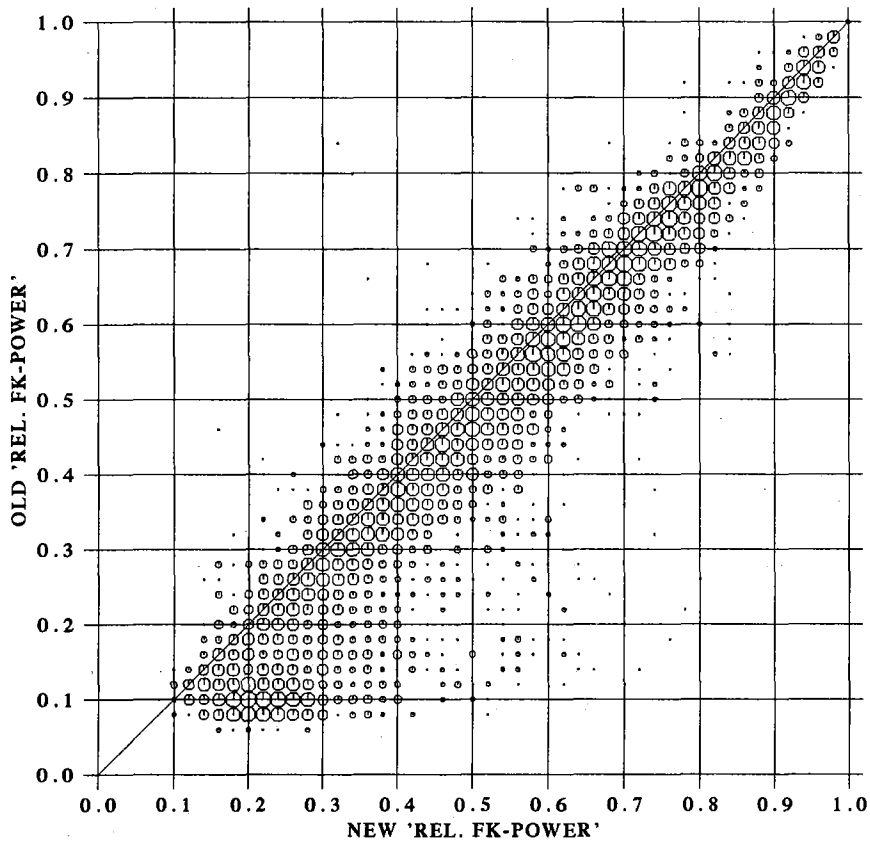

Fig. 7.4.5. New estimated 'rel. fk-power' with respect to the 'rel. fk-power' using the original recipes.

7.5 The 31 December 1992 seismic event on Novaya Zemlya

The small 31 December 1992 event (m_b 2.5) on Novaya Zemlya (Kværna and Ringdal, 1993) has attracted considerable attention in the nuclear monitoring research community. In particular, it has been used as an example to test the effectiveness of seismic identification tools.

Johnny Skorve of the Norwegian Institute of International Affairs is an expert in interpretation of satellite imagery and has previously conducted an investigation of the northern Novaya Zemlya test site (Skorve and Skogan, 1992). We have asked Johnny Skorve to study satellite imagery available from the general area to the NE of the test site where Carter et al. (1993) located the 31 December 1992 event. Even though both the location and nature of this event are very uncertain (a location at the test site cannot entirely be ruled out, and the event may well be a small earthquake), this study by Skorve serves to illustrate the potential and limitations of satellite imagery in a real monitoring situation. The text that follows is as provided by Skorve.

Svein Mykkeltveit

A magnitude 2.5 event was detected on Novaya Zemlya on 31 December 1992. NORSAR located the event to about 30 km NNE of the northern test site. The Norwegian Institute of International Affairs (NUPI) is studying the Novaya Zemlya nuclear test site using Landsat and SPOT images.

Fortunately the satellite imagery made available for this study also includes the area where the 31 December 1992 event probably took place. However, this part of the imagery had not been processed when considerable attention was focused on the event. NUPI is cooperating closely with Tokai University Research and Information Center (TRIC) in Tokyo, Japan. During a working session at TRIC in November 1993, Johnny Skorve (NUPI) and Masahiro Etaya (TRIC) produced sets of high quality satellite images of the 31 December 1992 event area. Both SPOT panchromatic 10 m resolution and Landsat - TM (multispectral) 30 m resolution images were made. In addition, the SPOT and Landsat data were digitally merged to produce high resolution color images of the area. This type of image processing makes it possible to utilize the strong sides of each satellite, i.e., the high resolution of SPOT and the discriminating capacity of the multispectral Landsat.

The study area was defined by the information in the report by Carter et al. (1993), in which the event was relocated using two different master event methods. The two event locations using method 1 (Herring and Ryaboy travel time curves, respectively) and the three event locations using method 2 (JB, IASPEI 91 and Ryaboy travel time curves, respectively) have all been located on the satellite images.

During the NUPI study of the Novaya Zemlya nuclear test sites, it has been possible to observe and map the infrastructure connected with these locations. The question was therefore raised: is it possible to see any infrastructure or activity that can be related to the 31 December 1992 event?

To facilitate such a search, during the working session in Tokyo in November 1993, subscenes both in black/white and color were produced that were centered around the calculated coordinates of the five locations mentioned above. The DMA digital terrain data of that area was also used. The available maps of Novaya Zemlya are all small-scaled, 1:1 mill. ONC and 1:500 000 TPC maps, and this is far from adequate for use in the study of this rather small area. The description of the area is to a large degree based on interpretation and analysis of satellite images.

The northern nuclear underground test site is situated in the southwestern part of the Matochkin Shar in the Shumilikha valley area. The 31 December 1992 event is, however, assumed to be located on the northern side of the Shar, on the eastern part of Novaya Zemlya (Fig. 7.5.1).

The 31 December event coincides with the central part of a valley running diagonally across the southernmost part of the Severny, the northern island (Fig. 7.5.1). The Matochkin Shar is wider in its eastern part and here the 12 km long Belushii bay branches off the Shar in a northerly direction. At its end a delta with shallow frontal water has been formed by fluvial sediment off-loading from the river's suspended material. The southeastern shore of the Belushii bay is situated at the foot of the Bremerhafen Mountain, and to the north of it is a low and flat area with some small lakes.

On the western side of the bay entrance, the Severnaya mountains rise directly from the sea to a height of more than 800 m above sea level. To the northeast of the Belushii valley is a glacier-covered mountain reaching 1140 m above sea level. In the northern part of the area, to the west of the valley, is another mountain. Its summit reaches 1175 m above sea level, and here glaciers are moving radially down. The largest of these goes all the way down to the valley floor where it has left a large semicircular terminal moraine 4 km in diameter. The glacier front had by the time image acquisition began receded approximately 4 1/2 km. The melt water from this large glacier drains northward to the Mityushikha fjord on the west coast of Novaya Zemlya. The poorly defined watershed is situated just east of the glacier. The color, multispectral Landsat-TM image enhances the low topography by the delineation of the vegetation cover. Satellite imaging during late August is most favorable in differentiating vegetational vigor. SPOT imagery for 1989 showed that all snow had melted except for the mountain summit areas and the upper parts of the glaciers.

The satellite images show that the summer of 1989 was considerably more favorable in the Matochkin Shar area compared with that of 1992. Generally, Novaya Zemlya is characterized by a severe climate with a cold, long winter. Meteorological data for the Malyye Karmakuly station on the west coast, south of the northern nuclear test site, show that the mean air temperature here rises above freezing in early June until the end of September. During very favorable weather conditions, the temperature can rarely, and for short periods, exceed 20°C, but the mean air summer temperature is between 4 and 5°C. The 31 December 1992 event area is located about 160 km north of the Malyye Karmakuly station, and the climate here is considerably more severe than on the southwest coast of Novaya Zemlya. Even the floor of the Belushii valley is probably completely snow-covered until late May/early June.

The color satellite image shows that the vegetation is present along the whole length of the valley, from Belushii bay to the inner part of the Mityushikha fjord. Due to the severity of the climate, the vegetation is only found in the coastal belt along the Matochkin Shar and in the low valleys. The vegetation is absent in areas above 150-200 m above sea level. Judging from the distribution of the vegetation alone, one may conclude that the Belushii valley is, as mentioned above, low levelled and flat at its base, and this is verified by the digital terrain data.

On the digitally merged SPOT and Landsat-TM images of the Belushii valley area, TRIC superimposed a geographical grid. By using this, the five seismically determined locations of the 31 December 1992 event were plotted on to the satellite images. The areas centered around these were photo-interpreted in an effort to trace and detect any human activities. The study area is shown in Fig. 7.5.2, with the five event locations from Carter et al. (1993) superimposed.

The event locations

A survey was made of the five locations. With respect to the accessibility, the locations denoted IASPEI 91 and Herrin have the best positions close to the innermost part of the Belushii bay and thus easy to reach by ship during the summer season. Ryaboy1 is further north, 2/3 of the way upstream between the bay and the watershed. The JB location is the most distant of the five. It is on the northern side of the valley that is draining towards the Mityushikha fjord. Ryaboy 2 is located on a mountain ridge about 7 km west of the IASPEI 91 site.

IASPEI 91

The coordinates of IASPEI 91 coincide with the southern rim of the large alluvial fan that is blocking most of the valley floor immediately north of the river-delta at the end of the Belushii bay. The alluvial fan measures 1.5 x 2.2 km. The material that accumulated on the western slope to form this impressive alluvial fan was transported by water through the canyon running in an ENE direction. The material is distributed in a fan shape way from the fan head at the lower end of the canyon. The scarp or the boundary between the distal side of the fan and the hard rock of the valley side is very distinct, as seen on the color satellite images. That is because the bedrock is apparently covered by quite dense vegetation while the surface of the fan is nearly devoid of vegetation except for some scattered patches on its lowest part.

On the rocky slope about 250 m west of the scarp and about 650 m south of the canyon, there is an area about 50-60 m in diameter that appears to be completely depleted of vegetation in strong contrast to the surroundings. This spot has a brown-grayish color similar to the barren topsoil on the surface of the alluvial fan below. There also seems to be a path from it and down to the scarp where a small alluvial fan meets the large one. The site is only some hundred meters southwest of the coordinates for IASPEI 91, but the resolution

of the satellite images is too poor to establish if this small feature is related to any human activity. It is more probable that the suspected track is a natural landscape feature like a creek or a scar caused by a small rockfall, landslide or avalanche. Fig. 7.5.3 shows a scene from the area around the IASPEI 91 location, with the large alluvial fan near the middle of the picture. The small feature discussed in the text above is marked by an arrow.

Herrin

Herrin is located 3 km north of IASPEI 91, northeast of the large alluvial fan and east of the Belushii braided river. The exact coordinates coincide with the somewhat elevated rocky shoulder about 200 m from the scarp down towards the riverside. The lowest part has rather dense vegetation, while the other half of the landscape seems to have more scattered vegetation. In some of the more shadowed locations, small snow patches can be seen. However, there are no signs of human activity in this area.

Ryaboy 1

Ryaboy 1 is found 8.8 km due north of IASPEI 91 and on the northern side of a large canyon. Its river deposits have formed an alluvial fan. The river constitutes the main discharge of water into the valley where the outer part of this alluvial fan transforms into the braided river system. The coordinates of Ryaboy 1 are just above the vegetation limit in an area where very reflective rocks are exposed. There is no indication of any human activity here.

JB

JB is located 23.5 km northwest of IASPEI 91 and about 5 km north of the largest glacier in the area, described earlier in the text. JB is situated above the vegetation limit and in a rather rough terrain on the western side of the valley leading to the Mityushikha fjord. It is not probable that any human activity is present on this valley slope covered by banks of snow.

Ryaboy 2

Ryaboy 2 is located 6 1/2 km due west of IASPEI 91. This is on a plateau stretching from the southern part of the Belushii valley to the Syedlho mountain near the Matoshkin Shar. Ryaboy 2 has the highest elevation of all five sites. The Ryaboy 2 coordinates coincide with an area about 800 m above sea level. The landscape is quite rugged and hostile. In the surroundings there are several small glaciers and many permanent snowfields. It is very unlikely that human activities should take place in such a desolate area.

Conclusions

The high quality of the satellite images produced for this study fail to show any certain signs of human activity that can be related to the 31 December 1992 event. This conclusion is based on experience gained during the satellite study of the Novaya Zemlya nuclear underground test site in the nearby Shumilikha valley on the southwestern side of the Matochkin Shar. The infrastructure and main feature related to the testing activities here are visible and have been mapped using satellite images. SPOT's 10 m resolution is, however, not fully satisfactory since a lot of the medium and almost all the fine details are lost. This has to be taken into consideration when the results of the 31 December 1992 event are evaluated.

However, if facilities and infrastructure such as those found in a number of places within the northern test site also had been present even to a limited extent in the 31 December 1992 event area, it would have been discovered during the photo-interpretation. It should also be noted that the presence of vegetation always facilitates the discovery of infrastructures and man-made features. In contrast, barren landscapes, of the type that dominate Novaya Zemlya, have generally the property of concealing such features.

J. Skorve, Norwegian Inst. of International Affairs

References

Carter, J., H. Israelsson and V. Ryaboy (1993): Location of the December 31, 1992, Novaya Zemlyan Event, Center for Seismic Studies, 12 April 1993.

Kværna, T. and F. Ringdal (1993): Monitoring a moratorium: An experiment in continuous seismic threshold monitoring of the northern Novaya Zemlya test site, in *Semi-annual Tech. Summ., 1 October 1992 - 31 March 1993*, NORSAR Sci. Rep. No. 2-92/93, Kjeller, Norway.

Skorve, J. and S.K. Skogan (1992): The NUPI Satellite Study of the Northern Underground Nuclear Test Area on Novaya Zemlya. NUPI Research Rep. No. 164, Oslo, Norway.

Fig. 7.5.1. The Matochkin Shar area of Novaya Zemlya with nuclear test site (circled) and the satellite imagery study area (shown enlarged in Fig. 7.5.2) to the east of the test site. (DMA DIGITAL TERRAIN DATA)

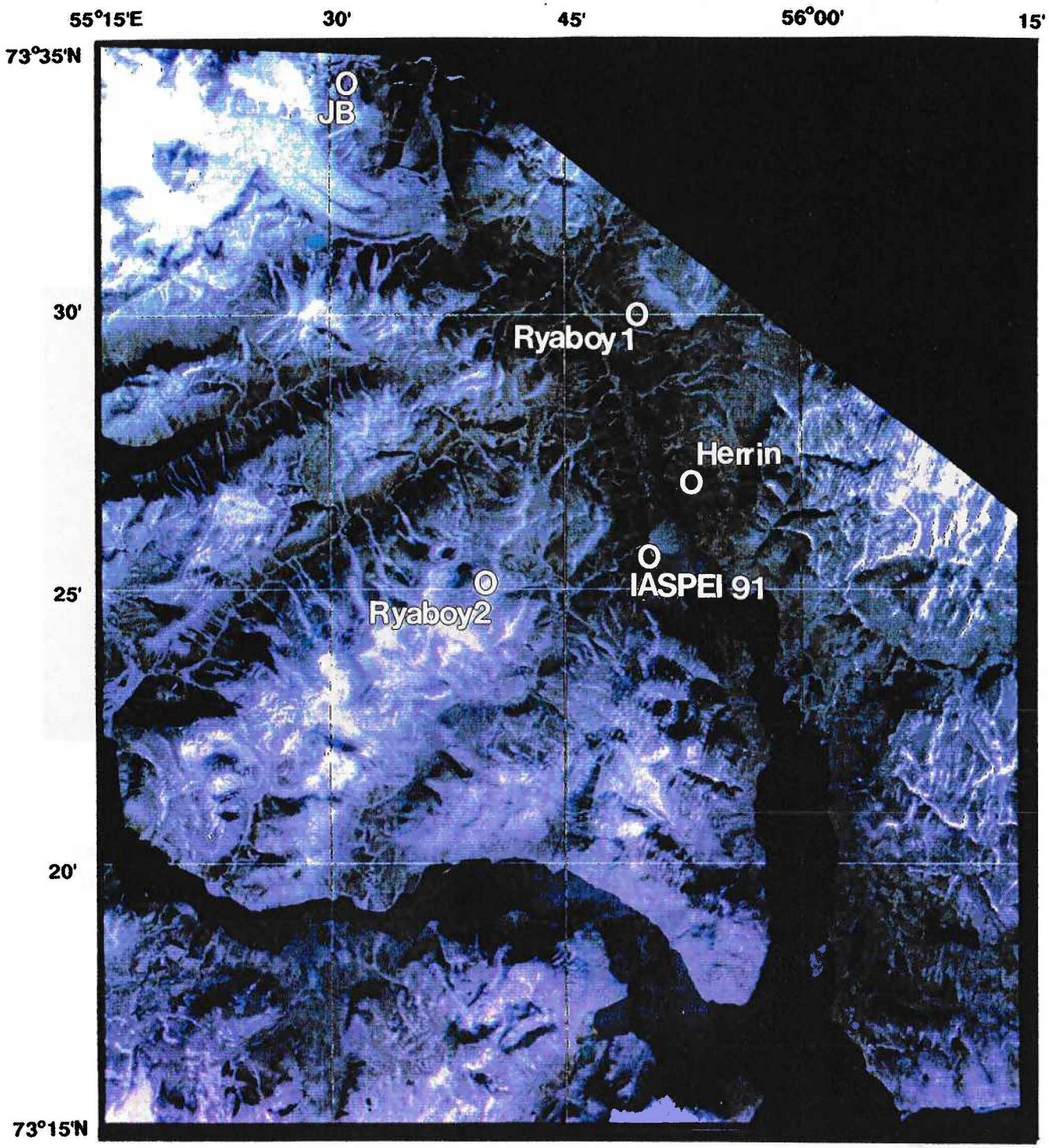

Fig. 7.5.2. Satellite imagery of the study area to the east of the northern Novaya Zemlya test site. The five different event locations for the 31 December 1992 event are from Carter et al (1993). Locations denoted "Herrin" and "Ryaboy1" refer to method 1 in Carter et al (1993), whereas locations denoted "JB", "IASPEI 91" and "Ryaboy2" refer to method 2. (PHOTO: SPOT IMAGE; IMAGE PRODUCTION: TRIC, TOKYO. DIGITALLY MERGED SPOT-P AND LANDSAT-TM IMAGES)

Fig. 7.5.3. Satellite imagery for an area around the IASPEI 91 event location. The small feature marked by an arrow is discussed in the text. (PHOTO: SPOT IMAGE; IMAGE PRODUCTION: TRIC, TOKYO. DIGITALLY MERGED SPOT-P AND LANDSAT-TM IMAGES)